



<https://theses.gla.ac.uk/>

Theses Digitisation:

<https://www.gla.ac.uk/myglasgow/research/enlighten/theses/digitisation/>

This is a digitised version of the original print thesis.

Copyright and moral rights for this work are retained by the author

A copy can be downloaded for personal non-commercial research or study, without prior permission or charge

This work cannot be reproduced or quoted extensively from without first obtaining permission in writing from the author

The content must not be changed in any way or sold commercially in any format or medium without the formal permission of the author

When referring to this work, full bibliographic details including the author, title, awarding institution and date of the thesis must be given

Enlighten: Theses

<https://theses.gla.ac.uk/>
research-enlighten@glasgow.ac.uk

THERMAL STRESSES IN SPHERICAL SHELLS

Thesis presented for the Degree of
Doctor of Philosophy of the
University of Glasgow

by

E. M. BARROWMAN, B.Sc.

May, 1970.

ProQuest Number: 10646297

All rights reserved

INFORMATION TO ALL USERS

The quality of this reproduction is dependent upon the quality of the copy submitted.

In the unlikely event that the author did not send a complete manuscript and there are missing pages, these will be noted. Also, if material had to be removed, a note will indicate the deletion.



ProQuest 10646297

Published by ProQuest LLC (2017). Copyright of the Dissertation is held by the Author.

All rights reserved.

This work is protected against unauthorized copying under Title 17, United States Code
Microform Edition © ProQuest LLC.

ProQuest LLC.
789 East Eisenhower Parkway
P.O. Box 1346
Ann Arbor, MI 48106 – 1346

THERMAL STRESSES IN SPHERICAL SHELLS

The subject matter of this thesis concerns the analytical and experimental investigation of the stress distributions caused by the steady state temperature distributions in spherical shells with various boundary conditions.

After a short critical review of the relevant literature, consideration is given in Chapter 1 to the analytic expressions for the temperature distributions in spherical shells exposed to ambient temperature and subject to the conductive, convective and radiant modes of heat transfer.

In Chapter 2 the equations for the stress resultants in a spherical shell as presented by Flugge are modified to include thermal effects. A particular solution of the shell equation is presented using the derived analytic temperature distributions. This solution, along with an asymptotic complementary function solution derived by Leckie, gives a general solution for the thermal stresses in spherical shells due to axisymmetric temperature distributions.

The problem of a heated opening in a spherical shell is considered and results are presented for the stresses for selected values of the shell parameters.

In Chapter 3 consideration is given to that region of the shell with large meridional angle whereas the region of shell appropriate to the shallow shell theory is considered in Chapter 4. In both these regions appropriate simplifications can be made to the complicated general solution for the spherical shell and somewhat simpler expressions for the stress resultants are obtained.

It is shown that the shallow shell theory is suitable for the evaluation of the thermal stresses in that region of the sphere which can be appropriately described as shallow.

Thermal stresses in cylindrical skirts are considered and comparisons are made with analytic work which has already been presented.

In Chapter 5 the stress concentrations at the junction of a uniformly heated cylindrical shell and a shallow spherical shell are investigated and computed results are presented for various cylinder to sphere thickness ratios.

Asymmetric temperature distributions on spherical shells are considered in Chapter 6 and methods of solution for the resulting stress distributions are discussed. An analytic solution is presented for a slowly varying line of temperature on a spherical shell.

The experimental investigations are described in Chapter 7 which also includes an examination of the problem of measuring thermal strains by the use of strain gauges.

Temperature distributions into three thicknesses of spherical shell from small uniformly heated circular openings are measured and agree favourably with the theoretical predictions.

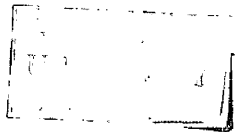
The stress distribution into a $\frac{1}{2}$ " spherical shell from a uniformly heated opening is measured using temperature compensated strain gauges and agreement is found between the experimental results and the analytic predictions.

In/

In Appendix 1 the computational procedures associated with the numerical evaluation of the analytic expressions developed in the thesis are considered.

The circular disc is considered in Appendix 2, while in Appendix 3 the convective and radiant modes of heat transfer are examined.

Appendix 4 gives the results obtained for the author by Babcock and Wilcox from a computer analysis, using the finite element technique, of a particular temperature distribution on a spherical shell. These results are compared with the equivalent theoretical predictions derived in the thesis.



INDEX

		Page No.
	NOMENCLATURE	2
	CRITICAL REVIEW	4
CHAPTER 1	TEMPERATURE DISTRIBUTION	21
CHAPTER 2	A GENERAL SOLUTION OF THE DIFFERENTIAL EQUATIONS FOR THE STRESS RESULTANTS IN SPHERICAL SHELLS SUBJECTED TO AXISYMMETRIC TEMPERATURE DISTRIBUTIONS	56
CHAPTER 3	STRESSES IN A SPHERICAL SHELL AT LARGE VALUES OF THE MERIDIONAL ANGLE	82
CHAPTER 4	SHALLOW SPHERICAL SHELLS	114
CHAPTER 5	STRESS CONCENTRATIONS AT THE JUNCTION OF A UNIFORMLY HEATED CYLINDRICAL SHELL AND A SHALLOW SPHERICAL SHELL	137
CHAPTER 6	UNSYMMETRIC TEMPERATURE DISTRIBUTIONS ON SPHERICAL SHELLS	157
CHAPTER 7	EXPERIMENTAL	203
	BIBLIOGRAPHY	250
	APPENDICES	256
	ACKNOWLEDGEMENTS	283

NOMENCLATURE

x, y, z	Rectangular co-ordinates
r, θ, ϕ	Polar co-ordinates
R_1, R_2	Radii of curvature of the middle surface of a shell
a	Radius of curvature of sphere or cylinder
A	Area, arbitrary constant, $A = \frac{D(1-\nu^2)\alpha(S^2+1-\nu)}{(S^2+1)^2 + 4\alpha^4}$
B	Biot number,
c	A heat transfer parameter, $c^2 = \frac{2m}{kh}$
D	Membrane stiffness, $D = \frac{Eh}{1-\nu^2}$
E	Young's modulus
F	Stress function
h	Thickness of a plate or shell
K	Bending stiffness, $K = \frac{Eh^3}{12(1-\nu^2)}$
k	The coefficient of thermal conductivity
l	A characteristic length
M_θ, M_ϕ	Moment resultants per unit length
m	The surface heat transfer coefficient
m_c	The convective heat transfer coefficient
m_r	The radiant heat transfer coefficient
N_θ, N_ϕ	The stress resultants per unit length
n	A summation index
Q_ϕ	Transverse shear per unit length
q	The rate of heat flow
S	Heat transfer parameter, $S^2 = \frac{2m}{kh} a^2$
T	Temperature of opening or boundary

t	Temperature
U, V	Independent shell variables
u, v	Displacement in the direction of the tangent to the parallel circle and the meridian respectively
w	Displacement in the direction of the normal to the shell surface
α	Coefficient of linear thermal expansion
$\gamma_{\theta\phi}$	Shear strain
$\epsilon_{\theta}, \epsilon_{\phi}$	Strains
α^4	Shell parameter $4\alpha^4 = \frac{D(1-\nu^2)}{k\alpha^2}$
μ	Intensity of plane hot-spot
ν	Poisson's ratio
$\sigma_{\theta}, \sigma_{\phi}$	Stress components
$\tau_{\theta\phi}$	Shear stress
χ	Angle of tangent rotation

INTRODUCTION

The determination of the thermal stresses play an important, and frequently even a primary role, in the design of nuclear reactors, gas and steam turbines, heat exchangers, supersonic aircraft and space structures and many other types of structure operating at elevated temperatures. The thermal stress calculations are generally based on linear elasticity and this often serves as a first step indicating whether further computations will be required to allow for non-linear effects caused either by plastic flow and creep or changes in the physical constants of the materials with temperature. This thesis concerns itself only with the assumptions of linear elasticity.

The formulation of elasticity problems which included the effect of temperature variation is credited to DUHAMEL⁽¹⁾. He presented the papers in 1835, which was not long after the basic formulation of the theory of elasticity, which discussed the generalisation of the fundamental theorems of elasticity to include thermal strains and stresses caused by non-uniform temperature distributions in an elastic body. The theory which he presented was at that time of only academic interest and was not at all developed until the postwar years when the rapid developments and advances in nuclear and chemical engineering, gas turbines, missiles and supersonic/

supersonic aircraft have stimulated further interest in thermo-elasticity and have led to extensive theoretical and experimental research on thermal stress problems.

Situations requiring the determination of the magnitude of thermal stress are to be found in many branches of engineering. Pressure vessels in process plants are subjected to varied conditions of operating temperature and pressure. The operating temperatures may be anywhere from extreme low levels to the maximum that construction materials will permit. Pressures may be high vacuum or several thousand pounds per square inch or anywhere between. Vessels when placed in service or shut down commonly undergo large changes in temperature or pressure, or both. These changes induce stresses in the support structures through variations in expansion between the vessel and its supports. Such stresses may on occasion be quite large.

In nuclear power engineering the containment vessels which house the nuclear reactor must be capable of withstanding thermal gradients particularly at skirts and nozzles. This is also true of the associated heat exchangers where the temperature gradients can be even more severe.

In chemical engineering many of the processes can be accelerated and carried out more efficiently by raising the temperature and the pressure. Hence, in designing vessels in which a high temperature is needed for chemical reactions, thermal stresses must be included in the design calculations and combined with the stresses due to pressure and other forms of loading to ensure adequate strength and life.

In producing power by heat engines, the heat cycle efficiency/

efficiency increases with the absolute temperature, this result being implicit from the Carnot efficiency for the conversion of heat into work in an ideal engine. An increase therefore in the operating temperature will produce a gain in efficiency but it also entails higher thermal stresses and higher creep rates for given stress. There have been recently many costly failures in the steam turbines of the Electricity Board due to thermal fatigue. This fatigue is caused by the shutting down of the plant in the evening when the demand for electricity falls off and restarting the following morning as the demand increases.

Aircraft structures designed for supersonic flight are subjected to aerodynamic heating. The air surrounding the aircraft in flight is progressively slowed down through the boundary layer and this process generates heat and consequently all external surfaces on the aircraft are heated. This leads to non-uniform transient temperatures of about 100°C and 250°C for Mach numbers of 2 and 3 respectively.

CRITICAL REVIEW

The analytical foundations of the thermoelastic theory were established by DUHAMEL⁽¹⁾ who, in 1835, presented a paper in which he modified the equations of isothermal elasticity which had been previously formulated in 1829 by POISSON⁽²⁾.

In DUHAMEL'S fundamental equation the temperature and the strain distribution are coupled, as functions of time and so an exact analysis would require the simultaneous determination of both the strain and temperature distributions. Examples of the solution of this coupled type of equation are presented by BOLEY and WEINER⁽³⁾.

Fortunately the thermoelastic coupling effect is small and it is not usual to include it in the stress analysis of plate and shell structures. It is possible therefore to determine independently as functions of time, the temperature distributions and the deformations of a body. DUHAMEL examined the implications of various simplifying assumptions and he propounded an analogy, appropriately named DUHAMEL'S analogy, which establishes a correspondence between the thermal stress problem and the body and surface stress problem which leads to identical strains. At first sight it may appear therefore that the solution of many thermal stress problems are readily available in elastic theory. Unfortunately/

Unfortunately this is not so since only a few body force problems have been solved and those which have are of little interest for thermal stresses. JOHNS⁽⁴⁾, in his recent book, outlines the underlying theory of this analogy which he describes as the "Body Force" analogy.

At about the same time as DUHAMEL'S original paper, NEUMANN⁽⁵⁾ deduced the thermoelastic stress equations, while, in 1879, HOPKINSON⁽⁶⁾ gave the full thermoelastic equations essentially in the same form as they are found to-day in the many books on thermal elasticity theory including the work by TIMOSHENKO and GOODIER⁽⁷⁾ and the two books already indicated.

One of the most outstanding workers in thermal elasticity was BIOT⁽⁸⁾ who as well as devising variational procedures for the numerical solutions of the heat conduction problem and the time dependent equations of thermal elasticity, was also the first to demonstrate the importance of a basic heat transfer parameter in the formation of thermal stresses within a body. This parameter, BIOT'S number (13) is defined by

$$B = \frac{m \ell}{k}$$

where m is the external heat transfer coefficient, ℓ is a characteristic length in the direction of heat flow, and k is the thermal conductivity of the material.

PRZEMIENIECKI⁽⁹⁾ observes that the magnitude of the thermal stresses increase with an increase in the BIOT number and that the increase is the more pronounced for the higher values of this number. This observation is confirmed by HEISLER⁽¹⁰⁾ who has prepared charts giving numerical values of the stresses in flat plates which are initially at zero temperature and are then suddenly exposed/

exposed to a uniform ambient temperature. These charts show the increase in magnitude of the stresses with an increase in the BIOT number. HLINKA ⁽¹¹⁾ demonstrates that the same is also true for slabs and cylinders. A form of BIOT'S number is also fundamental to the temperature distributions within this thesis and the effects of the magnitude of this number on the magnitudes of the resulting stresses for the cases considered can be seen to further confirm the general observation of PRZEMIENIECKI and thus highlight the importance of the BIOT number.

The governing differential equations for axisymmetrical shells of constant thickness were expressed as functions of two independent variables U and V by MEISSNER ⁽¹²⁾ and subsequently modified by EICHELBERG ⁽¹³⁾ and by PARKUS ⁽¹⁴⁾ to include axisymmetric temperature distributions.

The two dependent variables are determined from the differential equations in which the angle ϕ occurs as the independent variable

$$L(U) - \nu \frac{R_1}{R_2} U = - \frac{R_1^2}{KR_2} V + G(\phi) \quad (i)$$

$$L(V) + \nu \frac{R_1 V}{R_2} = E h \frac{R_1^2}{R_2^2} U - H(\phi) \quad (ii)$$

where

$$L(\dots) \equiv \frac{d^2(\dots)}{d\phi^2} + \left[\frac{R_1}{R_2} \frac{d}{d\phi} \left(\frac{R_2}{R_1} \right) + \cot \phi \right] \frac{d(\dots)}{d\phi} - \frac{R_1^2}{R_2^2} \cot^2 \phi \cdot (\dots)$$

(iii)

$$G(\phi) = \frac{R_1(1+\nu)\alpha}{R_2 h} \left\{ (R_1 - R_2) \cot \phi \cdot \bar{t} - \frac{dR_2}{d\phi} \bar{t} - R_2 \frac{d(\bar{t})}{d\phi} \right\} \quad (\text{iv})$$

$$H(\phi) = \frac{R_1^2 E h \alpha \cot \phi}{R_2} \left(1 - \frac{R_2}{R_1} - \frac{\tan \phi}{R_1} \frac{dR_2}{d\phi} \right) \bar{t} - E h R_1 \alpha \frac{d(\bar{t})}{d\phi} \quad (\text{v})$$

while the remaining parameters are as defined in Figures (i - ii) and in the index of nomenclature.

The stress-resultants and deformations are given in terms of U and V . Thus the problem of finding thermal stresses and the resulting deformations due to arbitrary axisymmetrical temperature distributions reduces to the solution of two simultaneous differential equations of the second order in which the 'temperature loading' terms occur on the right hand sides of the equations replacing the ordinary loading terms.

The general solution of equations (i) and (ii) can be separated into the homogeneous solution (complementary function) and the particular solution (particular integral). The complementary functions are used to satisfy the required boundary conditions while the particular integral depends on the temperature distribution only and is independent of the boundary conditions.

The method of describing the temperature loading in terms of the mean temperature, \bar{t} , and the temperature gradient, $\frac{d\bar{t}}{d\phi}$, through the shell thickness, h , is now almost uniformly adopted in problems involving shells and plates.

The exact solutions to cylindrical and conical shells are available in terms of trigonometric and modified Bessel functions respectively.

When/

When the two basic functions U and V have been solved the stress resultants and deformations can be obtained from relatively simple expressions. These are summarised below

$$N_1 = -\cot \phi \frac{V}{R_2}$$

$$N_2 = -\frac{V}{R_1}$$

$$Q = \frac{V}{R_2}$$

$$M_1 = -K \left(\frac{U}{R_1} + \frac{\nu \cot \phi}{R_2} \right) - \frac{\alpha E}{(1-\nu)} \frac{h^2}{12} \bar{t}$$

$$M_2 = -K \left(\frac{U \cot \phi}{R_2} + \frac{\nu U}{R_1} \right) + \frac{\alpha E}{(1-\nu)} \frac{h^2}{12} \bar{t}$$

$$W = \frac{R_2 \sin \phi}{Eh} \left(\frac{V}{R_1} + \frac{\nu \cot \phi}{R_2} \right) - \alpha R_2 \sin \phi \cdot t$$

where dots denote derivatives with respect to ϕ and W is the displacement in the direction normal to the shell surface, measured positive inwards.

For the spherical shell, where $R_1 = R_2 = a$, the mean radius of the sphere, these equations simplify considerably. Recognising $U = \frac{u+w}{a}$ for the angle of tangent rotation χ and since $V = aQ$ where Q is shear stress resultant, then equations (i) and (ii) can, for the spherical shell, be reduced to

$$L(\chi) - \nu \chi = -\frac{a^2}{K} Q - \frac{(1+\nu) a \alpha}{h} \bar{t} \quad (vi)$$

$$L(Q) + \nu Q = \frac{Eh}{a} \chi + Eh \alpha t \quad (vii)$$

which are similar to the equations which are derived, in Chapter 2 of this thesis, from the shell equation as presented by FLÜGGE⁽¹⁵⁾ and modified to include temperature effects.

The homogeneous portions of equations (vi) and (vii) can be combined to give a single equation in terms of the shear stress resultant Q and upon eliminating the operator L one obtains the "basic" equation for the spherical shell which was first suggested by H. REISSNER⁽¹⁶⁾ in 1912. MEISSNER proposed an analytic solution to this homogeneous equation in terms of a hypergeometric series and FLÜGGE reached a somewhat similar solution when with a suitable change in dependent function he transformed the equation into the hypergeometric form with two complex solutions whose real and imaginary parts are a set of four independent solutions.

A general analytic solution could therefore be obtained for the thermal stresses in a spherical shell provided the temperature loading on the right-hand side of the equations are also able to be expressed in the same form as the complementary function, that is as a hypergeometric series or in its associated form a series of Legendre polynomials of the first kind. This is the form of solution proposed by NOWACKI⁽¹⁷⁾ although he does suggest that because of the poor convergence of the series one could follow the approximate procedure which had been proposed by GECKELER⁽²⁵⁾. The poor convergence of the hypergeometric series for spherical shell problems has been commented upon by EKSTRÖM⁽¹⁹⁾ who, for values of $a/h = 62.5$, found it was necessary to consider not less than 18 terms of the series, and by FLÜGGE who considered that it was practically impossible (before the advent of modern computers?) to/

to apply his series to shells whose α/h value is substantially greater than 26 and where the edge to be considered has a co-latitude angle, ϕ , of not less than 70° . NOV0ZHILOV⁽²⁰⁾ concludes that the efforts to obtain the mathematically exact solution are to a great extent wasted since such solutions are inconvenient to use in practice and are moreover inconsistent since the basic assumptions of the original equations involve errors of the order $\sqrt{\alpha}$ in comparison with unity and hence, he claims, there is little sense in retaining terms in the final solution of a smaller order than $\sqrt{\alpha}$.

Because of the difficulties associated with the analytic solutions of the shell problems, various forms of asymptotic integration of the general equation have been considered. The approximate solutions thus derived are usually of a relatively simple form which makes them directly applicable to engineering calculations.

Following the method discussed by JEFFREYS⁽²¹⁾, for the asymptotic integration for second order differential equations which have one parameter large compared with unity, PRZEMIENIECKI⁽⁹⁾ proposed as a suitable parameter for axisymmetrical shells

$$k^2 = \sqrt{3(1-\nu^2)} \left(\frac{R_1^2}{h R_2} \right)_{ref.}$$

which is large for slender shells with thin walls. A second assumption which he introduced for the asymptotic integration was that the radius of curvature R_2 must not be equal to zero and therefore his solutions will break down near the pointed nose of a shell. Any practical slender shell will however usually have a solid nose to that $R_2 \neq 0$ and hence the asymptotic solution can be/

be used. PRZEMIENIECKI then presented the first order approximation of the asymptotic series solution for ring shells, conical shells and cylindrical shells which have axisymmetric temperature distributions. His results, which are summarised in Table (i), give the general solution for the two basic functions U and V , in equations (i) and (ii), in two parts; complementary functions with four arbitrary constants of integration C_1, C_2, β and δ and the particular integrals $R_2(EhR_1^2)^{-1}H(\phi)$ and $K R_2(R_1)^{-1}G(\phi)$ which are known functions depending upon the temperature distributions. In the solution for ring shells, that is shells where R_1 is a constant and where μ is as defined in Table (i), it is necessary to use the integral $\int (1 - \mu \cos \phi)^{-\frac{1}{2}} d\phi$ which cannot be expressed in terms of known tabulated functions. This integral has been evaluated numerically by PRZEMIENIECKI for a series of values of μ and some numerical results are shown in Figure (iii).

The particular integrals given by the asymptotic solutions are approximate. Better approximations can be obtained by using series expansion solutions whose coefficients are determined from the differential equations but this would require an appreciable amount of computation.

The asymptotic solutions for the ring shells can be modified, by putting $\mu = 0$ and $R_1 = a$, to include the special case of the spherical shell. The resulting expression for the shear stress resultant then becomes

$$Q = \frac{Eh}{a^3 \sin \phi} \left\{ c_1 e^{\sqrt{2}k\phi} \cos(\sqrt{2}k\phi + \beta) - c_2 e^{-\sqrt{2}k\phi} \sin(\sqrt{2}k\phi + \beta) \right\} - \frac{K}{ah} (1 + \nu) \alpha \bar{T} \quad \text{(viii)}$$

where the homogeneous portion of this solution is the same as the asymptotic solution of H. REISSNER'S spherical shell equation which was first proposed by BLUMENTHAL ⁽²³⁾. The same approximate solution for the complementary function was also obtained by HETENYI ⁽²⁴⁾ when he reduced the problem of a symmetrically loaded spherical shell to the problem of the flexure of elastically supported curved beams of variable width. For a somewhat coarser approximation, which is valid for large values of opening angle ϕ , GECKELER ⁽²⁵⁾ proposed a simplification to MEISSNER'S equations by dropping from the L operator of equation (iii) all terms other than the second derivative since, he argued, the second derivative is large in comparison with the other terms. The resulting equations are the same as the governing equations for the cylindrical shell and their solution is the same as equation (viii) with the exclusion of the $(\sin \phi)^{-\frac{1}{2}}$ term but, of course, $\sin \phi \approx 1$ for these larger values of ϕ .

All of the asymptotic solutions for the spherical shell so far listed suffer from the restrictions that they are not valid for small values of the angle ϕ . To overcome this difficulty, LECKIE ⁽²⁶⁾ transformed the homogeneous equation into the form of the LANGER ⁽²⁷⁾ equation for which an asymptotic solution is available. This solution is valid for all values of the angle ϕ and it gives for the shear stress resultant

$$Q = \left(\frac{-\phi}{\sin \phi} \right)^{\frac{1}{2}} (A_1 \text{ber} \sqrt{2} \alpha \phi + A_2 \text{bei} \sqrt{2} \alpha \phi + A_3 \text{ker} \sqrt{2} \alpha \phi + A_4 \text{kei} \sqrt{2} \alpha \phi) \quad (ix)$$

LECKIE demonstrated that this solution agrees with the shallow shell solution for small values of ϕ , where $\phi/\sin \phi \approx 1$ and/

and with the HETENYI type asymptotic solution for the larger values of the angle.

A full discussion of the relevance of all the approximate solutions is undertaken by TOOTH⁽²⁸⁾.

A method for the calculation of stresses and deformations in shallow shells subject to various forms of loading was developed by AMBARTSUMYAN⁽²⁹⁾. This method depends on the separation of the Fourier series solution into a portion recognisable as that of a flat plate under the same loading and the remainder due to the small curvature of the shell. Also using a Fourier analysis GRADOWCZYK⁽³⁰⁾ considered the thermal stresses on a shallow spherical shell and he evaluated numerical results after programming his Fourier coefficients. Of great interest are the solutions obtained by CONRAD and FLÜGGE⁽³¹⁾ for shallow spherical, cylindrical and hyperbolic shells under the action of plane and bending hot spots. The stresses and displacements at any point in a temperature field can be obtained by integrating the "effects" of the hot spots which comprise the field. The potentiality of this method for the numerical calculation of thermal stresses due to any temperature distribution has not yet been fully developed due perhaps to the lack of suitable algorithms for the Kelvin function, which describe the unit actions.

Though the homogeneous equation for the asymmetrically loaded shell has been solved by HAVERS⁽³²⁾, using an asymptotic method similar to that of BLUMENTHAL and by LECKIE using the LANGER asymptotic equation, little work has been done to consider the appropriate thermal loadings. STEELE⁽³³⁾, starting from the general shell equations as given by NOV0ZHIL0V, has shown using a/

a wave form, that for any type of loading, including thermal, which has a rapid variation with respect to one curvature co-ordinate relative to a slow variation in another then it is the rapid variation only which need be considered when estimating the stress distribution. A particular case of this general form had already been presented by BOUMA⁽³⁴⁾ who had investigated slowly varying edge loading of some shallow shell forms.

The junction problems, which arise where external members meet a spherical shell, have recently, because of their practical importance, received much attention by researchers. The analysis, usually involved, is carried out by combining existing solutions of the equations of the spherical shell and the penetrating member, often another shell shape, in such a way as to satisfy the appropriate compatibility and equilibrium conditions.

A great number of valuable papers on this subject were presented at the NUCLEAR REACTOR CONTAINMENT BUILDINGS AND PRESSURE VESSELS symposium. A paper by PENNY⁽³⁵⁾ treating the junction of a cylindrical with a spherical pressure vessel demonstrates the value of using matrix methods for the matching of the displacement of the adjoining elements. LECKIE and LIVESLEY⁽³⁶⁾ considered the meeting of the cylindrical supporting shell with a spherical shell while BAILEY and HICKS⁽³⁷⁾ investigated junction problems between a spherical shell and its supporting skirt.

Many conditions of mechanical loading of a cylindrical shell and the spherical dome which it intersects have been examined by BIJLAARD⁽³⁸⁾.

In a series of review articles on the supports for vertical pressure vessels, WOLOSEWICK⁽³⁹⁾ observes that "surveys of/
of/

of literature in the past number of years does not disclose any detailed studies of temperature variations in vertical skirts, insulated externally, internally or both". He presents the following empirical equation, based on test data, for the metal temperature t_x at some distance x inches below the tangent line on a vertical skirt

$$t_x = (t_v - 50^\circ) - 6.037x - 0.289x^2 + 0.009x^3 - 0.00007x^4$$

where t_v is the vapour or liquid temperature. In the tests from which the above relationship is formulated both surfaces of the skirt were insulated with equal amounts of insulation, the total insulation varying from 2 to $4\frac{1}{2}$ inches. It is assumed, though not explicitly stated by the author, that the temperature must be stated in $^\circ\text{F}$. WOLOSEWICK states that, "the above equation does not satisfy fully the experimental data, but it does give fairly reasonable average values".

It appears, from the papers by WOLOSEWICK, BERGMEN⁽⁴⁰⁾ and from the many technical reports within industry, to be common practice for full scale models to be constructed of portions of shell and skirt and the temperature distributions are then "fed into" computer programs for the full shell and the subsequent stresses and deformations determined. PENNY has stated that this was the procedure adopted by the C.E.G.B. and indeed at the present time this same organisation are performing full scale tests, involving temperature and strain measurement, on turbine casings. It has been found that the high thermal stresses associated with the daily "switching on" and "shutting down" have resulted in thermal fatigue and thus occasionally the total loss of a turbine set. The tests therefore, like those on pressure vessel skirts, are directed towards formulating/

formulating a design code to include thermal stresses.

Corresponding with the growing requirement for engineering structures to withstand higher and higher temperatures has been the necessity to determine the stresses on the structure when it is in service. This has motivated a great deal of research, particularly by strain gauge manufacturers such as BALDWIN⁽⁴¹⁾, MICRO-MEASUREMENT and BUDD, into experimental techniques of measurement at elevated temperature and in hostile environments.

Several large commercial organisations have undertaken their own research into measuring techniques and indeed some companies, such as Rolls Royce, even manufacture their own strain gauges. Much of the valuable research work, involving strain measurement, is contained within technical reports which are not made generally available. Fortunately there has grown a greater interest in experimental techniques and this has led to an increase in the publications dealing entirely with these topics. Such a publication is the journal STRAIN.

One experimental researcher who has made a valuable contribution to the understanding of the physical behaviour of different alloys, at elevated temperatures and subjected to stress, is BERTODO⁽⁴²⁾. He was seeking a material which would be suitable for the measurement of strains in the temperature range from ambient up to 1000°C. His published results give a clear assessment of the capabilities of most of the common strain gauge alloys and indicate their suitability for measurement over a particular temperature range.

The effects of the heating rates on strain gauges have been considered recently by BROAD⁽⁴³⁾. His experiments show that the rate of heating of a gauge affects the recorded strain reading.

The/

The magnitude of this apparent strain depends upon the type of gauge, the cement used and upon the rate of heating. A converse effect, to that of the heating rate, is commented upon in this thesis. The author observes that the sudden cooling of the surface of a strain gauge, due to small environmental changes, greatly affects the recorded strain reading.

Unfortunately, even with all these recent improvements in strain measurement techniques, there is still a dearth of published qualitative results from the measurement of strains due to temperature distributions on shell structures.

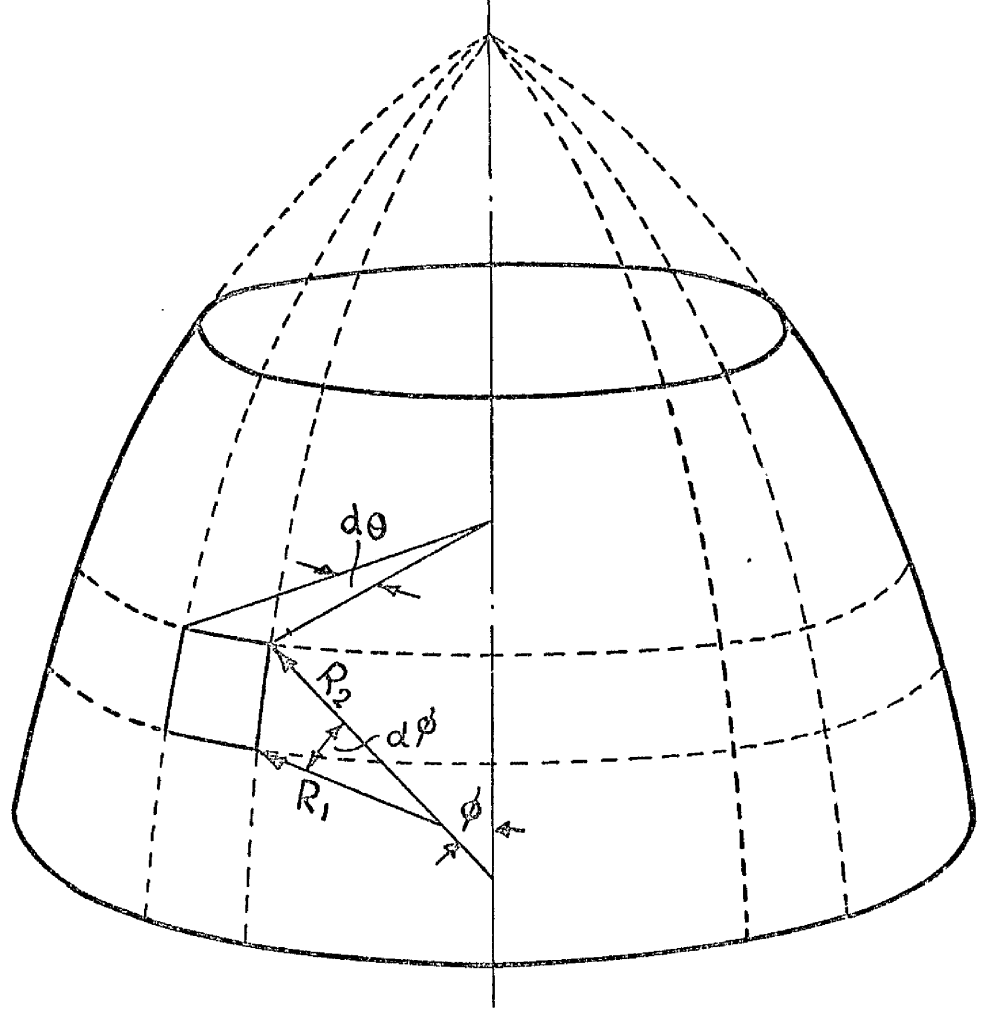


FIGURE (i) SLENDER AXI-SYMETRICAL SHELL

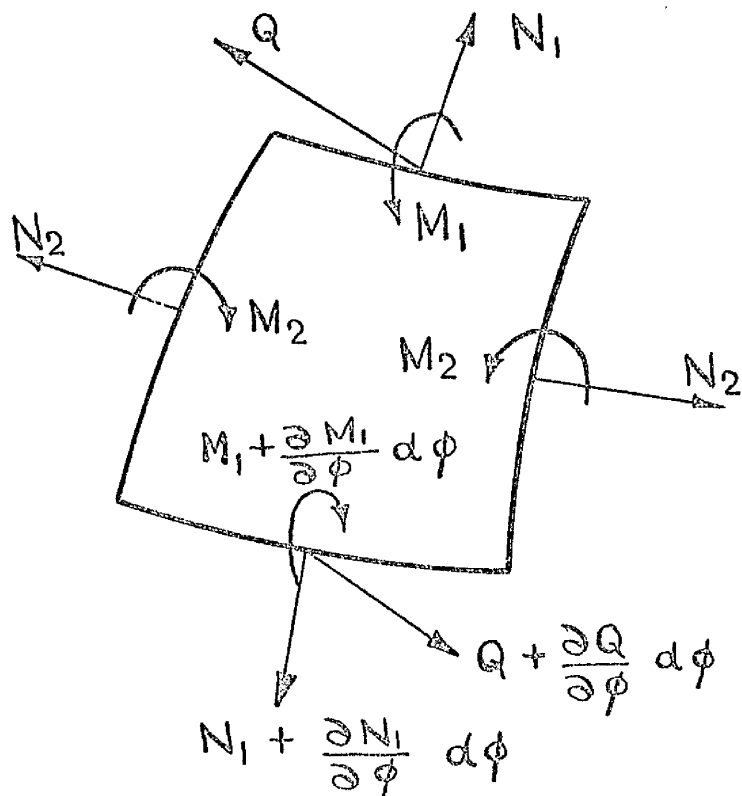


FIGURE (ii) POSITIVE DIRECTIONS OF STRESS-RESULTANTS AND STRESS-COUPLES

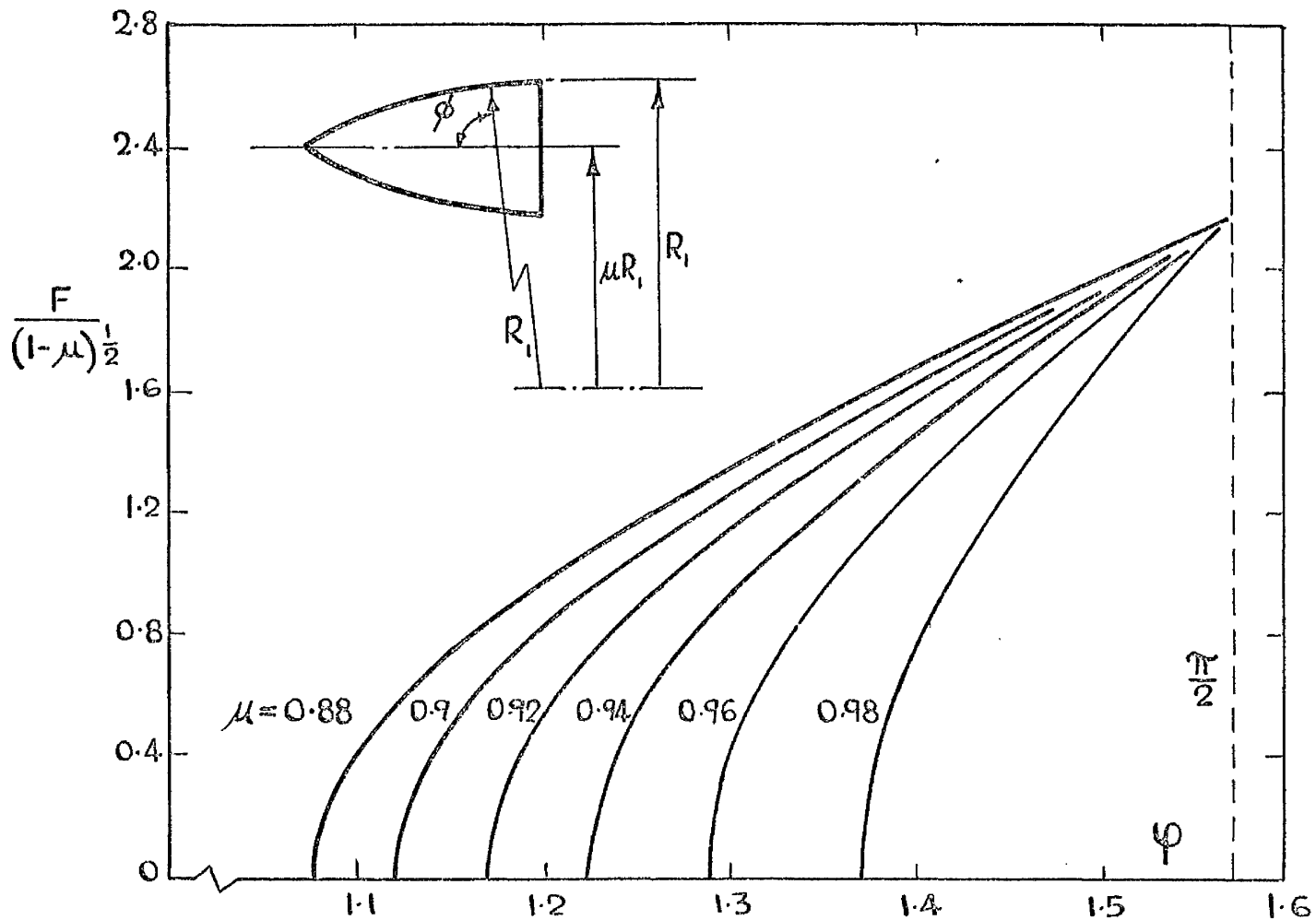


FIGURE iii VARIATION OF THE FUNCTION F WITH ϕ
FOR VARIOUS VALUES OF μ (RING SHELLS)

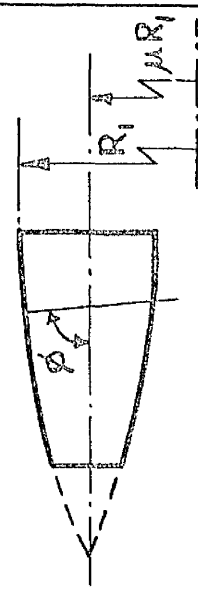
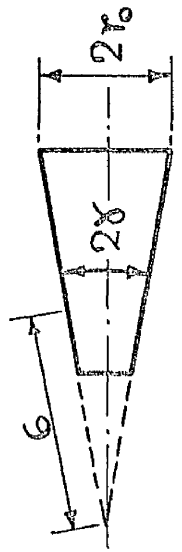
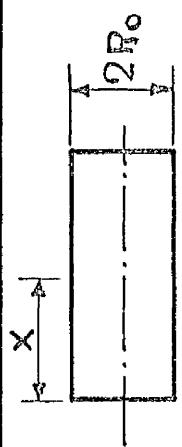
	RING SHELLS	CONICAL SHELLS	CYLINDRICAL SHELLS
			
U			$(K\Phi R_2 \sin \phi)^{-\frac{1}{2}} \left\{ C_1 e^{kF} \cos(kF+\beta) + C_2 e^{-kF} \cos(kF+\delta) \right\} + \frac{R_2}{EhR_1^2} H$
V			$\left(\frac{Eh}{\Phi R_2 \sin \phi} \right)^{\frac{1}{2}} \left\{ C_1 e^{kF} \sin(kF+\beta) - C_2 e^{-kF} \sin(kF+\delta) \right\} + \frac{KR_2}{R_1^2} G$
Φ	$\frac{(1-\mu)^{\frac{1}{2}}}{(1-\mu \operatorname{cosec} \phi)^{\frac{1}{2}}}$	$\left(\frac{r_0 \sec \delta}{S \tan \delta} \right)^{\frac{1}{2}}$	1
K	$[3(1-\nu^2)]^{\frac{1}{4}} \left[\frac{R_1}{(1-\mu)h} \right]^{\frac{1}{2}}$	$[3(1-\nu^2)]^{\frac{1}{4}} \left(\frac{R_1}{r_0 h \sec \delta} \right)^{\frac{1}{2}}$	$[3(1-\nu^2)]^{\frac{1}{4}} \left(\frac{R^2}{R_0 h} \right)^{\frac{1}{2}}$
kF	$[3(1-\nu^2)]^{\frac{1}{4}} \left(\frac{R_1}{h} \right)^{\frac{1}{2}} \int (1-\mu \operatorname{cosec} \phi)^{-\frac{1}{2}} d\phi$	$2 [3(1-\nu^2)]^{\frac{1}{4}} \left(\frac{S}{h \tan \delta} \right)^{\frac{1}{2}}$	$[3(1-\nu^2)]^{\frac{1}{4}} \frac{x}{(R_0 h)^{\frac{1}{2}}}$
R1	R1	∞	∞
R2	$R_1 (1 - \mu \operatorname{cosec} \phi)$	S tan δ	R0
G	$- \frac{R_1}{h} (1+\nu) \alpha \frac{dt}{d\phi}$	$- \frac{R_1^2}{h} (1+\nu) \alpha \frac{dF}{ds}$	$- \frac{R_1^2}{h} (1+\nu) \alpha \frac{dt}{dx}$
H	$- ER_1 h \alpha \frac{dt}{d\phi}$	$- ER_1^2 h \alpha \frac{dt}{ds}$	$- ER_1^2 h \alpha \frac{dt}{dx}$

TABLE (I) ASYMPTOTIC SOLUTIONS FOR SLENDER SHELLS (AFTER PRZEMIEŃIECKI)

CHAPTER I

TEMPERATURE DISTRIBUTION

Before seeking solutions of the uncoupled equations of thermal elasticity, it is first necessary to define mathematically temperature distributions which have some physical significance on a spherical shell.

A temperature distribution is derived for a spherical shell involving the conductive, convective and radiant modes of heat transfer. Analytic and asymptotic solutions are presented for the axisymmetric case. These solutions are compared with the appropriate known solutions for the flat circular plate and the cylindrical shell. All of the solutions contain a parameter which is identified as being similar in form to the BIOT number.

The special case of a slowly varying line of heat around a spherical shell is considered and an asymptotic solution is presented.

TEMPERATURE DISTRIBUTION

- 1.1 Heat Transfer
 - (a) The Equation for the Temperature Distribution in a Spherical Shell
 - (b) The Temperature in a Flat Plate with an Axisymmetric Distribution
 - (c) The Temperature in a Thin Cylinder with an Axisymmetric Distribution

- 1.2 Solutions of the Equation for the Axisymmetric Temperature Distribution in a Spherical Shell
 - (a) The Analytic Solution in Legendre Polynomials
 - (b) The Classical Method of Asymptotic Integration
 - (c) Langer's Asymptotic Solution
 - (d) Comparison of the three Solutions

- 1.3 Heat Transfer due to Conduction Only
 - (a) The Temperature Distribution in a Flat Circular Plate
 - (b) The Temperature Distribution in a Cylindrical Shell
 - (c) The Temperature Distribution in a Spherical Shell

- 1.4 General Comment on and Conclusions about Axisymmetric Temperature Distribution in Spherical Shells

- 1.5 A Slowly Varying Line of Heat Around a Spherical Shell

1.1 Heat Transfer

The basic law governing the heat conduction within a body, Fourier's Conduction Law, states that the flux of heat conducted across a surface is proportional to the temperature gradient, taken in a direction normal to the surface, at the point in question. This law is often expressed in the form

$$q = -kA \frac{dt}{dn} \quad 1.1$$

where q denotes the rate of heat flow across the area A , $\frac{dt}{dn}$ is the temperature gradient in the normal direction and the constant of proportionality, k , is called the thermal conductivity of the material.

The prediction of the rate at which heat is convected away from a solid surface by an ambient fluid requires an understanding of the principles of heat conduction, fluid dynamics and boundary layer theory. All these different phenomena have been included in terms of a single parameter by the assumption that the loss of convected heat at a surface is proportional to the temperature of that surface above ambient.

Thus if t_s is the surface temperature and t_f is the fluid temperature measured at some point suitably far removed from that surface, the heat loss, q_c , can then be expressed by

$$q_c = m_c A (t_s - t_f) \quad 1.2a$$

where the constant m_c is known as the convective heat transfer coefficient. This constant is a gross quantity which attempts only to represent an overall effect. It does not include any attempts/

attempts to explain the actual mechanism of the heat transfer, which must depend upon such things as the composition of the fluid and the nature and geometry of its motion past the surface. This linear relationship is known as Newton's Law of Cooling.

The final form of heat transfer is thermal radiation. its two distinguishing features are that it requires no medium of transport and that it depends upon the level of temperature of the emitting bodies. Whereas the rate of heat transfer by the modes of conduction and convection is proportional to the difference in temperature between the heat source and the heat sink this is not the case for thermal radiation. Here the quantity of heat exchanged is proportional to the differences of the fourth powers of the absolute temperatures of the radiating bodies. This relationship is known as the Stefan-Boltzmann Law for radiant heat emission. This law was proposed by Stefan based on his experimental evidence and was later derived by Boltzmann from the laws of Thermodynamics.

Even though the loss of radiant energy is proportional to the difference of the fourth powers of the temperatures, it is nevertheless found expedient in many engineering applications to define a "radiation coefficient" m_r on the basis of the linear temperature difference between the body and ambient. That is the coefficient

m_r is defined such that

$$q_r = A m_r (t_s - t_f) \tag{1.2b}$$

where q_r is the radiant heat loss.

Since this radiant heat transfer takes place simultaneously with, but independently of, the convective mode of transfer which we/

we have expressed in equation (1.2a), we can therefore combine these two results to give the total loss of heat from a surface as

$$q = q_r + q_c .$$

Substituting from equations (1.2a) and (1.2b) this becomes

$$q = A (m_c + m_r)(t_s - t_f)$$

or the two coefficients may be combined to give

$$q = Am(t_s - t_f) . \quad 1.2$$

This relationship, which contains the empiric coefficient, m , is used to estimate the heat losses from pipes, heat exchanges and from cooling fins.

The two relationships (given by equations (1.2) and (1.1)) can be made compatible provided the temperature is measured relative to a point removed from the boundary layer, in which case

$$t = t_s - t_f .$$

1.1(a) The Equation for the Temperature Distribution in a Spherical Shell

Consider a thin spherical shell of radius a and thickness h which has an asymmetric temperature distribution. Let us assume, however, that the temperature is constant through the thickness of the shell. An energy balance can be made on an element of the shell such as is shown in

Fig.1.1. Adopt the following notation:-

- q_1 = heat conducted into the element at ϕ
- q_2 = heat conducted out of the element at $\phi + \delta\phi$
- q_3 = heat conducted into the element at θ
- q_4 = heat conducted out of the element at $\theta + \delta\theta$
- q_5 = heat convected out of the element at the two surfaces

The principle of the conservation of energy, in the steady state, requires in the element that

$$q_1 + q_3 = q_2 + q_4 + q_5$$

From Fourier's Conduction Law and from Newton's Law of Cooling, the above equation may be written as

$$\begin{aligned} & -kh(a \sin\phi \cdot \delta\theta \frac{\partial t}{a \partial \phi})_{\phi} - kh(a \delta\phi \frac{\partial t}{a \sin\phi \partial \theta})_{\theta} \\ \text{Since} & = kh(a \sin\phi \delta\theta \frac{\partial t}{a \partial \phi})_{\phi + \delta\phi} - kh(a \delta\phi \frac{\partial t}{a \sin\phi \partial \theta})_{\theta + \delta\theta} + 2ma^2 \sin\phi \delta\phi \delta\theta t. \end{aligned}$$

In the limit where $\delta\phi \rightarrow 0$ and $\delta\theta \rightarrow 0$ we obtain the following differential equation

$$\frac{1}{\sin\phi} \frac{\partial}{\partial \phi} \sin\phi \frac{\partial t}{\partial \phi} + \frac{1}{\sin^2\phi} \frac{\partial^2 t}{\partial \theta^2} = S^2 t \tag{1.3}$$

where the parameter S is given by

$$S^2 = \frac{2m}{kh} \cdot a^2 \tag{1.4}$$

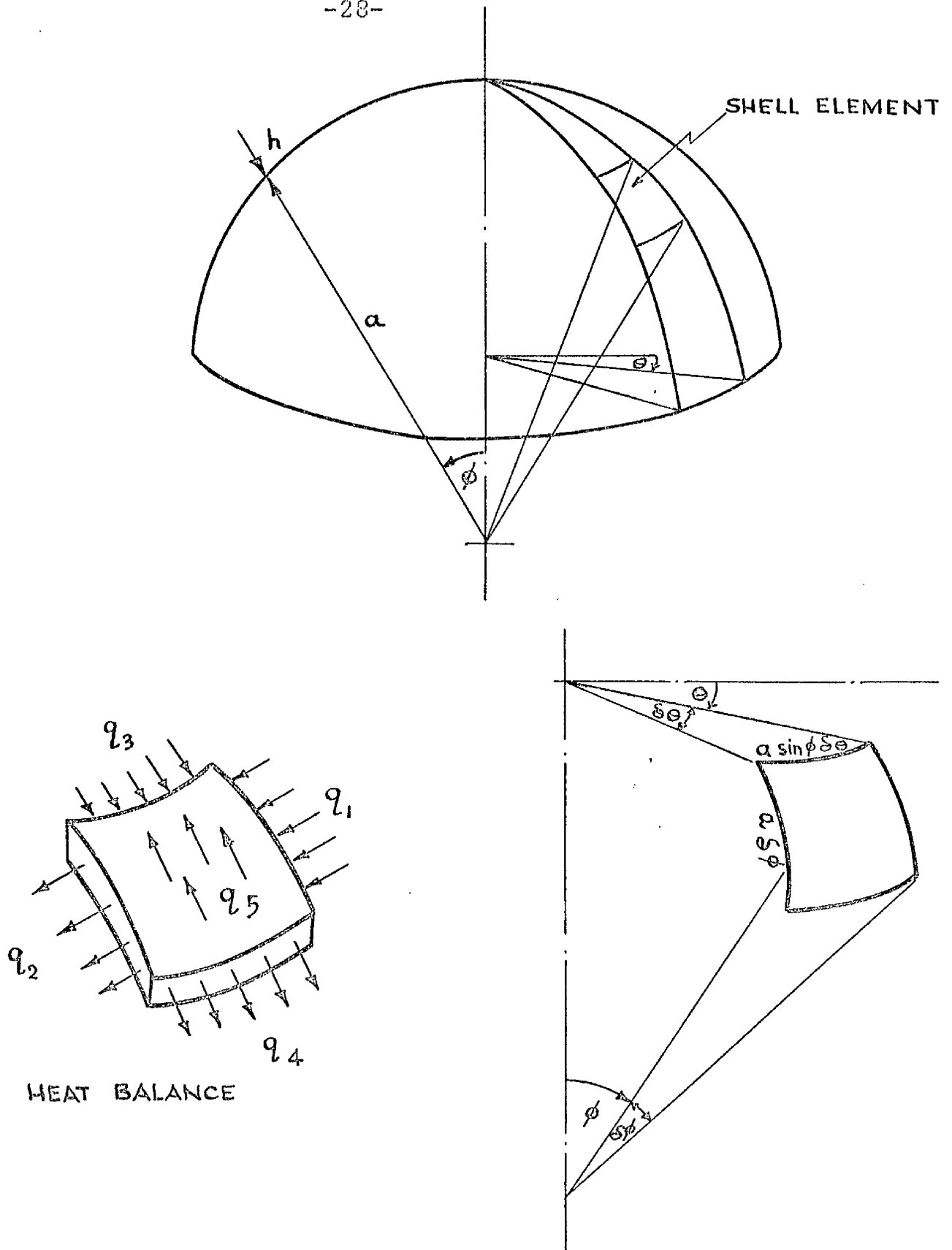


FIGURE (1.1) AN ELEMENT OF A SPHERICAL SHELL

Recognising the Laplace Operator in spherical polar co-ordinates as

$$\nabla^2(\dots) = \frac{1}{\sin\phi} \frac{\partial}{\partial\phi} \sin\phi \frac{\partial(\dots)}{\partial\phi} + \frac{1}{\sin^2\phi} \frac{\partial^2(\dots)}{\partial\theta^2}$$

then we can write equation (1.3) in a more concise form as

$$\nabla^2 t = S^2 t .$$

For the particular case where there is heat conduction only the heat transfer coefficient would be zero and the equation (1.3) would then become

$$\nabla^2 t = 0 \tag{1.5}$$

which is, of course, Laplace's Equation.

It is of interest to observe that the heat transfer parameter S^2 given by equation (1.4) is very similar to the BIOT number, B, which is

$$B = \frac{m \ell}{k}$$

where ℓ is the characteristic length in the direction of heat flow. BIOT⁽⁸⁾ showed that this thermal characteristic of a body influenced the magnitude of the resulting thermal stresses. The greater the magnitude of the BIOT number the greater the magnitude of the stress.

1.2 Solutions of the Equation for the Axisymmetric Temperature Distribution in a Spherical Shell

1.2(a) Analytic Solution in Legendre Polynomials

For a spherical shell, with axisymmetry, equation (1.3) becomes

$$\frac{1}{\sin \phi} \frac{\partial}{\partial \phi} \sin \phi \frac{\partial t}{\partial \phi} = S^2 t \quad 1.6$$

which may be further reduced to

$$t'' + \cot \phi \cdot t' - S^2 t = 0 \quad 1.7$$

where the dots indicate differentiation with respect to ϕ .

Using the substitution $x = \cot \phi$

equation (1.7) becomes

$$(1-x^2) \frac{d^2 t}{dx^2} - 2x \frac{dt}{dx} - S^2 t = 0 \quad 1.8$$

Legendre's Equation is of the form

$$(1-x^2) \frac{d^2 t}{dx^2} - 2x \frac{dt}{dx} + p(p+1)t = 0$$

Equation (1.8) can therefore be expressed as Legendre's

Equation provided we set

$$\begin{aligned} p &= -\frac{1}{2} \pm (S^2 - \frac{1}{4})^{\frac{1}{2}} \\ &= -\frac{1}{2} \pm iq \end{aligned}$$

and the solution can be then expressed in terms of Legendre Polynomials as

$$t = A P_{-\frac{1}{2}+iq}(\cos \phi) + B Q_{-\frac{1}{2}+iq}(\cos \phi) \quad 1.9$$

where /

where

$P_{-\frac{1}{2}+iq}(\cos\phi)$ = Legendre Polynomial, zero order, 1st kind

$Q_{-\frac{1}{2}+iq}(\cos\phi)$ = Legendre Polynomial, zero order, 2nd kind

and A and B the constants of integration.

Fortunately, these particular Legendre Polynomials of complex degree have been investigated and have been shown to be capable of representation in a series form of either sines or cosines of the angle. For a full discussion of their properties one can refer to Spherical and Ellipsoidal Harmonics by Hobson. There the functions are called CONIC FUNCTIONS and their series representation is given as

$$P_{-\frac{1}{2}+iq}(\cos\phi) = 1 + \frac{4q^2+1^2}{2^2} (\sin\phi/2)^2 + \frac{(4q^2+1^2)(4q^2+3^2)}{2^2 \cdot 4^2} (\sin\phi/2)^4 + \dots$$

$$Q_{-\frac{1}{2}+iq}(\cos\phi) = 1 + \frac{4q^2+1^2}{2^2} (\cos\phi/2)^2 + \frac{(4q^2+1^2)(4q^2+3^2)}{2^2 \cdot 4^2} (\cos\phi/2)^4 + \dots$$

$$0 \leq \phi < \pi$$

Unfortunately, in common with many solutions expressed as a series of Legendre Polynomials, the convergence of these solutions is very poor. It was found that the Sirius Computer took over one hour to calculate one point when the series was continued till a term less than 0.01 per cent of the sum of the preceding terms was reached. Thus, though we have an analytic solution for the temperature distribution, it has severe limitations which make it impracticable for use in the subsequent calculations of the stress functions. This is of course especially true of calculations near the apex of the shell, where the angle ϕ is very small, a region which is of particular interest in the stress analysis of the spherical shell.

1.2(b) The Classical Method of Asymptotic Integration

Since the analytic solution which we have just obtained yields a series with poor convergence, let us now consider an asymptotic solution using the method of asymptotic integration described by HILDEBRAND (44).

Assume that the temperature $t(\phi)$ can be expressed in the series form

$$t(\phi) = e^{s\zeta} \sum_{n=0}^{\infty} t_n S^{-n} \quad 1.10$$

where ζ, t_0, t_1 etc. are functions of ϕ . The expressions

$$t = e^{s\zeta} \sum t_n S^{-n}$$

$$t' = e^{s\zeta} \sum (s\zeta' t_n + t_n') S^{-n}$$

$$t'' = e^{s\zeta} \sum \{ (s\zeta')^2 t_n + s\zeta'' t_n + 2s\zeta' t_n' + t_n'' \} S^{-n}$$

are substituted in the differential equation (1.11) to give

$$\sum_0^{\infty} [\{ (s\zeta')^2 t_n + s\zeta'' t_n + 2s\zeta' t_n' + t_n'' \} + \cot\phi (s\zeta' t_n + t_n') - s^2 t_n] S^{-n} = 0$$

Regarding this expression as a series in descending powers of S we can equate the coefficients of S^2, S^1, S^0, S^{-1} , etc., to zero, and in so doing we obtain the following infinite set of equations

$$\zeta'^2 t_0 - t_0 = 0$$

$$\zeta'^2 t_1 - t_1 + \zeta'' t_0 + 2\zeta' t_0' + \cot\phi t_0 = 0$$

$$\zeta'^2 t_2 - t_2 + \zeta'' t_1 + 2\zeta' t_1' + \cot\phi t_1 + t_0'' + \cot\phi t_0' = 0$$

$$\zeta'^2 t_3 - t_3 + \zeta'' t_2 + 2\zeta' t_2' + \cot\phi t_2 + t_1'' + \cot\phi t_1' = 0$$

$$" \quad " \quad = 0$$

$$" \quad " \quad = 1.11 \text{abcd}$$

From the first of these equations (1.15a) we deduce

that

$$\xi' = \pm 1$$

that is, on integrating

$$\xi = \pm \phi + C_1$$

The constant C_1 can be dropped since its effect is merely to multiply the entire series by a constant. The remaining equations (1.11 bcd) may now be simplified to read

$$2t_0' + \cot \phi \cdot t_0 = 0$$

$$2t_1' + \cot \phi \cdot t_1 = -\xi^{-1} (t_0'' + \cot \phi \cdot t_0')$$

$$2t_2' + \cot \phi \cdot t_2 = -\xi^{-1} (t_1'' + \cot \phi \cdot t_1')$$

$$\cdot \quad \quad \quad \cdot \quad \quad \quad \cdot \quad \quad \quad \cdot \quad \quad \quad \cdot$$

1.16 abc

Equation (1.12a) can be readily solved and found to be

$$t_0 = C_2 \sin^{-\frac{1}{2}} \phi$$

where C_2 is the constant of integration. Since the right-hand side of equation (1.12b) is proportional to C_2 it is clear that the particular integrals of the remaining equations are also proportional to C_2 . Substituting this value of t_0 in the right hand side of equation (1.12b) yields the differential equations

$$\begin{aligned} 2t_1' + \cot \phi \cdot t_1 &= -C_2 \xi^{-1} \left[\frac{1}{2} \sin^{-\frac{1}{2}} \phi \left(\frac{1}{2} \cot^2 \phi + 1 \right) \right] \\ &= \mp \frac{1}{2} C_2 (1 + \frac{1}{2} \cot^2 \phi) \sin^{-\frac{1}{2}} \phi \end{aligned}$$

which has the solution

$$t_1 = C_3 \sin^{-\frac{1}{2}} \phi \mp C_2 \frac{1}{8} \sin^{-\frac{1}{2}} \phi (\phi - \cot \phi)$$

A two term series solution for the temperature would then be

$$t = e^{\pm s \phi} \left[C_2 \sin^{-\frac{1}{2}} \phi + C_3 s^{-1} \sin^{-\frac{1}{2}} \phi \mp C_2 \sin^{-\frac{1}{2}} \phi \cdot \frac{1}{8} (\phi - \cot \phi) \right]$$

The effects of the constants of integration

C_2, C_3 etc. can be traced through and the expression written in the form

$$t = \left(C_2 + \frac{C_3}{s} + \frac{C_4}{s^2} + \dots \right) e^{\pm s\phi} \left\{ \sin^{-\frac{1}{2}}\phi \mp \frac{1}{8s} \sin^{-\frac{1}{2}}\phi (\phi - \cot\phi) \pm \dots \right\}$$

to demonstrate that only the particular integrals of equation (1.12 bc) need be considered.

Thus the two term series solution is

$$t = A e^{s\phi} \left\{ \sin^{-\frac{1}{2}}\phi - \frac{1}{8s} \sin^{-\frac{1}{2}}\phi (\phi - \cot\phi) \right\} + B e^{-s\phi} \left\{ \sin^{-\frac{1}{2}}\phi + \frac{1}{8s} \sin^{-\frac{1}{2}}\phi (\phi - \cot\phi) \right\}.$$

1.13

For large values of ϕ this solution may be reduced to the form

$$t = e^{\pm s\phi} \left(1 \mp \frac{1}{8s} \phi \right)$$

For small values of ϕ the representation of the temperature will be

$$t = \frac{e^{\pm s\phi}}{\phi^{\frac{1}{2}}} \left(1 \pm \frac{1}{8s\phi} \right)$$

1.2(c) Langer's Asymptotic Solution

LANGER⁽²⁷⁾ has presented a method of asymptotic expansion which has been recently applied to shell theory by various authors.

Formerly it had been the practice when dealing with small openings to replace $\cot \phi$ by ϕ^{-1} , which in this case would give the equation of the flat plate and the solution would then be valid for small values of ϕ only. The Langer solution however does not suffer from this restriction and is valid for all values of ϕ .

Using the substitution $x = \sin \phi/2$ the differential equation (1.6) becomes

$$\frac{1}{4x} \frac{d}{dx} x(1-x^2) \frac{dt}{dx} - S^2 t = 0 \quad 1.14$$

If we normalise this equation by means of the substitution $t = wy$, where

$$w = [x(1-x^2)]^{-\frac{1}{2}} = [\cos^2 \phi/2 \sin \phi/2]^{-\frac{1}{2}}$$

the resulting equation in y is then

$$\frac{d^2 y}{dx^2} + \left[\frac{-4S^2}{(1-x^2)} + \frac{\frac{1}{4} - 0}{x^2} + \frac{2-x^2}{(1-x^2)^2} \right] y = 0 \quad 1.15$$

Since x is limited to $1 > x \geq 0$ and providing S is sufficiently large, then the dominant terms in the coefficient of y are the first two.

The general form of the differential equation for which Langer gives the asymptotic solution is

$$\frac{d^2 u}{dz^2} + \left\{ \rho^2 \gamma^2(z) + \frac{\frac{1}{4} - A^2}{z^2} + \lambda(z) \right\} u = 0 \quad 1.16$$

where/

where

(i) e^z is a large constant

(ii) $Y^z(z) = z^{\frac{1}{2}-z} \psi_1(z)$ where $\psi_1(z)$

is analytic and bounded in the range $|z| > z \geq 0$

and $\mu > 0$

(iii) A^z is a constant

(iv) $\lambda(z)$ is analytic and bounded in the range $|z| > z \geq 0$

The asymptotic solution of equation (1.20) is

$$u = \Psi(z) \xi^\mu C_\beta(\xi)$$

where

(a) $\beta = 2\mu A$

(b) $\Phi(z) = \int_0^z Y(z) dz$

(c) $\Psi(z) = Y^{-\frac{1}{2}} \Phi^{\frac{1}{2}-\mu}$

(d) $\xi(z) = e^{\Phi(z)}$

and (e) $C_\beta(\xi)$

is any cylinder function of order β

Comparing equations (1.15) and (1.16) we find

(i) $e^z = -(2S)^z$

(ii) $Y^z(z) = \frac{1}{1-x^2}$; $\mu = \frac{1}{2}$

(iii) $A^z = 0$

(iv) $\lambda(z) = \frac{z-t^2}{(1-t^2)^2}$

and therefore

$$y = \frac{1}{(1-x^2)^{\frac{1}{4}}} (i 2S \sin^{-1} x) [A J_0(i 2S \sin^{-1} x) + B Y_0(i 2S \sin^{-1} x)]$$

From/

From the properties of Bessel functions, we have

$$J_0(iz) = I_0(z)$$

$$Y_0(iz) = K_0(z)$$

Recalling that

$$t = (\cos^2 \frac{\phi}{2} \sin \frac{\phi}{2})^{-\frac{1}{2}} y$$

it is then possible to write the general solution in the form

$$t = (\phi / \sin \phi)^{\frac{1}{2}} [A I_0(s\phi) + B K_0(s\phi)] \tag{1.17}$$

which is valid for all values of ϕ in the range $\pi > \phi \geq 0$ provided S^2 is large.

When the angle ϕ is small

$$\phi / \sin \phi \approx 1, \quad r \approx a\phi$$

and the equation (1.17) can be written as

$$t = A I_0(s \frac{r}{a}) + B K_0(s \frac{r}{a})$$

which is the equation for a flat circular plate.

For large values of $s\phi$ we may replace the Bessel Functions I_0 and K_0 by their asymptotic representation.

If $s\phi \geq 10$ then

$$I_0(s\phi) \approx (2\pi s\phi)^{-\frac{1}{2}} e^{s\phi} \left[1 - \frac{-1}{8s\phi} + \frac{-1 \cdot -9}{2! (8s\phi)^2} - \dots \right]$$

$$K_0(s\phi) \approx \left(\frac{\pi}{2s\phi} \right)^{\frac{1}{2}} e^{-s\phi} \left[1 + \frac{-1}{8s\phi} + \frac{-1 \cdot -9}{2! (8s\phi)^2} + \dots \right] \tag{1.18}$$

If therefore S is sufficiently large and ϕ is in the region of $\frac{\pi}{2}$

then/

then

$$I_0(s\phi) \approx (2\pi s\phi)^{-\frac{1}{2}} e^{s\phi}$$

$$K_0(s\phi) \approx \left(\frac{\pi}{2s\phi}\right)^{\frac{1}{2}} e^{-s\phi}$$

so that for these conditions equation (1.17) becomes

$$t = e^{s\phi} \cdot C + e^{-s\phi} \cdot D.$$

where C and D are constants. This is the form of the equation for a thin cylindrical shell.

The expression for the temperature distribution which we have developed using the Langer Asymptotic Expansion agrees with the known theory at the apex and at the equator, where the spherical shell approximates to a flat plate and to a cylindrical shell respectively.

The expression also provides an original asymptotic form for the Conic functions or the Mehler functions as they are called by the Russian authors.

1.2(d) A Comparison of the three solutions

Each of the solutions has been computed over a range of values of the angle, ϕ , for selected values of the parameter S .

These numerical results are presented in tables 1.1 to 1.3. The three selected values of S are $S = 3, 6$ and 12 .

It is shown in Chapter 7 that a reasonable value of S , for a $\frac{1}{2}$ inch thick semi-polished mild steel spherical shell of radius 58 inches, is $S = 7$. The values of S used in the tables, however, were not chosen with any particular material or shell geometry in mind but rather to illustrate the limitations of the various forms of solution of the temperature equation.

The tables present the values, for specific values of the angle ϕ , of each of the functions which, along with their integration constants, make up each of the three solutions. Each of these solutions has two parts, the temperature equation being of second order, one part being a function which increase with ϕ the other a decreasing function with ϕ . It is not possible to compare the three sets of results directly but all of them can be normalised to a common value at some specific value of ϕ .

This is not unreasonable since an identical procedure is adopted when they are "fitted" to any boundary conditions. The value of ϕ chosen for normalising in the tables is $\phi = 1.5$ which is the nearest tabulated value to the equator of the spherical shell.

The Conic Function series were continued till a term less than .01 per cent of the sum of the preceding terms was reached. The Sirius computer used for the calculation took almost/

ϕ	Langer		Conic		Asymptotic		Langer		Conic		Asymptotic	
	$\sqrt{\frac{\phi}{\sin\phi}} K_0$	$\sqrt{\frac{\phi}{\sin\phi}} I_0$	$Q_{-\frac{1}{2}+iq}$	$P_{-\frac{1}{2}+iq}$	$e^{-s\phi} f(\phi)$	$e^{+s\phi} g(\phi)$	'Normalised'	'Normalised'	'Normalised'	'Normalised'	'Normalised'	'Normalised'
.1	3191	1397	2312	1394	8553	1159	5823	1831	5679	1867	5527	1789
.3	1762	8084	1286	8060	4873	6938	3215	1060	3159	1080	3149	1071
.5	1270	6864	9296	6823	3530	5907	2318	9001	2284	9139	2281	9121
.7	991	6481	7335	6424	2787	5569	1823	8498	1802	8604	1801	8598
.9	8247	6457	6070	6379	2307	5533	1505	8467	1491	8545	1491	8542
1.1	7028	6657	5188	6558	1972	5689	1283	8730	1274	8784	1274	8784
1.3	6140	7046	4547	6921	1729	6004	1120	9240	1117	9269	1117	9270
1.5	5480	7626	4071	7466	1548	6476	1000	1000	1000	1000	1000	1000
1.7	4989	8422	3720	8219	1414	7130	9104	1104	9138	1101	9136	1101
1.9	4637	9500	3469	9236	1319	8010	8462	1246	8521	1237	8517	1237
2.1	4406	1096	3311	1061	1258	9201	8039	1437	8133	1421	8129	1421
2.3	4274	1336	3250	1252	1234	1085	7799	1751	7983	1677	7974	1676
2.5	4358	1598	3315	1531	1258	1326	7953	2095	8143	2050	8129	2048
2.7	4680	2083	3601	1978	1364	1712	8540	2732	8846	2650	8812	2643
2.9	5675	3068	4509	2859	1689	2462	1036	4023	1108	3830	1091	3802
3.1	1235	8109	12	12	4394	5036	2254	1063	9	9	2839	7776

TABLE(1.1)

Solutions of the differential equation describing the temperature distribution on a thin spherical shell for $S = 12$. Right hand side of the table contains the solutions 'normalised' to a value of 1000 at $\phi = 1.5$.

ϕ	Langer		Conic		Asymptotic		Langer 'Normalised'		Conic 'Normalised'		Asymptotic 'Normalised'	
	$\frac{\phi}{\sin\phi} K_0$	$\frac{\phi}{\sin\phi} I_0$	$Q_{-\frac{1}{2}+iq}$	$P_{-\frac{1}{2}+iq}$	$e^{-s\phi} f(\phi)$	$e^{+s\phi} g(\phi)$						
.05	1006 -3	2050 -3	1006 -3	7004	9511 -3	6524 -4	2612 2	5065 -2	2336 2	1122 -1	5534	
.1	1023 -3	1374 -3	1023 -3	4795	6030 -3	1381 -3	1750 2	5150 -2	1599 2	7112 -2	1171	
.3	1221 -3	4901 -4	1214 -3	1738	5079 -3	6567 -4	6245 1	6113 -2	5797 1	5990 -2	5570	
.5	1681 -3	2182 -4	1654 -3	7832 -1	6833 -3	3044 -4	2780 1	8330 -2	2613 1	8059 -2	2582	
.7	2549 -3	1050 -4	2480 -3	3814 -1	1038 -2	1495 -4	1338 1	1249 -1	1278 1	1225 -1	1268	
.9	4118 -3	5280 -5	3957 -3	1940 -1	1674 -2	7627 -5	6728	1993 -1	6470	1975 -1	6469	
1.1	6936 -3	2734 -5	6584 -3	1017 -1	2801 -2	4003 -5	3484	3316 -1	3393	3304 -1	3394	
1.3	1204 -2	1450 -5	1130 -2	5464 -2	4818 -2	2150 -5	1848	5689 -1	1822	5684 -1	1823	
1.5	2144 -2	7848 -6	1985 -2	2998 -2	8477 -2	1179 -5	1000	1000	1000	1000	1000	
.05	1373 -3	1023 -3	6230 4	1023 -3	1938 -3	8546 -3	7625 -4	2082 4	7945 -4	1523 4	1086	
.1	7783 -4	1093 -3	3567 4	1092 -3	1380 -3	6952 -3	8152 -4	1192 4	8485 -4	1084 4	8832	
.3	1469 -4	2004 -3	6798 3	1994 -3	2855 -4	1181 -2	1494 -3	2272 3	1549 -3	2244 3	1500	
.5	3546 -5	4983 -3	1650 3	4928 -3	6991 -5	2981 -2	3716 -3	5515 2	3829 -3	5494 2	3787	
.7	9302 -6	1401 -2	4353 2	1378 -2	1849 -5	8393 -2	1044 -2	1455 2	1070 -2	1453 2	1066	
.9	2556 -6	4181 -2	1203 2	4087 -2	5115 -6	2496 -1	3118 -2	4020 1	3175 -2	4020 1	3171	
1.1	7244 -7	1295 -1	3430 1	1258 -1	1459 -6	7691 -1	9655 -2	1146 1	9774 -2	1146 1	9770	
1.3	2103 -7	4120 -1	1002 1	3979 -1	4263 -7	2433	3072 -1	3349	3091 -1	3350	3091	
1.5	6239 -8	1341	2992	1287	1272 -7	7872	1000	1000	1000	1000	1000	

TABLES (1.2 - 3)

Solutions of the differential equation describing the temperature distribution on a thin spherical shell for $S = 3$ (upper table) and $S = 6$ (lower).
The right hand side of the table contains the solutions 'normalised' to a value of 1000 at $\phi = 1.5$.

almost one hour to determine each value at the extremities of the angle shown in the tables. The time required is such a severe limitation that it makes this form of solution impractical for further work.

The "classical" Asymptotic solution was, obviously, easy and quick to compute. The values obtained compare favourably with those from the other two methods of solution except near the apex of the sphere. It would appear that this solution is not suitable for small values of ϕ but very suitable for the remainder of the shell. Unfortunately, we do wish to investigate the stress resultants in the vicinity of small openings and therefore this very attractive form of solution is also unsuitable.

The Langer Asymptotic solution agrees well with the Conic Function solution, particularly near the origin. It has already been demonstrated that the Langer solution approximates to the solution for a flat plate in that region. It is, however, noticed that for small values of the parameter S the Langer solutions near the values of $\phi = \frac{\pi}{2}$ are not in so good agreement with the Conic Function solutions as are the "classical" Asymptotic solutions.

Since we are particularly interested in conditions near the origin, it would appear that the most "suitable" expression for the temperature distribution is the Langer Asymptotic solution, namely, equation (1.17)

1.3 Heat Transfer due to Conduction Only

If there is no loss of heat from the surfaces of the shell due to convection or radiation, then the heat transfer coefficient, m , defined in the relationship (1.2) is zero. The equations, for each of the three shell forms considered, will reduce in each case to Laplace's Equation in the appropriate co-ordinate system.

The problem of heat transfer due to conduction alone is important since it describes exactly conditions in an insulated body.

When the equation (1.6) for the spherical shell with an axisymmetric temperature distribution is modified to include $m = 0$ it becomes

$$\frac{d}{d\phi} \sin\phi \frac{dt}{d\phi} = 0 \tag{1.19}$$

If we integrate once we find

$$t' = \frac{dt}{d\phi} = \frac{C}{\sin\phi} \tag{1.20}$$

and if we integrate a second time

$$t = C \ln(\operatorname{cosec}\phi - \cot\phi) + D \tag{1.21}$$

where, as before, C and D are the constants of integration.

These constants may be found by inserting the boundary

$$\begin{aligned} t = T & \quad \text{at } \phi = \phi_1 & \quad \text{and} \\ t = T_2 & \quad \text{at } \phi = \phi_2 \end{aligned} \tag{1.22}$$

in equation (1.21) whence

$$\begin{aligned} T &= C \ln(\operatorname{cosec}\phi_1 - \cot\phi_1) + D \\ T_2 &= C \ln(\operatorname{cosec}\phi_2 - \cot\phi_2) + D \end{aligned}$$

and/

and solving these two equations

$$C = \frac{T - T_2}{\ln \frac{\operatorname{cosec} \phi_1 - \cot \phi_1}{\operatorname{cosec} \phi_2 - \cot \phi_2}}$$

$$D = \frac{(T_2 - T) \ln (\operatorname{cosec} \phi_2 - \cot \phi_2)}{\ln \frac{\operatorname{cosec} \phi_1 - \cot \phi_1}{\operatorname{cosec} \phi_2 - \cot \phi_2}}$$

1.23

Examination of equation (1.19) reveals that for small values of the angle ϕ , where $\cos \phi \approx 1$, the equation reduces to that of the flat plate whereas for large values of ϕ where $\sin \phi \approx 1$ the equation becomes that of the cylinder.

1.4 General Comment on and Conclusions about
Axisymmetric Temperature Distribution in
Spherical Shells

Let us as an example consider the particular case of a spherical shell which has the following boundary conditions

$$\begin{aligned}t &= T \quad \text{at} \quad \phi = 0.1 \\t &= 0 \quad \text{at} \quad \phi = 1.5\end{aligned}$$

Let us find the temperature distributions corresponding to the following values of the parameter S ;

$$S = 0, 1, 3, 5 \text{ and } 10.$$

It has been already demonstrated that the most suitable form of expression of the temperature distribution is

$$t = (\phi/\sin\phi)^{\frac{1}{2}} [A I_0(S\phi) + B K_0(S\phi)]$$

which result was obtained by the use of the Langer Asymptotic Equation.

Taking each of the values of S in turn and substituting in the boundary conditions the constants A and B are easily evaluated and thus the temperature can be computed for discrete values of ϕ in the range $0.1 \leq \phi \leq 1.5$. This can be repeated for all the values of S except for $S = 0$, the heat conduction case, where we must use, in the same manner as described above, the equation (1.21)

$$t = C \ln(\operatorname{cosec} \phi - \cot \phi) + D$$

for the temperature distribution.

These computations have been performed and the results are presented in Figure (1. 2)

It/

BOUNDARY CONDITIONS

TEMPERATURE, $t = T$ AT $\phi = 0.1$
 $t = 0$ AT $\phi = 1.5$

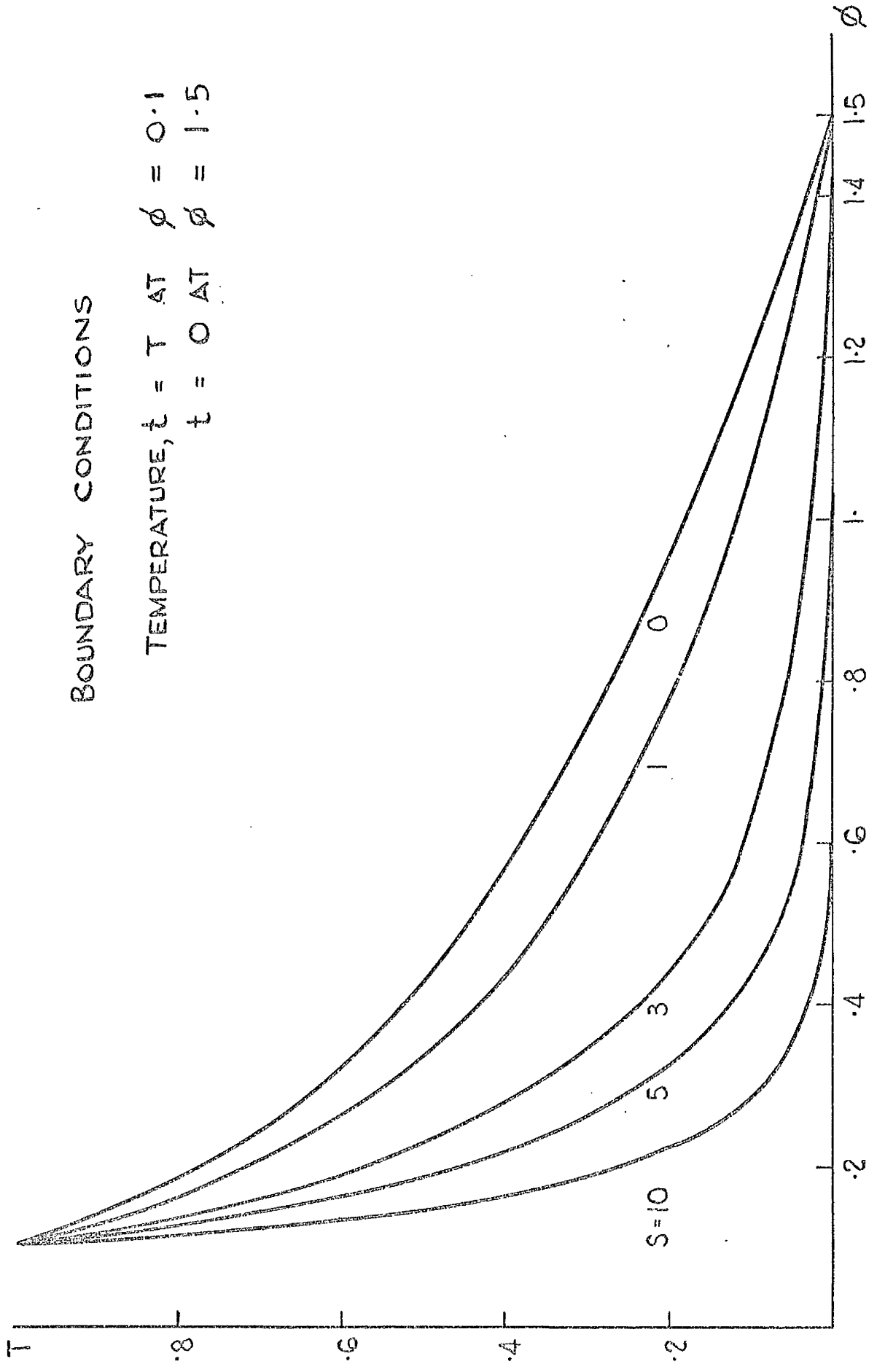


FIGURE (1.2) THE THEORETICAL TEMPERATURE DISTRIBUTION IN A SPHERICAL SHELL FOR VARIOUS VALUES ON THE PARAMETER S.

It is observed from this graph that for $S = 0$ and l that there are non-zero temperature gradients at $\phi = 1.5$. For all other values of S the temperature has died out before the outer boundary has been reached with the greater the value of S the quicker the die out. This of course is shown in the computation where it is found that the constant A , associated with the I_0 term, is also zero for these larger values of S . This prompts us to examine the form of these Modified Bessel Functions I_0 and K_0 . We can see from Figure (1.3) that the function K_0 is particularly associated with the inner boundary $\phi = \phi_1$, where we have the temperature T . Further, if the temperature dies out before the outer boundary is reached, then the constant A must be zero and the equation (1.17) is then reduced to

$$t = \left(\frac{\phi}{\sin \phi} \right)^{\frac{1}{2}} B K_0(S\phi) \quad 1.24$$

Thus, depending on the value of S and the angle between the two boundaries, we can use this simpler expression for the temperature and in the particular example which we are considering it appears to be true for values of $S \geq 3$. It will be demonstrated, in the experimental section, that where there is convection present usually $S \gg 3$.

The temperature distribution curve for $S = 0$ is noticed to be almost linear for values of $\phi > 1.0$. This, however, is only to be expected since, from equation (1.20)

$$t = \frac{c}{\sin \phi}$$

and we have already observed that the corresponding temperature in a cylindrical shell would be linear.

This/

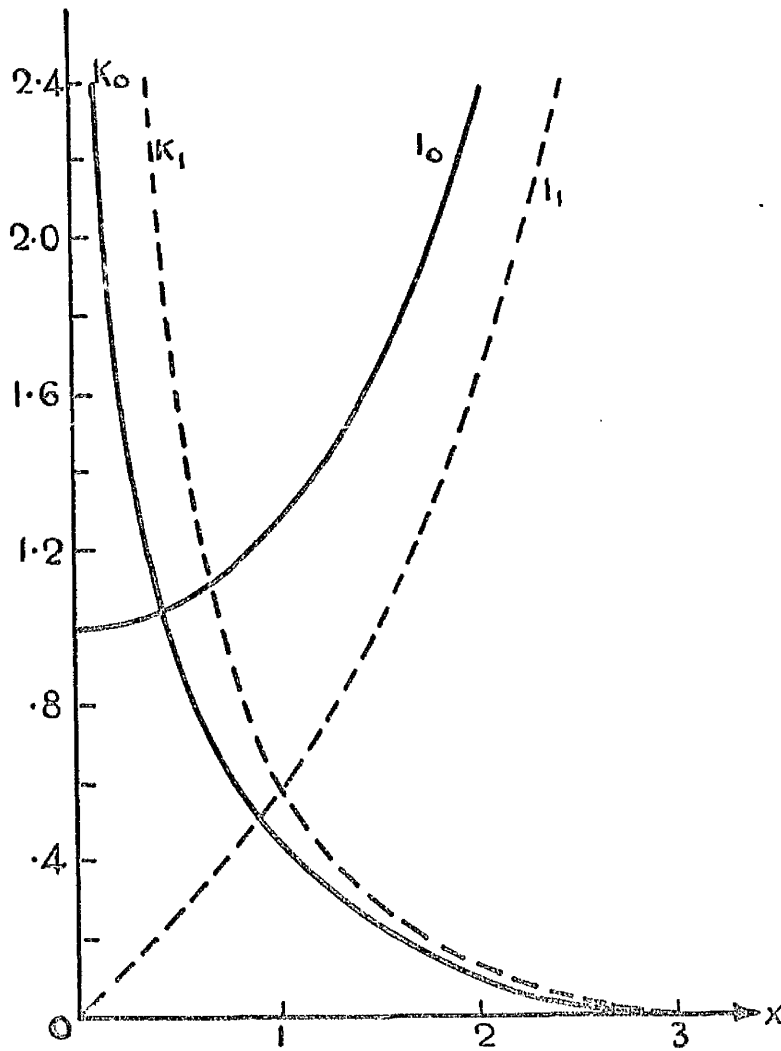


FIGURE (1.3) THE MODIFIED BESSEL FUNCTIONS $I_0(x)$, $K_0(x)$, $I_1(x)$ AND $K_1(x)$

This observation of the linear temperature distribution is important since it has been shown by DEN HARTOG⁽⁵⁰⁾ that such a temperature distribution in cylindrical shells causes zero stress resultants.

Conclusions

Expressions for the symmetric temperature distribution have been derived for a spherical shell which has conductivity within the thickness of the shell and heat convection and radiation at the surfaces. The convective heat loss from an element of area is assumed to be proportional to the temperature at the element as is the radiant heat loss.

The solution which appears most satisfactory for ease of computation, is that obtained by using the Langer asymptotic expansion form for the basic heat equation. This solution

$$t = \left(\frac{\phi}{\sin\phi}\right)^{\frac{1}{2}} [AI_0(s\phi) + BK_0(s\phi)]$$

agrees reasonably with the analytic solution and with the solutions for the flat plate and the cylinder over these regions of the sphere which approximate to these configurations. This therefore is the form of the solution which will be used in the subsequent investigation.

Where the temperature gradient reduces to zero on the shell the simplified form of the solution

$$t = \left(\frac{\phi}{\sin\phi}\right)^{\frac{1}{2}} BK_0(s\phi)$$

may be used.

If there is no convection loss from the surface of the shell, $S = 0$ and the temperature is then given by

$$t = C \ln(\operatorname{cosec}\phi - \cot\phi) + D$$

where the temperature gradient could never be zero since no heat is lost at the surfaces. For this particular case one would always require two boundary conditions to evaluate the temperature equation.

1.5 A Slowly Varying Line of Heat Around a Spherical Shell

We shall now extend the scope of the present chapter to include the unsymmetric problem of a slowly varying line of heat around a spherical shell. That is for some specific value of the angle ϕ , say $\phi = \phi_1$, we have a temperature distribution which can be defined as $T_n(\Theta)$. The small suffix n is used to avoid any confusion with the problem, for which we have developed a solution, of a uniform line of temperature around a spherical shell.

Let us impose a limitation to the argument and propose that this line of heat is in the central portion of the shell where it can be assumed that

$$\sin \phi \approx 1.$$

The unsymmetric temperature distribution on a spherical shell is, from equation (1.3), given by

$$\frac{1}{\sin \phi} \frac{\partial}{\partial \phi} \sin \phi \frac{\partial t}{\partial \phi} + \frac{1}{\sin^2 \phi} \frac{\partial^2 t}{\partial \Theta^2} = S^2 t.$$

For the central portion of the sphere, where it can be assumed that

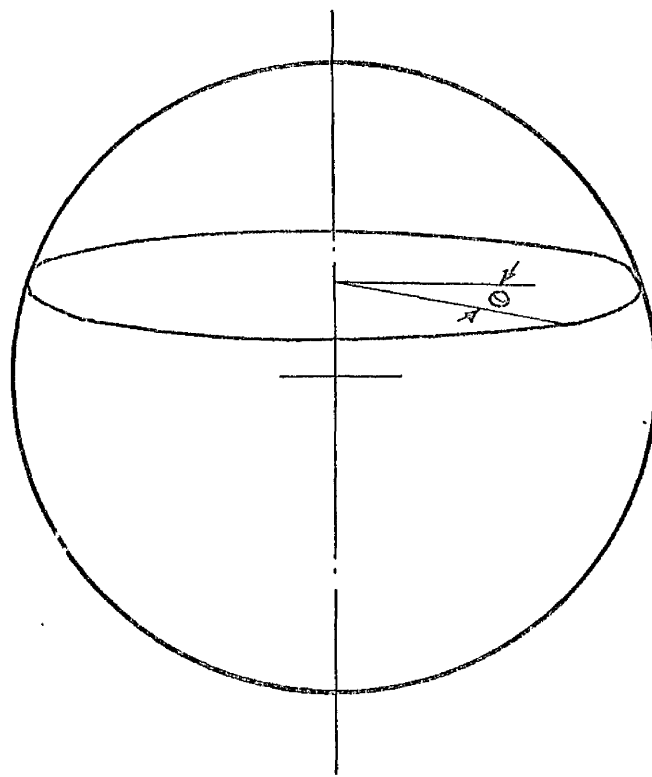
$\sin \phi \approx 1$, this equation reduces to

$$\frac{\partial^2 t}{\partial \phi^2} + \frac{\partial^2 t}{\partial \Theta^2} = S^2 t. \quad 1.25$$

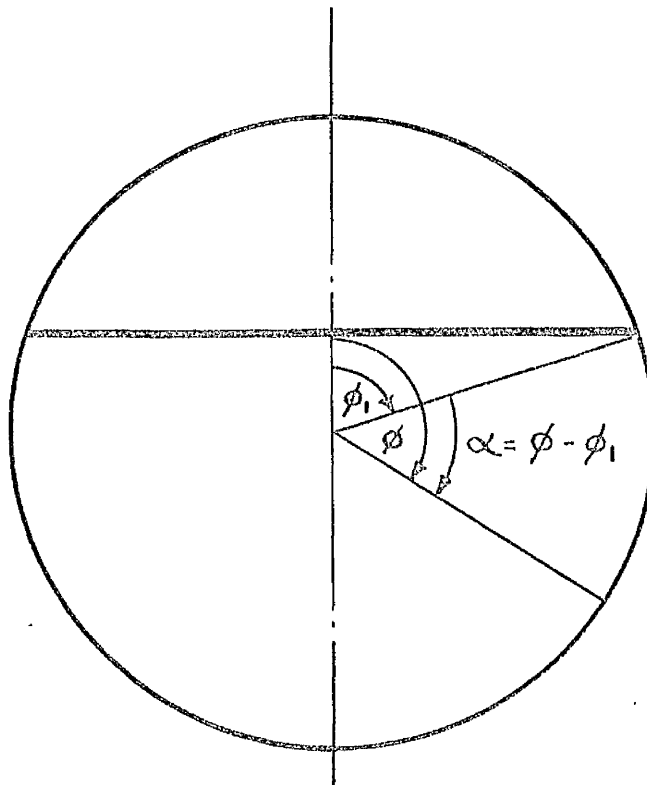
It is possible to change the reference for the co-ordinate system from the pole, where $\phi = 0$, by defining an angle α , measured from the line of heat, such that

$$\alpha = \phi - \phi_1$$

This is shown in Figure (1.4) Equation (1.25) can now be written/



LINE OF SLOWLY
VARYING TEMPERATURE
 $t = T_n(\theta)$



NEW PLANE OF
REFERENCE OF THE
CO-LATITUDINAL ANGLE

FIGURE (1.4) CHANGE OF CO-ORDINATE SYSTEM FOR A
LINE OF SLOWLY VARYING TEMPERATURE
ROUND A SPHERICAL SHELL

written as

$$\frac{\partial^2 t}{\partial \alpha^2} + \frac{\partial^2 t}{\partial \theta^2} = S^2 t \quad 1.26$$

Let us suppose that the variation of temperature with Θ is slow. Propose

$$\omega = \epsilon \Theta \quad 1.27$$

where ϵ is some small constant. This implies

$$t = t(\alpha, \omega)$$

and gives

$$\frac{\partial t}{\partial \theta} = \epsilon \frac{\partial t}{\partial \omega}$$

Let us express the temperature in the series form

$$t(\alpha, \omega) = t_0(\alpha, \omega) + \epsilon^2 t_1(\alpha, \omega) + \epsilon^4 t_2(\alpha, \omega) + \dots \quad 1.28$$

and substitute this series for t in equation (1.26) to find

$$\begin{aligned} \frac{\partial^2 t_0}{\partial \alpha^2} + \epsilon^2 \frac{\partial^2 t_1}{\partial \alpha^2} + \epsilon^4 \frac{\partial^2 t_2}{\partial \alpha^2} + \dots + \epsilon^2 \frac{\partial^2 t_0}{\partial \omega^2} + \epsilon^4 \frac{\partial^2 t_1}{\partial \omega^2} + \dots \\ = S^2 (t_0 + \epsilon^2 t_1 + \epsilon^4 t_2 + \dots) \end{aligned}$$

Regarding this expression as a series in ascending powers of ϵ we can equate the coefficients of $\epsilon^0, \epsilon^2, \epsilon^4$ etc. to zero and thereby obtain an infinite set of equations. Since, however, ϵ is small, let us examine the first two equations of the set. They are

$$\begin{aligned} \frac{\partial^2 t_0}{\partial \alpha^2} &= S^2 t_0 \\ \frac{\partial^2 t_1}{\partial \alpha^2} + \frac{\partial^2 t_0}{\partial \omega^2} &= S^2 t_1 \end{aligned} \quad 1.29-30$$

From the first of these equations the expression for t_0 is found to be

$$t_0 = A_0(\omega) e^{-s\alpha}$$

when we are considering the particular case of the temperature decreasing with angle α . Equation (1.30) then becomes

$$\frac{\partial^2 t_1}{\partial \alpha^2} + e^{-s\alpha} \frac{\partial^2 A_0}{\partial \omega^2} = s^2 t_1,$$

which has the solution

$$t_1 = A_1(\omega) e^{-s\alpha} + \frac{1}{2s} \frac{\partial^2 A_0}{\partial \omega^2} \alpha e^{-s\alpha}$$

Thus if we consider only the first two terms in the set the series solution of equation (1.26) is

$$t = A_0 e^{-s\alpha} + \varepsilon^2 \left(A_1 e^{-s\alpha} + \frac{1}{2s} \frac{\partial^2 A_0}{\partial \omega^2} \alpha e^{-s\alpha} \right). \quad 1.31$$

If the constant ε is sufficiently small that we can neglect the terms involving ε^2 then this expression reduces to

$$t = A_0 e^{-s\alpha} + \frac{1}{2s} \frac{\partial^2 A_0}{\partial \omega^2} \alpha e^{-s\alpha} \quad 1.32$$

Let us now postulate the boundary condition that

$$t = T_n(\Theta) \text{ at } \alpha = 0$$

where $T_n(\Theta)$ varies slowly with the angle Θ . Substitute this condition in equation (1.32). We have therefore that

$$A_0(\omega) = T_n(\Theta)$$

so that we may rewrite equation (1.32) as

$$t = T_n e^{-s\alpha} + \frac{1}{2s} \frac{\partial^2 T_n}{\partial \Theta^2} \alpha e^{-s\alpha} \quad 1.33$$

Since T_n varies slowly with Θ then $\frac{\partial^2 T_n}{\partial \Theta^2}$ must be of small magnitude. Because of this and since S is a reasonably large number, then it would appear to be a satisfactory approximation to drop the second term in equation (1.33) so that the temperature distribution can be expressed as

$$t = T_n(\Theta) e^{-S\alpha} \quad \dots \quad 1.34$$

This agrees, in the limit, where $T_n(\Theta) = T$ with the result which we have already obtained for a uniform line of heat around the shell.

The result obtained in equation (1.34) has practical significance since there are many situations in which it is possible for the temperature to vary slowly in one direction relative to the other, for example, where a flat plate meets the shell or at the junction of a skirt with a shell.

A result similar to this was obtained by BOUMA (34) for the stress resultants in a shallow shell due to a slowly varying edge load. BOUMA in his argument used an assumption of the type

$$t(\Theta, \phi) = t(\phi) A_n \cos n\Theta$$

where $A_n \cos n\Theta$ varies slowly with Θ , to describe his edge loading. We could have used this same assumption but the argument involves a more intuitive type of reasoning to produce the same final result.

CHAPTER 2

A GENERAL SOLUTION OF THE DIFFERENTIAL EQUATIONS
FOR THE STRESS RESULTANTS IN SPHERICAL SHELLS
SUBJECTED TO AXISYMMETRIC TEMPERATURE DISTRIBUTIONS

- 2.1 Solution of the Differential Equations .
- (a) The Differential Equations including Temperature Effects
 - (b) A Solution for the Complementary function
 - (c) The Particular Integral
- 2.2 The Spherical Shell with the Uniformly Heated Circular Opening

The well known differential equations for the stress resultants in a spherical shell of uniform thickness are extended to include the effects of temperature.

The particular integrals of these equations are found for the axisymmetric temperature distributions investigated in the previous Chapter. These particular integrals are added to known complementary function solutions to provide a general solution for the stress resultants in spherical shells.

The case of a uniformly heated circular opening, which is free of external constraints, is considered in detail. The effect of varying the shell and temperature parameters on the magnitudes of the stress resultants is investigated and the results are presented in graphical form.

2.1 Solution of the Differential Equations

The derivation of the differential equations for a spherical shell have occupied the attentions of a great number of researchers over a great number of years and indeed controversy still can be aroused over the order of accuracy of terms to be included or excluded. However, the form of the differential equations described in great detail by TIMOSHENKO⁽⁷⁾ and by FLÜGGE⁽¹⁵⁾ are now generally accepted. The author will develop the equations presented by FLÜGGE to include thermal effects. The sign conventions adopted by FLÜGGE (which are shown in Figures (2.1 - 2)) are maintained.

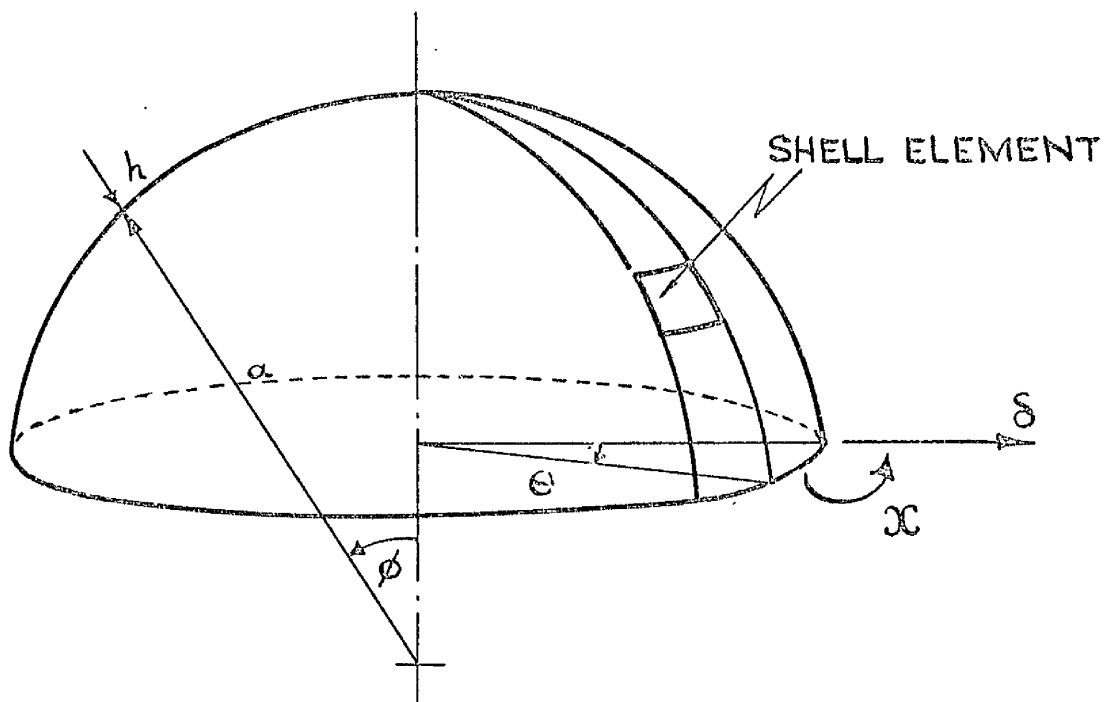
2.1(a) The Differential Equations including Temperature Effects

To include the effects of temperature in the equations as developed by FLÜGGE let us assume that the temperature variation through the shell thickness is linear and that it can be represented as

$$t(\theta, \phi, z) = \tau(\theta, \phi) + \frac{z}{h} \bar{\tau}(\theta, \phi) \quad 2.1$$

where, $\tau(\theta, \phi)$ is the average temperature over the thickness, $\bar{\tau}(\theta, \phi)$ is the temperature difference between the inner and the outer shell surfaces and Z is the distance out from the middle surface.

This /



ANGLE OF TANGENT ROTATION - θ
HORIZONTAL DISPLACEMENT - S

FIGURE 2.1. SPHERICAL SHELL

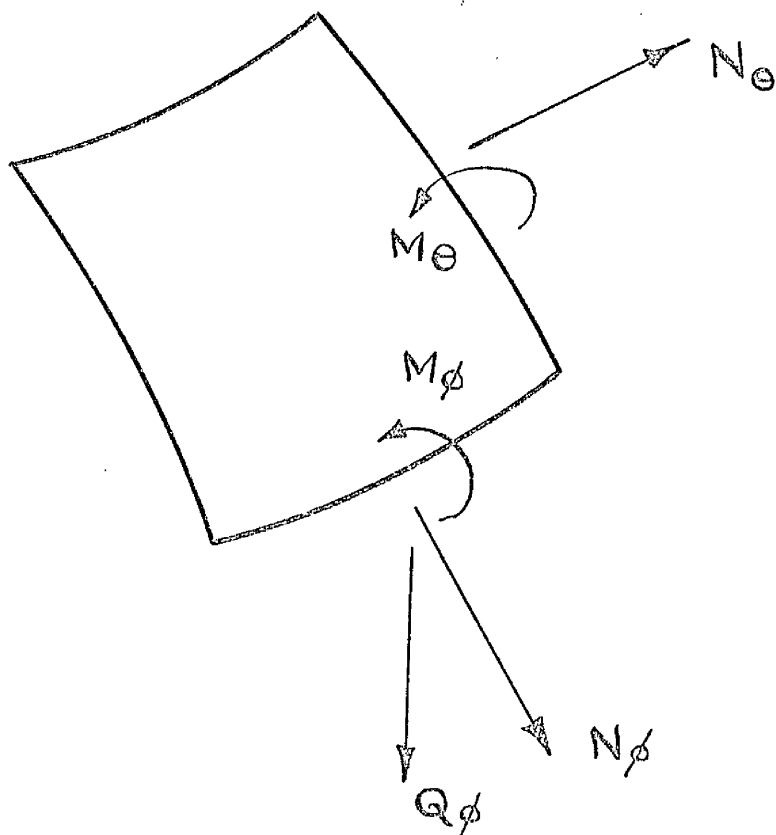


FIGURE (2.2.) STRESS RESULTANTS ON SHELL ELEMENT.

This heating of the shell will produce the strains

$$\varepsilon_{\theta} = \varepsilon_{\phi} = \alpha t + \frac{z}{h} \alpha \bar{t} , \quad \gamma_{\theta\phi} = 0 \quad 2.2$$

where α is the coefficient of thermal expansion of the material of the shell. Hooke's law must now be modified to include this thermal expansion and the problem is then reduced by expressing the stress resultants in terms of the tangent rotation χ and the transverse shear stress resultant Q_{ϕ} through the relationships

$$N_{\phi} = -Q_{\phi} \cot \phi$$

$$N_{\theta} = -Q_{\phi}$$

$$M_{\phi} = \frac{K}{\alpha} [\chi' + \nu \chi \cot \phi] - \frac{K}{h} (1 + \nu) \alpha \bar{t}$$

$$M_{\theta} = \frac{K}{\alpha} [\chi \cot \phi + \nu \chi'] - \frac{K}{h} (1 + \nu) \alpha \bar{t} \quad 2.3-6$$

The differential equations, in terms of these dependent variables, assume the form

$$L(\chi) - \nu \chi = \frac{\alpha^2}{K} Q_{\phi} + \frac{\alpha \alpha (1 + \nu)}{h} \bar{t}$$

$$L(Q_{\phi}) + \nu Q_{\phi} = -D(1 - \nu^2) \chi + D(1 - \nu^2) \alpha t'$$

when the operator L is introduced where

$$L(\dots) \equiv (\dots)'' + (\dots)' \cot \phi - (\dots) \cot^2 \phi \quad 2.7$$

The constants K and D are the bending and membrane stiffness of the shell respectively and are given by

$$K = \frac{Eh^3}{12(1 - \nu^2)} , \quad D = \frac{Eh}{1 - \nu^2}$$

The/

The two coupled equations above can be separated to obtain the two independent fourth order equations in ϕ and χ

$$L.L(Q\phi) - \nu^2 Q\phi = \frac{\alpha^2 D(1-\nu^2)}{K} Q\phi + D(1-\nu^2)\alpha \left[L(\bar{t}') - \nu \bar{t}' + \frac{1+\nu}{h} \alpha \bar{t}' \right]$$

$$L.L(\chi) - \nu^2 \chi = -\frac{\alpha^2 D(1-\nu^2)}{K} \chi + D(1-\nu^2)\alpha \left[\frac{\alpha^2 \bar{t}'}{K} + \frac{\alpha}{Dh(1-\nu)} [L(\bar{t}') - \nu \bar{t}'] \right]$$

which can be rewritten in the form

$$L.L(Q\phi) + 4\alpha^4 Q\phi = D(1-\nu^2)\alpha [L(\bar{t}') - \nu \bar{t}'] - \frac{D}{h} (1-\nu^2)(1+\nu)\alpha \alpha \bar{t}'$$

$$L.L(\chi) + 4\alpha^4 \chi = \frac{D}{K} (1-\nu^2)\alpha^2 \alpha \bar{t}' + \frac{\alpha \alpha (1+\nu)}{h} [L(\bar{t}') - \nu \bar{t}']$$

2.8-9

where

$$4\alpha^4 = \frac{D}{K} (1-\nu^2)\alpha^2 - \nu^2 \simeq 12(1-\nu^2)\frac{\alpha^2}{h^2}$$

2.10

The fully expanded form of the equation (2.8)

when the temperature effect is zero, is

$$\frac{d^4 Q\phi}{d\phi^4} + \frac{2\cos\phi}{\sin\phi} \frac{d^3 Q\phi}{d\phi^3} - \frac{3-\sin^2\phi}{\sin^2\phi} \frac{d^2 Q\phi}{d\phi^2} + \frac{\cos\phi(3+2\sin^2\phi)}{\sin^3\phi} \frac{dQ\phi}{d\phi}$$

$$+ \left[(1-\nu^2)\left(1 + \frac{12\alpha^2}{h^2}\right) - \frac{3}{\sin^2\phi} \right] Q\phi = 0$$

2.11

This equation was derived by H. REISSNER⁽¹⁶⁾ in 1912.

The equations (vi, vii) are similar to the equations (vi - vii) which were derived from the work of MEISSNER⁽¹²⁾.

2.1(b) A Solution for the Complementary Function

Many solutions for H.REISSNER'S differential equation for the stress resultant Q_ϕ have been proposed. These range from analytic solutions in terms of hypergeometric functions or Legendre polynomials, with of course poor convergence, to approximate solutions usually valid for only a particular portion of the sphere. A detailed description and critical review of these various solutions is undertaken by TOOTH⁽²⁸⁾.

An asymptotic solution, which is valid for all values of the angle ϕ is

$$Q_\phi = \left(\frac{\phi}{\sin\phi}\right)^{\frac{1}{2}} (A_1 \text{ber}'\sqrt{2}\alpha\phi + A_2 \text{bei}'\sqrt{2}\alpha\phi + A_3 \text{ker}'\sqrt{2}\alpha\phi + A_4 \text{kei}'\sqrt{2}\alpha\phi) \quad 2.12$$

This result was presented by LECKIE⁽²⁶⁾. It is obtained by using the method of asymptotic integration developed by LANGER⁽²⁷⁾.

This method is described in detail in Chapter I where it was used to find the temperature distribution on a spherical shell.

The solution, equation (2.12), has also been obtained by GALLETLY⁽⁴⁶⁾ using a different approach.

It is proposed to use this solution as our complementary function in the ensuing investigation into the thermal stresses on a spherical shell. There now remains the problem of finding appropriate particular integrals and hence a general solution of the problem.

The Particular Integral

Consider the action of the $L (\dots)$ operator on the temperature gradient. It gives

$$\begin{aligned} L(t') &\equiv t''' + t'' \cot \phi - t' \cot^2 \phi \\ &= (t'' + t' \cot \phi)' + t' \end{aligned}$$

The equation (1.7) for the temperature distribution is

$$t'' + t' \cot \phi = S^2 t$$

which gives

$$L(t') = t' (S^2 + 1)$$

Substituting this value for $L(t')$ into equation (2.8)

we find

$$L.L(Q_\phi) + 4\alpha^4 Q_\phi = D(1-\nu^2)\alpha(S^2 + 1 - \nu)t' \tag{2.13}$$

Propose a particular integral for this equation of the form

$$Q_\phi = At'$$

where, as usual, A is a constant and substitute this expression for Q_ϕ back into equation (2.13) to yield

$$A[(S^2 + 1)^2 t' + 4\alpha^4 t'] = D(1-\nu^2)\alpha(S^2 + 1 - \nu)t'$$

whence

$$A = \frac{D(1-\nu^2)\alpha(S^2 + 1 - \nu)}{(S^2 + 1)^2 + 4\alpha^4} \tag{2.14}$$

It is observed that for the particular case where $S = 0$, that is no heat loss due to convection, the value of A becomes

$$A = \frac{D(1-\nu^2)\alpha(1-\nu)}{4\alpha^4}$$

It should be observed that whereas it requires, in the many cases where the temperature gradient becomes zero on the surface of the shell, only one boundary condition to define the constant A, the conduction only case requires a thermal gradient at some outer boundary and hence there will be resulting boundary effects to be considered at that boundary.

For the general case, the general solution for the stress resultant, Q_ϕ , on a spherical shell, due to an axisymmetric temperature distribution and subject to the heat transfer laws which have been postulated, is

$$Q_\phi = \left(\frac{\phi}{\sin\phi}\right)^{\frac{1}{2}} (A_1 \text{ber}'\sqrt{2\alpha}\phi + A_2 \text{bei}'\sqrt{2\alpha}\phi + A_3 \text{ker}'\sqrt{2\alpha}\phi + A_4 \text{kei}'\sqrt{2\alpha}\phi) + A t \quad 2.15$$

where the constant A is defined in equation (2.14)

Using this value for Q_ϕ we can now substitute back into the linking equations (2.8 - 9) and obtain the corresponding expressions for the stress resultants and the displacements as :

$$N_\phi = -\cot\phi \left(\frac{\phi}{\sin\phi}\right)^{\frac{1}{2}} (A_1 \text{ber}'z + A_2 \text{bei}'z + A_3 \text{ker}'z + A_4 \text{kei}'z) - A \cot\phi \cdot t$$

$$N_\theta = \sqrt{2\alpha} \left(\frac{\phi}{\sin\phi}\right)^{\frac{1}{2}} \left\{ A_1 \left[\text{bei}z + \frac{1}{2\sqrt{2\alpha}} \left(\frac{1}{\phi} + \cot\phi\right) \text{ber}'z \right] \right. \\ - A_2 \left[\text{ber}z - \frac{1}{2\sqrt{2\alpha}} \left(\frac{1}{\phi} + \cot\phi\right) \text{bei}'z \right] \\ + A_3 \left[\text{kei}z + \frac{1}{2\sqrt{2\alpha}} \left(\frac{1}{\phi} + \cot\phi\right) \text{ker}'z \right] \\ \left. - A_4 \left[\text{ker}z - \frac{1}{2\sqrt{2\alpha}} \left(\frac{1}{\phi} + \cot\phi\right) \text{kei}'z \right] \right\} \\ + A (t \cot\phi - s^2 t)$$

$$\chi = \frac{2\alpha^2}{D(1-\nu^2)} \left(\frac{\phi}{\sin\phi}\right)^{\frac{1}{2}} \left\{ A_1 \left[\text{bei}'z - \frac{\nu}{2\alpha^2} \text{ber}'z \right] - A_2 \left[\text{ber}'z + \frac{\nu}{2\alpha^2} \text{bei}'z \right] \right. \\ \left. + A_3 \left[\text{kei}'z - \frac{\nu}{2\alpha^2} \text{ker}'z \right] - A_4 \left[\text{ker}'z + \frac{\nu}{2\alpha^2} \text{kei}'z \right] \right\} \\ + \frac{4\alpha^4}{(s^2+1)^2 + 4\alpha^4} \cdot \alpha t$$

$$M_{\phi} = \frac{\alpha}{\sqrt{2}\alpha} \left(\frac{\phi}{\sin\phi}\right)^{\frac{1}{2}} \left\{ A_1 \left[\text{ber} Z - \frac{f_1}{2\sqrt{2}\alpha} \text{bei}' Z \right] + \frac{\nu}{2\alpha^2} \left(\text{bei} Z + \frac{f_1}{2\sqrt{2}\alpha} \text{ber}' Z \right) \right. \\ + A_2 \left[\left(\text{bei} Z + \frac{f_1}{2\sqrt{2}\alpha} \text{ber}' Z \right) - \frac{\nu}{2\alpha^2} \left(\text{ber} Z - \frac{f_1}{2\sqrt{2}\alpha} \text{bei}' Z \right) \right] \\ + A_3 \left[\left(\text{ker} Z - \frac{f_1}{2\sqrt{2}\alpha} \text{kei}' Z \right) + \frac{\nu}{2\alpha^2} \left(\text{kei} Z + \frac{f_1}{2\sqrt{2}\alpha} \text{ker}' Z \right) \right] \\ + A_4 \left[\left(\text{kei} Z + \frac{f_1}{2\sqrt{2}\alpha} \text{ker}' Z \right) - \frac{\nu}{2\alpha^2} \left(\text{ker} Z - \frac{f_1}{2\sqrt{2}\alpha} \text{kei}' Z \right) \right] \left. \right\} \\ + \frac{\alpha A}{(s^2+1-\nu)} [s^2 t - (1-\nu) \cot\phi \cdot t]$$

$$M_{\theta} = \frac{\nu\alpha}{\sqrt{2}\alpha} \left(\frac{\phi}{\sin\phi}\right)^{\frac{1}{2}} \left\{ A_1 \left[\left(\text{ber} Z - \frac{f_2}{2\sqrt{2}\alpha} \text{bei}' Z \right) + \frac{\nu}{2\alpha^2} \left(\text{bei} Z + \frac{f_2}{2\sqrt{2}\alpha} \text{ber}' Z \right) \right] \right. \\ + A_2 \left[\left(\text{bei} Z + \frac{f_2}{2\sqrt{2}\alpha} \text{ber}' Z \right) - \frac{\nu}{2\alpha^2} \left(\text{ber} Z - \frac{f_2}{2\sqrt{2}\alpha} \text{bei}' Z \right) \right] \\ + A_3 \left[\left(\text{ker} Z - \frac{f_2}{2\sqrt{2}\alpha} \text{kei}' Z \right) + \frac{\nu}{2\alpha^2} \left(\text{kei} Z + \frac{f_2}{2\sqrt{2}\alpha} \text{ker}' Z \right) \right] \\ + A_4 \left[\left(\text{kei} Z + \frac{f_2}{2\sqrt{2}\alpha} \text{ker}' Z \right) - \frac{\nu}{2\alpha^2} \left(\text{ker} Z - \frac{f_2}{2\sqrt{2}\alpha} \text{kei}' Z \right) \right] \left. \right\} \\ + \frac{\alpha A}{(s^2+1-\nu)} [(1-\nu)t \cot\phi + \nu s^2 t]$$

$$u_h = \frac{\alpha \sin\phi}{Eh} (N_{\theta} - \nu N_{\phi}) + \alpha \sin\phi \cdot \alpha t$$

2.16-21

where

$$Z = \sqrt{2}\alpha\phi$$

$$f_1 = \left[\frac{1}{\phi} + (1-2\nu) \cot\phi \right]$$

$$f_2 = \left[\frac{1}{\phi} + \left(1 - \frac{2\nu}{\nu}\right) \cot\phi \right]$$

$$A = \frac{D(1-\nu^2)\alpha(s^2+1-\nu)}{(s^2+1)^2 + 4\alpha^4}$$

and

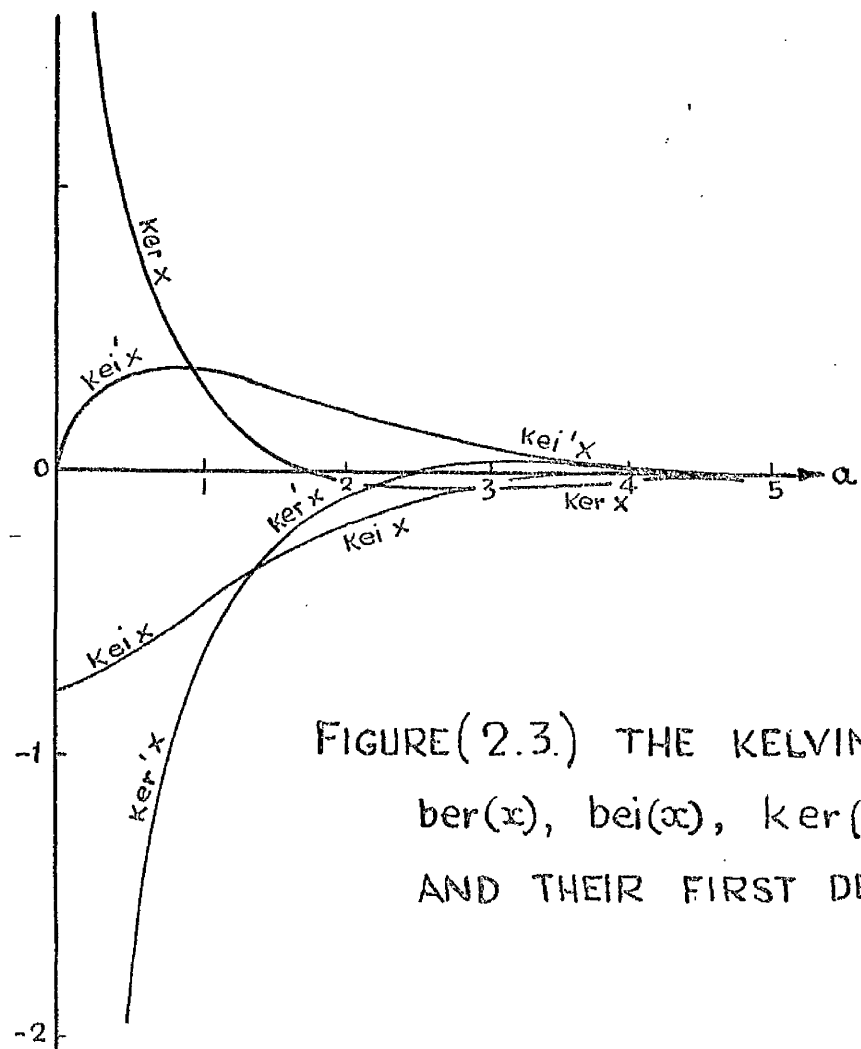
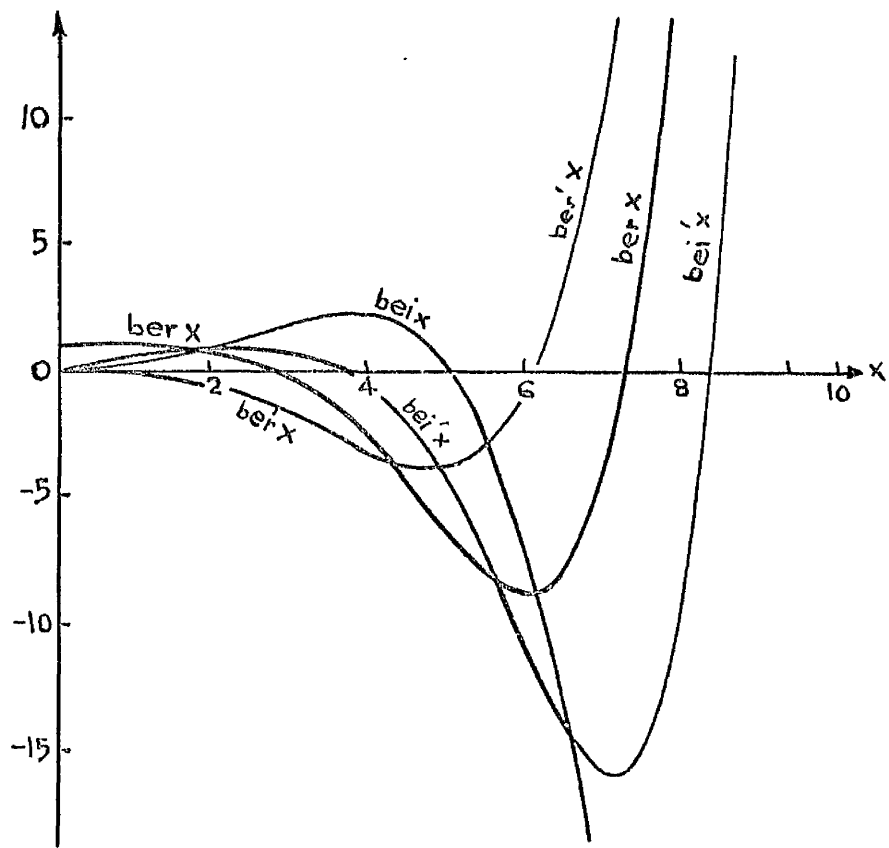
$$\text{ber}' Z = \frac{d}{dz} (\text{ber} Z)$$

etc.

These equations for the stress resultants and the displacements are somewhat involved. Simplification of various types are possible, however. The most obvious is the use of the usual approximations for the trigonometric functions in the region of the apex where ϕ is small and in the region of the equator where $\phi = \frac{\pi}{2}$. Another possibility is the use of the asymptotic forms of the Kelvin functions which are valid for arguments greater than 6. The various simplifications will be discussed in subsequent chapters as they become applicable.

The Kelvin functions found in equations (2.16-21) are of two distinct types. The ber-bei functions and their derivations represent waves which are zero or small at the origin but which increase rapidly with the argument; this can be easily observed in Figure (2.3). The converse is true for the ker-kei functions and their derivatives. Expressions involving the Kelvin functions therefore represent waves starting at the boundaries but decaying rapidly into the shell. The terms involving the ber-bei's, which in our case are the terms associated with the constants A_1 and A_2 , represent conditions at the outer boundary which die out rapidly into the shell, whereas the terms involving the ker-kei functions are associated with the inner boundary. It is possible therefore, in those problems where the temperature gradient is associated with one boundary but is zero before the other boundary is reached, to make the two appropriate integration constants zero.

The equations, which have been developed, can be applied to a number of specific problems. The first to be considered is that of the uniformly heated circular opening.



FIGURE(2.3.) THE KELVIN FUNCTIONS $ber(x)$, $bei(x)$, $ker(x)$, $kei(x)$ AND THEIR FIRST DERIVATIVES

2.2 The Spherical Shell with the Uniformly Heated Circular Opening

Consider a spherical shell which has an axisymmetric circular opening at $\phi = \phi_1$. Let this opening be free of external constraints and be heated to a constant temperature T . Further permit the temperature gradient, into the shell, away from this boundary, to become zero before some outer boundary is reached. Let us for such a shell as described above investigate the magnitude and the distribution of the stresses and the displacements.

The boundary conditions of the shell may be expressed as

$$\begin{aligned} N_{\phi_1} &= M_{\phi_1} = 0 \\ t_{\phi_1} &= T \end{aligned}$$

and for large values of the angle

$$t^{\cdot} = 0$$

This final condition allows us to discard the terms involving the constants A_1 and A_2 in equations (2.16-21).

The first two boundary conditions, in conjunction with equations (2.16) and (2.17), now give

$$\begin{aligned} N_{\phi_1} = 0 &= -\cot \phi_1 \left(\frac{\phi_1}{\sin \phi_1} \right)^{\frac{1}{2}} \left[A_3 \operatorname{ker}' Z_1 + A_4 \operatorname{kei}' Z_1 \right] - A \cot \phi_1 t_1^{\cdot} \\ M_{\phi_1} = 0 &= \frac{a}{\sqrt{2}\alpha} \left(\frac{\phi_1}{\sin \phi_1} \right)^{\frac{1}{2}} \left[A_3 \left\{ (\operatorname{ker} Z_1 - \frac{f_{11}}{2\sqrt{2}\alpha} \operatorname{kei}' Z_1) + \frac{\nu}{2\alpha^2} (\operatorname{kei} Z_1 + \frac{f_{11}}{2\sqrt{2}\alpha} \operatorname{ker}' Z_1) \right\} \right. \\ &\quad \left. + A_4 \left\{ (\operatorname{kei} Z_1 + \frac{f_{11}}{2\sqrt{2}\alpha} \operatorname{ker}' Z_1) + \frac{\nu}{2\alpha^2} (-\operatorname{ker} Z_1 + \frac{f_{11}}{2\sqrt{2}\alpha} \operatorname{kei}' Z_1) \right\} \right] \\ &\quad + \frac{aA}{s^2 + 1 - \nu} \left[(1 - \nu) t_1^{\cdot} \cot \phi_1 + \nu s^2 T \right] \end{aligned}$$

where, it is recalled,

$$A = \frac{E \alpha h (s^2 + 1 - \nu)}{(s^2 + 1)^2 + 4\alpha^4}$$

After introducing a new constant B such that

$$B = \frac{1}{E \alpha h} A = \frac{(s^2 + 1 - \nu)}{(s^2 + 1)^2 + 4\alpha^4} \quad 2.24$$

we can solve equations (2.22--23) for the constants A_3 and A_4 to find

$$A_3 = E h \alpha T B \left[\frac{-\frac{t_1}{T} J + \sqrt{2} \alpha k e^{i' z_1} \frac{s^2 - (1 - \nu) \cot \phi_1 \frac{t_1}{T}}{s^2 + 1 - \nu}}{I k e^{i' z_1} - J k e^{i' z_1}} \right] \left(\frac{\phi_1}{\sin \phi_1} \right)^{\frac{1}{2}}$$

$$A_4 = E h \alpha T B \left[\frac{-\sqrt{2} \alpha k e^{i' z_1} \frac{s^2 - (1 - \nu) \cot \phi_1 \frac{t_1}{T}}{s^2 + 1 - \nu} + \frac{t_1}{T} J}{I k e^{i' z_1} - J k e^{i' z_1}} \right] \left(\frac{\phi_1}{\sin \phi_1} \right)^{\frac{1}{2}}$$

where

$$I = \left[(k e^{i z_1} + \frac{f_{11}}{2\sqrt{2}\alpha} k e^{i' z_1}) + \frac{\nu}{2\alpha^2} (k e^{i z_1} - \frac{f_{11}}{2\sqrt{2}\alpha} k e^{i' z_1}) \right]$$

$$J = \left[(k e^{i z_1} - \frac{f_{11}}{2\sqrt{2}\alpha} k e^{i' z_1}) + \frac{\nu}{2\alpha^2} (k e^{i z_1} + \frac{f_{11}}{2\sqrt{2}\alpha} k e^{i' z_1}) \right]$$

For simplicity of expression let us introduce two further constants B_3 and B_4 such that

$$A_3 = E h \alpha T B_3$$

$$A_4 = E h \alpha T B_4$$

2.25-26

and of course these new constants B_3 and B_4 can be found from the appropriate expressions for A_3 and A_4 given above.

Since/

Since the temperature gradient becomes zero before an outer boundary is reached, we may write the temperature equation (1.37) as

$$t = \left(\frac{\phi}{\sin\phi}\right)^{\frac{1}{2}} F K_0(S\phi)$$

and using the boundary condition that $t_{\phi_1} = T$ we find the constant F to be

$$F = \frac{T \left(\frac{\phi_1}{\sin\phi_1}\right)^{-\frac{1}{2}}}{K_0(S\phi_1)}$$

The expression for the temperature in our problem is therefore

$$t = T \frac{\left(\frac{\phi}{\sin\phi}\right)^{\frac{1}{2}} K_0(S\phi)}{\left(\frac{\phi_1}{\sin\phi_1}\right)^{\frac{1}{2}} K_0(S\phi_1)} \quad 2.27$$

Using the well known properties of Bessel functions we can differentiate this expression to find t' , the temperature gradient, as

$$t' = \frac{T}{\left(\frac{\phi_1}{\sin\phi_1}\right)^{\frac{1}{2}} K_0(S\phi_1)} \left[\frac{1}{2} \left(\frac{\phi}{\sin\phi}\right)^{-\frac{1}{2}} \frac{\sin\phi - \phi \cos\phi}{\sin^2\phi} K_0(S\phi) - \left(\frac{\phi}{\sin\phi}\right)^{\frac{1}{2}} S K_1(S\phi) \right] \quad 2.28$$

The value of this gradient at the opening, when $\phi = \phi_1$, is then

$$t'_1 = T \left[\frac{\sin\phi_1 - \phi_1 \cos\phi_1}{2\phi_1 \sin\phi_1} - S \frac{K_1(S\phi_1)}{K_0(S\phi_1)} \right]$$

with which value we can evaluate the constants B_3 and B_4 .

The equations (2.16-21) for the stress resultants can now be computed for the effects into the shell for each particular opening value.

The results obtained can be expressed in terms of stresses. For the membrane stress resultants N_Θ and N_ϕ we need only divide the results by the thickness of the shell to obtain the actual membrane stresses $\sigma_{\Theta m}$ and $\sigma_{\phi m}$ where/

where the second subscript, m , indicates a membrane action. If in the case of the bending stress resultants we assume that the stress distribution is linear across the thickness of the section, then the relationship between these stress resultants and the maximum stresses at the surface are

$$M_{\theta} = \frac{h^2}{6} \sigma_{\theta b}$$

$$M_{\phi} = \frac{h^2}{6} \sigma_{\phi b}$$

where the subscript, b , indicates a bending action.

The expressions for the stress distribution in the problem which we have considered are therefore

$$\frac{\sigma_{\phi m}}{E \alpha T} = -\cot \phi \left(\frac{\phi}{\sin \phi} \right)^{\frac{1}{2}} (B_3 \operatorname{ker}' Z + B_4 \operatorname{kei}' Z) - B \cot \phi \cdot \frac{t}{T}$$

$$\frac{\sigma_{\theta m}}{E \alpha T} = \sqrt{2} \alpha \left(\frac{\phi}{\sin \phi} \right)^{\frac{1}{2}} \left[B_3 \left\{ \operatorname{ker} Z + \frac{1}{2\sqrt{2}\alpha} (\frac{1}{\phi} + \cot \phi) \operatorname{ker}' Z \right\} - B_4 \left\{ \operatorname{ker} Z - \frac{1}{2\sqrt{2}\alpha} (\frac{1}{\phi} + \cot \phi) \operatorname{kei}' Z \right\} \right] + B \left(\frac{t}{T} \cot \phi - s^2 \frac{t}{T} \right)$$

$$\frac{\chi}{\alpha T} = 2\alpha^2 \left(\frac{\phi}{\sin \phi} \right)^{\frac{1}{2}} \left[B_3 \left\{ \operatorname{ker}' Z - \frac{\nu}{2\alpha^2} \operatorname{ker}' Z \right\} - B_4 \left\{ \operatorname{ker}' Z + \frac{\nu}{2\alpha^2} \operatorname{kei}' Z \right\} \right] + \frac{4\alpha^4}{(s^2+1)^2 + 4\alpha^4} \cdot \frac{t}{T}$$

$$\frac{\sigma_{\phi m}}{E \alpha T} = \frac{6\alpha}{\sqrt{2}\alpha h} \left(\frac{\phi}{\sin \phi} \right)^{\frac{1}{2}} \left[B_3 \left\{ \left(\operatorname{ker} Z - \frac{f_1}{2\sqrt{2}\alpha} \operatorname{kei}' Z \right) + \frac{\nu}{2\alpha^2} \left(\operatorname{kei} Z + \frac{f_1}{2\sqrt{2}\alpha} \operatorname{ker}' Z \right) \right\} + B_4 \left\{ \left(\operatorname{kei} Z + \frac{f_1}{2\sqrt{2}\alpha} \operatorname{ker}' Z \right) - \frac{\nu}{2\alpha^2} \left(\operatorname{ker} Z - \frac{f_1}{2\sqrt{2}\alpha} \operatorname{kei}' Z \right) \right\} \right] + \frac{B}{s^2 + 1 - \nu} \left[s^2 \frac{t}{T} - (1-\nu) \cot \phi \frac{t}{T} \right]$$

$$\frac{\sigma_{\theta b}}{E \alpha T} = \frac{6\alpha \nu}{\sqrt{2}\alpha h} \left(\frac{\phi}{\sin \phi} \right)^{\frac{1}{2}} \left[B_3 \left\{ \left(\operatorname{ker} Z - \frac{f_2}{2\sqrt{2}\alpha} \operatorname{kei}' Z \right) + \frac{\nu}{2\alpha^2} \left(\operatorname{kei} Z + \frac{f_2}{2\sqrt{2}\alpha} \operatorname{ker}' Z \right) \right\} + B_4 \left\{ \left(\operatorname{kei} Z + \frac{f_2}{2\sqrt{2}\alpha} \operatorname{ker}' Z \right) - \frac{\nu}{2\alpha^2} \left(\operatorname{ker} Z - \frac{f_2}{2\sqrt{2}\alpha} \operatorname{kei}' Z \right) \right\} \right] + \frac{B}{(s^2+1-\nu)} \left[(1-\nu) \frac{t}{T} \cot \phi + \nu s^2 \frac{t}{T} \right]$$

$$\frac{u_h}{\alpha \sin \phi \cdot \alpha T} = \frac{1}{E} (\sigma_{\theta m} - \nu \sigma_{\phi m}) + \frac{t}{T}$$

where

$$B = \frac{s^2 + 1 - \nu}{(s^2+1)^2 + 4\alpha^4}$$

Let us now consider the graphical results which are presented. These results can be divided into two main types. They are:

- (1) the stresses and the displacements at the actual shell opening (these we shall call henceforth the opening values), and
- (2) the stresses and the displacements into the shell from a particular value of opening.

In both sets of results, it is assumed that the value of the temperature at the opening is T and that the temperature and the stress distribution terminate within the portion of the shell being investigated so that no outer boundary conditions need be considered.

Using the results of equations (2.29-34), a series of opening values has been computed for certain selected values of the shell parameters. These opening values are presented as full lines in Figures (2.4-10). From the same equations the stress distributions into the shell from certain selected values of opening were also computed. These results are presented as broken lines in the same figures and the value of the particular opening from which they emulate is found alongside each line. Details of the computation are given in Appendix 1.

The values of the shell parameter a/h selected for presentation are 30, 90 and 150. The reason for this choice is the popularity of these values in shell literature. These values cover a fair range of practical shell forms. The choice of values for the parameter S was more difficult. Consideration was given to/

to the shells which are discussed in the experimental section and it was felt that values of 6, 9 and 12 for S would adequately demonstrate the variations due to heat transfer effects.

The value of 0.255 for the Poisson's ratio was also chosen from experimental considerations. It is the value obtained for the mild steel of the experimental shell. Now let us examine in detail Figures (2.4 - 10) where some of these results are presented.

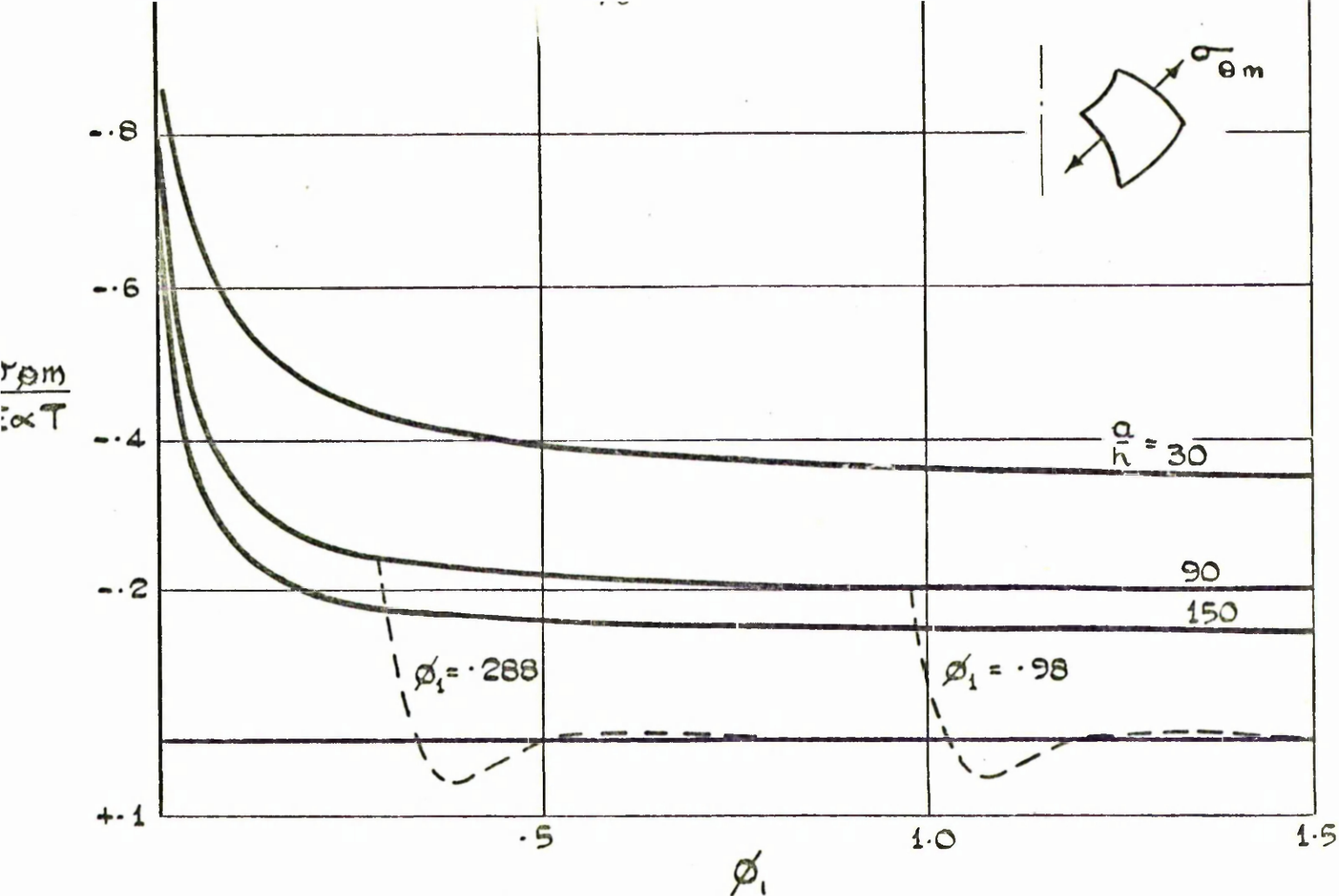


FIGURE (2.4) OPENING VALUES OF CIRCUMFERENTIAL MEMBRANE STRESS ($S=12, \nu=0.255$) THE STRESS DISTRIBUTION INTO A SHELL FROM A PARTICULAR OPENING VALUE IS SHOWN BY A BROKEN LINE.

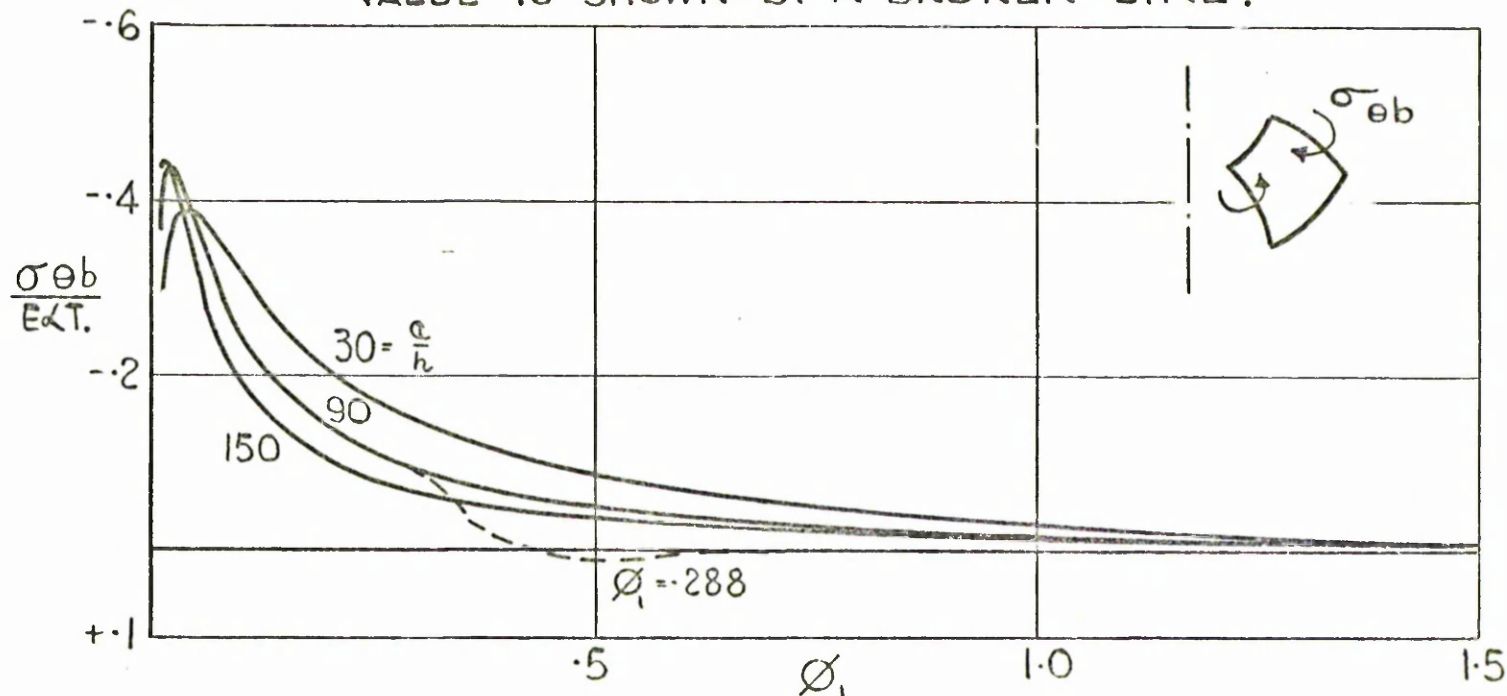


FIGURE (2.5) OPENING VALUES OF CIRCUMFERENTIAL BENDING STRESS ($S=12, \nu=0.255$)

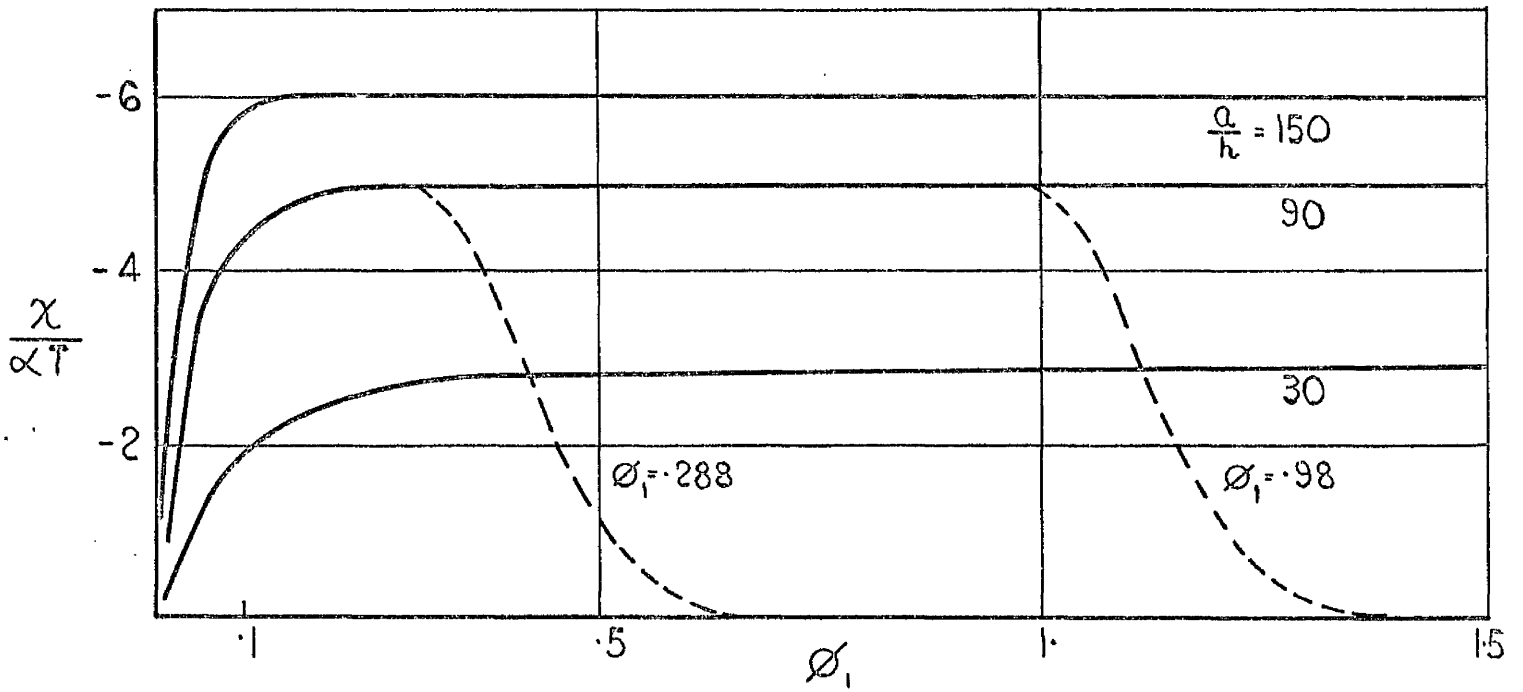


FIGURE (2.6) THE TANGENT ROTATION AT THE OPENING ($S = 12$, $V = 0.255$)

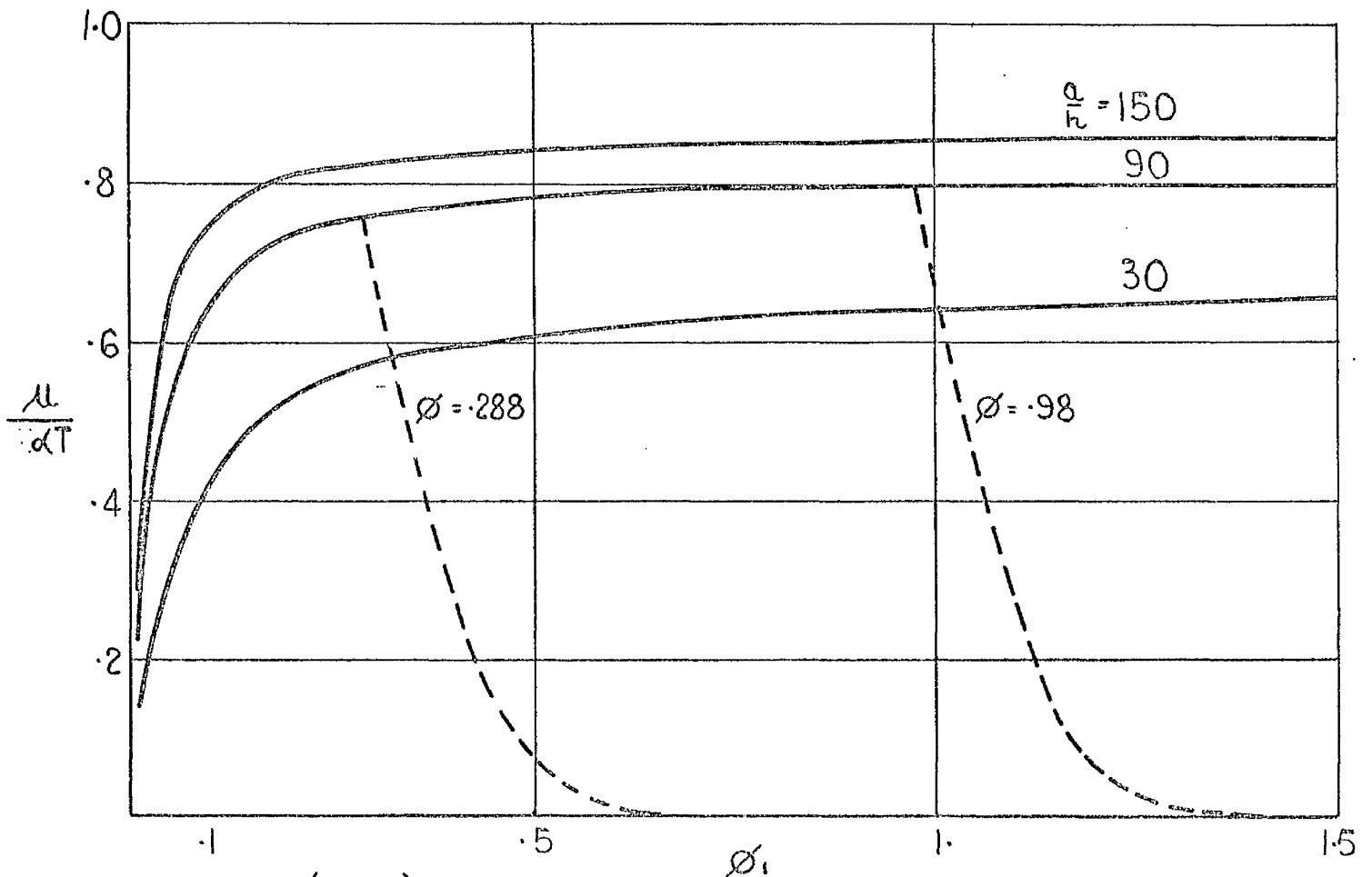


FIGURE (2.7) THE HORIZONTAL DISPLACEMENT OF THE OPENING. ($S = 12$, $V = 0.255$)

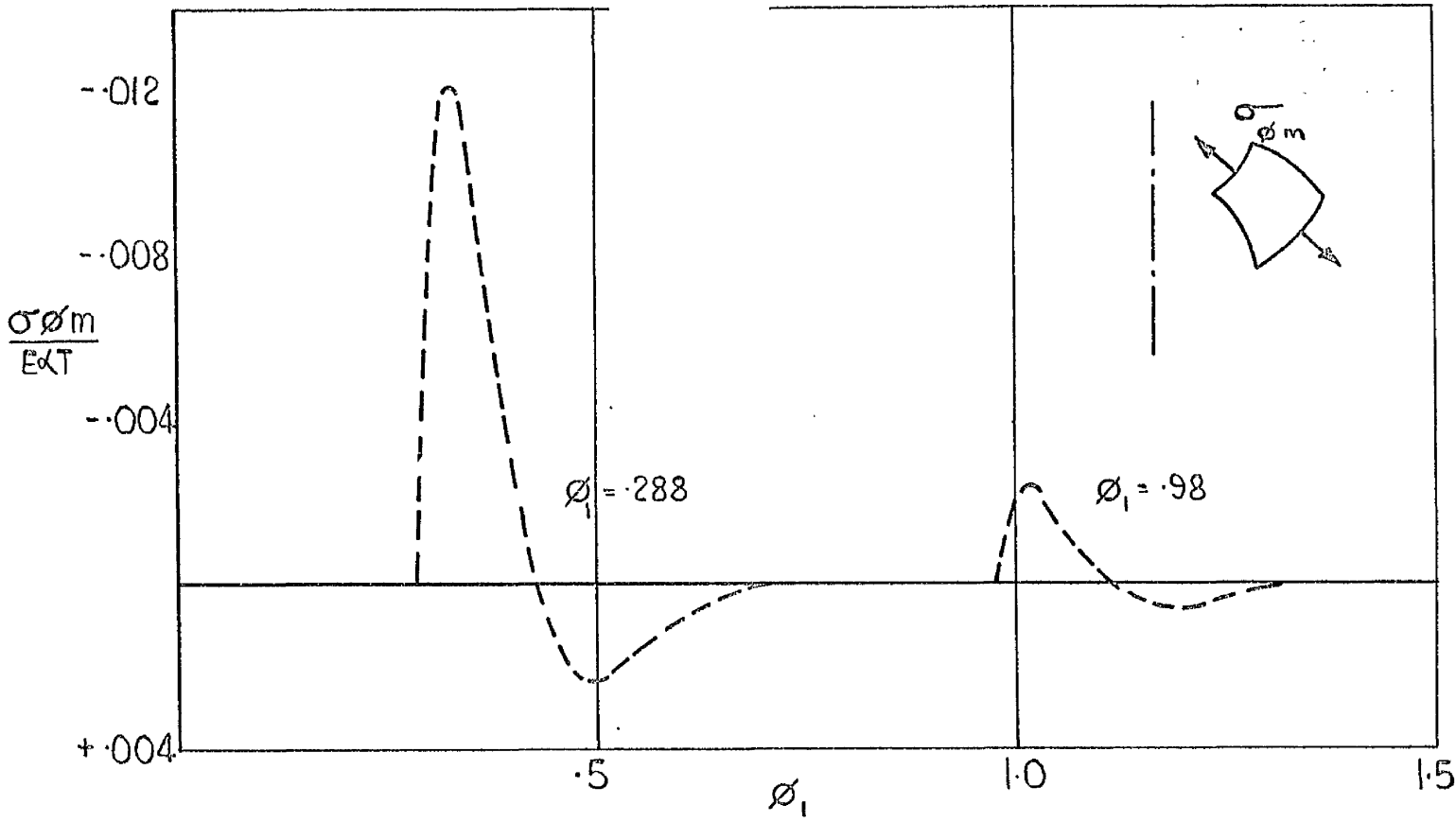


FIGURE (2.8) CIRCUMFERENTIAL BENDING STRESS DISTRIBUTION INTO SHELL FOR TWO OPENING VALUES ($\frac{\alpha}{R} = 90, S=12, \nu = 0.255$)

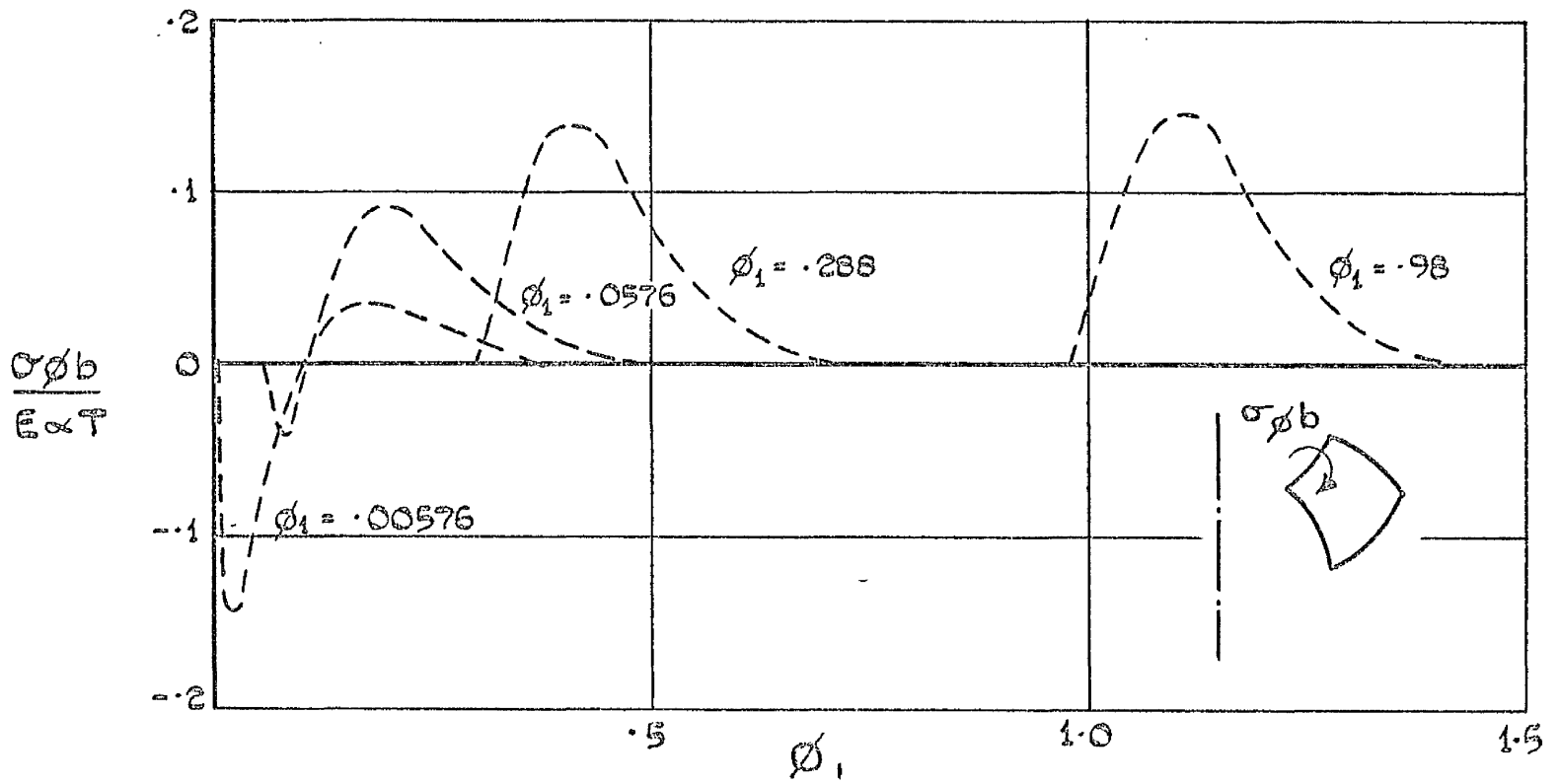


FIGURE (2.9) MERIDIONAL BENDING STRESS DISTRIBUTION INTO THE SHELL FOR VARIOUS OPENING VALUES ($\frac{\alpha}{R} = 90, S=12, \nu = 0.255$)

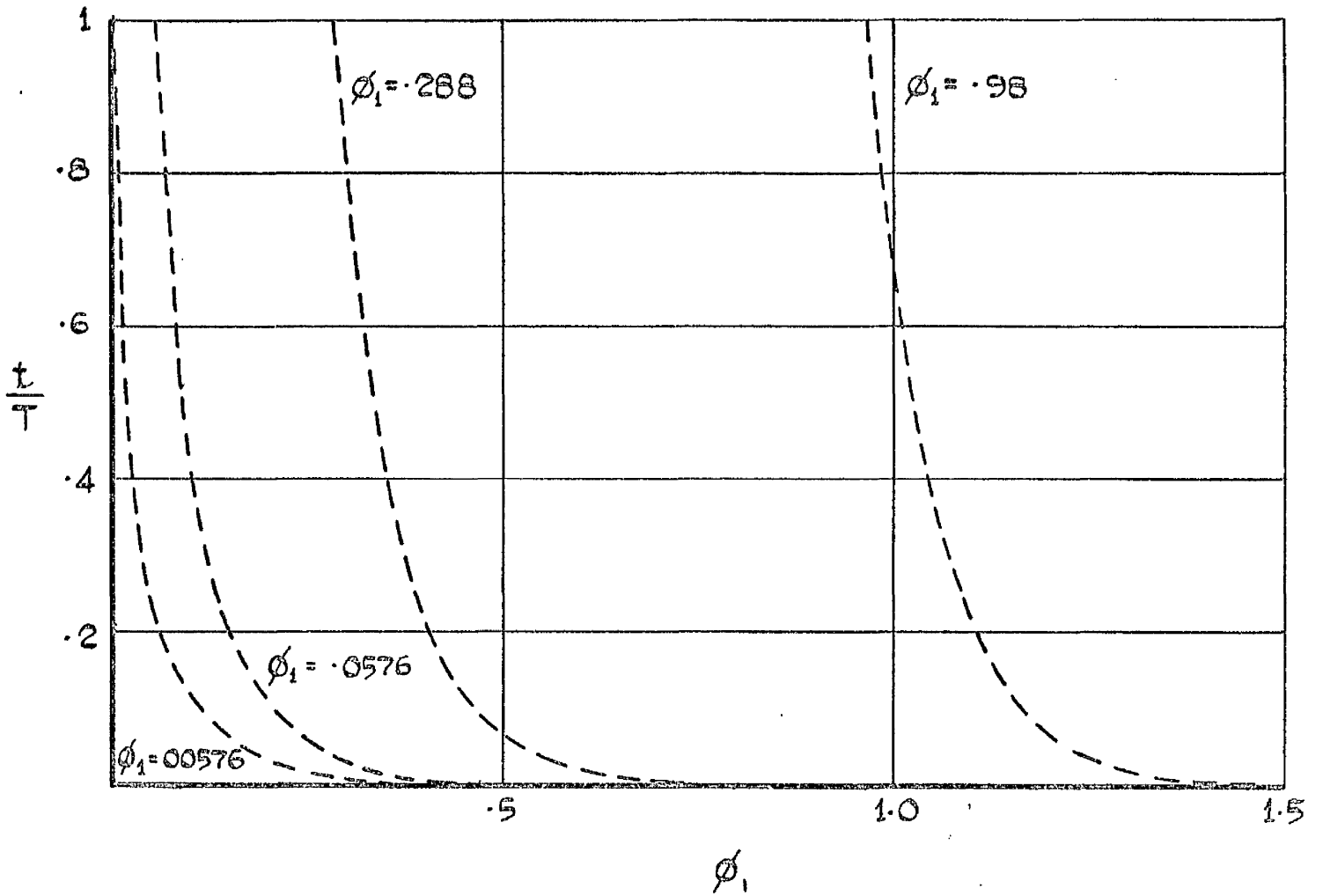


FIGURE (2.10) THE TEMPERATURE DISTRIBUTION INTO THE SHELL FOR VARIOUS OPENING VALUES ($\frac{a}{R} = 90, S=12, v = 0.255$)

ϕ	.01152	.0230	.0346	.0461	.0576	.0691	.0921	.1152	.1728	.2880	.4032	.5184	.7487	1.037	1.497
$-\sigma_{\phi m}^2 (E_{AT})^{-1}$.5934	.4809	.4010	.3423	.2984	.2649	.2181	.1878	.1459	.1128	.0993	.0919	.0841	.0793	.0739
$-\sigma_{\phi b}^2 (E_{AT})^{-1}$.4348	.4355	.4015	.3608	.3223	.2883	.2341	.1945	.1331	.0781	.0533	.0393	.0236	.0125	.0015
$-\chi^2 (AT)^{-1}$.9016	1.806	2.498	2.994	3.345	3.593	3.894	4.081	4.081	4.061	4.095	4.036	3.942	3.815	3.801
$-\sigma_{\phi m}^2 (E_{AT})^{-1}$.6643	.5569	.4781	.4191	.3743	.3398	.2911	.2591	.2142	.1780	.1629	.1547	.1523	.1396	.1336
$-\sigma_{\phi b}^2 (E_{AT})^{-1}$.4353	.4462	.4175	.3796	.3422	.3085	.2537	.2128	.1483	.0888	.0614	.0457	.0252	.0151	.0018
$-\chi^2 (AT)^{-1}$.9026	1.851	2.598	3.150	3.552	3.844	4.220	4.432	4.653	4.736	4.718	4.6899	4.616	4.589	4.518
$-\sigma_{\phi m}^2 (E_{AT})^{-1}$.7167	.6158	.5401	.4826	.4387	.4044	.3558	.3236	.2780	.2407	.2253	.2217	.2067	.2003	.1939
$-\sigma_{\phi b}^2 (E_{AT})^{-1}$.4212	.4391	.4154	.3806	.3453	.3129	.2594	.2189	.1541	.0935	.0650	.0465	.0298	.0163	.0020
$-\chi^2 (AT)^{-1}$.8733	1.821	2.585	3.159	3.584	3.899	4.314	4.560	4.842	4.985	4.992	4.977	4.979	4.950	4.906

TABLES (2.1 - 3)

OPENING VALUES FOR VARIOUS VALUES OF S

WITH $\frac{\rho}{\gamma} = 90$ AND $\nu = 0.255$.

The graphs of the opening values show up two distinct regions. In the first region, approximately defined by $0 < \phi_1 < 0.5$ there are great variations in the values of the stresses and of the displacements. Beyond the value of $\phi_1 = 0.5$ these opening values tend toward a more constant value. In the next Chapter we shall investigate this region of the shell.

It is observed that the opening value of the membrane circumferential stress, for all values of the parameters, appear to tend to the same value at the origin, namely, $-E\alpha T$ while the corresponding values of the bending stress, angular rotation and the displacement all tend to a value of zero. These limiting conditions shall be proved later to be the case. These limiting values are the same as those for a circular flat plate. However, it would appear wrong from these results to consider any portion of the spherical form as a flat plate, although this has been done by certain researchers.

Stresses whose magnitude is in the region of $E\alpha T$ are high and may require careful thought from the design viewpoint. Further, it must be remembered that these results are for a completely free opening. Stresses due to edge restraints must be added to the stress values which we have just considered. This problem we shall consider when we are investigating the interaction of a cylindrical shell with a shallow spherical shell. The stress distributions shown by the broken lines, into a shell from a particular opening, die out very rapidly. This justifies our confidence in dropping the terms involving the constants of integration A_3 and A_4 from equations (2.16-21) when we consider the thermal effects associated with the lower boundary of the angle.

The/

The Tables (2.1 - 3) along with the appropriate Figures show that for a fixed value of a/h (a value of 90 was the one chosen to illustrate this effect) the stresses and the displacements vary with the parameter S . The greater the value of S the greater are the stresses. The variation appears more pronounced for larger values of opening where each of the opening terms tends to a constant value. This constant value we will investigate. This variation of the magnitude of the stress term with the parameter S we would rather expect but not, perhaps, that the effect would appear greater for the larger values of opening.

It has already been observed that the constant S , which is a heat transfer parameter, is very similar to the BIOT number. BIOT⁽⁸⁾ has already demonstrated that the greater the number the larger are likely to be the magnitude of the stresses. The results in this example, for the uniformly heated circular opening, confirm the importance of this parameter. The reduction of the magnitude of the thermal stresses in a spherical shell therefore becomes the problem of reducing the magnitude of the parameter S .

CHAPTER 3

STRESSES IN A SPHERICAL SHELL AT
LARGE VALUES OF THE MERIDIONAL ANGLE

For larger values of the meridional angle the Kelvin functions can be replaced by their asymptotic form. This results in greater simplification of the expressions for the stresses and the displacements on a spherical shell. These expressions are shown to be similar to and, in the region of the equator of the shell, the same as, the results for a cylindrical shell.

The problem of a line of heat around a spherical shell is considered and graphical results are presented illustrating the effects of varying the main parameters.

3.1 Stresses in a Spherical Shell at Large Values
of the Meridional Angle

- (a) The Simplified Equations of the Spherical
Shell for Large Values of Angle

- (b) The Spherical Shell with a Large Heated Opening

- (c) A Line of Heat Around a Spherical Shell

3.1 (a) The Simplified Equations of the Spherical Shell for Large Values of Angle

In order to simplify the rather involved expressions for the stress resultants which were derived in Chapter 2, we could first consider replacing the Kelvin functions by their asymptotic forms. They are

$$\text{ber } Z = (2\pi Z)^{-\frac{1}{2}} e^{\frac{Z}{\sqrt{2}}} \cos\left(\frac{Z}{\sqrt{2}} - \frac{\pi}{8}\right) ; \quad \text{ber}' Z = (2\pi Z)^{-\frac{1}{2}} e^{\frac{Z}{\sqrt{2}}} \cos\left(\frac{Z}{\sqrt{2}} + \frac{\pi}{8}\right)$$

$$\text{bei } Z = (2\pi Z)^{-\frac{1}{2}} e^{\frac{Z}{\sqrt{2}}} \sin\left(\frac{Z}{\sqrt{2}} - \frac{\pi}{8}\right) ; \quad \text{bei}' Z = (2\pi Z)^{-\frac{1}{2}} e^{\frac{Z}{\sqrt{2}}} \sin\left(\frac{Z}{\sqrt{2}} + \frac{\pi}{8}\right)$$

$$\text{ker } Z = \left(\frac{\pi}{2Z}\right)^{\frac{1}{2}} e^{-\frac{Z}{\sqrt{2}}} \cos\left(\frac{Z}{\sqrt{2}} + \frac{\pi}{8}\right) ; \quad \text{ker}' Z = -\left(\frac{\pi}{2Z}\right)^{\frac{1}{2}} e^{-\frac{Z}{\sqrt{2}}} \cos\left(\frac{Z}{\sqrt{2}} - \frac{\pi}{8}\right)$$

$$\text{kei } Z = -\left(\frac{\pi}{2Z}\right)^{\frac{1}{2}} e^{-\frac{Z}{\sqrt{2}}} \sin\left(\frac{Z}{\sqrt{2}} + \frac{\pi}{8}\right) ; \quad \text{kei}' Z = \left(\frac{\pi}{2Z}\right)^{\frac{1}{2}} e^{-\frac{Z}{\sqrt{2}}} \sin\left(\frac{Z}{\sqrt{2}} - \frac{\pi}{8}\right)$$

3.1 - 81

TIMOSHENKO and REISSNER⁽⁴⁸⁾ suggest that these expressions are valid for values of $Z > 6$. However, FLÜGGE states that the larger value $Z > 10$ is more correct and he observes that at $Z = 10$ the errors made in using these formulae are in the order of several per cent.

Using these asymptotic forms in the expression for the shear stress resultant, Q_ϕ , equation (2.26) will reduce to

$$Q_\phi = \frac{1}{\sqrt{\sin\phi}} \left[e^{\alpha\phi} (A_1 \cos \alpha\phi + A_2 \sin \alpha\phi) + e^{-\alpha\phi} (A_3 \cos \alpha\phi + A_4 \sin \alpha\phi) \right] \quad (24)$$

This is, however, the form of the solution obtained by HETENYI when he reduced the problem of the spherical shell to that of a beam/

beam on an elastic foundation. BLUMENTHAL⁽²³⁾ arrived at the same solution, by simplifications of REISSNER'S basic equation (2.11), as did LECKIE by using the classical method of asymptotic integration.

Replacing the Kelvin functions in equations (2.16-21) by their asymptotic form as given in equations (3.1 - 8), we arrive at the following expressions for the stress resultants and the displacements:-

$$Q_\phi = (\sin\phi)^{-\frac{1}{2}} \left\{ e^{\alpha\phi} (A_1 \cos \alpha\phi + A_2 \sin \alpha\phi) + e^{-\alpha\phi} (A_3 \cos \alpha\phi + A_4 \sin \alpha\phi) \right\} + \alpha t$$

$$N_\phi = -\cot\phi \cdot Q_\phi$$

$$N_\theta = -\sqrt{2}\alpha (\sin\phi)^{-\frac{1}{2}} \left\{ e^{\alpha\phi} [A_1 \cos(\alpha\phi + \frac{\pi}{4}) + A_2 \sin(\alpha\phi + \frac{\pi}{4})] - e^{-\alpha\phi} [A_3 \sin(\alpha\phi + \frac{\pi}{4}) - A_4 \cos(\alpha\phi + \frac{\pi}{4})] \right\} + \alpha (t \cot\phi - s^2 t)$$

$$M_\phi = \frac{\alpha}{\sqrt{2}\alpha} (\sin\phi)^{\frac{1}{2}} \left\{ e^{\alpha\phi} [A_1 \sin(\alpha\phi + \frac{\pi}{4}) - A_2 \cos(\alpha\phi + \frac{\pi}{4})] - e^{-\alpha\phi} [A_3 \cos(\alpha\phi + \frac{\pi}{4}) + A_4 \sin(\alpha\phi + \frac{\pi}{4})] \right\} + \frac{\alpha A}{s^2 + 1 - \nu} [s^2 t - (1 - \nu) \cot\phi \cdot t]$$

$$M_\theta = \frac{\nu\alpha}{\sqrt{2}\alpha} (\sin\phi)^{\frac{1}{2}} \left\{ e^{\alpha\phi} [A_1 \sin(\alpha\phi + \frac{\pi}{4}) - A_2 \cos(\alpha\phi + \frac{\pi}{4})] - e^{-\alpha\phi} [A_3 \cos(\alpha\phi + \frac{\pi}{4}) + A_4 \sin(\alpha\phi + \frac{\pi}{4})] \right\} + \frac{\alpha A}{s^2 + 1 - \nu} [(1 - \nu) t \cot\phi + \nu s^2 t]$$

$$\chi = \frac{2\alpha^2}{Eh} (\sin\phi)^{-\frac{1}{2}} \left[e^{\alpha\phi} (A_1 \sin \alpha\phi - A_2 \cos \alpha\phi) - e^{-\alpha\phi} (A_3 \sin \alpha\phi - A_4 \cos \alpha\phi) \right] + \frac{4\alpha^4}{(s^2 + 1)^2 + 4\alpha^4} \alpha t$$

$$\frac{u}{a \sin\phi} = \frac{1}{Eh} (N_\theta - \nu N_\phi) + \alpha t$$

3.1 (b) The Spherical Shell with a Large Heated Opening

Let us now reconsider the problem in the previous Chapter of a spherical shell with a uniformly heated axisymmetric opening. However, let us impose the further condition that

$$\sqrt{2} \alpha \phi > 10$$

so that the opening must be large.

Since we have stipulated that the opening, at

$\phi = \phi_1$, is free of external constraints and that the temperature distribution reduces to zero before the outer boundary is reached then the appropriate boundary conditions are

$$N_{\phi_1} = M_{\phi_1} = 0,$$

$$t_{\phi_1} = T$$

and

$$t^* \rightarrow 0$$

for large values of ϕ . It is recalled that this last condition allows us to drop the terms with the coefficients A_1 and A_2 in equations (3.9 - 15).

Substituting for the first two boundary conditions in equations (3.10 & 12) yields

$$N_{\phi_1} = 0 = -\cot \phi_1 \left[(\sin \phi_1)^{-\frac{1}{2}} (A_3 \cos \alpha \phi_1 + A_4 \sin \alpha \phi_1) e^{-\alpha \phi_1} + A t_1 \right]$$

$$M_{\phi_1} = 0 = -\frac{\alpha}{\sqrt{2} \alpha} (\sin \phi_1)^{-\frac{1}{2}} e^{-\alpha \phi_1} \left[A_3 \cos (\alpha \phi_1 + \frac{\pi}{4}) + A_4 \sin (\alpha \phi_1 + \frac{\pi}{4}) \right] \\ + \frac{\alpha A}{s^2 + 1 - \nu} \left[s^2 t_1 - (1 - \nu) \cot \phi_1 t_1 \right]$$

or /

or expressing these two equations in matrix notation

$$\begin{bmatrix} 0 \\ 0 \end{bmatrix} = \begin{bmatrix} \cos \alpha \phi_1 & \sin \alpha \phi_1 \\ \cos (\alpha \phi_1 + \frac{\pi}{4}) & \sin (\alpha \phi_1 + \frac{\pi}{4}) \end{bmatrix} \begin{bmatrix} A_3 \\ A_4 \end{bmatrix} - A e^{+\alpha \phi_1} (\sin \phi_1)^{\frac{1}{2}} \begin{bmatrix} -t_1 \\ \frac{\sqrt{2} \alpha}{s^2+1-\nu} [s^2 t_1 - (1-\nu) \cot \phi_1 t_1] \end{bmatrix}$$

We may now transpose this matrix to give

$$\begin{bmatrix} A_3 \\ A_4 \end{bmatrix} = \sqrt{2} e^{+\alpha \phi_1} \sin^{\frac{1}{2}} \phi_1 \begin{bmatrix} \sin (\alpha \phi_1 + \frac{\pi}{4}) & -\sin \alpha \phi_1 \\ -\cos (\alpha \phi_1 + \frac{\pi}{4}) & \cos \alpha \phi_1 \end{bmatrix} \begin{bmatrix} -t_1 \\ \frac{\sqrt{2} \alpha}{s^2+1-\nu} [s^2 t_1 - (1-\nu) \cot \phi_1 t_1] \end{bmatrix}$$

Let us now evaluate some of the stress resultants for our problem using these values of the integration constants.

From equation (3.11)

$$N_{\theta} = \sqrt{2} \alpha (\sin \phi)^{-\frac{1}{2}} e^{-\alpha \phi} [\sin (\alpha \phi + \frac{\pi}{4}) - \cos (\alpha \phi + \frac{\pi}{4})] \begin{bmatrix} A_3 \\ A_4 \end{bmatrix} + A (t \cot \phi - s^2 t)$$

After substituting in this expression the values of the constants of integration which we have just found, it becomes

$$N_{\theta} = 2 \alpha A \left(\frac{\sin \phi_1}{\sin \phi} \right)^{\frac{1}{2}} (e^{-\alpha (\phi - \phi_1)}) [\sin (\alpha \phi + \frac{\pi}{4}) - \cos (\alpha \phi + \frac{\pi}{4})] \begin{bmatrix} \sin (\alpha \phi_1 + \frac{\pi}{4}) - \sin \alpha \phi_1 \\ -\cos (\alpha \phi_1 + \frac{\pi}{4}) \cos \alpha \phi_1 \end{bmatrix} \begin{bmatrix} t_1 \\ \frac{\sqrt{2} \alpha}{s^2+1-\nu} [s^2 t_1 - (1-\nu) \cot \phi_1 t_1] \end{bmatrix} + A (t \cot \phi - s^2 t)$$

For the opening value of N_{θ} , that is the value at $\phi = \phi_1$,

the expression reduces to

$$N_{\theta_1} = 2 \alpha A \left[-t_1 - \frac{\alpha}{s^2+1-\nu} \{ s^2 t_1 - (1-\nu) \cot \phi_1 t_1 \} + \frac{t_1 \cot \phi_1 - s^2 t_1}{2 \alpha} \right] \quad (3.16)$$

By substituting in equation (3.14) we can find, by the same method, the opening value of the angular rotation to be

$$\chi_1 = \frac{-2 \sqrt{2} \alpha^2 A}{E h} \left\{ -\frac{t_1}{\sqrt{2}} - \frac{\sqrt{2}}{s^2+1-\nu} [s^2 t_1 - (1-\nu) \cot \phi_1 t_1] \right\}$$

We could now evaluate these results for particular values of the main parameters (ν , $\frac{a}{h}$, S) but first let us examine the expressions for the temperature distribution. For the evaluation of the results in our previous graphs, we assumed that the temperature distribution was given by equation (1.21) as

$$t = BK_0(s\phi) \cdot \left(\frac{\phi}{\sin\phi}\right)^{\frac{1}{2}} .$$

We have already seen however, in section 1.2 (c), that for larger values of $s\phi$ the asymptotic form for the Modified Bessel Function $K_0(s\phi)$ would give

$$t = B e^{-s\phi} . \tag{3.18}$$

It would seem reasonable therefore to use this expression for the temperature in problems of the type we are considering where

$\sqrt{2} s\phi > 10$ although we realise that there could be cases (for small values of S) where the two criteria, for using the asymptotic forms, are not compatible.

Applying the boundary condition

$$t_{\phi_1} = T$$

to equation (3.18) yields

$$t = T \frac{e^{-s\phi}}{e^{-s\phi_1}} \tag{3.19}$$

which when differentiated gives

$$t^\circ = -sT \frac{e^{-s\phi}}{e^{-s\phi_1}} \tag{3.20}$$

At the opening where $\phi = \phi_1$, the temperature gradient will be

$$t_1' = -5T \quad 3.21$$

Assuming that the two criteria for the asymptotic forms are compatible, we can now substitute this value for the temperature gradient into the equations (3.16 - 17) to yield

$$N_{\theta_1} = \frac{ET\alpha h (S^2+1-\nu)}{(S^2+1)^2 + 4x^4} \left[2x - \frac{2x^2 S}{S^2+1-\nu} - 5 - \cot\phi_1 \cdot \left(1 + \frac{2x^2 - \nu 2x^2}{S^2+1-\nu} \right) \right]$$

$$\chi_1 = \frac{\alpha T 2x^2 S}{(S^2+1)^2 + 4x^4} \left[-(S^2+1-\nu) + 2xS - 2x^2 + \cot\phi_1 (1-\nu) 2x \right]$$

3.22-23

Where the parameter $S = 12$ and the Poisson's ratio $\nu = 0.255$, these expressions, for the selected values of $\frac{\alpha}{h}$ given, reduce to:

$$N_{\theta_1} \left(\frac{\alpha}{h} = 30 \right) = (-0.3435 - 0.08467 \cot\phi_1) ET\alpha h$$

$$N_{\theta_1} \left(\frac{\alpha}{h} = 90 \right) = (-0.1931 - 0.03961 \cot\phi_1) ET\alpha h$$

$$N_{\theta_1} \left(\frac{\alpha}{h} = 150 \right) = (-0.1395 - 0.02278 \cot\phi_1) ET\alpha h$$

$$\chi_1 \left(\frac{\alpha}{h} = 30 \right) = (-2.9913 + 0.4091 \cot\phi_1) \alpha T$$

$$\chi_1 \left(\frac{\alpha}{h} = 90 \right) = (-4.9007 + 0.5912 \cot\phi_1) \alpha T$$

$$\chi_1 \left(\frac{\alpha}{h} = 150 \right) = (-5.8832 + 0.5206 \cot\phi_1) \alpha T$$

We may now compare these expressions with the graphical solutions presented in the preceding Chapter. It has already been observed that the two graphs in question, those for N_{θ} and χ_1 , quickly attain constant values for the larger values of the opening angle. The value of $\cot \phi_1$ is very small for the large values of ϕ_1 and the constant term associated with it is also relatively small. Thus with the expressions above we could have predicted the "linear" portions of the graphs.

If we carry the approximation consequential to the dropping of the $\cot \phi$ terms back to equations (3.9 - 15) and indeed back to the equations in Chapter 2 from which the equations (3.9 - 15) were developed, we find an interesting result. For example, the shear stress resultant Q_{ϕ} would be, omitting the t^* term

$$Q_{\phi} = e^{\alpha\phi} (A_1 \cos \alpha\phi + A_2 \sin \alpha\phi) + e^{-\alpha\phi} (A_3 \cos \alpha\phi + A_4 \sin \alpha\phi) .$$

The complementary function portion of this expression is the solution of the differential equation

$$Q_{\phi}^{\dots} + 4\alpha^4 Q_{\phi} = 0 \tag{3.24}$$

Alternatively, if we consider the $L(\dots)$ operator

$$L(\dots) \equiv (\dots)^{\dots} + (\dots)^{\dot{}} \cot \phi - (\dots) \cot^2 \phi$$

and drop there the terms involving $\cot \phi$ the equation (2.24) will also reduce to this form.

This is the form of the solution, for large values of the angle, proposed by GECKELER⁽²⁵⁾. It is also the solution for a cylindrical shell so that in effect we are approximating this region/

region of the spherical shell to a cylindrical shell.

Full discussions of the implications of this approximation are found in FLÜGGE and HETÉNYI. It is of interest to us to notice that our "temperature" terms in the stress resultants simplify considerably. The constant A would also simplify since the numerator would become S^2 and the denominator $S^4 + 4\alpha^4$ in place of $(S^2 + 1 - \nu)$ and $(S^2 + 1)^2 + 4\alpha^4$ respectively if the same simplifying assumptions are carried into the temperature equations.

The equations (3.9 - 15) have thus been simplified even further but, as HETÉNYI observes, it is a somewhat coarser approximation that results. The equations for the stress resultants in this case are

$$Q_\phi = e^{\alpha\phi} (A_1 \cos \alpha\phi + A_2 \sin \alpha\phi) + e^{-\alpha\phi} (A_3 \cos \alpha\phi + A_4 \sin \alpha\phi) + At$$

$$N_\phi = 0$$

$$N_\theta = -\sqrt{2}\alpha \left\{ e^{\alpha\phi} \left[A_1 \cos \left(\alpha\phi + \frac{\pi}{4} \right) + A_2 \sin \left(\alpha\phi + \frac{\pi}{4} \right) \right] - e^{-\alpha\phi} \left[A_3 \sin \left(\alpha\phi + \frac{\pi}{4} \right) - A_4 \cos \left(\alpha\phi + \frac{\pi}{4} \right) \right] \right\} - As^2t$$

$$M_\phi = \frac{a}{\sqrt{2}\alpha} \left\{ e^{\alpha\phi} \left[A_1 \sin \left(\alpha\phi + \frac{\pi}{4} \right) - A_2 \cos \left(\alpha\phi + \frac{\pi}{4} \right) \right] - e^{-\alpha\phi} \left[A_3 \cos \left(\alpha\phi + \frac{\pi}{4} \right) + A_4 \sin \left(\alpha\phi + \frac{\pi}{4} \right) \right] \right\} + \frac{aAs^2t}{S^2 + 1 - \nu}$$

$$M_{\theta} = \gamma M_{\phi}$$

$$\chi = \frac{2\alpha^2}{Eh} \left[e^{\alpha\phi} (A_1 \sin \alpha\phi - A_2 \cos \alpha\phi) - e^{-\alpha\phi} (A_3 \sin \alpha\phi - A_4 \cos \alpha\phi) \right] + \frac{4\alpha^4}{S^4 + 4\alpha^4} \alpha t^{\circ}$$

$$\frac{u}{\alpha} = \frac{1}{Eh} \cdot N_{\theta} + \alpha t \quad 3.25 - 31$$

where

$$A = \frac{Eh\alpha S^2}{S^4 + 4\alpha^4}$$

The simplified results of equations (3.25 - 31) are of considerable interest since they are also the equations for a cylindrical shell with a longitudinal temperature distribution. For a cylindrical shell it is customary to change from the meridional co-ordinate ϕ to an axial co-ordinate x where $x = \alpha\phi$. For the region of the shell, where the GECKELER equations are valid, the equations (3.22 - 23), for the opening values of the circumferential membrane stress and tangent rotation, become

$$N_{\theta_1} = ET\alpha h \frac{S^3}{S^4 + 4\alpha^4} \left[2\alpha - \frac{2\alpha^2}{S} - S \right]$$

$$\chi_1 = \frac{\alpha T \cdot 2\alpha^2 S}{S^4 + 4\alpha^4} [-S^2 + 2\alpha S - 2\alpha^2]$$

3.32 - 33

The horizontal displacement u is given by equation (3.31) as

for/
$$u = \frac{\alpha}{Eh} \cdot N_{\theta} + \alpha \alpha T$$

for large values of ϕ . The value of U at the shell opening will, from equations (3.32) then be

$$U_1 = \alpha \Delta T \frac{1}{S^4 + 4\alpha^4} [4\alpha^4 + 2\alpha S^3 - 2\alpha^2 S^2] \quad 3.34$$

Equations (3.33 - 34) can be written as

$$\chi_1 = \frac{2\alpha T_s}{(4 + \frac{S^4}{\alpha^4})} \left[-\frac{S^2}{\alpha^2} + 2\frac{S}{\alpha} - 2 \right]$$

$$U_1 = \frac{2\alpha \Delta T}{(4 + \frac{S^4}{\alpha^4})} \left[2 + \frac{S^3}{\alpha^3} - \frac{S^2}{\alpha^2} \right]$$

3.35 - 36

The equations for the tangent rotation χ_1 , contains the term ST . It has been shown, in equation (3.21), that this is in fact the temperature gradient at the opening so that

$$ST = -\dot{t}_1$$

and equation (3.35) can be written as

$$\chi_1 = \frac{-2\alpha \dot{t}_1}{\frac{S^4}{\alpha^4} + 4} \left[-\frac{S^2}{\alpha^2} + 2\frac{S}{\alpha} - 2 \right] \quad 3.37$$

It is observed that the two equations (3.36 - 37) contain terms which are powers of the ratio of the heat transfer parameter, S , to the basic shell parameter, α . The value of this ratio is

$$\frac{S}{\alpha} = \frac{\left(\frac{2m}{kh}\right)^{\frac{1}{2}} \cdot a}{(3 \cdot (1-\nu^2))^{\frac{1}{4}} \left(\frac{a}{h}\right)^{\frac{1}{2}}} = \left[\left(\frac{2m}{k}\right)^2 \frac{1}{3(1-\nu^2)} \right]^{\frac{1}{4}} \cdot a^{\frac{1}{2}}$$

Thus, provided the two heat transfer parameters and the Poisson's ratio/

ratio remain constant, the ratio $\frac{S}{\alpha} = \text{const.} \sqrt{a}$. This implies that the opening values of the displacements are independent of the shell thickness but are functions of \sqrt{a} . This confirms what has already been observed, that the "size effect" is of importance on the magnitudes of the thermal effects.

For the special case of heat conduction only, that is where there is no loss of heat from the surfaces, then $S = 0$ and the equations (3.36 - 37) reduce to

$$\begin{aligned} \chi_1 &= -\alpha t_1 \\ u_1 &= \alpha \Delta T \end{aligned} \tag{3.38 - 39}$$

Further, since both $N_{\phi_1} = 0$ and $M_{\theta_1} = 0$ then it can be seen from equations (3.25 - 31) that there is no stress distribution into the shell for this temperature distribution.

It has been shown in section 1.3(b) of Chapter I that the temperature distribution of a cylindrical shell, due to heat conduction only, will be linear.

TIMOSHENKO⁽⁴⁹⁾ and DEN HARTOG⁽⁵⁰⁾ have investigated the case of a cylindrical shell with a linearly varying axial temperature distribution and have confirmed that there should be no stress distribution in the shell and that the edge displacements are as given by equations (3.38 - 39).

It is of interest to compare the opening values of the displacements for the various combinations of shell parameter,

$\frac{a}{h}$, and heat transfer parameter, S , which have been used in the earlier graphs and tables. The values of $\chi_1 / \alpha t_1$ and $\frac{u_1}{\alpha \Delta T}$ have been evaluated from equations (3.36 - 37).

$\frac{u_1}{\alpha \Delta T} \approx$

The opening values are presented in tables (3.1 - 2).

The results show excellent agreement with the corresponding graphical results in Figures (2.6 - 7) for the larger values of opening.

For the horizontal displacement, u_1 , it is observed that its value decreases with an increase in S so that the greatest displacement is associated with the conduction only mode of heat transfer, $S=0$, that is with a fully insulated shell.

One cannot draw a general conclusion from table (3.2) because the temperature gradient at the opening, t_1' , is itself a function of S , since from equation (3.21)

$$t_1' = -St$$

It is possible to express the dependent term as $\chi_{\alpha T}$ for all the values of S except $S=0$ for which values the equation (3.21) is no longer valid. For this special case the temperature gradient is linear between the opening and some other defined boundary.

Table (3.3) shows $\chi_{\alpha T}$ for all the parameters so far considered except $S=0$. It is difficult to draw any general conclusions from the values presented. One could be tempted into predicting that the value of the tangent rotation at opening would increase with the value of S for any particular value of $\frac{a}{h}$. A comparison between the values at $S=9$ and $S=12$ for $\frac{a}{h} = 30$ shows, however, that this is not the case. These particular results indicate that there must be a turning value in equation (3.37) in the region of $\frac{S}{\alpha} = 1.3$ and that beyond this value the tangent rotation χ_1 will decrease with increasing S .

HICKS⁽⁴⁷⁾, in his investigation of the junction problem/

S / a/h	30	90	150
0	1	1	1
6	.8375	.9257	.9506
9	.7379	.8658	.9068
12	.6527	.8054	.8598

Table (3.1) The value of $\frac{u_i}{\alpha T}$ for various values of the shell parameters S and α .
($\nu = 0.255$)

S / a/h	30	90	150
0	1	1	1
6	.4536	.6218	.6896
9	.3251	.4996	.5784
12	.2424	.4073	.4893

Table (3.2) The value of $\frac{\chi_i}{\alpha T}$ for various values of the paramters S and α .
($\nu = 0.255$)

S / a/h	30	90	150
6	-2.7214	-3.7310	-4.1373
9	-2.9261	-4.4961	-5.2051
12	-2.9084	-4.8878	-5.8717

Table (3.3) The value of $\frac{\chi_i}{\alpha T}$ for various values of the shell parameters.
($\nu = 0.255$)

problem between a spherical shell and its cylindrical skirt, made the assumption that the temperature distribution on the skirt could be expressed as

$$t = C e^{-\mu x}$$

where C and μ are constants and x is the axial co-ordinate.

He then substituted this expression in the HETÉNYI equation for the displacement of a cylindrical shell due to an axial temperature distribution. HICKS thus obtained solutions for the horizontal displacement and the tangent rotation of the opening which are the same as those given in equations (3.36 - 37). HICKS then states that when $\frac{S}{\alpha}$ is sufficiently small these formulae will reduce to

$$\chi_1 = \alpha t_1$$

$$u_1 = \alpha \alpha T$$

This is, of course, the result which was obtained, in equations (3.38 - 39), for the condition of heat conduction only, where $S = 0$. HICKS proceeds to develop all of his interaction equations on the assumption that $\frac{S}{\alpha}$ is small.

WEIL and MURPHY⁽⁵¹⁾ who investigated the problem of a cylindrical skirt supporting a pressure vessel also made the assumption that the opening displacements are as those which are produced by a linear temperature distribution and are therefore given by equations (3.38 - 39). These authors indicate, however, by the examples which they present, that they are considering well insulated skirts with insulations of 4" thickness on both surfaces. BERGMAN⁽⁴⁰⁾ presents experimental results which indicate that a 2" insulation would reduce the value of S to $0.46S$ whereas a 3" insulation would reduce the value to $0.092 S$

WEIL and MURPHY present, as an example, the problem of/

of cylindrical skirt which has the following experimentally measured values:-

$$\begin{aligned} \alpha &= 114.9 \text{ ins} & \alpha &= 7.7 \times 10^{-6} / \text{F}^{\circ} \\ E &= 25.5 \times 10^6 \text{ lb/in}^2 & T &= 880^{\circ}\text{F} \approx 800\text{F}^{\circ} \\ h &= 0.9063 \text{ in} & t_1 &= -32.7 \text{ F}^{\circ}/\text{in} \end{aligned}$$

insulation thickness = 4" per surface.

If we assume a Poisson's ratio for the skirt material of

$$\nu = 0.255$$

then the value of the parameter α for the shell will be

$$\alpha = \left[3(1-\nu^2) \frac{\alpha^2}{h^2} \right]^{\frac{1}{4}} = 14.57$$

and since, from equation (3.21),

$$t_1 = -ST$$

then

$$S = -\frac{t_1}{T} = 0.040875$$

The appropriate value of the parameter $\frac{S}{\alpha}$ for their shell is therefore

$$\frac{S}{\alpha} = \frac{0.040875}{14.57} = 0.002805$$

Substituting this value in the appropriate expressions for the displacements, equations (3.36 - 37), gives

$$\begin{aligned} \chi_1 &= -\alpha t_1 (0.99719) \\ u_1 &= 0.999996 \alpha \alpha T \end{aligned}$$

This result somewhat justifies the assumption made by the authors, provided cylindrical skirts have 4" insulation. It is interesting to observe that taking a value of 30 Btu/hr ft F^o for the conductivity of the steel and 1.4 Btu/hr ft² F^o for the coefficient of surface heat transfer between steel and atmosphere will give, for the equivalent uninsulated,

uninsulated skirt

$$S = \left(\frac{2m}{kh} \right)^{\frac{1}{2}} \alpha = \left(\frac{2 \times 1.4 \times 12}{0.9063 \times 30} \right)^{\frac{1}{2}} \cdot \frac{114.9}{12} = 10.644$$

which value can be compared with the value of $S = 0.040875$ obtained earlier, for the 4" insulated skirt. Moreover a value of $S = 10.644$ would lead us to expect, after equations (3.36 - 37), displacements of the order

$$u_1 = 0.433 \alpha \Delta T = 0.307''$$

$$\chi_1 = 33.8 \times 10^{-3}$$

as compared with

$$u_1 = 0.707''$$

$$\chi_1 = 0.252 \times 10^{-3}$$

for the insulated skirt.

On the basis of these assumptions about the relationship between the temperature distributions and the displacements WEIL and MURPHY then evaluated their interaction equations between the skirt and the pressure vessel. BERGMAN, after commenting upon the great number of pressure vessels with skirt supports which had been constructed since the 1930's and which were in successful operation comments, "had the analysis and examples given by WEIL and MURPHY and CHENG and WEIL for the three intersecting cylinder problem been available during this period, they might have been a powerful deterrent to the use of skirt supports. Their calculations show stresses on an elastic basis well over double the cold yield point of the steel".

3.1(c) A Line of Heat Round a Spherical Shell

Before proceeding to investigate the problem of a uniform line of heat around a spherical shell, let us first consider the relationship existing between the edge loadings and their corresponding displacements in that region of the shell where these GECKELER type equations are valid.

The stress resultants M_ϕ and Q_ϕ at $\phi = \phi_1$ are given by equations (3.25) and (3.28) as

$$Q_{\phi_1} = e^{-\alpha\phi_1} (A_3 \cos \alpha\phi_1 + A_4 \sin \alpha\phi_1) + \alpha T_1$$

$$M_{\phi_1} = -\frac{a}{\sqrt{2}\alpha} \cdot e^{-\alpha\phi_1} \left[A_3 \cos \left(\alpha\phi_1 + \frac{\pi}{4} \right) + A_4 \sin \left(\alpha\phi_1 + \frac{\pi}{4} \right) \right] + \alpha T_1$$

where only the displacements, stress resultants and temperature distributions in the portion of the sphere below the circle are considered. In matrix form these two equations can be written as

$$e^{+\alpha\phi_1} \begin{bmatrix} Q_{\phi_1} - \alpha T_1 \\ -\frac{\sqrt{2}\alpha}{a} M_{\phi_1} + \sqrt{2}\alpha T_1 \end{bmatrix} = \begin{bmatrix} \cos \alpha\phi_1 & \sin \alpha\phi_1 \\ \cos \left(\alpha\phi_1 + \frac{\pi}{4} \right) & \sin \left(\alpha\phi_1 + \frac{\pi}{4} \right) \end{bmatrix} \begin{bmatrix} A_3 \\ A_4 \end{bmatrix}$$

and hence transposed to give the expressions for the integration constants

$$\begin{bmatrix} A_3 \\ A_4 \end{bmatrix} = \sqrt{2} e^{+\alpha\phi_1} \begin{bmatrix} \sin \left(\alpha\phi_1 + \frac{\pi}{4} \right) & -\sin \alpha\phi_1 \\ -\cos \left(\alpha\phi_1 + \frac{\pi}{4} \right) & \cos \alpha\phi_1 \end{bmatrix} \begin{bmatrix} Q_{\phi_1} - \alpha T_1 \\ -\frac{\sqrt{2}\alpha}{a} M_{\phi_1} + \sqrt{2}\alpha T_1 \end{bmatrix}$$

The corresponding expression for the angular rotation χ_1 , equation (3.30), also written in matrix form is

$$\chi_1 = -\frac{2\alpha^2}{Eh} e^{-\alpha\phi_1} \begin{bmatrix} \sin \alpha\phi_1 & -\cos \alpha\phi_1 \end{bmatrix} \begin{bmatrix} A_3 \\ A_4 \end{bmatrix} + \frac{4\alpha^4}{5^4 + 4\alpha^4} \alpha t_1$$

Substituting for A_3 and A_4 and then simplifying leads to

$$\chi_1 = -\frac{2\sqrt{2}\alpha^2}{Eh} \begin{bmatrix} \bar{r}^{\frac{1}{2}} & -1 \end{bmatrix} \begin{bmatrix} Q_{\phi_1} - \alpha t_1 \\ -\frac{\sqrt{2}\alpha}{a} M_{\phi_1} + \sqrt{2}\alpha \alpha t_1 \end{bmatrix} + \frac{4\alpha^4}{5^4 + 4\alpha^4} \alpha t_1$$

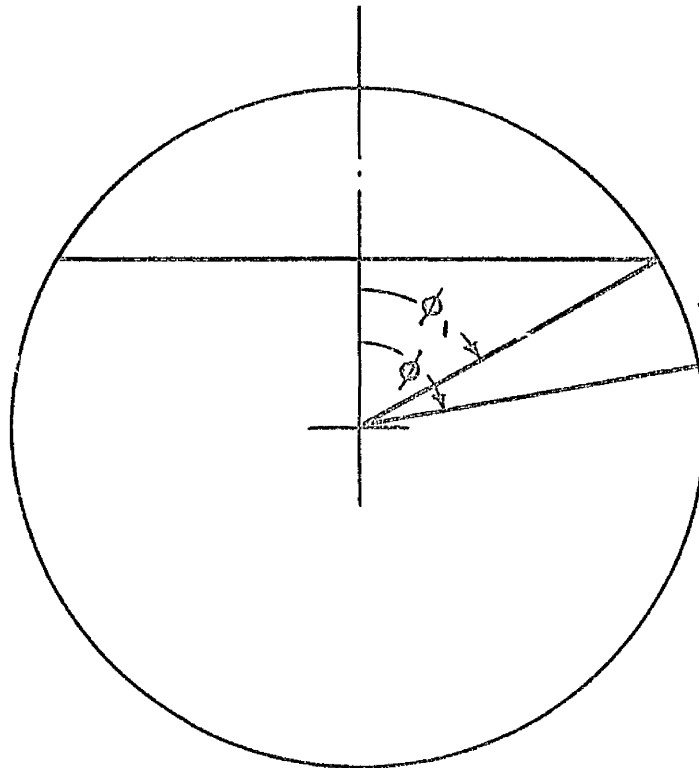
This relationship shows that the rotation at the opening is independent of the value of ϕ_1 , which could similarly be shown of the horizontal displacement in the same region of the sphere. The independence of the stress resultants and their corresponding displacements from the position on the sphere greatly simplifies any problem in this region. This factor has been made use of by researchers, including HICKS when he considered the interaction of a spherical shell with a cylindrical skirt, and can be readily shown from FLÜGGE'S equations. FLÜGGE changed the independent variable from ϕ to ϕ_2 where

$$\phi_2 = \phi - \phi_1$$

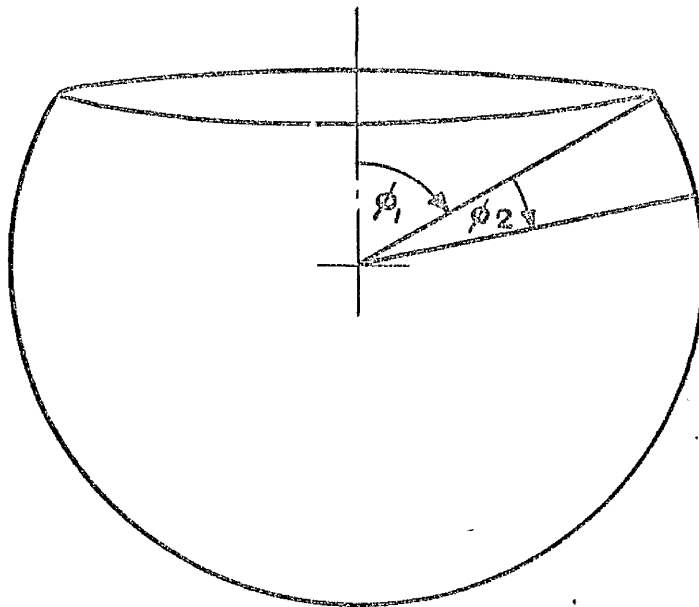
as shown in Figure (3.1), and demonstrated that the "effects" from a condition at ϕ_1 are the same into both portions of the sphere.

The above results are of course compatible with equation (3.18) and indeed could be said to be consequential upon GECKELER'S assertion that this portion of a spherical shell can be considered as a cylindrical shell.

Proceeding now with the problem of a line of heat causing a uniform temperature T around a spherical shell at $\phi = \phi_1$, we must first limit our argument to region where $\cot \phi$ is very small/



SPHERICAL SHELL DIVIDED INTO TWO PORTIONS
BY THE MERIDIONAL $\phi = \phi_1$



LOWER PORTION OF SHELL SHOWING NEW
VARIABLE ϕ_2 WHERE $\phi_2 = \phi - \phi_1$

FIGURE (3.1)

small and the GECKELER forms of solution are applicable. It is more convenient to consider the spherical shell as comprising an upper and lower portion heated uniformly at their boundary ϕ_1 to a temperature T . From the foregoing discussion it can be seen that the two portions are symmetric with respect to the stress resultants and the displacements although ϕ_1 is not necessarily at the equator of the shell. This enables us to consider only one portion of the shell, the lower, and requires that portion to satisfy the following boundary conditions

$$Q_{\phi_1} = \chi_1 = 0$$

to make it compatible with the upper portion.

The temperature distribution into the lower portion of the shell is, after equation (3.18), given by

$$t = B e^{-s\phi}$$

which after satisfying the temperature boundary condition at becomes

$$t = T \frac{e^{-s\phi}}{e^{-s\phi_1}}$$

and it is appreciated that a similar form of temperature distribution exists in the upper portion of the shell.

Substituting for the boundary conditions into equations (3.25, 30) gives

$$Q_{\phi_1} = 0 = e^{-\alpha\phi_1} (A_3 \cos \alpha\phi_1 + A_4 \sin \alpha\phi_1) + A t_1$$

$$\chi_1 = 0 = \frac{-2\alpha^2}{Eh} e^{-\alpha\phi_1} (A_3 \sin \alpha\phi_1 - A_4 \cos \alpha\phi_1) + \frac{4\alpha^4}{5^4 + 4\alpha^4} \alpha t_1$$

In/

In matrix form this can be written as

$$\begin{bmatrix} 0 \\ 0 \end{bmatrix} = \begin{bmatrix} \cos \alpha \phi_1 & \sin \alpha \phi_1 \\ \sin \alpha \phi_1 & -\cos \alpha \phi_1 \end{bmatrix} \begin{bmatrix} A_3 \\ A_4 \end{bmatrix} + e^{\alpha \phi_1} \begin{bmatrix} At_1 \\ -\frac{2\alpha^2 At_1}{s^2} \end{bmatrix}$$

which we can transpose to give

$$\begin{bmatrix} A_3 \\ A_4 \end{bmatrix} = At_1 e^{-\alpha \phi_1} \begin{bmatrix} -\cos \alpha \phi_1 & -\sin \alpha \phi_1 \\ -\sin \alpha \phi_1 & \cos \alpha \phi_1 \end{bmatrix} \begin{bmatrix} 1 \\ -\frac{2\alpha^2}{s^2} \end{bmatrix}$$

Let us now evaluate each of the stress resultants using these values of the integration constants. Substituting first into equation (3.25) for the shear stress resultant Q_ϕ yields

$$Q_\phi = At_1 e^{-\alpha \phi + \alpha \phi_1} \begin{bmatrix} \cos \alpha \phi & \sin \alpha \phi \\ -\sin \alpha \phi & \cos \alpha \phi \end{bmatrix} \begin{bmatrix} -\cos \alpha \phi_1 & -\sin \alpha \phi_1 \\ -\sin \alpha \phi_1 & \cos \alpha \phi_1 \end{bmatrix} \begin{bmatrix} 1 \\ -\frac{2\alpha^2}{s^2} \end{bmatrix} + At_1$$

Evaluating this matrix we find

$$Q_\phi = -AsT e^{-\alpha(\phi - \phi_1)} \left\{ -\cos \alpha(\phi - \phi_1) - \frac{2\alpha^2}{s^2} \sin \alpha(\phi - \phi_1) \right\} + At_1$$

If we now change the dependent variable by defining

$$\phi_2 = \phi - \phi_1$$

where the physical meaning of ϕ_2 is as shown in Figure (3.1), we have

$$Q_\phi = Eh\alpha T \left\{ -\frac{s^3}{s^4 + 4\alpha^4} \left[e^{-\alpha \phi_2} \left(-\cos \alpha \phi_2 - \frac{2\alpha^2}{s^2} \sin \alpha \phi_2 \right) - e^{-s \phi_2} \right] \right\}$$

Similar/

Similar substitutions for the other stress resultants lead to the following expressions for the stresses into the shell from the line of uniform temperature

$$\begin{aligned} \sigma_{\theta m} &= \frac{N_{\theta}}{h} = -E\alpha T \frac{s^3}{s^4 + 4\alpha^4} \left\{ \sqrt{2}\alpha e^{-\alpha\phi_2} \left[-\sin(\alpha\phi_2 + \frac{\pi}{4}) + \frac{2\alpha^2}{s^2} \cos(\alpha\phi_2 + \frac{\pi}{4}) \right] + s e^{-s\phi_2} \right\} \\ \sigma_{\phi b} &= \frac{6M_{\phi}}{11} = \frac{6\alpha}{h} E\alpha T \frac{s^3}{s^4 + 4\alpha^4} \left\{ \frac{1}{\sqrt{2}\alpha} e^{-\alpha\phi_2} \left[-\cos(\alpha\phi_2 + \frac{\pi}{4}) - \frac{2\alpha^2}{s^2} \sin(\alpha\phi_2 + \frac{\pi}{4}) \right] + \frac{1}{s} e^{-s\phi_2} \right\} \\ \chi &= \frac{\alpha T 2\alpha^2 s^3}{s^4 + 4\alpha^4} \left[e^{-\alpha\phi_2} \left(-\sin \alpha\phi_2 + \frac{2\alpha^2}{s^2} \cos \alpha\phi_2 \right) - \frac{2\alpha^2}{s^2} e^{-s\phi_2} \right] \\ u &= \alpha \left(\frac{1}{Eh} N_{\theta} + \alpha T e^{-s\phi_2} \right) \end{aligned}$$

The equations for the stresses and displacements have been programmed and numerical results have been obtained for the same values of the main parameters $(\nu, \frac{\alpha}{h}, s)$ which were considered in Chapter 2. The results are presented in graphical form, using the same conventions as previously, in Figures (3.2 - 7).

The heat conduction case, where $S = 0$, has not been presented. We have already shown that, for this case, the temperature distribution is linear and that for a "free" open shell the stress resultants are zero. This latter property implies that the problem would only be one of matching the displacement and the rotation. The linear temperature case, for a cylindrical shell, has been presented, as an example, by HETENYI. If we substitute our/

our temperature distribution $t = T e^{-s\phi_2}$ in the equation obtained by HETENYI for the cylindrical shell, using his simplified approach, then we obtain results identical to those presented.

The same problem, however, occurs in one of the earliest papers on thermal stress in shells which was written by DEN HARTOG⁽⁵⁰⁾.

This paper reminds us that the lower end of the temperature distribution must also be considered since there will be a rotational term, though no displacement at that end of the field.

The importance of this problem and of the results presented is that they could be considered as describing the effects of a line of heat around the central portion of a spherical shell with a temperature distribution away from the line such as is shown in Figure (3.8a). Theoretically, such a situation is impossible since the heat must be transferred on to the shell through a finite area. In practice it is likely to be transferred through a band of uniform width, for example through a plate welded to the sphere. The width of this band is likely to be of the order of the thickness of the shell so that the assumption of a line of heat seems not unreasonable. We could if we wished, however, take the width of the band into consideration by dividing the shell into the regions

$$0 \leq \phi \leq |\frac{b}{2}| \quad \text{where} \quad t = T$$

$$\phi - \phi_2 \geq |\frac{b}{2}| \quad \text{where} \quad t = t(\phi_2)$$

which are as shown in Figure (3.8b), then matching up the resulting boundary conditions.

The graphical results are presented in Figures (3.2 - 7) for two values of the temperature parameter S ($S=6, S=12$) and/

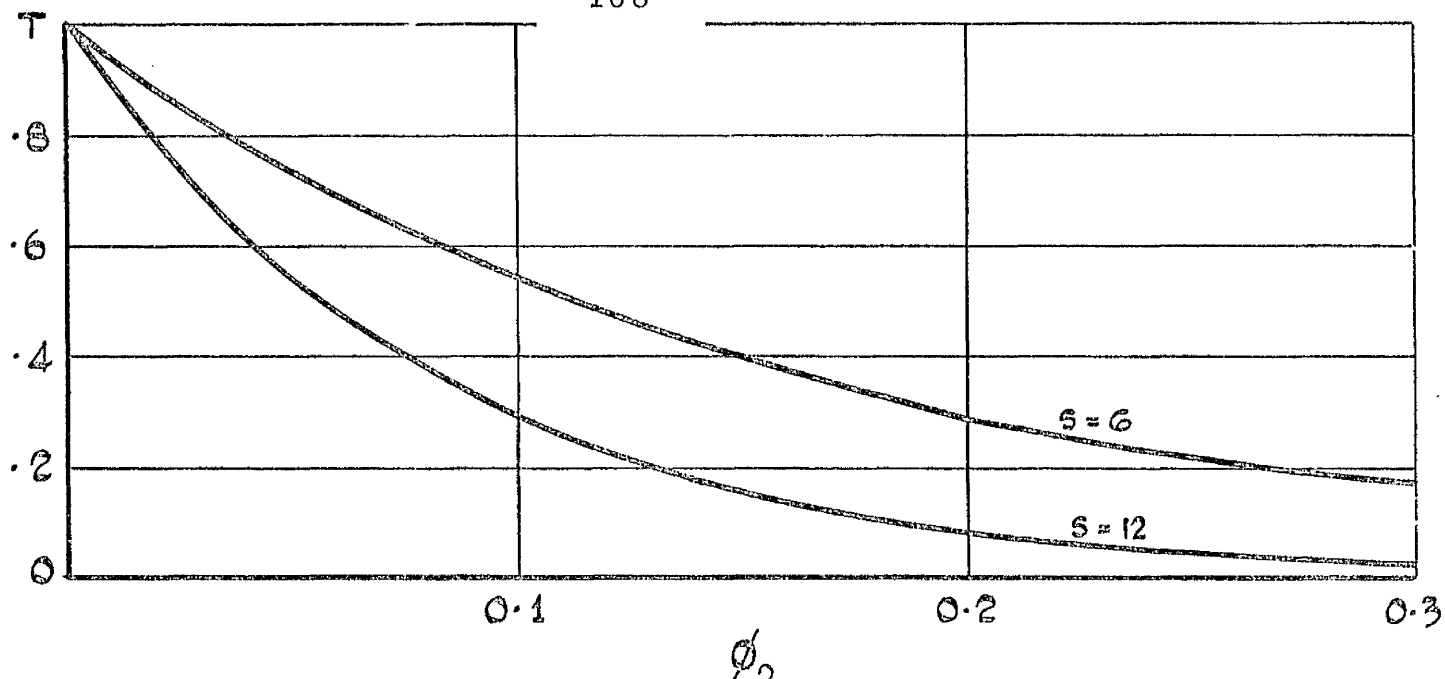


FIGURE (3.2) TEMPERATURE DISTRIBUTIONS INTO A SPHERICAL SHELL FROM A LINE OF TEMPERATURE T. FOR S = 6 AND S = 12

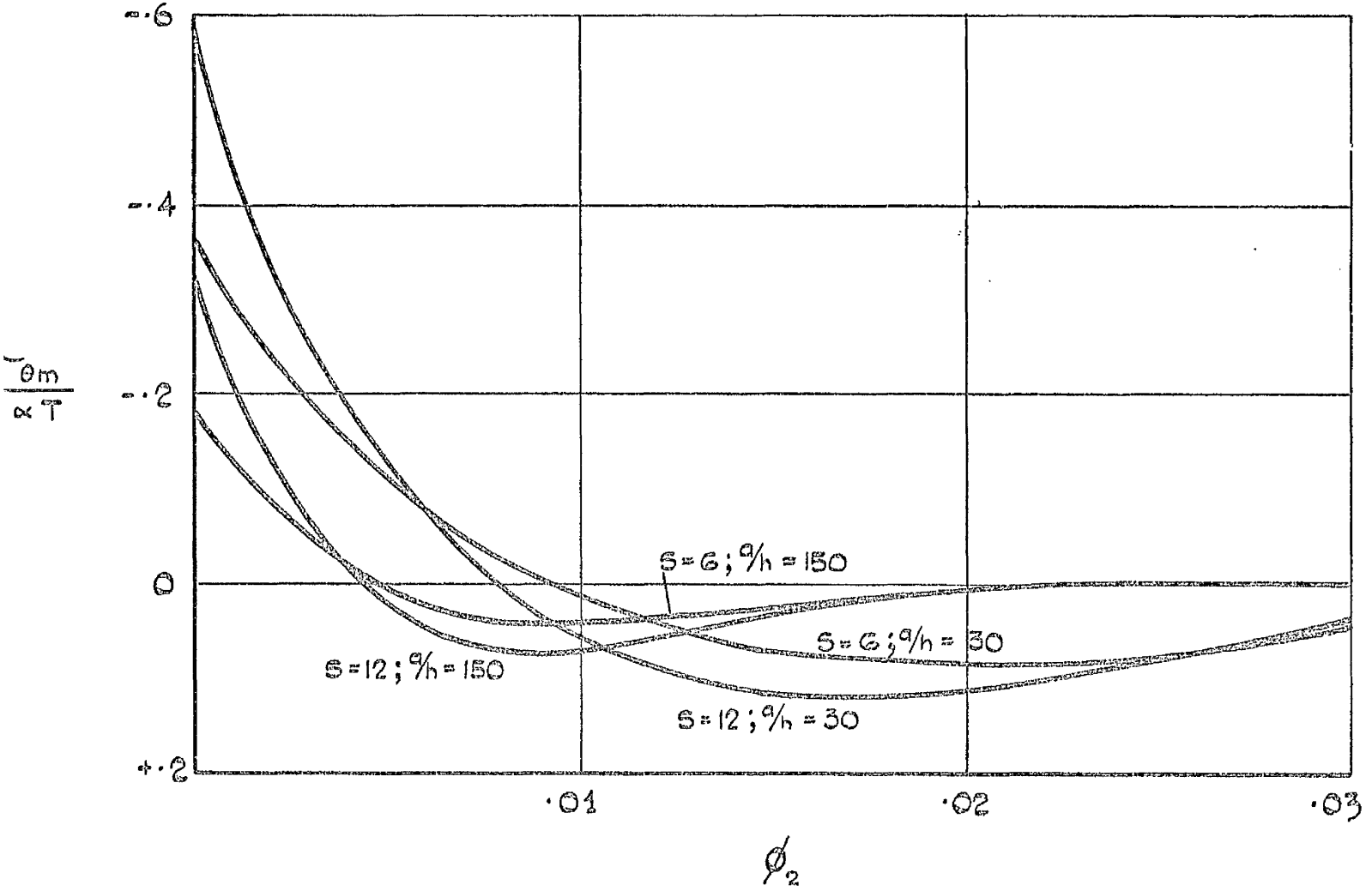


FIGURE (3.3) THE CIRCUMFERENTIAL MEMBRANE STRESS DISTRIBUTION INTO A SPHERICAL SHELL FROM A LINE OF TEMPERATURE T.

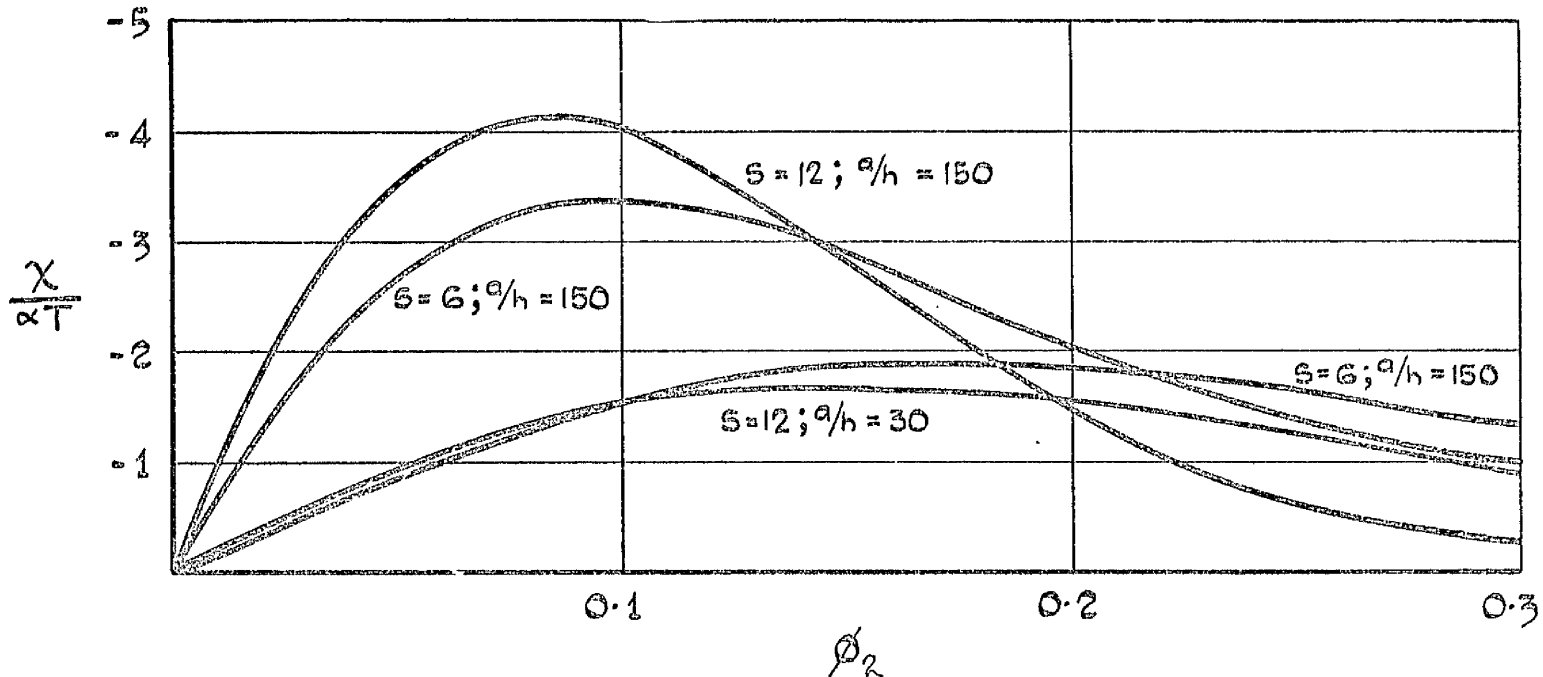


FIGURE (3.4) THE TANGENT ROTATION DISTRIBUTION INTO A SPHERICAL SHELL FROM A LINE OF TEMPERATURE \bar{T} .

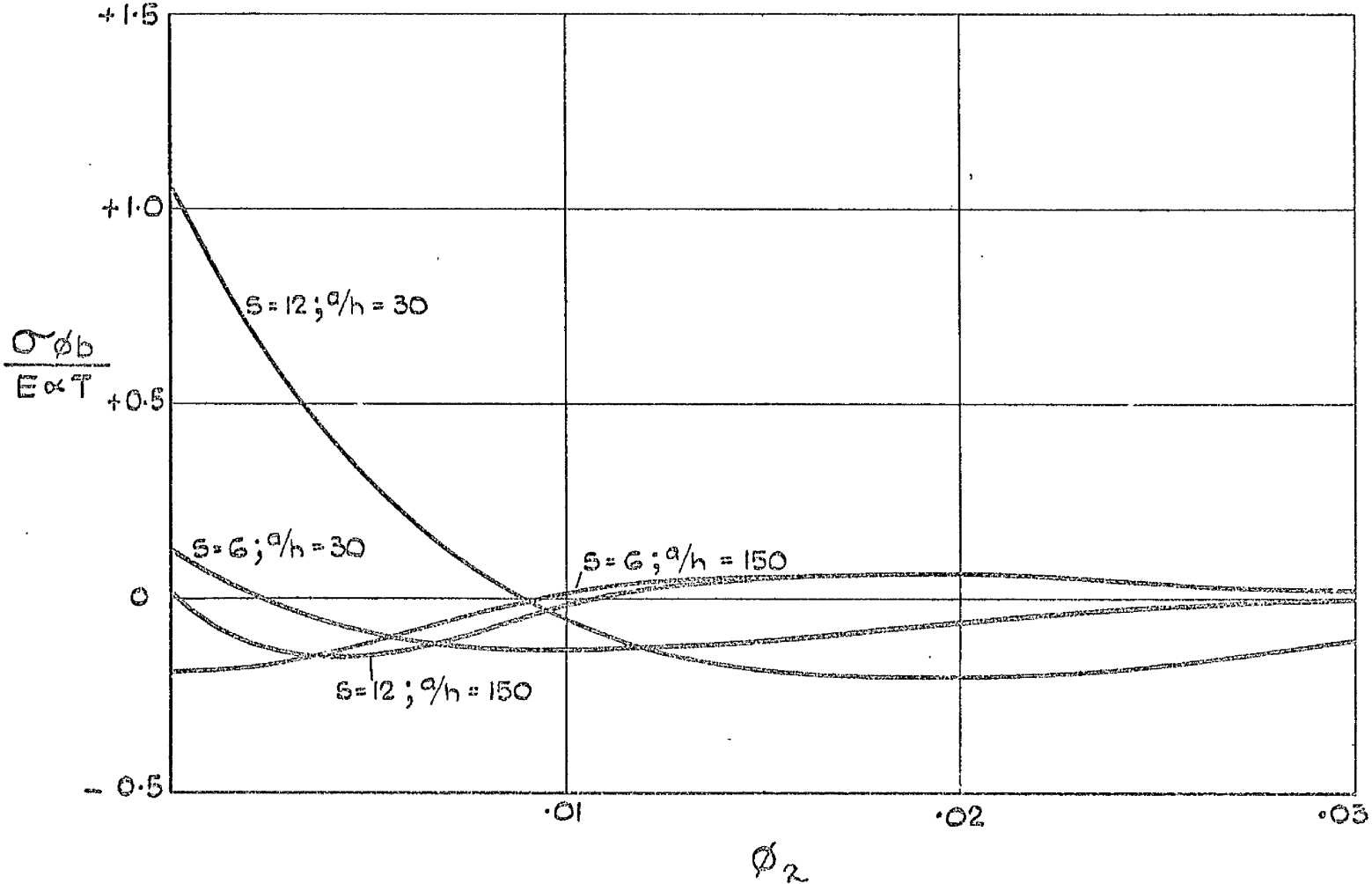


FIGURE (3.5) THE MERIDIONAL BENDING STRESS DISTRIBUTION INTO A SPHERICAL SHELL FROM A LINE OF TEMPERATURE \bar{T} .

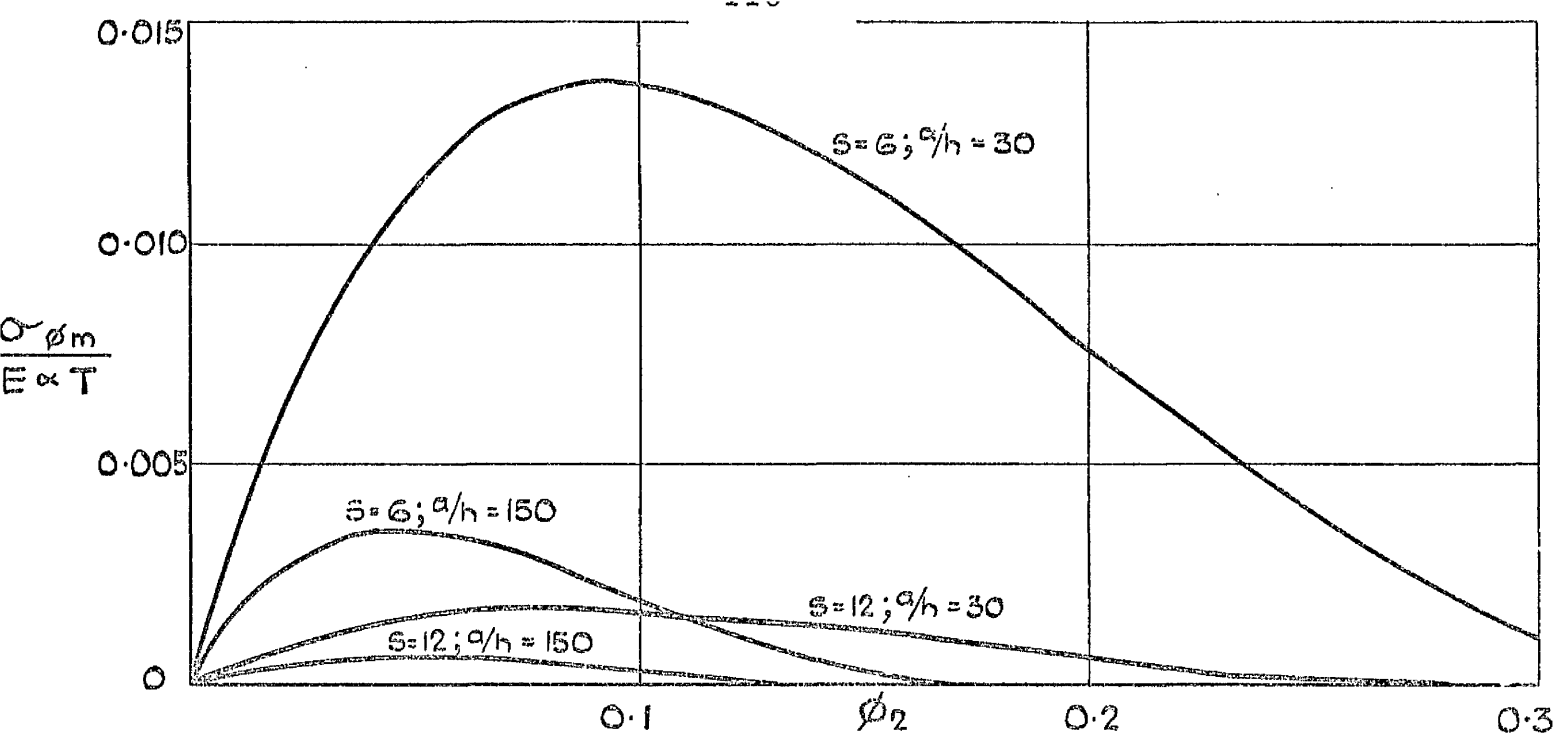


FIGURE (3.6) THE MERIDIONAL MEMBRANE STRESS DISTRIBUTION INTO A SPHERICAL SHELL FROM A LINE OF TEMPERATURE T .

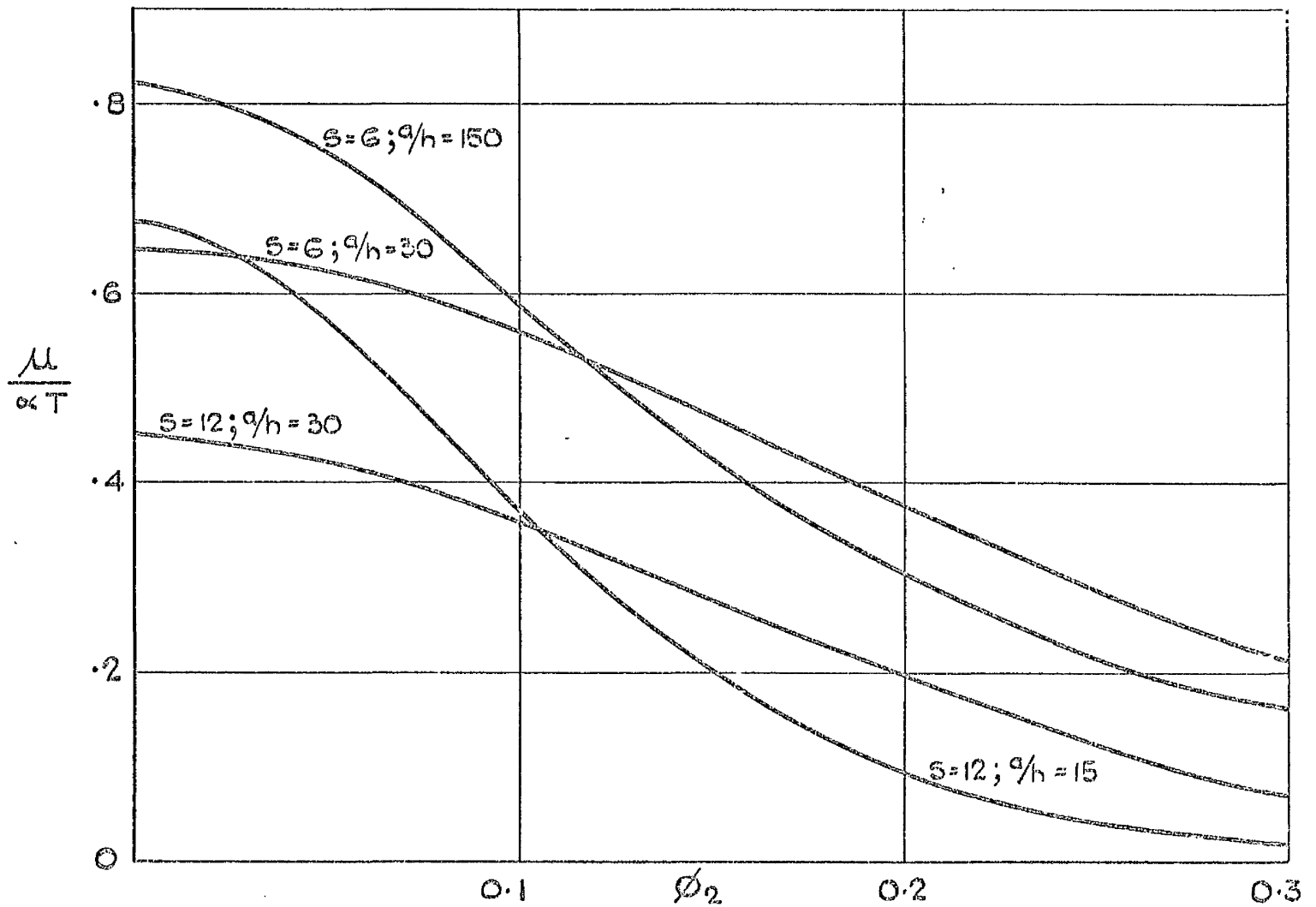


FIGURE (3.7) THE HORIZONTAL DISPLACEMENT DISTRIBUTION OF A SPHERICAL SHELL FROM A LINE OF TEMPERATURE T .

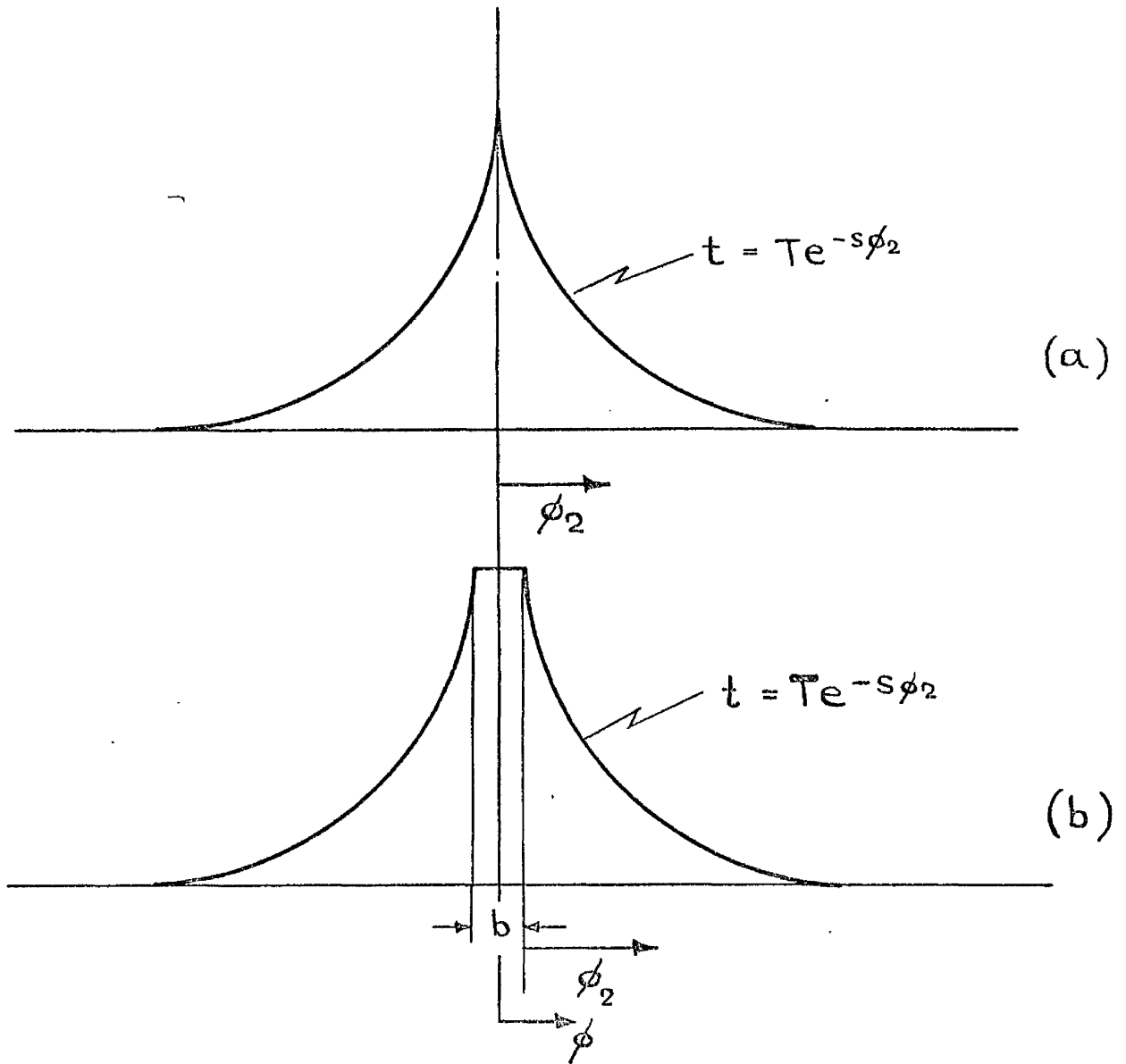


FIGURE (3.8) CROSS SECTION OF THE TEMPERATURE DISTRIBUTION DUE TO (a) A LINE OF TEMPERATURE (b) A BAND OF UNIFORM TEMPERATURE, AROUND A SPHERE.

and for two values of the shell parameter $\frac{a}{h}$ ($\frac{a}{h} = 30, \frac{a}{h} = 150$). Combinations of the same values of these parameters have been considered in the previous sets of graphs.

It is observed once more that the highest values of the stresses are likely to occur at the temperature boundary.

Larger values of the stresses are associated with larger values of S but with smaller values of $\frac{a}{h}$.

The maximum value of the meridional bending stress, which has a magnitude of $1.05 E \alpha T$ for $S = 12$ and $\frac{a}{h} = 30$ is very pronounced. In the circumferential direction the same combination of parameters give a total maximum stress of magnitude $0.82 E \alpha T$. These stresses are comparable in magnitude with those found in our previous problem at small heated openings.

It is noticed that the magnitudes of the stresses at the line of temperature depend upon the value of the ratio $\frac{S}{\alpha}$. Recalling from the earlier discussion, in the preceding section, that

$$\frac{S}{\alpha} \propto \left(\frac{S}{a/h}\right)^{\frac{1}{2}}$$

it is interesting to observe that two of the cases presented have very similar $\frac{S}{\alpha}$ ratios. These are

$$\frac{S}{\left(\frac{a}{h}\right)^{\frac{1}{2}}} = \frac{6}{\sqrt{30}} = 1.1$$

and

$$\frac{S}{\left(\frac{a}{h}\right)^{\frac{1}{2}}} = \frac{12}{\sqrt{150}} = 0.983$$

Examination of the various "line" values of the stresses for these two particular cases demonstrates that their values are very similar with the larger value being associated with the larger ratio. The "line" values of the horizontal displacement display, as before, are/

are contrary effect with a smaller displacement being associated with the larger s/α ratio.

It is recalled, from the earlier discussion, that when the parameter s/α is broken into its components

$$\frac{s}{\alpha} = \text{const} \sqrt{a}$$

Thus, as with the shell with the free opening, it is demonstrated that the magnitudes of the stress and displacement at the line of temperature depend upon the radius a that is upon the actual size of the sphere or of the cylinder.

CHAPTER 4

SHALLOW SPHERICAL SHELLS

Shallow Shell theory has been used, because of its great simplifications, to investigate localised effects in spherical shells. It has also been used in the investigation of the interaction effects between cylindrical nozzle and a spherical shell.

In this Chapter it is demonstrated that the Shallow Shell theory can be used to investigate certain problems involving thermal gradients even though much of the temperature field extends beyond that region of the shell which could properly be described as "shallow".

- 4.1 The Stress Resultants for a Symmetric Temperature
 Distribution on a Shallow Spherical Shell
 - (a) The Solution of the Linking Equations
 - (b) A Comparison with the Spherical Shell Theory

- 4.2 The Shallow Spherical Shell with the Uniformly
 Heated Axisymmetric Opening
 - (a) A Comparison of the Results with those for the
 Spherical Shell
 - (b) The Limiting Values of the Stress Resultants for
 Small Angles of Opening

- 4.3 The Shallow Shell Equations Expressed in
 Cartesian Co-ordinates

4.1 The Stress Resultants for a Symmetric Temperature Distribution on a Shallow Spherical Shell

To investigate the effects of thermal gradients near the apex of a spherical shell simplifying assumptions, of the type

$$\frac{\phi}{\sin \phi} = 1$$

could be made in the equations which have already been derived for the spherical shell.

Since the concept of "shallowness" is of such great importance in shell literature, because of the great simplifications it brings to the involved expressions for the stress resultants, it is of interest to see if it can be usefully applied to the problems which have already been considered. It could however have the added complication that the temperature field may extend beyond the region which could properly be considered as shallow. In this connection E. REISSNER⁽⁴⁸⁾, who did much of the pioneer work on shallow shell theory, indicates that a segment will be called shallow if the ratio of its height to base diameter is less than 1/8th

(this would indicate on our spherical shell the surface included by

$$\phi < 30^\circ)$$

4.1(a) The Solution of the Linking Equations

In his investigation of temperature hot spots CONRAD⁽³¹⁾ derived the equations for the shallow spherical shell including the temperature effects. Although CONRAD'S work will be discussed later, it is interesting at this point to observe that he likened the top portion of a sphere to a parabaloid of revolution whose equation he used. One can accept CONRAD'S two basic linked equations which are given in terms of the normal deflection W , positive inwards, and a stress function F . The deflection is shown in Figure (4.1a). These equations are

$$\begin{aligned} \nabla^4 W - \frac{1}{\alpha k} \nabla^2 F &= - \frac{1-\nu}{h} \alpha \nabla^2 \bar{t} \\ \nabla^4 F + \frac{D(1-\nu^2)}{a} \nabla^2 W &= -D(1-\nu^2) \alpha \nabla^2 \bar{t} \end{aligned} \tag{4.1-2}$$

where ∇^2 is the Laplacian operator, defined for this coordinate system as

$$\nabla^2(\dots) = \frac{d^2(\dots)}{dr^2} + \frac{1}{r} \frac{d(\dots)}{dr} \tag{4.3}$$

The relationships between the stress resultants and the dependent variables are, for the rotationally symmetric case,

$$\begin{aligned} Q_r &= -K (\nabla^2 W)' \\ N_r &= \frac{1}{r} F' \\ N_\theta &= F'' \\ M_r &= -K \left(\frac{1}{r} W'' + \nu \frac{W'}{r} \right) \\ M_\theta &= -K \left(\frac{1}{r} W' + \nu W'' \right) \\ \chi &= W' \end{aligned} \tag{4.4-9}$$

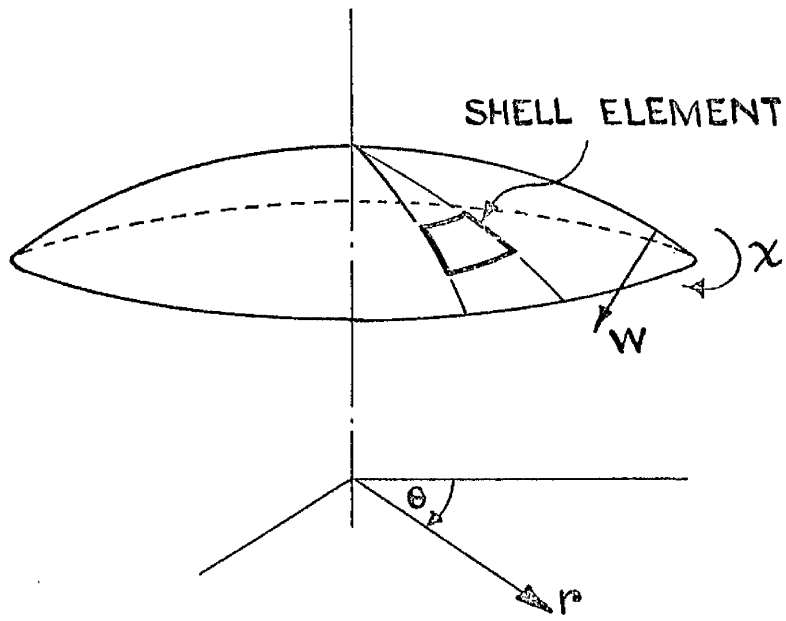


FIGURE (4.1a) SHELL ELEMENT OF A SHALLOW SPHERICAL SHELL

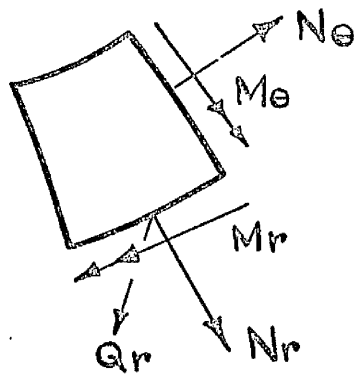


FIGURE (4.1b) STRESS RESULTANTS ON SHELL ELEMENT

where the primes denote differentiation with respect to r

Using the technique described by REISSNER the coupled equations (4.1-2) can be solved to give

$$F = A_1 \text{ber} z + A_2 \text{bei} z + A_3 \text{ker} z + A_4 \text{kei} z + A_5 \ln z + A_6 - \frac{Eh\alpha^2 s^2 t}{s^4 + 4\alpha^4}$$

$$W = \frac{2\alpha^2}{\alpha D(1-\nu^2)} (A_1 \text{bei} z - A_2 \text{ber} z + A_3 \text{kei} z - A_4 \text{ker} z) + A_7 \ln r + A_8 - \frac{4\alpha^4 \alpha t}{s^4 + 4\alpha^4}$$

4.10-11

where $z = \sqrt{2}\alpha \frac{r}{a}$.

After eliminating the constants of integration the stress resultants can be written as

$$F = A_1 \text{ber} z + A_2 \text{bei} z + A_3 \text{ker} z + A_4 \text{kei} z - \frac{Eh\alpha^2 s^2 t}{s^4 + 4\alpha^4}$$

$$W = \frac{2\alpha^2}{\alpha D(1-\nu^2)} (A_1 \text{bei} z - A_2 \text{ber} z + A_3 \text{kei} z - A_4 \text{ker} z) - \frac{4\alpha^4 \alpha t}{s^4 + 4\alpha^4}$$

$$N_r = \frac{2\alpha^2}{\alpha^2} \left(A_1 \frac{\text{ber}' z}{z} + A_2 \frac{\text{bei}' z}{z} + A_3 \frac{\text{ker}' z}{z} + A_4 \frac{\text{kei}' z}{z} \right) - \frac{\sqrt{2}\alpha Eh\alpha s^2 t}{(s^4 + 4\alpha^4) z}$$

$$N_\theta = \frac{2\alpha^2}{\alpha^2} \left[A_1 \left(-\text{bei} z - \frac{1}{z} \text{ber}' z \right) + A_2 \left(\text{ber} z - \frac{1}{z} \text{bei}' z \right) + A_3 \left(-\text{kei} z - \frac{1}{z} \text{ker}' z \right) + A_4 \left(\text{ker} z - \frac{1}{z} \text{kei}' z \right) \right] - \frac{Eh\alpha s^2}{s^4 + 4\alpha^4} \left(s^2 t - \sqrt{2}\alpha \frac{t}{z} \right)$$

$$M_r = -\frac{1}{\alpha} \left[A_1 (\text{ber}z - \frac{1-\nu}{z} \text{bei}'z) + A_2 (\text{ber}z + \frac{1-\nu}{z} \text{ber}'z) \right. \\ \left. + A_3 (\text{ker}z - \frac{1-\nu}{z} \text{kei}'z) + A_4 (\text{ker}z + \frac{1-\nu}{z} \text{ker}'z) \right] \\ + \frac{Eh\alpha}{S^4 + 4\alpha^4} \left[S^2 t - (1-\nu) \sqrt{2} \alpha \frac{t}{z} \right]$$

$$\chi = \frac{2\sqrt{2}\alpha^3}{\alpha^2 D (1-\nu^2)} (A_1 \text{bei}'z - A_2 \text{ber}'z + A_3 \text{kei}'z - A_4 \text{ker}'z) \\ - \frac{4\alpha^4 \alpha t}{S^4 + 4\alpha^4}$$

$$u = \frac{r}{Eh} [N_\theta - \nu N_r] + r\alpha t$$

4.12 - 18

For convenience and consistency with earlier sections the primes and the dots imply

$$\text{ber}'z \equiv \frac{d(\text{ber}z)}{dz} \quad ; \quad (\dots)' \equiv \frac{d(\dots)}{d\left(\frac{r}{\alpha}\right)}$$

This latter operator is used since in the range of the shallow shell

$$\frac{r}{\alpha} \approx \phi$$

and this affords direct comparison with the general spherical shell theory.

4.1(b)

A Comparison with the Spherical Shell Theory

In Chapter 2 was developed, in equation (2.16), the expression for the stress resultant, N_ϕ , in a spherical shell as

$$N_\phi = -\cot\phi \left(\frac{\phi}{\sin\phi}\right)^{\frac{1}{2}} (A_1 \text{ber}'z + A_2 \text{bei}'z + A_3 \text{ker}'z + A_4 \text{kei}'z) - A \cot\phi \cdot t$$

For small values of the angle ϕ if the following assumptions are made

$$\begin{aligned} \frac{\phi}{\sin\phi} &\approx 1 \\ \cot\phi &\approx \phi^{-1} \\ \phi &\approx \frac{r}{a} \end{aligned}$$

then they lead to

$$N_\phi = -\frac{a}{r} \left(A_1 \text{ber}'\sqrt{2}\alpha\frac{r}{a} + A_2 \text{bei}'\sqrt{2}\alpha\frac{r}{a} + A_3 \text{ker}'\sqrt{2}\alpha\frac{r}{a} + A_4 \text{kei}'\sqrt{2}\alpha\frac{r}{a} \right) - A \frac{a}{r} t$$

We see immediately that the form of this agrees with the complementary function portion of equations (4.14) for N_r in a shallow spherical shell.

To compare the particular integral portions we must examine the constant A in equation (2.16) in more detail. It has the value, equation (2.14), of

$$A = \frac{E h \alpha (S^2 + 1 - \nu)}{(S^2 + 1)^2 + 4\alpha^4}$$

When it is realised that $4\alpha^4$ is a very large number and that $|\nu| < 1$ then it can be seen that the two solutions are perfectly compatible, within a small order of magnitude, for all values of S .

It can therefore be concluded that the equations which have been developed using the shallow shell theory appear to be in agreement, over the appropriate range of the sphere, with the general expressions of Chapter 2 which were based upon Langer's Asymptotic Equation. It will be of interest now to compare actual numerical results from both theories and this shall be done in the next section.

4.2 The Shallow Spherical Shell with the Uniformly Heated Axisymmetric Opening

This problem has already been considered for the general case of the spherical shell and for the case of large angles of opening. One can now specialise the problem for small angles of opening and use the theory which has just been developed for shallow spherical shells.

In the previous Chapters were postulated the boundary conditions, for this particular problem, as

$$\begin{aligned} N_{r_1} &= M_{r_1} = 0 \\ t_1 &= T \end{aligned}$$

where the small subscript 1 refers to the conditions at the unrestrained opening at $r = r_1$. Further assume, as was also done previously, that the temperature distribution into the shell is described by the equation (1.6) as

$$\nabla^2 t = \frac{\Sigma^2}{a^2} t$$

and that the temperature gradient becomes zero within the boundaries of the shell.

After equation (1.7) the temperature at any point is given by

$$t = A K_0\left(\frac{\Sigma r}{a}\right) + B I_0\left(\frac{\Sigma r}{a}\right)$$

Substituting for the temperature boundary conditions this equation becomes

$$t = T \frac{K_0\left(\frac{\Sigma r}{a}\right)}{K_0\left(\frac{\Sigma r_1}{a}\right)}$$

and, upon differentiating, it gives

$$\frac{dt}{dr} = -T \frac{s}{a} \frac{K_1\left(\frac{sr}{a}\right)}{K_0\left(\frac{sr}{a}\right)} \quad 4.20$$

so that the value of the temperature gradient at the opening is

$$\left(\frac{dt}{dr}\right)_1 = -T \frac{s}{a} \frac{K_1\left(\frac{sr_1}{a}\right)}{K_0\left(\frac{sr_1}{a}\right)} \quad 4.21$$

Now use the stress free boundary conditions. They give

$$N_{r_1} = 0 = \frac{2\alpha^2}{a^2} \left(A_3 \frac{\ker' z_1}{z_1} + A_4 \frac{\kei' z_1}{z_1} \right) - \frac{\sqrt{2}\alpha Ehs^2 t_1}{(s^4 + 4\alpha^4) z_1}$$

$$M_{r_1} = 0 = -\frac{1}{a} \left\{ A_3 \left[\ker z_1 - (1-\nu) \frac{\kei' z_1}{z_1} \right] + A_4 \left[\kei z_1 - (1-\nu) \frac{\ker' z_1}{z_1} \right] \right. \\ \left. + \frac{Eha\alpha}{s^4 + 4\alpha^4} \left[s^2 T - (1-\nu) \sqrt{2}\alpha \frac{t_1}{z_1} \right] \right\}$$

and can be more conveniently expressed in a matrix form as

$$\begin{bmatrix} 0 \\ 0 \end{bmatrix} = \begin{bmatrix} \frac{2\alpha^2}{a^2} \frac{\ker' z_1}{z_1} & \frac{2\alpha^2}{a^2} \frac{\kei' z_1}{z_1} \\ -\left(\ker z_1 - \frac{1-\nu}{z_1} \kei' z_1\right) \frac{1}{a} & -\left(\kei z_1 + \frac{1-\nu}{z_1} \ker' z_1\right) \frac{1}{a} \end{bmatrix} \begin{bmatrix} A_3 \\ A_4 \end{bmatrix} + \frac{Eha}{s^4 + 4\alpha^4} \begin{bmatrix} -\sqrt{2}\alpha s^2 t_1 \\ \alpha \left[s^2 T - (1-\nu) \sqrt{2}\alpha \frac{t_1}{z_1} \right] \end{bmatrix}$$

This matrix can be transposed to yield

$$\begin{bmatrix} A_3 \\ A_4 \end{bmatrix} = \frac{Eha}{\Delta (s^4 + 4\alpha^4)} \begin{bmatrix} -\ker z_1 - \frac{1-\nu}{z_1} \ker' z_1 & -\frac{2\alpha^2}{a^2} \frac{\kei' z_1}{z_1} \\ \ker z_1 + \frac{1-\nu}{z_1} \kei' z_1 & \frac{2\alpha^2}{a^2} \frac{\ker' z_1}{z_1} \end{bmatrix} \begin{bmatrix} \sqrt{2}\alpha s^2 t_1 \\ -s^2 T + (1-\nu) \sqrt{2}\alpha \frac{t_1}{z_1} \end{bmatrix} \quad 4.22$$

where

$$\Delta = \frac{2\alpha^2}{a^2} \left\{ \frac{\text{ker}'z_1}{z_1} \left(-\text{kei}z_1 - \frac{1-\nu}{z_1} \text{ker}'z_1 \right) - \frac{\text{kei}'z_1}{z_1} \left(-\text{ker}z_1 + \frac{1-\nu}{z_1} \text{kei}'z_1 \right) \right\}$$

One can now substitute these constants of integration back into the equations (4.12 - 18) to give the full solution, for the stress resultants and displacement, of the problem.

4.2(a) A Comparison of the Results with those for the Spherical Shell

The values of the stress resultants have been computed for a range of opening values. The values of the parameters used were the same as those of the spherical shell. The computed results are tabulated in Tables (4.1 - 2) alongside the corresponding values obtained using our general spherical shell equations. Although only the "opening" values are presented, it is appreciated from the earlier work that these are usually the maximum values of the particular "effect" examined. In fact the stress resultants into the shell from various size of opening were also computed. Their values and the relative divergence from the spherical shell results merely parallel the opening values which are shown tabulated. For that reason and since a fair sample would have to be shown, they are not presented.

One can conclude from these tabulated results that it is possible, with a fair degree of accuracy, to use the shallow shell theory. In effect, one can use the shallow shell theory for temperature problems in situations where one would be using the normal/

	Z ₁	1	2	3	4	5	6	7	8	9	10	11	12
$\frac{\sigma_{1em}}{E\alpha C}$	$\phi_1 \approx \frac{r_1}{a}$.0576	.1152	.1728	.2304	.2880	.3456	.4032	.4608	.5184	.5760	.6335	.6911
	Shallow Shell	.4008	.1414	.0701	.0416	.0276	.0196	.0147	.0114	.0092	.0076	.0064	.0054
$\frac{\sigma_{1eb}}{E\alpha C}$	General Shell	.3985	.1392	.0685	.0402	.0262	.0183	.0134	.0102	.0080	.0064	.0052	.0042
	Shallow Shell	.5856	.2435	.1301	.0805	.0547	.0396	.0301	.0237	.0192	.0159	.0134	.0115
$\frac{\chi_1}{\alpha C}$	General Shell	.5886	.2440	.1297	.0797	.0537	.0385	.0288	.0223	.0177	.0143	.0118	.0098
	Shallow Shell	6.071	5.049	4.046	3.339	2.836	2.467	2.186	1.967	1.792	1.650	1.533	1.435
$\frac{\chi_1}{\alpha C}$	General Shell	6.109	5.081	4.076	3.366	2.863	2.492	2.211	1.992	1.817	1.675	1.558	1.461

Table 4.1 A comparison between the opening values obtained by the shallow shell theory and by the general shell theory for a free heated opening in a spherical shell with $\nu = 0.255$, $\mu = 90$ and $S = 0$.

Z	1	2	3	4	5	6	7	8	9	10	11	12
$\phi \approx \frac{r_1}{d}$.0576	.1152	.1728	.2304	.2880	.3456	.4032	.4608	.5184	.5760	.6335	.6911
Shallow Shell	.3765	.2616	.2169	.1944	.1812	*	.1665	.1622	.1587	.1562	.1549	.1546
General Shell	.3743	.2591	.2142	.1915	.1780	.1691	.1629	.1583	.1547	.1520	.1505	.1485
Shallow Shell	.3404	.2126	.1491	.1134	.0911	*	.0649	.0566	.0502	.0450	.0403	.0361
General Shell	.3422	.2128	.1483	.1118	.0888	.0730	.0614	.0526	.0457	.0399	.0347	.0307
Shallow Shell	3.529	4.409	4.637	4.702	4.720	*	4.710	4.694	4.688	4.665	4.598	4.492
General Shell	3.552	4.432	4.653	4.720	4.736	4.732	4.717	4.700	4.690	4.663	4.593	4.577

Table 4.2 A comparison between the opening values obtained by the shallow shell theory, and by the general shell theory for a free heated opening in a spherical shell with $\nu = 0.255$, $\mu = 90$ and $S = 9$.

* Computer failure.

normal shallow shell theory. One of these situations is the meeting of a cylindrical shell with a shallow shell and since this is such an important problem the next Chapter is devoted entirely to it.

4.2(b) The Limiting Values of the Stress Resultants for Small Angles of Opening

The graphs presented in Chapter 2 for the opening values of the stresses and the displacements in a spherical shell, with a free heated opening, indicated that as the angle of opening was reduced to zero, these values tended to the same limit as for a flat plate under the same conditions. The more simple shallow shell equations enable this phenomena to be examined in some detail.

For small values of the argument the asymptotic form of the Kelvin functions is

$$\begin{aligned}
 \text{ker } z &= -\ln z + 0.1159 + \frac{\pi z^2}{16} + \dots \\
 \text{kei } z &= -\frac{z^2}{4} \ln z - \frac{\pi}{4} + 1.1159 \frac{z^2}{4} + \dots \\
 z^{-1} \text{ker}' z &= -z^{-2} + \frac{\pi}{8} + \frac{z^2}{16} \ln z + \dots \\
 z^{-1} \text{kei}' z &= -\frac{1}{2} \ln z - \frac{1}{4} + 0.558 + \dots \quad 4.23
 \end{aligned}$$

Since the limiting case is being considered where

$\phi \rightarrow 0$ and hence $z \rightarrow 0$ then it would be sufficient to take

$$\begin{aligned}
 \text{ker } z &\approx -\ln z \\
 \text{kei } z &\approx -\frac{\pi}{4} \\
 z^{-1} \text{ker}' z &\approx \frac{z^2}{16} \ln z - z^{-2} \\
 z^{-1} \text{kei}' z &\approx -\frac{1}{2} \ln z \quad . \quad 4.24
 \end{aligned}$$

Examine first the circumferential stress resultant which after equation (4.30) is, in matrix notation,

$$N_{\theta} = \frac{2\alpha^2}{a^2} \begin{bmatrix} -keiz - \frac{1}{z} ker'z & kerz - \frac{1}{z} keiz' \end{bmatrix} \begin{bmatrix} A_3 \\ A_4 \end{bmatrix} - \frac{EhS^2\alpha}{S^4 + 4\alpha^4} (S^2t - \sqrt{2}\alpha \frac{t'}{z})$$

For the particular problem of the free heated opening the integration constants A_3 and A_4 have the value given in equations (4.22).

Substituting therefore for them in the above equation yields

$$N_{\theta} = \frac{2\alpha^2}{a^2} \begin{bmatrix} -keiz - \frac{1}{z} ker'z & kerz - \frac{1}{z} keiz' \end{bmatrix} \begin{bmatrix} -keiz_1 - \frac{1-\nu}{z_1} ker'z_1 & -\frac{2\alpha^2}{a^2} \frac{keiz_1'}{z_1} \\ + kerz_1 - \frac{1-\nu}{z_1} keiz_1' & \frac{2\alpha^2}{a^2} \frac{ker'z_1}{z_1} \end{bmatrix}$$

$$\begin{bmatrix} \sqrt{2}\alpha S^2 t_1' \\ -S^2 T + (1-\nu)\frac{\sqrt{2}\alpha t_1'}{z_1} \end{bmatrix} \frac{Eh\alpha}{(S^4 + 4\alpha^4)\Delta} - \frac{EhS^2\alpha}{S^4 + 4\alpha^4} (S^2t - \sqrt{2}\alpha \frac{t'}{z})$$

where, as before,

$$\Delta = \frac{2\alpha^2}{a^2} \left\{ \frac{ker'z_1}{z_1} \left(-keiz_1 - \frac{1-\nu}{z_1} ker'z_1 \right) - \frac{keiz_1'}{z_1} \left(-kerz_1 + \frac{1-\nu}{z_1} keiz_1' \right) \right\}$$

For simplicity first consider the limiting value of this denominator Δ by substituting into it the appropriate values from equations (4.24). It becomes

$$\Delta \approx \frac{2\alpha^2}{a^2} \left\{ \left(-\frac{1}{z_1} + \frac{\pi}{8} \right) \left[\frac{\pi}{4} - (1-\nu)\chi - \frac{1}{z_1} + \frac{\pi}{8} \right] - \left(\frac{1}{2} \ln z_1 + 0.308 \right) \left[\ln z - 0.1159 + (1-\nu) \left(\frac{1}{2} \ln z + 0.308 \right) \right] \right\}$$

which with a rearrangement of terms, is

$$\Delta_{z_1 \rightarrow 0} \approx \frac{2\alpha^2}{a^2} \frac{1}{Z^4} \left\{ -(1-\nu) - \frac{1}{4}(1-\nu) Z_1^4 \ln 2Z_1 + \text{terms involving powers of } z_1 \right\}$$

It is observed that the lowest powers of Z_1 in the numerator of N_{θ} also involve Z_1^{-4} . One can therefore consider multiplying both the numerator and the denominator by Z_1^4 before taking the limit as $Z_1 \rightarrow 0$. This would greatly simplify the task. One need only include terms of the order of Z^{-4} when evaluating the matrix since all the other terms will eventually tend to zero.

Substituting from the equations (4.24) in the expression for N_{θ_1} and following the method as described above, gives

$$N_{\theta_1} = \frac{Eh\alpha}{S^4 + 4\alpha^4} \left\{ -\sqrt{2}\alpha S^2 \frac{t_1}{Z_1} - 2\alpha^2 \sqrt{2}\alpha t_1 Z_1 \ln Z_1 - \left(S^4 T - \frac{S^2 \sqrt{2}\alpha t_1}{Z_1} \right) \right\}$$

This can be simplified to

$$N_{\theta_1} = \frac{Eh\alpha T}{S^4 + 4\alpha^4} \left(-2\sqrt{2}\alpha^3 \frac{t_1}{T} Z_1 \ln Z_1 - S^4 \right)$$

4.25

Recalling from equation (4.20) that the expression for the temperature gradient is

$$\frac{dt}{dr} = -\frac{S}{a} \frac{T K_1\left(\frac{sr}{a}\right)}{K_0\left(\frac{sr}{a}\right)}$$

hence

$$t_1 \equiv \left[\frac{dt}{d\left(\frac{r}{a}\right)} \right]_1 = -ST \frac{K_1\left(\frac{sr}{a}\right)}{K_0\left(\frac{sr}{a}\right)}$$

For small arguments the asymptotic values of these Modified Bessel functions are

$$K_0(x) \approx -\ln x$$

$$K_1(x) \approx x^{-1}$$

Hence the expression

$$\frac{t_1}{T} z_1 \ln z_1 \approx \frac{s z_1 \ln z_1}{s \left(\frac{r_1}{a}\right) \ln \frac{s r_1}{a}}$$

Further, since $z_1 = \sqrt{2} \alpha \frac{r_1}{a}$ this expression reduces in the limit to

$$\frac{t_1}{T} z_1 \ln z_1 \approx \sqrt{2} \alpha$$

Substituting this value back in equation (4.25) it gives

$$N_{\theta_1} = \frac{E h \alpha T}{s^4 + 4 \alpha^4} (-4 \alpha^4 - s^4) = -E h \alpha T$$

$$\text{lt. as } \begin{matrix} \phi \rightarrow 0 \\ r_1 \rightarrow 0 \end{matrix} \quad 4.26$$

Equation (4.18) has for the opening value of the horizontal displacement

$$\left(\frac{u}{r}\right)_1 = \frac{1}{E h} N_{\theta_1} + \alpha T$$

Using the result of equation (4.26) this becomes

$$\left(\frac{u}{r}\right)_1 = 0$$

$$\text{lt. } r_1 \rightarrow 0$$

In a similar manner it can also be shown that

$$M_{r_1} = \chi_1 = 0$$

$$\text{lt. as } r_1 \rightarrow 0$$

These results for the various limiting values confirm the graphical results as presented in Chapter 2. Further, as has been already stated, these values are the same as the appropriate values for a flat plate. It must however be emphasised again that this correspondence is only true at the limit where r approaches zero and it would not appear practical to consider the spherical shell as a flat plate. Indeed this is well illustrated in Chapter 7 where very small opening values are considered and the corresponding stresses are evaluated. It is shown there that the bending stresses are considerable.

It is of interest to note that HICKS⁽⁶⁰⁾ in his analysis of small holes (and similarly in analysis by WATERS⁽⁶¹⁾) makes the assumption that regions of the pressure vessel local to the opening can be treated as a flat plate. PENNY⁽³⁵⁾ suggests that such treatment will be of limited application. This appears to be the case for the thermal gradients which have been examined.

4.3 The Shallow Shell Equations Expressed in Cartesian Co-ordinates

The linking equations (4.1 - 2) express the normal deflection W and the stress function F in the cartesian co-ordinate system provided the Laplacian Operator reads

$$\nabla^2(\dots) \equiv \frac{\partial^2(\dots)}{\partial x^2} + \frac{\partial^2(\dots)}{\partial y^2} \tag{4.27}$$

and where the co-ordinates x and y are as shown in Figure (4.2). Separate these linked equations by acting upon equation (4.1) with the operator ∇^2 , multiplying equation (4.2) by $(\alpha K)^{-1}$ and then adding the resulting equations to give

$$\nabla^6 W + \frac{4\alpha^4}{a^4} \nabla^2 W = \frac{4\alpha^4}{a^3} \alpha \nabla^2 t \tag{4.28}$$

This equation may be specialised for the single dimensional problem if there is no variation of W in the y direction and the operator then becomes

$$\nabla^2(\dots) \equiv \frac{\partial^2(\dots)}{\partial x^2} \tag{4.29}$$

The solution for the complementary function of equation (4.28) for this case is

$$W = e^{+\frac{\alpha x}{a}} \left[A_1 \cos \frac{\alpha x}{a} + A_2 \sin \frac{\alpha x}{a} \right] + e^{-\frac{\alpha x}{a}} \left[A_3 \cos \frac{\alpha x}{a} + A_4 \sin \frac{\alpha x}{a} \right] + A_5 x + A_6 \tag{4.30}$$

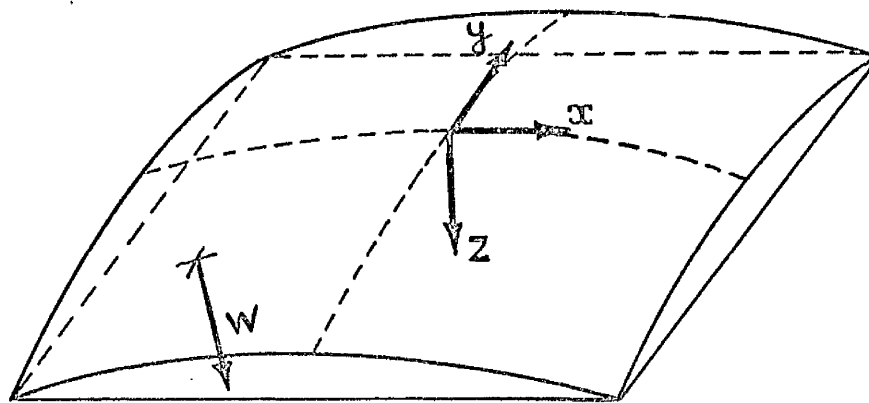


FIGURE (4.2) SHALLOW SHELL WITH CARTESIAN CO-ORDINATE SYSTEM SHOWING POSITIVE DIRECTION OF DISPLACEMENT W .

To find the appropriate particular integral one may use the well tried technique of proposing that

$$W = At$$

where A is some constant to be determined.

After substituting for W in equation (4.28) and recalling from Chapter 1 and section 4.2 that

$$\nabla^2 t = \frac{s^2}{a^2} t$$

for such linear cases it yields

$$A = \frac{-4\alpha^4}{s^4 + 4\alpha^4} \cdot a\alpha$$

The general solution of equation (4.28) for W is therefore

$$W = e^{\frac{+\alpha x}{a}} \left[A_1 \cos \frac{\alpha x}{a} + A_2 \sin \frac{\alpha x}{a} \right] + e^{\frac{-\alpha x}{a}} \left[A_3 \cos \frac{\alpha x}{a} + A_4 \sin \frac{\alpha x}{a} \right] + A_5 x + A_6 - \frac{4\alpha^4}{s^4 + 4\alpha^4} \cdot a\alpha t$$

4.31

The constant A_6 , which represents a rigid body movement, can be discarded and if the geometric compatibility of the shell portion is examined it can show that the constant A_5 is also zero.

It is observed that this solution for W is the same as the solution for U , equation (3.31), obtained using the GECKELER assumptions for large angles of opening. It is recalled that the GECKELER solution is the solution for cylindrical shells.

It would appear that the shallow shell solutions are compatible, at the equator of the shell, to the GECKELER solutions of /

of Chapter 3.

The shallow shell equations in cartesian co-ordinates have been used by many researchers including GRADOWCZYK ⁽³⁰⁾ CONRAD ⁽³¹⁾ and BOUMA ⁽³⁴⁾

These cartesian forms of the shell equations are developed at this stage and are made use of in subsequent Chapters.

CHAPTER 5

STRESS CONCENTRATIONS AT THE JUNCTION
OF A UNIFORMLY HEATED CYLINDRICAL SHELL
AND A SHALLOW SPHERICAL SHELL

The problem of determining the stress distribution in a shallow spherical shell which is joined to a heated cylindrical shell is considered. It is assumed that the cylindrical shell is at a uniform elevated temperature and that the thermal gradients into the spherical shell are as described in Chapter I.

The problem is evaluated in matrix notation and the final results computed.

It is demonstrated that this problem is the general case since the two limiting values of thickness ratio describe respectively a free opening and a rigid insert.

The results presented are for various common thickness ratios of cylinder to sphere and indicate therefore the possible variations in the magnitudes of the stresses at a spherical shell opening with differing boundary conditions.

5.1 The Heated Cylinder and the Shallow Spherical Shell

- (a) The Equations for the Cylindrical Shell
- (b) The Equations for the Shallow Spherical Shell
- (c) The Linked Equations for the Two Shell Forms
- (d) Computed Results
- (e) Conclusions and Observations

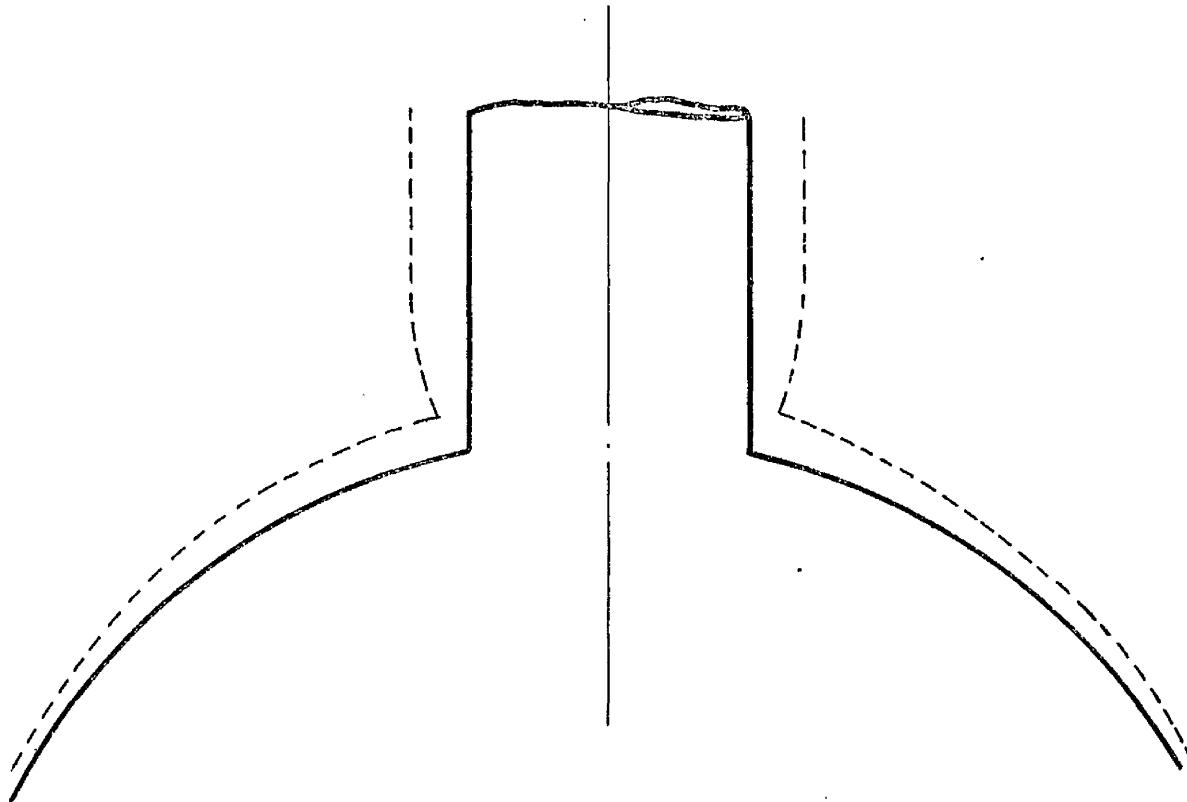


FIGURE (5.1) INTERACTION OF A HEATED CYLINDRICAL SHELL WITH A SHALLOW SPHERICAL SHELL.

5.1 The Heated Cylinder and the Shallow Spherical Shell

The problems associated with the interaction between cylindrical and spherical shells have been considered by a number of authors for various loading conditions. BIJLAARD⁽³⁸⁾, in his work for the Welding Research Council, has considered many of the local loading effects transferred from a pipe to a shallow spherical shell. Mention must also be made of the many papers presented at the symposium on Reactor Containment Buildings and Nuclear Pressure Vessels held in the Royal College of Science and Technology. Many of the papers demonstrate the value of the matrix approach to the interaction problems where complex cases can be presented with greater clarity. Perhaps one paper in particular could be referred to - 'Stresses at the Junction of Pressure Vessel and Duct' by PENNY⁽³⁵⁾, as being relevant to the method which is now followed.

Let us first define the problem. A cylindrical shell is joined axisymmetrically to a spherical shell as shown in Figure (5.1). For simplicity of computation one can, like BIJLAARD, use the shallow shell theory for the spherical shell portion. This limits somewhat the range of application but allows the problem to be programmed for a small computer like Sirius. This point is elaborated in Appendix 1 where the computational difficulties are discussed. The cylinder is now assumed to be heated to a uniform temperature and the spherical shell to have a steady state temperature distribution which is defined by the relationships investigated in Chapter 1.

5.1(a) The Equation for the Cylindrical Shell

For an open cylindrical shell heated to a uniform temperature T , the following relationships between the edge loadings and the corresponding deflections are given by TIMOSHENKO;

$$W_c = \frac{-1}{2\beta^3 K} (\beta M_c + Q_c) - R\alpha_c T$$

$$\chi_c = \frac{1}{2\beta^2 K} (2\beta M_c + Q_c)$$

5.1 - 2

where the shell constant β is defined by

$$4\beta^4 = \frac{12(1-\nu^2)}{R^2 h_c^2}$$

The small subscript c is used to refer to the cylinder and the sign convention, which is of great importance, is as shown in Figure (5.2). The above equations have been used earlier in Chapter 3, where mention was made of their association with the work of HETENYI.

In order to express these equations in a more suitable form for linking to the shallow shell equations, introduce a new parameter γ where

$$4\gamma^4 = 12(1-\nu^2) \frac{R^2}{h_c^2} = 4R^4\beta^4 \quad 5.3$$

which parameter corresponds more closely to \mathfrak{X} , the parameter for the spherical shell. Rewriting equations (5.1 - 2) in matrix notation and introducing this new parameter gives

$$\begin{bmatrix} -\chi_c \\ -\frac{W_c}{R} \end{bmatrix} = \frac{2\gamma^2}{E_c h_c} \begin{bmatrix} -1 & -2\gamma \\ \frac{1}{\gamma} & 1 \end{bmatrix} \begin{bmatrix} Q_c \\ \frac{M_c}{R} \end{bmatrix} + \begin{bmatrix} 0 \\ \alpha_c T \end{bmatrix} \quad 5.4$$

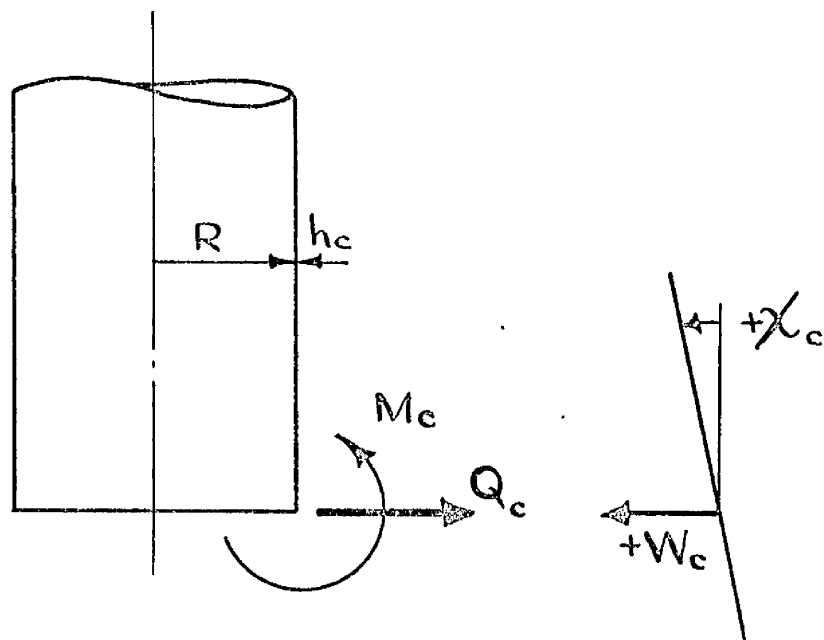


FIGURE (5.2) SIGN CONVENTION FOR A CYLINDRICAL SHELL.

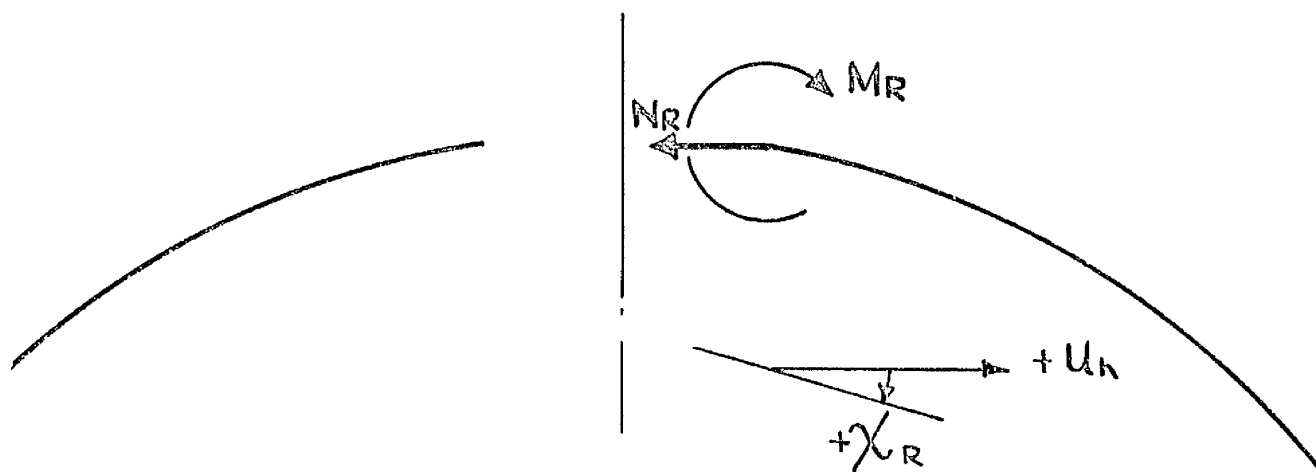


FIGURE (5.3) SIGN CONVENTION FOR A SHALLOW SPHERICAL SHELL.

A still more suitable form of expression of these equations for subsequent matching is

$$\begin{bmatrix} -\chi_c \\ -\frac{w_c}{R} \end{bmatrix} = \frac{2\gamma^2}{Ech_c} \begin{bmatrix} M_1 \end{bmatrix} \begin{bmatrix} Q_c \\ \frac{M_c}{a} \end{bmatrix} + \begin{bmatrix} 0 \\ \alpha_c T \end{bmatrix} \quad 5.5$$

where the matrix $[M_1]$ is

$$M_1 = \begin{bmatrix} -1 & -\frac{2\gamma a}{R} \\ \frac{1}{\gamma} & \frac{a}{R} \end{bmatrix} \quad 5.6$$

5.1(b) The Equation for the Shallow Spherical Shell

In Chapter 4 the equations (4.12 - 18) were developed for the stress resultants and the displacements in an open shallow spherical shell which has a temperature distribution described by

$$\nabla^2 t = \frac{s^2}{a^2} t$$

The sign convention for the shallow shell is shown, once again, in Figure (5.3).

The stress resultants N_r and M_r at the boundary $r = R$ can be written as

$$\begin{bmatrix} N_r \\ \frac{M_r}{a} \end{bmatrix} = \begin{bmatrix} M_2 \end{bmatrix} \begin{bmatrix} \frac{A_3}{a^2} \\ \frac{A_4}{a^2} \end{bmatrix} - \frac{Eh\alpha}{5^4 + 4\alpha^4} \begin{bmatrix} M_3 \end{bmatrix} \quad 5.7$$

where the matrices $[M_2]$ and $[M_3]$ are

$$[M_2] = \begin{bmatrix} 2\alpha^2 \frac{\text{ker}' z_1}{z_1} & 2\alpha^2 \frac{\text{kei}' z_1}{z_1} \\ -\text{ker} z_1 + \frac{1-\nu}{z_1} \text{kei}' z_1 & -\text{kei} z_1 - \frac{1-\nu}{z_1} \text{ker}' z_1 \end{bmatrix}$$

$$[M_3] = \begin{bmatrix} S^2 \sqrt{2} \alpha \frac{T'}{z_1} \\ -S^2 T + (1-\nu) \sqrt{2} \alpha \frac{T'}{z_1} \end{bmatrix}$$

and

$$z_1 = \sqrt{2} \alpha \frac{R}{a}$$

$$T' = \left(\frac{dt}{d\left(\frac{r}{a}\right)} \right)_{r=R}$$

Solving the equation (5.7) for the constants A_3 and A_4 yields

$$\begin{bmatrix} A_3 \\ \alpha^2 \\ A_4 \\ \alpha^2 \end{bmatrix} = \begin{bmatrix} \cdot \\ \cdot \\ \cdot \\ \cdot \end{bmatrix}^{-1} \begin{bmatrix} N_R \\ \frac{M_R}{\alpha} \end{bmatrix} + \begin{bmatrix} \cdot \\ \cdot \\ \cdot \\ \cdot \end{bmatrix}^{-1} \begin{bmatrix} \cdot \\ \cdot \\ \cdot \\ \cdot \end{bmatrix} \quad 5.8$$

The equation for the horizontal displacement and the angular rotation at $r = R$ then become

$$\begin{bmatrix} \chi_R \\ u_R \end{bmatrix} = \frac{2\alpha^2}{Eh} \begin{bmatrix} \cdot \\ \cdot \\ \cdot \\ \cdot \end{bmatrix} \begin{bmatrix} \frac{A_3}{\alpha^2} \\ \frac{A_4}{\alpha^2} \end{bmatrix} + \frac{\alpha}{S^4 + 4\alpha^4} \begin{bmatrix} \cdot \\ \cdot \\ \cdot \\ \cdot \end{bmatrix} \begin{bmatrix} \cdot \\ \cdot \\ \cdot \\ \cdot \end{bmatrix} + \begin{bmatrix} 0 \\ \alpha T \end{bmatrix}$$

5.9

where the matrices $[M_4]$ and $[M_5]$ are

are

$$[M_4] = \begin{bmatrix} \sqrt{2}\alpha \operatorname{kei}'z_1 & -\sqrt{2}\alpha \operatorname{ker}'z_1 \\ -\operatorname{kei}z_1 - \frac{1+\nu}{z_1} \operatorname{ker}'z_1 & \operatorname{ker}z_1 - \frac{1+\nu}{z_1} \operatorname{kei}'z_1 \end{bmatrix}$$

$$[M_5] = \begin{bmatrix} 4\alpha^4 T \\ -S^2 \left\{ S^2 T - (1-\nu) \sqrt{2}\alpha \frac{T}{z_1} \right\} \end{bmatrix}$$

Substituting for the constants A_3 and A_4 from

equation (5.8) into equation (5.9) gives

$$\begin{bmatrix} \chi_R \\ \frac{U}{R} \end{bmatrix} = \frac{2\alpha^2}{Eh} \begin{bmatrix} M_4 \\ M_2 \end{bmatrix} \begin{bmatrix} N_R \\ \frac{M_R}{\alpha} \end{bmatrix} + \begin{bmatrix} M_2 \\ M_3 \end{bmatrix} + \frac{\alpha}{S^4 + 4\alpha^4} \begin{bmatrix} M_5 \\ 0 \\ \alpha T \end{bmatrix}$$

5.10

5.1(c) The Linked Equations for the Two Shell Forms

One now can consider joining the two heated shell forms at their common boundary which in the case of the shallow spherical shell, is at $r = R$. Assuming that the joint is rigid so that the angular rotation and the horizontal displacement of the cylinder and the sphere are equal, will give, after considering the sign convention and notation,

$$\begin{bmatrix} -\chi_c \\ -\frac{W_c}{R} \end{bmatrix} = \begin{bmatrix} \chi_R \\ \frac{U}{R} \end{bmatrix} \quad 5.11$$

Further, the stress resultants at this boundary must also be equal so that

$$\begin{aligned} Q_c &= N_R \\ M_c &= M_R \end{aligned}$$

Now substitute from equations (5.5) and (5.10) into equation (5.11) to find

$$\begin{aligned} \frac{2\gamma^2}{E_c h_c} \begin{bmatrix} M_1 \\ M_1 \end{bmatrix} \begin{bmatrix} Q_c \\ \frac{M_c}{a} \end{bmatrix} + \begin{bmatrix} 0 \\ \alpha_c T \end{bmatrix} = \\ \frac{2\alpha^2}{E h} \begin{bmatrix} M_4 \\ M_4 \end{bmatrix} \begin{bmatrix} -1 \\ -1 \end{bmatrix} \begin{bmatrix} N_R \\ \frac{M_R}{a} \end{bmatrix} + \begin{bmatrix} -1 \\ -1 \end{bmatrix} \begin{bmatrix} M_2 \\ M_3 \end{bmatrix} + \frac{\alpha}{5^4 + 4\alpha^4} \begin{bmatrix} M_5 \\ M_5 \end{bmatrix} + \begin{bmatrix} 0 \\ \alpha T \end{bmatrix} \quad 5.12 \end{aligned}$$

These are a pair of equations for N_R and M_R which can be solved/

solved to yield

$$\begin{bmatrix} N_R \\ \frac{M_R}{a} \end{bmatrix} = \begin{bmatrix} \frac{2\gamma^2}{Ech_c} \begin{bmatrix} M_1 \end{bmatrix} - \frac{2\alpha^2}{Eh} \begin{bmatrix} M_4 \end{bmatrix} \begin{bmatrix} M_2 \end{bmatrix}^{-1} \\ \frac{2\alpha^2}{Eh} \begin{bmatrix} M_4 \end{bmatrix} \begin{bmatrix} M_2 \end{bmatrix}^{-1} \begin{bmatrix} M_3 \end{bmatrix} + \frac{\alpha}{S^4 + 4\alpha^4} \begin{bmatrix} M_5 \end{bmatrix} + \begin{bmatrix} 0 \\ T(\alpha - \alpha_c) \end{bmatrix} \end{bmatrix} \quad 5.13$$

The values obtained for N_R and M_R may be substituted back into equation (5.8) and hence the constants A_4 and A_3 found. With these constants the stress resultants and the displacements into the shallow spherical shell can be calculated for the particular opening value of R , under consideration.

If the cylindrical and the spherical shells are constructed of the same material, with the same values of the material constants, then equation (5.13) may be simplified to

$$\begin{bmatrix} N_R \\ \frac{M_R}{a} \end{bmatrix} = \begin{bmatrix} 2\gamma^2 \frac{h}{h_c} \begin{bmatrix} M_1 \end{bmatrix} - 2\alpha^2 \begin{bmatrix} M_4 \end{bmatrix} \begin{bmatrix} M_2 \end{bmatrix}^{-1} \\ 2\alpha^2 \begin{bmatrix} M_4 \end{bmatrix} \begin{bmatrix} M_2 \end{bmatrix}^{-1} \begin{bmatrix} M_3 \end{bmatrix} + \frac{Eh\alpha}{S^4 + 4\alpha^4} \begin{bmatrix} M_5 \end{bmatrix} \end{bmatrix} \quad 5.14$$

5.1(d) Computed Results

A program was prepared for a Sirius computer to evaluate the matrix (5.14). After obtaining values for the two stress resultants N_R and M_R the integration constants were then calculated from the matrix (5.8). It was then possible to find the opening values of all the stress resultants and displacements in the shallow shell.

It should also have been possible for the computer to find the values of the stress resultants into the shell from a particular value of opening but unfortunately the storage capacity of the machine could not cope. The Sirius is rather a small machine. One can, however, take the values of the integration constants A_3 and A_4 from one program and use them in a second program to find the resultants into the shell. This was, however, not very successful.

The values of the shell parameters used to obtain numerical results were the same as those used earlier. The value of Poisson's ratio is taken as 0.255 for both the cylinder and the shallow shell. A selection of values for the ratio of the thickness of the shallow shell to the thickness of the cylinder was used for computation. Graphical results are presented in Figures (5.4 - 9) for the stresses and the displacements of the shallow shell for certain of the thickness ratios. The two limiting values of these ratios, namely

$$\frac{h}{h_c} = 0 \quad ; \quad \frac{h}{h_c} = 10 \times 10^6 (\infty) ,$$

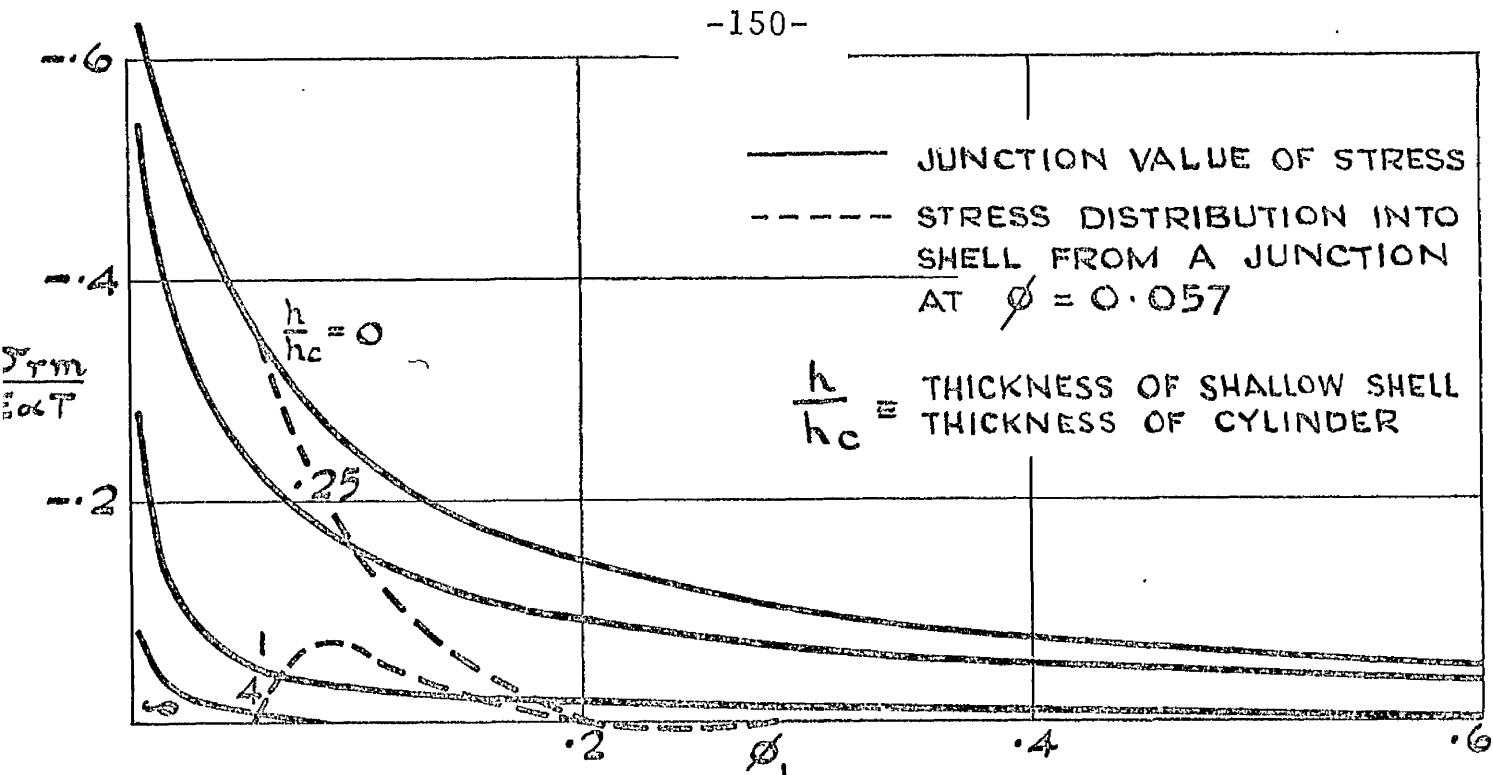


FIGURE (5.4) JUNCTION VALUES OF THE MERIDIONAL MEMBRANE STRESS ON A SHALLOW SPHERICAL SHELL.

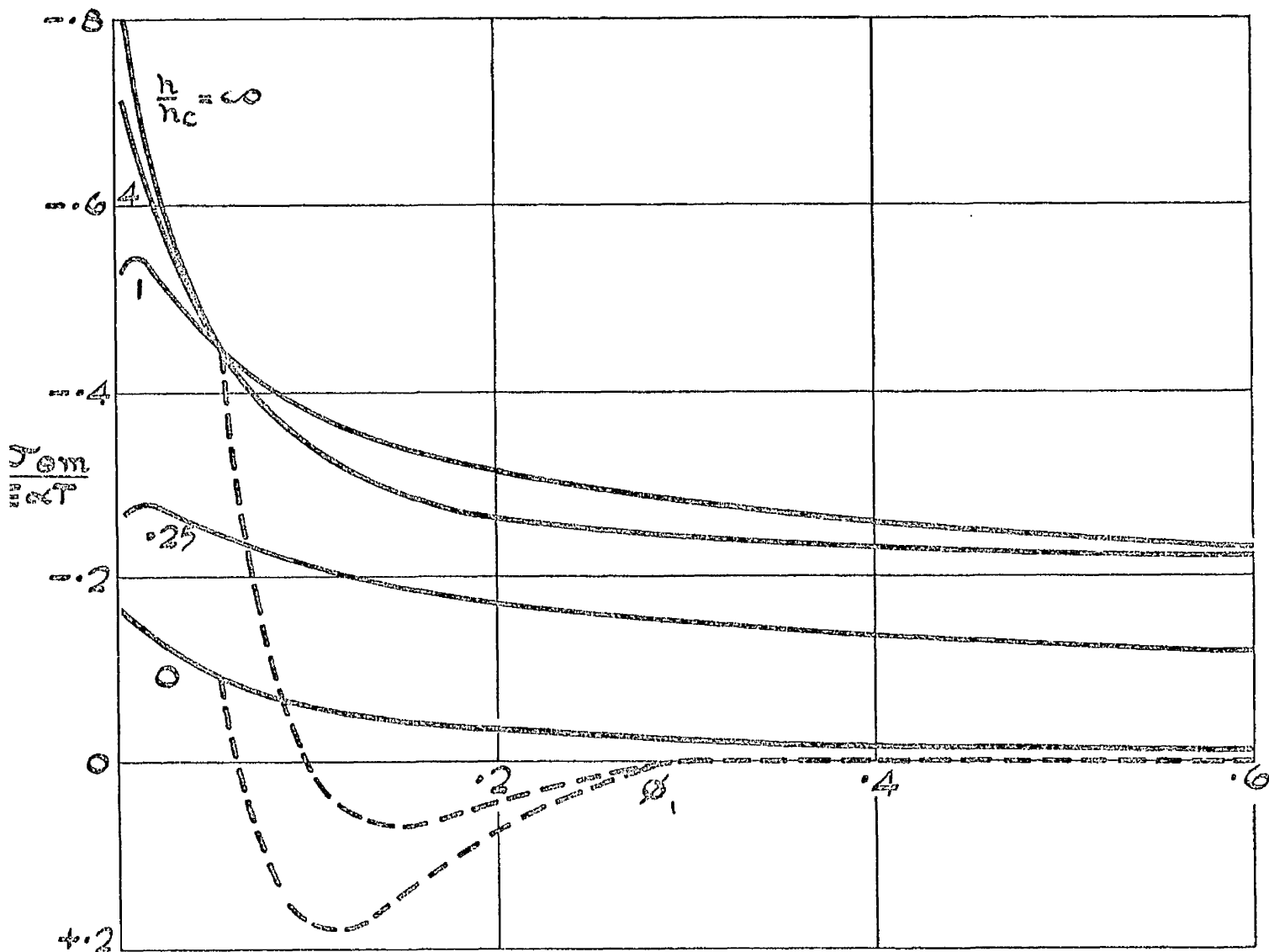


FIGURE (5.5) CIRCUMFERENTIAL MEMBRANE STRESS

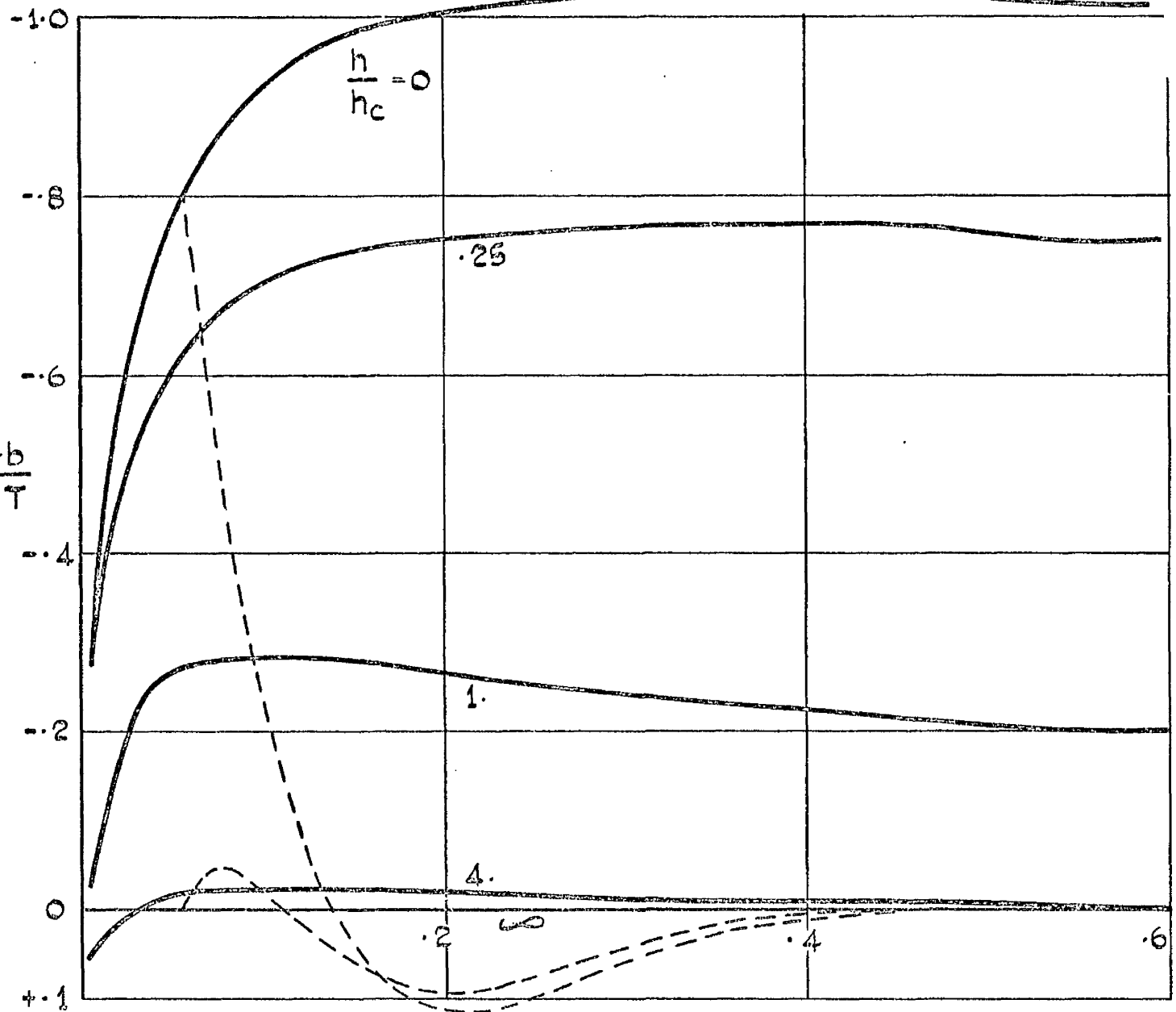


FIGURE (5.6) MERIDIONAL BENDING STRESS

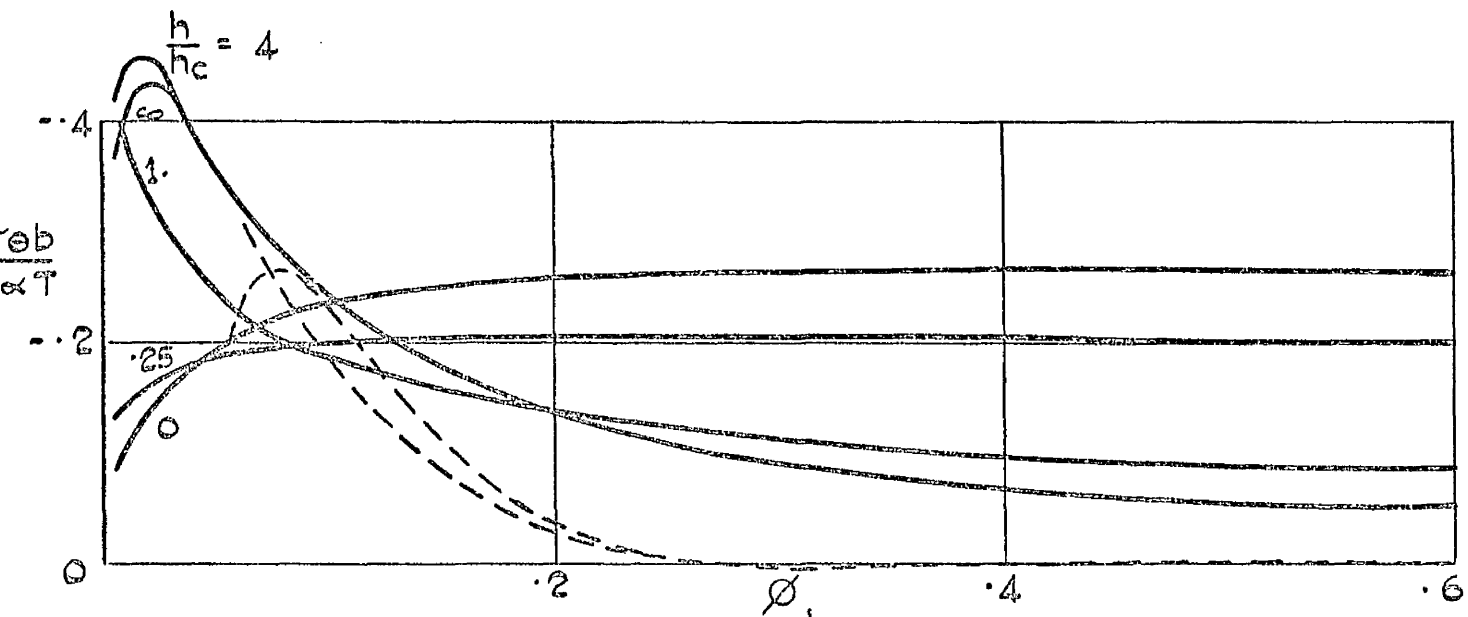


FIGURE (5.7) CIRCUMFERENTIAL BENDING STRESS

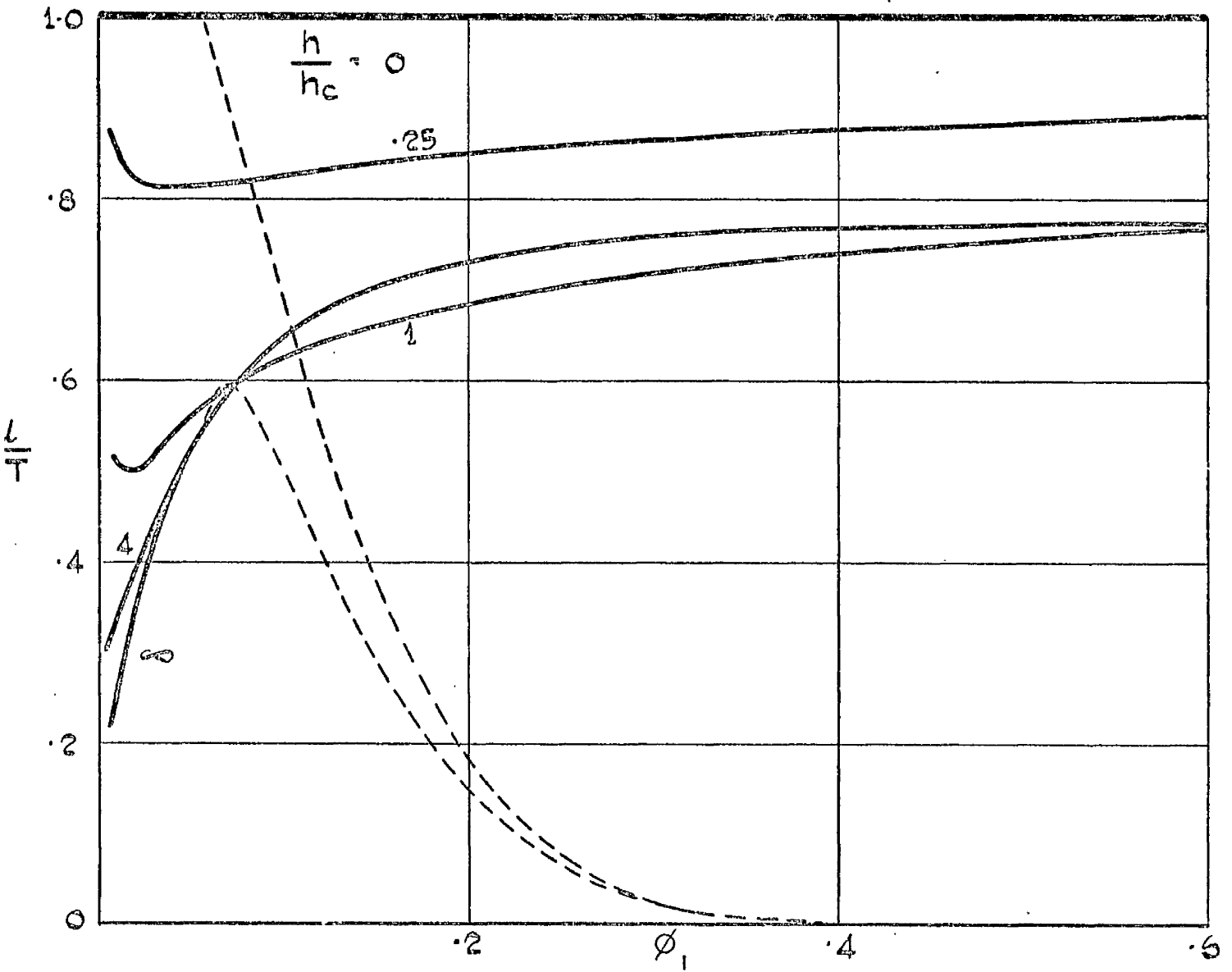


FIGURE (5.8) HORIZONTAL DISPLACEMENT

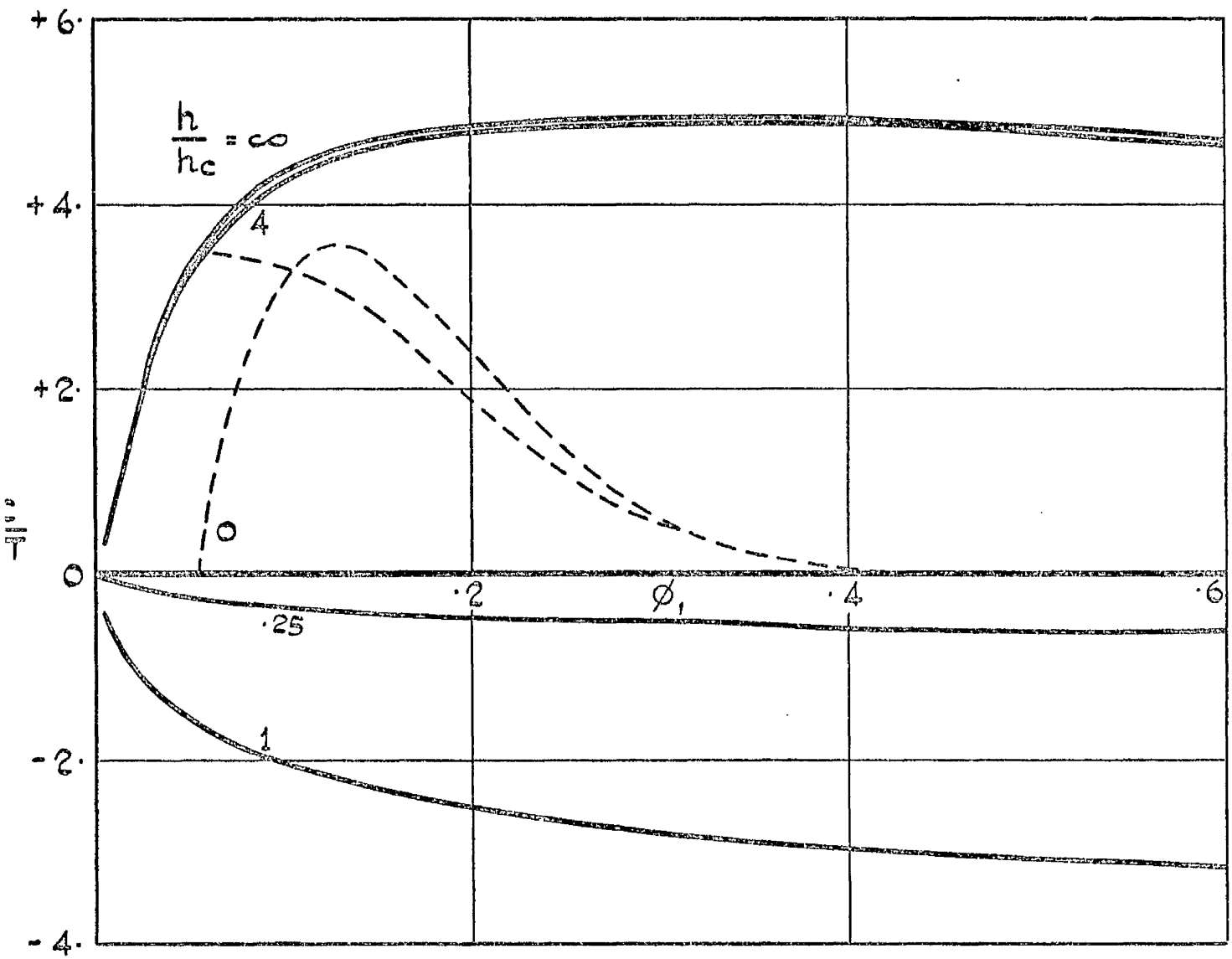


FIGURE (5.9) ANGULAR ROTATION

are included. The importance of these two values is that the first could represent a rigid insert in a shallow shell and the second represent an open shell. As in all the previous graphs presented, a full line gives the opening value of the stress for each particular value of opening.

It was considered of value to show also the stress distribution into the shallow shell from a particular opening. The value chosen $\phi = 0.057$ has already been illustrated. These stresses are shown as before by broken line. Only the two limiting values of thickness ratio were thought necessary to illustrate the stress distribution into the shell.

The value taken for the heat transfer parameter, S , is, for all cases, $S = 12$.

5.1(e) Conclusions and Observations

It is observed that there is a slight "falling away" in many of the graphs for larger values of the angle ϕ . This is particularly noticeable when the values are of greater magnitude. This "falling away" seems to correspond to the approximate limit of the shallow shell theory.

The graphs for the limiting case, $\frac{h}{h_c} = \infty$, correspond to the graphs for the open spherical shell, with of course the same parameters, presented in Chapter 2.

The graphs for the other limiting condition, $\frac{h}{h_c} = 0$, show correspondence, for the larger values of opening, with the graphs shown in Chapter 3 for a line of temperature round a spherical shell.

Let/

Let us examine now the magnitude of the total stress, that is the sum of the bending and the membrane stresses, on the surface of the shallow shell. Although it is only possible to add these stresses for the opening values, it has already been observed that the stress at the opening is likely to be the one of the greatest magnitude. For the open shell, $\frac{h}{h_c} = \infty$, it is seen that the total circumferential stress is much greater than the total meridional stress, whereas for the rigid insert the converse is the case. The values of the total circumferential stress for the open shell are

$$\begin{array}{rcccc} \phi_1 & = & .02 & .05 & .1 \\ \frac{\sigma_{\theta(m+b)}}{E\alpha T} & = & 1.07 & 1.03 & 0.59 \end{array}$$

for these three selected junction values. Where the shell has a rigid insert the values of the total meridional stress for certain junction values are

$$\begin{array}{rcccc} \phi_1 & = & .05 & .1 & .2 & .3 \\ \frac{\sigma_r(m+b)}{E\alpha T} & = & .14 & 1.164 & 1.144 & 1.13 \end{array}$$

These total values are quite considerable. For all the cases examined, however, the total principal stress has not been found to be greater than $\frac{E\alpha T}{1-\nu}$, the maximum stress for a totally restrained flat plate. It should however be emphasised that the rigid insert considered in the foregoing results is of the same material as the shallow shell. If different material were used with different coefficients of linear thermal expansion, then there would be greater stresses to be considered.

No/

No account has been taken of the vertical movement of the shallow shell and of course of the cylinder. If this movement were restrained in any way, further stresses are probable. These could be estimated using the results of BIJLAARD⁽³⁸⁾ who considered the case of a vertical load on the cylinder.

The results demonstrate that it is possible to have thermal stresses of quite a high magnitude at any heated opening on a spherical shell. These stresses are supplemented by boundary conditions which are also due to the temperature distribution.

CHAPTER 6

UNSYMMETRIC TEMPERATURE DISTRIBUTIONS
ON SPHERICAL SHELLS

The general problem of unsymmetric temperature distributions is considered.

The stresses and displacements on a spherical shell due to a temperature distribution which varies rapidly with respect to one line of curvature and slowly with respect to the other are investigated. This problem is of practical significance in that such a situation can arise from a slowly varying "line" of heat on the shell. The results are similar in form to those obtained by other authors for the corresponding boundary value problem of a slowly varying edge load on a spherical shell.

A general method of solution for any temperature distribution is considered involving temperature "hot spots" and the "influence line technique".

A general method of solution for any axisymmetric temperature in cylindrical shells is presented which involves dividing the shell into a number of bands each of uniform temperature.

Examples are presented which illustrate the various techniques of solution.

- 6.1. The Stresses Arising from a Temperature Distribution which Varies Slowly Along One Axis of Curvature but Rapidly Along the Other.

- 6.2.
 - (a) The Influence Line Technique
 - (b) Conrad's Solution for a Plain Hot Spot
 - (c) An Influence Band of Uniform Temperature Around a Spherical Shell.
 - (d) EXAMPLES

6.1 The Stresses Arising from a Temperature Distribution which Varies Slowly Along One Axis of Curvature but Rapidly Along the Other

The case of a varying line of heat on a spherical shell was considered in Chapter 1 where it was demonstrated that the temperature distribution could be expressed in the form

$$t(x,y) \approx T(y) e^{-\frac{s}{a}x} + \frac{1}{2sa} \frac{\partial^2 T}{\partial y^2} x e^{-\frac{s}{a}x} \tag{6.1}$$

where $T(y)$ is the temperature of the line of heat which lies along the ordinate at $x = 0$. It was argued that provided the temperature of the line of heat was slowly varying and $2sa$ reasonably large in magnitude, then it would be reasonable to drop the second term in this approximation since $\frac{\partial^2 T}{\partial y^2}$ must be very small. The temperature distribution into the shell is therefore, with these conditions,

$$t(x,y) \approx T e^{-\frac{s}{a}x} \tag{6.2}$$

Let us now examine the stress distribution likely to arise from such a temperature field. For the analysis, let us specialise cartesian co-ordinates. The two appropriate basic linked equations are given by CONRAD⁽³¹⁾ as

$$\nabla^4 W - \frac{1}{\alpha K} \cdot \nabla^2 F = 0 \tag{6.3}$$

$$\nabla^4 F + \frac{Eh}{a} \nabla^2 W = -D(1-\nu^2)\alpha \nabla^2 t \tag{6.4}$$

They may be separated to give

$$\nabla^6 W + 4\rho^4 \nabla^2 W = -4\rho^4 a \alpha \nabla^2 t \quad 6.5$$

$$\nabla^6 F + 4\rho^4 \nabla^2 F = -Eh \alpha \nabla^2 t \quad 6.6$$

where the constant ρ is given by

$$\rho^4 = \frac{\alpha x^4}{a^4}$$

Let us now obtain a solution for equation (6.5).

Following the same analytical method as was adopted in Chapter 1, first propose a new function ω where

$$\omega = \epsilon y$$

and ϵ is some small constant. Further, let us assume that the deflection W can be expressed in the series form as

$$W(x, y) \equiv W(x, \omega) = W_0(x, \omega) + \epsilon^2 W_1(x, \omega) + \epsilon^4 W_2(x, \omega) + \dots \quad 6.7$$

This series expression for W can now be substituted in equation (6.5) to give

$$\begin{aligned} \frac{\partial^6 W_0}{\partial x^6} + 4\rho^4 \frac{\partial^2 W_0}{\partial x^2} + \epsilon^2 \left(3 \frac{\partial^6 W_0}{\partial x^4 \partial \omega^2} + 4\rho^4 \frac{\partial^2 W_0}{\partial \omega^2} + 4\rho^4 \frac{\partial W_1}{\partial x^2} + \frac{\partial^6 W_1}{\partial x^6} \right) \\ + \epsilon^4 (\dots) + \dots = -4\rho^4 a \alpha \frac{\partial^2}{\partial x^2} T e^{-\frac{\alpha}{a} x} \end{aligned} \quad 6.8$$

Regarding this expression as a series in ascending powers of ϵ equate the coefficients of $\epsilon^0, \epsilon^2, \epsilon^4, \dots$, etc. to zero./

zero. In so doing obtain an infinite set of equations. The temperature term on the right hand side of equation (6.8) arose from τ_0 term in equation (1.28) and it is therefore of the order ε^0 .

Consider the first of these equations, that is the equation from the zero order coefficients. It is

$$\frac{\partial^2 W_0}{\partial x^2} + 4\rho^4 \frac{\partial^2 W_0}{\partial x^2} = -4\rho^4 \alpha \alpha \frac{s^2}{a^2} t \quad 6.9$$

The solution for the complementary function of this equation obtained by the author is

$$W_0 = e^{\rho x} [A_1(\omega) \sin \rho x + A_2(\omega) \cos \rho x] + e^{-\rho x} [A_3(\omega) \sin \rho x + A_4(\omega) \cos \rho x] + A_5(\omega) x + A_6$$

If this displacement is due to a line of temperature which decays rapidly in the x direction, then one can, provided the temperature is ambient before the outer boundary is reached, discard the terms involving the constants A_1 , A_2 and A_5 . One can also, since it represents a rigid body movement, discard the constant A_6 .

To determine the particular integral solution, assume that it is of the form

$$W_0 = At$$

where A is some constant. Upon substituting this value for W_0 in equation (6.8) this constant is found to be

$$A = - \frac{4\rho^4 \alpha \alpha}{s^2/a^4 + 4\rho^4}$$

The general solution of equation (6.9) is therefore

$$W_0 = e^{-\rho x} [A_3(\omega) \sin \rho x + A_4(\omega) \cos \rho x] - \frac{4\rho^4 \alpha \alpha t}{s^2/a^4 + 4\rho^4} \quad 6.10$$

It is observed that this solution for W_0 is identical to the solution for/

for W in the one dimensional problem except that whereas the coefficients A_3 and A_4 in the one dimensional case were constants they are now functions of ω .

The second equation in the series, found by equating the coefficients of ε^2 , is

$$\frac{\partial^6 W_1}{\partial x^6} + 4\rho^4 \frac{\partial^2 W_1}{\partial x^2} = -3 \frac{\partial^2 W_0}{\partial x^4 \partial \omega^2} - 4\rho^4 \frac{\partial^2 W_0}{\partial \omega^2}$$

Upon substituting for the value of W_0 from equation (6.9) it becomes

$$\begin{aligned} \frac{\partial^6 W_1}{\partial x^6} + 4\rho^4 \frac{\partial^2 W_1}{\partial x^2} &= 8\rho^4 e^{-\rho x} \left(\frac{\partial^2 A_3}{\partial \omega^2} \sin \rho x + \frac{\partial^2 A_4}{\partial \omega^2} \cos \rho x \right) \\ &+ 4\rho^4 \alpha \frac{\partial^2 t}{\partial \omega^2} \cdot \frac{3 \frac{s^2}{a^2} + 4\rho^4}{\frac{s^4}{a^4} + 4\rho^4} \end{aligned}$$

The complementary function can be recognised as being similar in form to that of the preceding equation in the series and indeed to that of all the subsequent equations. The particular integral has been determined using the "D" operation method. The general solution of this equation is

$$\begin{aligned} W_1 &= e^{-\rho x} (A_7 \sin \rho x + A_8 \cos \rho x) + A_9 x + A_{10} \\ &+ \frac{x}{4\rho} e^{-\rho x} \left[\frac{\partial^2 A_3}{\partial \omega^2} (\sin \rho x + \cos \rho x) + \frac{\partial^2 A_4}{\partial \omega^2} (\cos \rho x - \sin \rho x) \right] \end{aligned}$$

6.11

One can, as before, discard the terms involving the constants A_9 and A_{10} and also, since it involves the term $\frac{\partial^2 t}{\partial \omega^2}$ drop the final term in the equation.

The series solution for W considering only the first/

first two terms in that series, is

$$W = W_0 + \varepsilon^2 W_1 \quad .$$

Substituting in the values of W_0 and W_1 presented in equations (6.9) and (6.10) respectively, this becomes

$$W = e^{-\rho x} \left\{ \left[A_3 \sin \rho x + \frac{x}{4\rho} \frac{\partial^2 A_3}{\partial y^2} (\sin \rho x + \cos \rho x) \right] + \right. \\ \left. \left[A_4 \cos \rho x + \frac{x}{4\rho} \frac{\partial^2 A_4}{\partial y^2} (\cos \rho x - \sin \rho x) \right] \right\} \\ - \frac{4\rho^4 a \alpha}{\frac{s^4}{a^4} + 4\rho^4} \cdot t \\ + \varepsilon^2 \left[e^{-\rho x} (A_7 \sin \rho x + A_8 \cos \rho x) \right] \quad .$$

If ε is a small number, then, considering only the first order terms, the solution for the normal deflection W is

$$W = e^{-\rho x} \left\{ \left[A_3 \sin \rho x + \frac{x}{4\rho} \frac{\partial^2 A_3}{\partial y^2} (\sin \rho x + \cos \rho x) \right] + \right. \\ \left. \left[A_4 \cos \rho x + \frac{x}{4\rho} \frac{\partial^2 A_4}{\partial y^2} (\cos \rho x - \sin \rho x) \right] \right\} \\ - \frac{4\rho^4 a \alpha}{\frac{s^4}{a^4} + 4\rho^4} \cdot t$$

6.12

where t , A_3 and A_4 are all functions of y

In a similar manner, one can solve equations (6.6) for the stress function F to find

$$F = e^{-\rho x} \left\{ \left[a_3 \sin \rho x + \frac{x}{4\rho} \frac{\partial^2 a_3}{\partial y^2} (\sin \rho x + \cos \rho x) \right] + \right. \\ \left. \left[a_4 \cos \rho x + \frac{x}{4\rho} \frac{\partial^2 a_4}{\partial y^2} (\cos \rho x - \sin \rho x) \right] \right\} \\ - \frac{E h \alpha}{\frac{s^4}{a^4} + 4\rho^4} \cdot \frac{s^2}{a^2} \cdot t$$

There/

6.13

There is, however, an obvious relationship between the constants of the two equations. This relationship can be found by substituting both these basic functions into the linking equation (6.3) to yield

$$F = e^{-\rho x} \left\{ \left[A_3 \sin \rho x + \frac{x}{4\rho} \frac{\partial^2 A_3}{\partial y^2} (\sin \rho x + \cos \rho x) \right] - \left[A_4 \cos \rho x + \frac{x}{4\rho} \frac{\partial^2 A_4}{\partial y^2} (\cos \rho x - \sin \rho x) \right] \right\} \cdot 2\rho^2 a K - \frac{Eh\alpha}{\frac{s^4}{a^4} + 4\rho^4} \cdot \frac{s^2}{a^2} \cdot t \quad 6.14$$

The stress resultants given in terms of the deflection W and the stress function F are, after CONRAD, for the cartesian co-ordinate system

$$N_x = F, yy$$

$$N_y = F, xx$$

$$M_x = -K (W, xx + \nu W, yy)$$

$$M_y = -K (W, yy + \nu W, xx)$$

$$N_{xy} = -F, xy$$

$$M_{xy} = -(1-\nu)K W, xy \quad 6.15 - 20$$

The expression of stress resultants N_x and M_x are therefore

$$N_x = e^{-\rho x} \left\{ \left[\frac{\partial^2 A_4}{\partial y^2} \sin \rho x + \frac{x}{4\rho} \frac{\partial^2 A_4}{\partial y^2} (\sin \rho x + \cos \rho x) \right] - \left[\frac{\partial^2 A_3}{\partial y^2} \cos \rho x + \frac{x}{4\rho} \frac{\partial^2 A_3}{\partial y^2} (\cos \rho x - \sin \rho x) \right] \right\} a K 2\rho^2 - \frac{Eh\alpha}{\frac{s^4}{a^4} + 4\rho^4} \cdot \frac{s^2}{a^2} \cdot \frac{\partial^2 t}{\partial y^2}$$

and

$$\begin{aligned}
 M_x = & -e^{-\rho x} K \left\{ -2\rho^2 \cos \rho x \cdot A_3 + \right. \\
 & \frac{1}{2} \frac{\partial^2 A_3}{\partial y^2} \left[\rho x \sin \rho x - \rho x \cos \rho x - 2(1-\nu) \sin \rho x \right] + \\
 & \frac{\nu x}{4\rho} \frac{\partial^4 A_3}{\partial y^4} (\sin \rho x + \cos \rho x) + 2\rho^2 \sin \rho x \cdot A_4 + \\
 & \frac{1}{2} \frac{\partial^2 A_4}{\partial y^2} \left[\rho x \sin \rho x + \rho x \cos \rho x - 2(1-\nu) \cos \rho x \right] + \\
 & \left. \frac{\nu x}{4\rho} \frac{\partial^4 A_4}{\partial y^4} (\cos \rho x - \sin \rho x) \right\} \\
 & + \frac{4\rho^4 \alpha x K}{\frac{s^4}{a^4} + 4\rho^4} \left(\frac{s^2 t}{a^2} + \nu \frac{\partial^2 t}{\partial y^2} \right)
 \end{aligned}$$

6.21 - 22

To determine the form of the constants $A_3(y)$ and $A_4(y)$ two distinct situations seem possible for investigation. One is where the shell is open at $x = 0$ and has a temperature distribution $t = T(y)$ along that boundary. The second situation is where there is a "line source of heating" along $x = 0$ so that the temperature is $t = T(y)$ on that line. The boundary conditions along this line are zero rotation and zero shear stress through the thickness.

Consider in detail the case of the open shell where at

$$x = 0, \quad N_x = M_x = 0$$

and

$$t = T(y)$$

and where of course the various assumptions with regard to the temperature distribution, which were made earlier, are still valid.

For/

For the condition of zero normal stress at the boundary $x = 0$ equation (6.21) yields

$$(N_x)_{x=0} = 0 = -\frac{\partial^2 A_3}{\partial y^2} \cdot aK2\rho^2 - \frac{Eh\alpha}{\frac{s^4}{a^4} + 4\rho^4} \cdot \frac{s^2}{a^2} \cdot \left(\frac{\partial^2 t}{\partial y^2}\right)_{x=0}$$

that is

$$\frac{d}{dy^2} \left[A_3 + \frac{Eh\alpha \frac{s^2}{a^2}}{2\rho^2 a K \left(\frac{s^4}{a^4} + 4\rho^4 \right)} \cdot T \right] = 0$$

Thus

$$A_3 = -\frac{Eh\alpha 2\rho^2 \frac{s^2}{a^2}}{\frac{s^4}{a^4} + 4\rho^4} \cdot T(y) + C_y + D \quad 6.23.$$

where C and D are constants. Though they both must be zero for the problem which we are considering, it is of interest to observe that the constant D would represent the edge loading in the boundary value problem. This equation is discussed later.

From the boundary condition of zero edge moment equation (6.22) gives, at $x = 0$,

$$(M_x)_{x=0} = 0 = 2\rho^2 A_3 + (1-\nu) \frac{\partial^2 A_4}{\partial y^2} + \frac{4\rho^4 a \alpha}{\frac{s^4}{a^4} + 4\rho^4} \left[\frac{s^2}{a^2} T + \nu \left(\frac{\partial^2 t}{\partial y^2} \right)_{x=0} \right]$$

Substituting into this equation the value of the constant A_3 yields

$$\frac{\partial^2 A_4}{\partial y^2} = \frac{-4\rho^4 a \alpha \nu}{(1-\nu) \left(\frac{s^4}{a^4} + 4\rho^4 \right)} \cdot \frac{\partial^2 T}{\partial y^2}$$

which can be integrated to give

$$A_4 = \frac{-4\rho^4 a \alpha \nu}{(1-\nu) \left(\frac{s^4}{a^4} + 4\rho^4 \right)} \cdot T$$

6.24

plus/

plus of course the two constants of integration which again are zero.

It has therefore been shown that for this particular problem

$$\begin{aligned} A_3(y) &= B_3 \cdot T(y) \\ A_4(y) &= B_4 \cdot T(y) \end{aligned}$$

where B_3 and B_4 are constants. The normal deflection W and the stress function F can now be written as

$$\begin{aligned} W = e^{-\rho x} \left\{ \left[T B_3 \sin \rho x + \frac{x}{4\rho} B_3 \frac{\partial^2 T}{\partial y^2} (\sin \rho x + \cos \rho x) \right] + \right. \\ \left. \left[T B_4 \cos \rho x + \frac{x}{4\rho} B_4 \frac{\partial^2 T}{\partial y^2} (\cos \rho x - \sin \rho x) \right] \right\} \\ - \frac{4\rho^4 a \alpha}{\frac{s^4}{a^4} + 4\rho^4} \cdot T e^{-\frac{s}{a} x} \end{aligned}$$

$$\begin{aligned} F = e^{-\rho x} \left\{ \left[T B_4 \sin \rho x + \frac{x}{4\rho} B_4 \frac{\partial^2 T}{\partial y^2} (\sin \rho x + \cos \rho x) \right] - \right. \\ \left. \left[T B_3 \cos \rho x + \frac{x}{4\rho} B_3 \frac{\partial^2 T}{\partial y^2} (\cos \rho x - \sin \rho x) \right] \right\} 2\rho^2 a k \\ - \frac{E h \alpha}{\frac{s^4}{a^4} + 4\rho^4} \frac{s^2}{a^2} T e^{-\frac{s}{a} x} \end{aligned}$$

6.25 - 26

This could be further simplified by realising that the term involving $\frac{\partial^2 T}{\partial y^2}$ must be very small and thus one can, for a slightly coarser approximation, drop these terms and the equation then becomes

$$W = T(y) e^{-\rho x} (B_3 \sin \rho x + B_4 \cos \rho x) - \frac{4\rho^4 a \alpha}{\frac{s^4}{a^4} + 4\rho^4} \cdot T e^{-\frac{s}{a} x}$$

$$F = T(y) e^{-\rho x} (B_4 \sin \rho x - B_3 \cos \rho x) - \frac{E h \alpha}{\frac{5^4}{a^4} + 4\rho^4} \cdot \frac{5^2}{a^2} \cdot T e^{-\frac{5}{a} x}$$

6.27 - 28

This is a most interesting result: Provided the temperature distribution at the open boundary, $x=0$, varies slowly in the y direction, then the two equations (6.26 - 27) will give us a reasonable approximation to the effects within the shell. It is noticed that these equations are identical to those for the constant temperature distribution along the open edge with, of course, the term $T(y)$ replacing the term T (a constant).

Many authors have considered the problem of varying boundary loading on shells. BOUMA⁽³⁴⁾, investigating the problem of shells with slowly varying edge loads, described that loading as the cosine series

$$Z(x, y) = Z_n(x) \cos n y .$$

He then showed that the normal deflection W could be expressed as

$$W = e^{-\lambda x} [B_{11} \cos \lambda x + B_{12} \sin \lambda y] \cos n y .$$

If we reconsider equation (6.22), in which the constants C and D were zero for the problem under consideration, we see that if there were no temperature distribution then this equation would become

$$A_3 = C y + D$$

and the meaning of this expression, since $\frac{\partial^2 A_3}{\partial y^2} = 0$ is a slowly varying boundary loading. This result to some extent confirms the slowly varying edge loading case investigated by BOUMA.

GRADOWCZYK⁽³⁰⁾ /

GRADOWCZYK⁽³⁰⁾ argued that the errors occurred in replacing the effects of a temperature distribution by a bending couple and a membrane force along an edge, for the one dimensional problem on a shallow spherical shell, are small. He then suggested that the results of BOUMA'S work could be applied to the equivalent thermal gradient problem.

STEELE⁽³³⁾ has shown, using the shell equations of NOVOYHILOV, that for any loading which varies like a series of waves rapidly with respect to one ordinate and slowly with respect to the other, then a solution is possible in terms of the expression for the distribution in the direction of rapid variation. The value of STEELE'S contribution is that it embraces all types of loading, including thermal, and though the wave form is quite general, as is shown in Figure (6.1), a half wave could be considered as equivalent to the problem which has been considered in this section.

STEELE suggests that if $\alpha_n \cos n\theta$ denotes a typical term in the Fourier expansion of some applied load and if $n \ll \sqrt{R}$ then the applied load be termed "slowly varying". For such slowly varying loads however SIMMONDS shows that the conventional influence coefficient matrix which relates the Fourier components of the edge loads to the Fourier components of the edge values of the displacements and axial rotation is ill-conditioned.

A limitation of the results presented by the author is that the angle ϕ is sufficiently large. That is the results apply only to that portion of a shell where the GECKELER solutions, for the symmetrically loaded shell, are applicable. Further, in order to obtain the final results presented in equations (6.27-28) it was assumed that the magnitude of the term of modulus

$$\frac{\alpha}{4 \nu / \alpha} \cdot \frac{\partial^2 T}{\partial y^2}$$

in equations (6.25-26), was such that this term could be neglected. Changing the longitudinal distance x into the non-dimensional form ϕ , where $x = a\phi$, means that the assumption would require that

$$\frac{n^2}{4x} \ll 1$$

The foregoing analysis presents a simplified solution for the class of asymmetric thermal distributions on spherical shells which fulfil the requirement of being slowly varying with respect to one principal axis of curvature relative to the other.

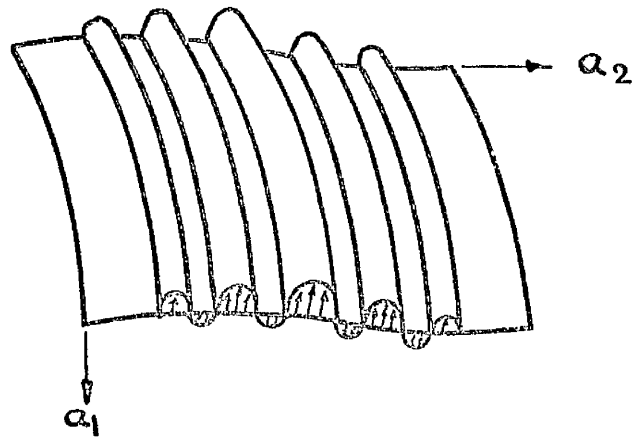


FIGURE (6.1) SHELL SURFACE WITH SURFACE LOADS OF RAPID VARIATION WITH RESPECT TO ONE COORDINATE.

6.2(a) The Influence Line Technique

A more general method of tackling any two dimensional temperature distribution is by a modification of the Influence Line Technique. This technique is described in several papers by KENEDI and TOOTH⁽⁶²⁾.

The influence line technique assumes the application of the principle of superposition and is based on the construction of appropriate influence lines or surfaces corresponding to a condition of 'reciprocal symmetry', which satisfies the linear theory between all points on the surface of the shell. This condition expressed by Maxwell's Reciprocal Theorem links the cause and effect at any two arbitrarily selected points on an elastic shell.

The 'influence line' gives the variation of some selected effect at any point C say of a structure as a unit action travels from A to B along the path S of the 'loading' applied to the structure. The selected effect δ may be stress, deflection, etc. and the unit action may be representative of radial or tangential load, 'bending or twisting' moment, or temperature depending on the nature of the applied 'loading' w .

The total effect at the point C due to the 'loading' applied along S then becomes $\int_S w \delta ds$ which can be evaluated numerically or graphically whichever is most convenient.

With temperature gradients where the effect is over an area, influence surfaces in place of influence lines are considered. Where the condition of 'reciprocal symmetry' exists the constructions of the appropriate influence line or surface becomes quite simple. Considering two points, F, on the load path AB, and C, any other point/

point on the surface, the condition of reciprocity may be stated as

$$\delta_{CF} = \delta_{FC}$$

where δ_{CF} is the selected effect at F due to the unit action applied at C, and δ_{FC} is the same effect at C due to the unit action at F. In such cases the influence line required for C may be obtained directly by applying the unit action at C to the otherwise unloaded structure and evaluating its selected effect along the load path AB. THIS IS SHOWN IN FIGURE (6.2).

To be able to make use of this method, however, it is necessary to know the effect of the unit action imposed. In thermal analysis the plane temperature hot spot investigated by CONRAD and FLÜGGE⁽³¹⁾ for a shallow spherical dome may be utilised for this purpose.

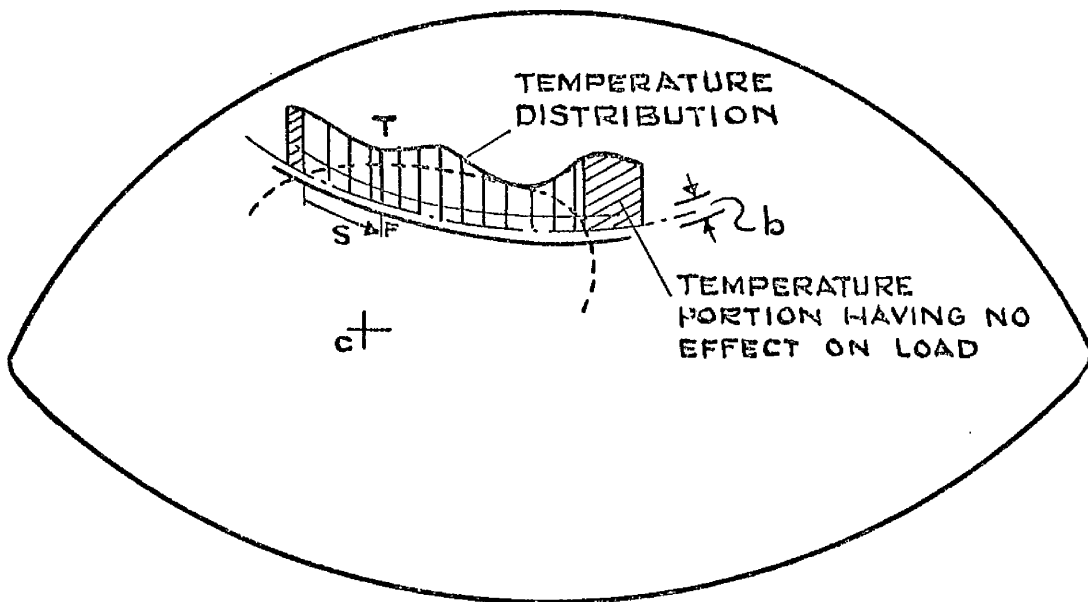
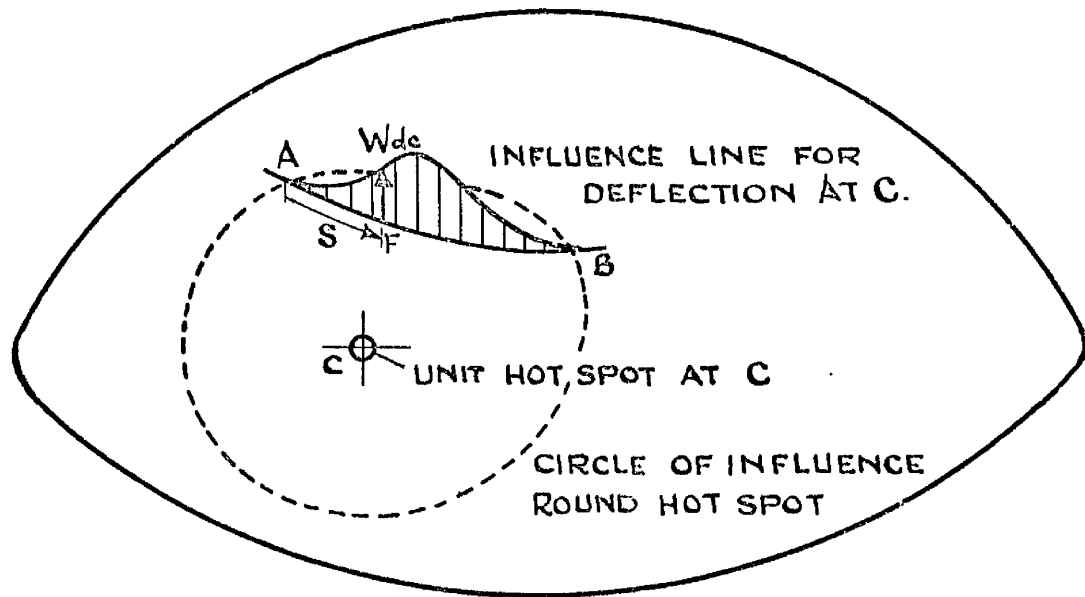


FIGURE (6.2) THE INFLUENCE LINE TECHNIQUE FOR FINDING THE DEFLECTION AT C DUE TO A BAND OF VARYING TEMPERATURE. TOTAL DEFLECTION W AT C DUE TO TEMPERATURE DISTRIBUTION T ALONG THE BAND A.B. IS GIVEN BY $W = \sum_A^B (T_b s_s) W$

6.2(b) Conrad's Solution for a Plain Hot Spot

Consider a circular area A of a shell, heated to a uniform temperature T as shown in Figure (6.3). A plane hot spot can be defined as the limiting case of a temperature distribution such that as its area $A \rightarrow 0$ then $T \rightarrow \infty$ so that the quantity $\mu \equiv \lim_{A \rightarrow 0} \Delta T A$ remains always finite. This definition, which is analogous to that for the intensity of a concentrated force, is chosen so that a finite stress system will result and the quantity μ is therefore a measure of the intensity of the hot spot.

The solution for the functions W and F in the region outwith the hot spot, are

$$W = \frac{\mu \alpha^2}{\pi a} \operatorname{kei} \sqrt{2\alpha} \frac{r}{a}$$

$$F = D(1-\nu^2) \frac{\mu}{2\pi} \operatorname{ker} \sqrt{2\alpha} \frac{r}{a}$$

6.29 - 30

from which can be derived expressions for the stresses and the displacements, some of which are

$$N_r = D(1-\nu^2) \frac{\mu \sqrt{2\alpha}}{2\pi a r} \operatorname{ker}' \sqrt{2\alpha} \frac{r}{a}$$

$$N_\theta = D(1-\nu^2) \frac{\mu 2\alpha^2}{2\pi a^2} \operatorname{ker}'' \sqrt{2\alpha} \frac{r}{a}$$

$$M_r = \frac{D(1-\nu^2)\mu}{2\pi a} \left[\operatorname{ker} \sqrt{2\alpha} \frac{r}{a} - \frac{(1-\nu)a}{\sqrt{2\alpha}} \operatorname{kei} \sqrt{2\alpha} \frac{r}{a} \right]$$

6.31 - 33

By/

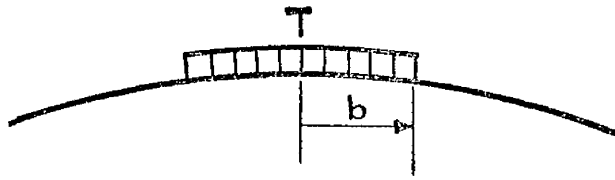


FIGURE (6.3) TEMPERATURE HOT SPOT

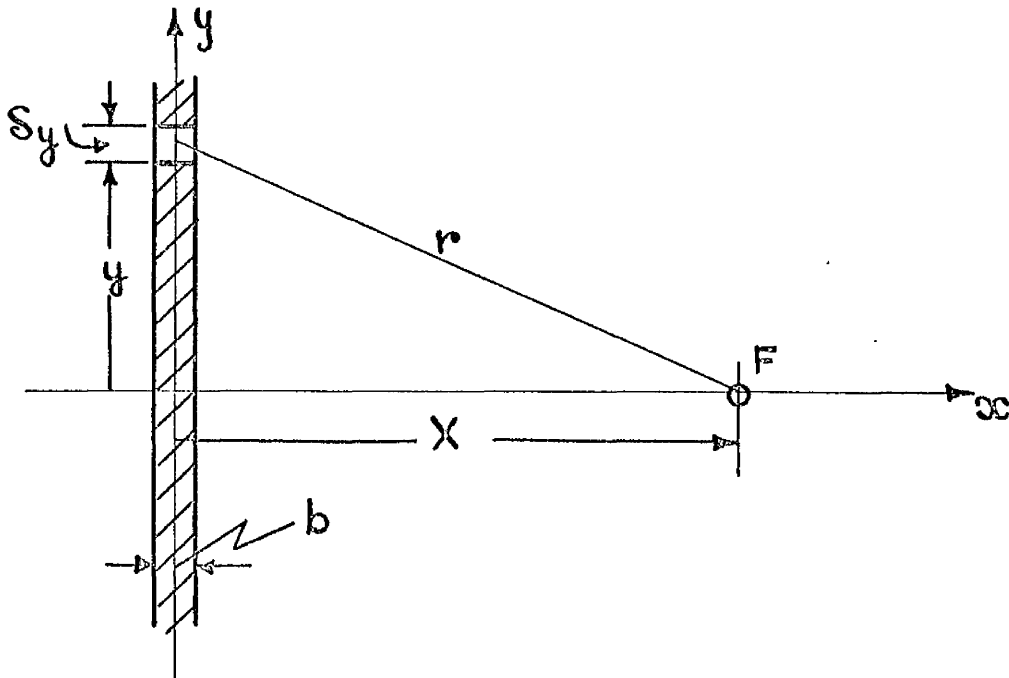


FIGURE (6.4) A POINT F DISTANCE X FROM A BAND OF UNIFORM TEMPERATURE T .

By using the appropriate asymptotic expansion forms for the KELVIN functions it can be shown that in the vicinity of the hot spot (but not within the hot spot itself) these singularities are of the form

$$\begin{aligned}
 W &= -\frac{\mu \alpha^2}{4a} & * \\
 N_r &= -\frac{Eh\mu}{2\pi} \left(\frac{1}{r^2}\right) \\
 N_\theta &= \frac{Eh\mu}{2\pi} \left(\frac{1}{r^2}\right) \\
 M_r &= \frac{(1+\nu)Eh\mu}{4\pi a} \ln \sqrt{2\alpha} \frac{r}{a} .
 \end{aligned}$$

6.34 - 37

*

The expression for the radial deflection

equation (6.34), is not in agreement with the result given by CONRAD. This disparity is due to CONRAD making the assumption that when approaching the origin

$$kei z \approx -z^2 \ln z$$

which can be seen by reference to any of the tables of these KELVIN functions or by inspection of Figure (2.3) to be incorrect.

DWIGHT in his book "Tables of Integrals and other Mathematical Data" gives, for small arguments,

$$kei z \approx -\left(\frac{z^2}{4}\right) \ln z - \frac{\pi}{4} + O(z^2)$$

The value, when approaching the origin, should therefore be

$$kei z \approx -\frac{\pi}{4}$$

and this is the value which was used by the author to derive equation (6.34).

If one considers the effects at the boundary of the hot spot, where $r = b$, then equations (6.34-37) yield

$$W = -\frac{\pi \alpha^2 b^2 \Delta T}{4a}$$

$$N_r = -\frac{1}{2} E h \alpha T$$

$$N_\theta = \frac{1}{2} E h \alpha T$$

$$M_r = E h \alpha T \frac{(1+\nu)}{4a} b^2 \ln \sqrt{2} \alpha \frac{b}{a}$$

6.38-41

These expressions agree with the corresponding values for the effects within the same hot spot. There is of course a difference in sign for the hoop stress, N_θ , which must be compressive within the heated region.

Using these solutions of CONRAD for a temperature hot spot, it should be possible to estimate the stresses at any point on a continuous spherical shell for any temperature distribution.

This could be done by integration or by using the influence line technique which has already been described. Unfortunately the integrals must involve the KELVIN functions and this makes any solutions difficult. Attempts by the author to numerically generate these functions were not wholly successful for the reasons given in Appendix 1. However, with the larger computers now becoming available, this could be a fruitful line of approach, especially/

especially since it is possible, without added difficulty, to include loading and bending hot spots in any calculation.

Let us now consider a number of examples in which these results are made use of in thermal stress problems.

6.2(c) An Influence Band of Uniform Temperature
Around a Spherical Shell

As a first example of the use of the hot spot technique let us find the normal deflection W at some point F distance x from an infinite band, of uniform temperature T and width b which lies along the y axis as shown in Figure (6.4).

This problem can be tackled by the influence line technique by "erecting" a unit hot spot at F and integrating the "effect" of temperature and area along the length of the band. Since, however, an analytic solution of the integral is possible in this case, let us divide the band into a number of hot spots each of area $b \delta y$ and of temperature T . The deflection at the point F due to the hot spot at y is, from equation (6.29)

$$W = \frac{b \delta y \alpha T x^2}{\pi a} \operatorname{kei} \frac{\sqrt{2} x}{a} (x^2 + y^2)^{\frac{1}{2}} .$$

The total deflection at F due to the band of temperature is therefore

$$W = \frac{b \alpha T x^2}{\pi a} \int_{-\infty}^{+\infty} \operatorname{kei} \frac{\sqrt{2} x}{a} (x^2 + y^2)^{\frac{1}{2}} dy .$$

Consider the integral

$$I(x) = 2 \int_0^{\infty} \operatorname{kei} \frac{\sqrt{2} x}{a} (x^2 + y^2)^{\frac{1}{2}} dy$$

with the substitutions

$$v = \frac{\sqrt{2} x}{a} x$$

$$u = \frac{\sqrt{2} x}{a} y$$

it becomes

$$I(v) = \frac{\sqrt{2} a}{x} \int_0^{\infty} \operatorname{kei} (v^2 + u^2)^{\frac{1}{2}} du .$$

Using that known relationship between the Bessel functions

$$K_0(i^{\frac{1}{2}} z) = \operatorname{ker}(z) + i \operatorname{kei}(z)$$

the integral can be expressed as

$$I(v) = \frac{\sqrt{2}a}{\alpha} \int_m \int_0^{\infty} K_0 (iv^2 + u^2)^{\frac{1}{2}} du .$$

Finally, with the substitution

$$r = i^{\frac{1}{2}} u$$

the integral takes the form

$$I(v) = \frac{\sqrt{2}a}{\alpha} \int_m -i^{\frac{1}{2}} \int_0^{\infty} K_0 [r^2 + (i^{\frac{1}{2}}v)^2]^{\frac{1}{2}} dr$$

for which WATSON⁽¹⁸⁾ gives the solution as

$$I(v) = -\frac{\alpha\pi}{2\alpha} e^{-\frac{v}{\sqrt{2}}} \left(\cos \frac{v}{\sqrt{2}} + \sin \frac{v}{\sqrt{2}} \right) .$$

The total deflection W at the point F is therefore

$$W = -\frac{\alpha T \alpha b}{2} e^{-\frac{\alpha x}{a}} \left(\cos \frac{\alpha x}{a} + \sin \frac{\alpha x}{a} \right)$$

6.42

and this result is shown graphically in Figure (6.5).

Similar integrations lead to the following expressions for the stress resultants and rotation into a shell from a uniform band of temperature -

$$Q_x = \frac{Eh\alpha T}{2\alpha a} \alpha b e^{-\frac{\alpha x}{a}} \cos \frac{\alpha x}{a}$$

$$M_x = \frac{Eh\alpha T}{4\alpha} b e^{-\frac{\alpha x}{a}} \left(\sin \frac{\alpha x}{a} - \cos \frac{\alpha x}{a} \right)$$

$$\chi = \frac{\alpha T \alpha^2 b}{a} e^{-\frac{\alpha x}{a}} \sin \frac{\alpha x}{a}$$

and

$$N_y = Eh \left[\frac{W}{a} + \alpha T \right]$$

6.43 - 46

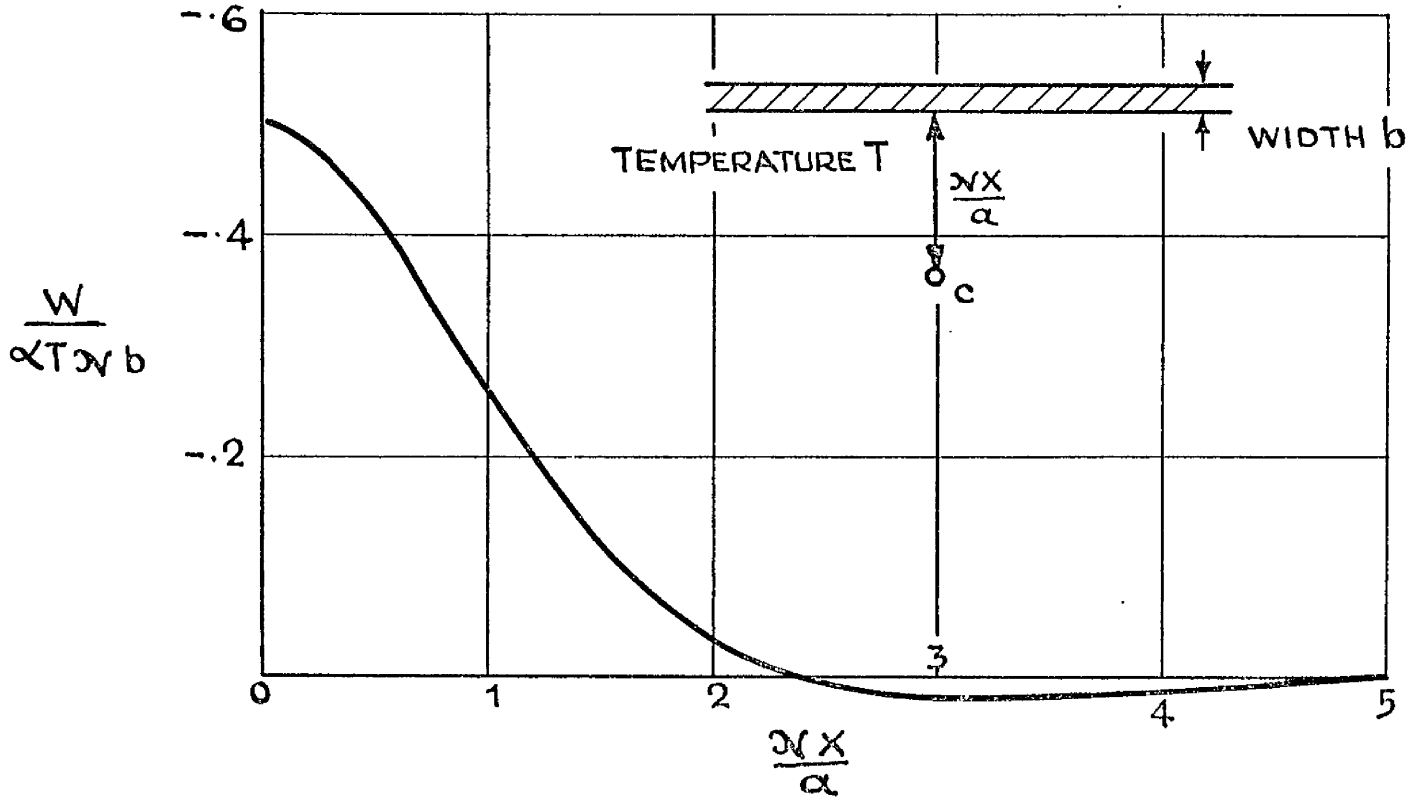


FIGURE (6.5)
RADIAL DEFLECTION W AT A POINT C
DISTANCE $\frac{r}{a}$ FROM A UNIFORM BAND
OF WIDTH b AND TEMPERATURE T .

One would be tempted to think that the use of a band of infinite length was a rather severe limitation, unfortunately necessary for the evaluation of the integrals involved. An inspection of Figure (6.6), which is a graph showing the normal deflection at a distance from a hot spot reveals a quick "die out" of effect with distance from the hot spot. This is also true for the other stress resultants. By a simple application of the influence technique whereby the point under consideration is enclosed within a hot spot, it is observed that there is therefore a circle of influence round any point and any "effects" outwith this circle need not be considered. This in the case of the normal deflection W we see from Figure (6.6) a suitable radius of influence would be of the order of

$$r \approx \frac{a}{\sqrt{2\alpha}} \cdot 4$$

The rapid falling off in value of the KELVIN functions, whose integrals are required, is shown in Figure (2.3). Thus, although a band is taken as infinite, the same results are reasonably true for all bands greater than a certain finite length which is governed by the shell parameters.

With these derived results for a uniform band of temperature, it is now possible to evaluate the stress resultants due to any axisymmetric temperature around a spherical shell. This can be accomplished either by the integration of the temperature effects over the surface or by considering an influence band of temperature at a discrete point and summing the effects. Unlike the case of temperature hot spot the functions involved are easily "manipulated".

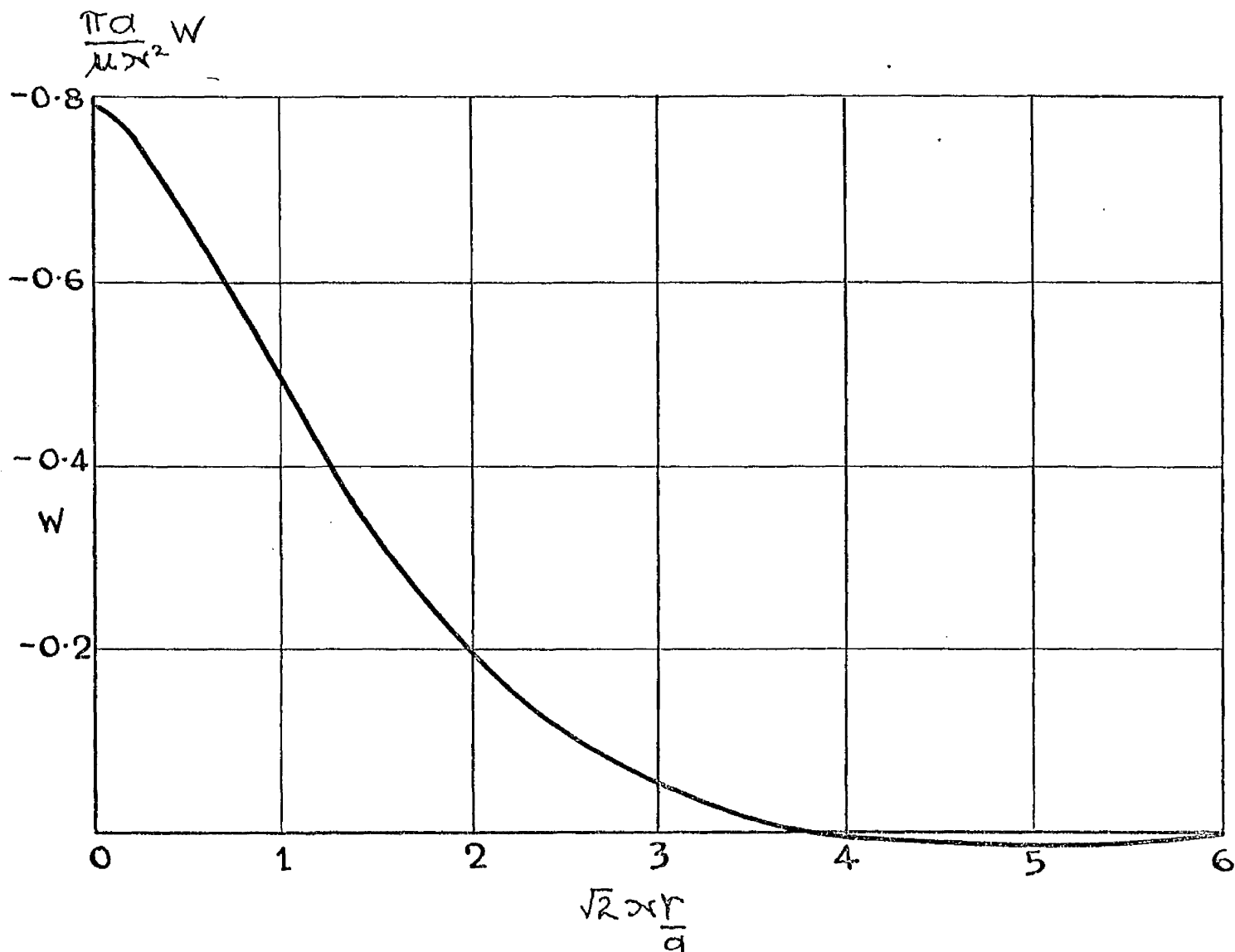


FIGURE (6.6)

RADIAL DEFLECTION W OF THE SHELL AT A DISTANCE $\sqrt{2} \frac{\alpha r}{a}$ FROM A HOT SPOT OF INTENSITY μ .

The case of the uniform line of heat around a sphere, which was considered in Chapter 3, should suitably demonstrate the ease with which a solution can be obtained by adding, analytically, the effects of a number of bands of temperature.

The temperature distribution into the shell from such a line of heat is

$$t = T e^{\pm \frac{s}{a} x}$$

where T is the temperature at the line $x = 0$

Let us find the deflection at the point $x = 0$ due to this temperature field. After dividing the shell into a number of bands each of width δx and of temperature $t(x)$ we can integrate the effects of all these bands to give

$$W_{x=0} = 2 \int_0^{\infty} -\alpha T \delta x e^{-\frac{s}{a} x} e^{-\frac{\alpha x}{a}} \left(\cos \frac{\alpha x}{a} + \sin \frac{\alpha x}{a} \right) dx$$

which when evaluated yields

$$W_{x=0} = \frac{-\alpha \delta T (\alpha s + 2\alpha^2)}{s^2 + 2\alpha s + 2\alpha^2}$$

By multiplying both numerator and denominator by $(s^2 - 2\alpha s + 2\alpha^2)$ this reduces to

$$W_{x=0} = \frac{-\alpha \delta T (s^3 \alpha - 2s\alpha^3 + 4\alpha^4)}{s^4 + 4\alpha^4}$$

This is the same result, except for a sign change, as was obtained in the equations (3.40 - 43) by the general solution of the basic differential equation for large values of the meridional.

The/

The sign change is due to CONRAD assuming that a positive normal deflection is inward.

We have thus demonstrated that the hot spot technique can give the same result as was obtained using the more direct approach. Let us now consider a numerical example using the same influence band technique.

EXAMPLE *

To evaluate the deflections and the stresses in a cylindrical support skirt of dimensions, length 48 in, thickness 1.75 in, mean radius 186 in. These stresses are caused by the symmetric longitudinal temperature distribution which is expressed as

$$t(^{\circ}C) = 300 - 100 e^{-0.18x} + 0.0025 e^{+0.18x}$$

where x is the longitudinal distance in inches. This distribution is shown in Figure (6.7). The shell material properties are, the coefficient of linear thermal expansion, α , = 13.0×10^{-6} per C° , Poisson's ratio, ν , = 0.3.

Considering the influence line approach and using the results derived in equations (6.42 - 46) for a band of uniform temperature, let us numerically evaluate the desired effect at a number of locations along the shell. Numerically this is not a particularly easy problem since the temperature distribution, and hence the stress distribution, does not become zero within the rather short length of the cylindrical shell. This requires the effects at the boundaries to be considered.

To illustrate the numerical method of approach, let us find the normal deflection at the point C distance $x = 1.6 \frac{a}{\lambda}$ along /

* This example and the following asymmetric problem, is due to PAYNE⁽⁶⁷⁾ He presents analytic and finite difference solutions for this particular problem.

along the shell, as shown in Figure (6.7b) At this point erect an "influence band" of width $\frac{\alpha b}{a}$. The deflection distribution due to such a band is given by equation (6.42) as

$$W = -\frac{\alpha T \alpha b}{2} e^{-\frac{\alpha x}{a}} \left(\cos \frac{\alpha x}{a} + \sin \frac{\alpha x}{a} \right)$$

and this distribution is also shown in the Figure.

The "effect" at C of a band of width $\frac{\alpha b}{a} = 0.2$ located about a point D distance $0.75 \frac{a}{\alpha}$ from C is therefore

$$\begin{aligned} W &= -0.34 \alpha T \alpha b \\ &= -0.34 \times 101 \times 0.2 \times a \alpha \\ &= -6.87 a \alpha \end{aligned}$$

In a similar manner the effect of all of the other bands which make up the surface of the shell, have been obtained and they give a total deflection at C of

$$W = -96.3 a \alpha$$

The values for the stress resultants, obtained in a similar manner, are shown in Table (6.1).

Figure (6.7) shows, however, that the effect of the influence band at C is still considerable at both of the shell boundaries. It is therefore obvious that the boundary conditions must, in this problem, be considered. To do this an influence band is now "erected" at each of the boundaries and the resulting effects are estimated as before. These results are presented in Table (6.1) from which it is observed there are bending moments and transverse shears at both the boundaries. Since this is not the case for an open shell/

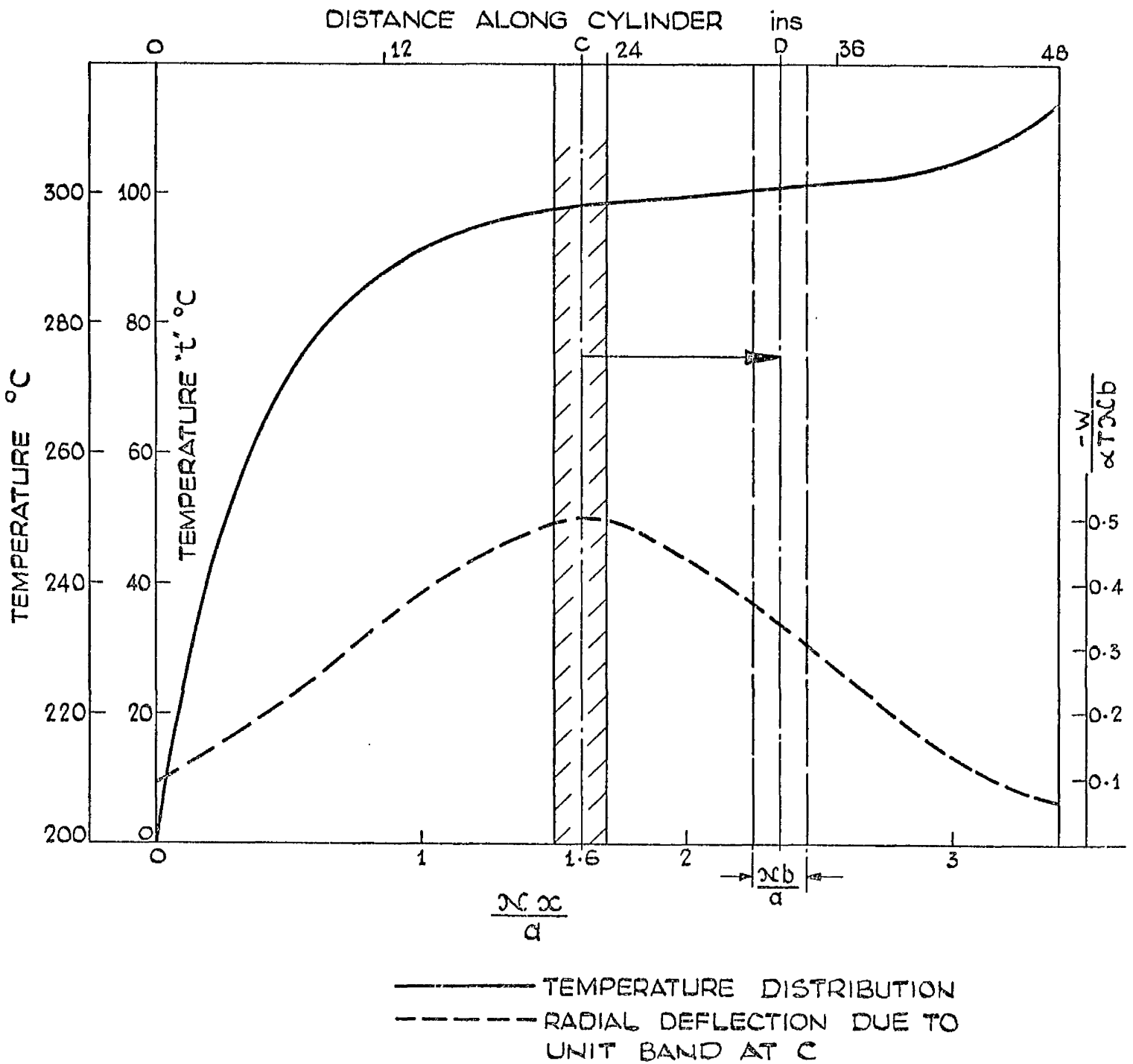


FIGURE (6.7b) INFLUENCE ON DEFLECTION AT 'C'
OF A TEMPERATURE BAND OF WIDTH Δxb AT D

$\frac{\partial x}{\partial a}$	0	0.8	1.6	2.4	3.4
x in.	0	11.2	22.5	33.6	48
$\frac{-W}{a\alpha}$	34.0	72.0	96.3	91.8	54.7
$\frac{4x^2}{Eha\alpha} M$	21.0	-23.0	-38.8	-43.2	-4.0
$\frac{2x}{Eha} Q$	23.9	-18.6	-4.9	1.76	56.6
$\frac{1}{\alpha x} \chi$	44.6	60.5	80.5	72.0	52.7

TABLE (6.1) STRESSES AND DISPLACEMENTS AT SELECTED POINTS ALONG THE CYLINDER.

$\frac{\partial x}{\partial a}$	$\frac{-W_M}{a\alpha}$	$\frac{-W_Q}{a\alpha}$	$\frac{4x^2}{Eha\alpha} M_M$	$\frac{4x^2}{Eha\alpha} M_Q$	$\frac{2x}{Eha} Q_M$	$\frac{2x}{Eha} Q_Q$
0	-10.5	23.78	-21.0	0	0	-23.9
0.8	0.097	7.444	-13.254	15.336	6.724	-0.221
1.6	2.173	-0.140	-4.087	9.598	4.210	-4.939
2.4	1.337	-1.591	+0.117	2.914	1.278	-3.048
3.4	0.249	-0.771	+0.855	-0.408	-0.179	-0.567

TABLE (6.2) STRESSES AND DISPLACEMENTS AT SELECTED POINTS ON THE CYLINDER DUE TO THE BOUNDARY BENDING MOMENT AND THE TRANSVERSE SHEAR AT $\frac{\partial x}{\partial a} = 0$

$\frac{\partial x}{\partial a}$	$\frac{-W_M}{a\alpha}$	$\frac{-W_Q}{a\alpha}$	$\frac{4x^2}{Eha\alpha} M_M$	$\frac{4x^2}{Eha\alpha} M_Q$	$\frac{2x}{Eha} Q_M$	$\frac{2x}{Eha} Q_Q$
0	0.048	-1.834	-0.165	-0.969	-0.034	1.348
0.8	0.205	-3.600	-0.102	4.330	0.153	5.765
1.6	0.398	-2.124	0.495	18.207	0.646	11.228
2.4	0.222	11.241	2.041	35.012	1.243	6.265
3.4	2.0	56.60	4.0	0	0	-56.60

TABLE (6.3) EFFECT OF BENDING MOMENT AND TRANSVERSE SHEAR AT EDGE $\frac{\partial x}{\partial a} = 3.4$

shell, "corrections" must be made relating these edge boundary values to conditions within the shell. These corrections are indicated in Tables (6.2-3). The values of the various effects at the ends remote from the loaded boundary are small and have consequently been neglected.

To find the deflection at C, in an open shell we must also include the terms due to the bending moment and the transverse shear at both of the boundaries. Finally, a term must be included which will involve the uniform rise in temperature of 200 C° . Using Tables (6.1-3) the deflection at C due to all of these effects is therefore

$$\begin{aligned} W_c &= -\alpha \alpha (200 + 96.3 + 2.173 - 0.14 + 0.398 - 2.124) \\ &= -0.717 \text{ in.} \end{aligned}$$

The values for the deflections and the stresses, calculated in a similar manner as the deflection above, are presented in Figures (6.8-10) where they may be compared with the analytic results of PAYNE.

Considering the magnitudes of the terms involved, the results are most encouraging and show that the procedure was quite satisfactory. The width of influence band used to estimate the effects given in Table (6.1) was $\frac{\alpha b}{a} = 0.2$. A check at the left-hand boundary, $\alpha = 0$, showed that there was substantially little difference between band widths of 0.1, 0.2 and 0.4.

Like the previous case considered, this example could also have been "solved" analytically by straightforward integration of the band effects. However, it does illustrate the capability of the numerical approach.

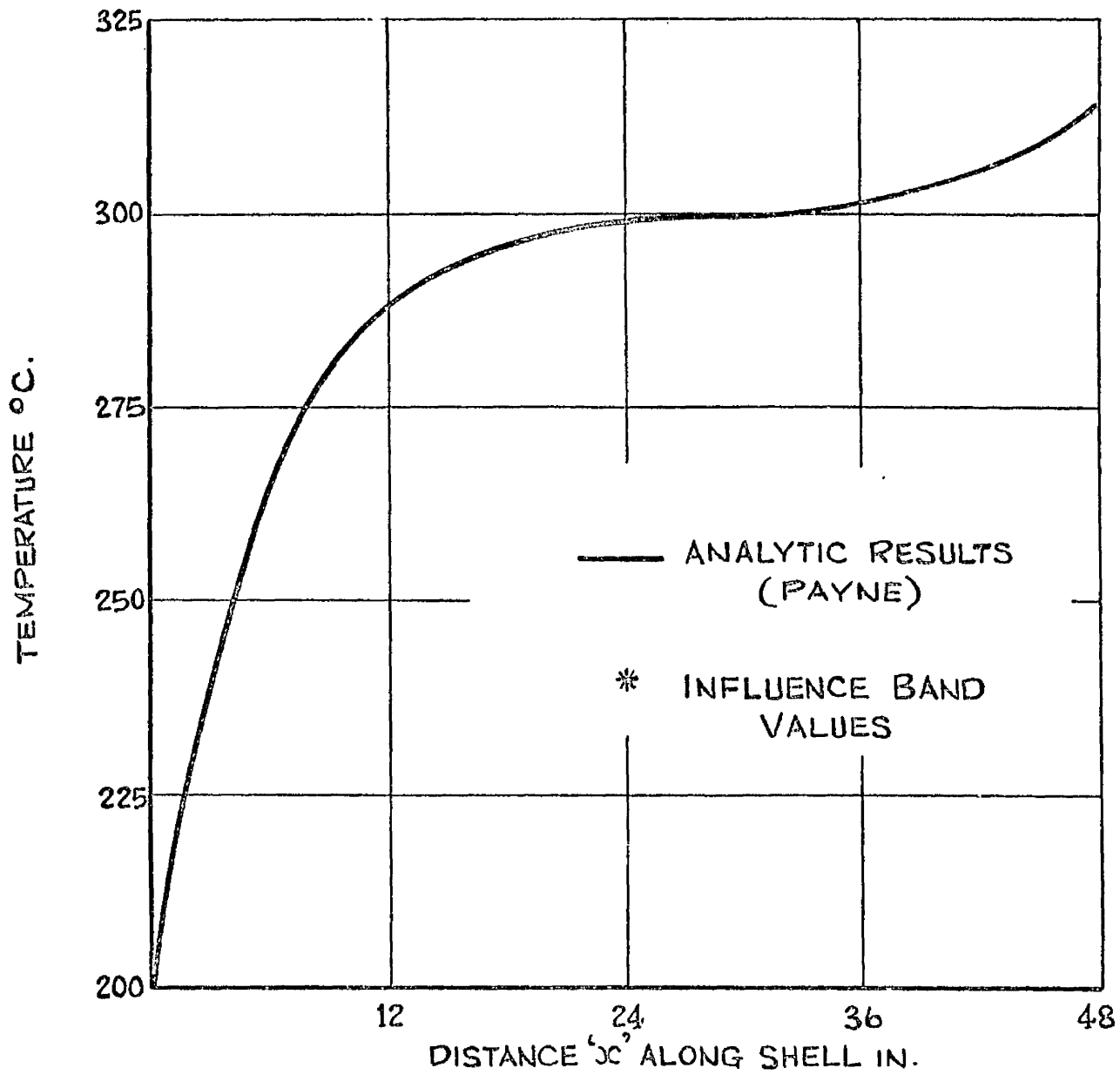


FIGURE (6.7) TEMPERATURE DISTRIBUTION ALONG SHELL

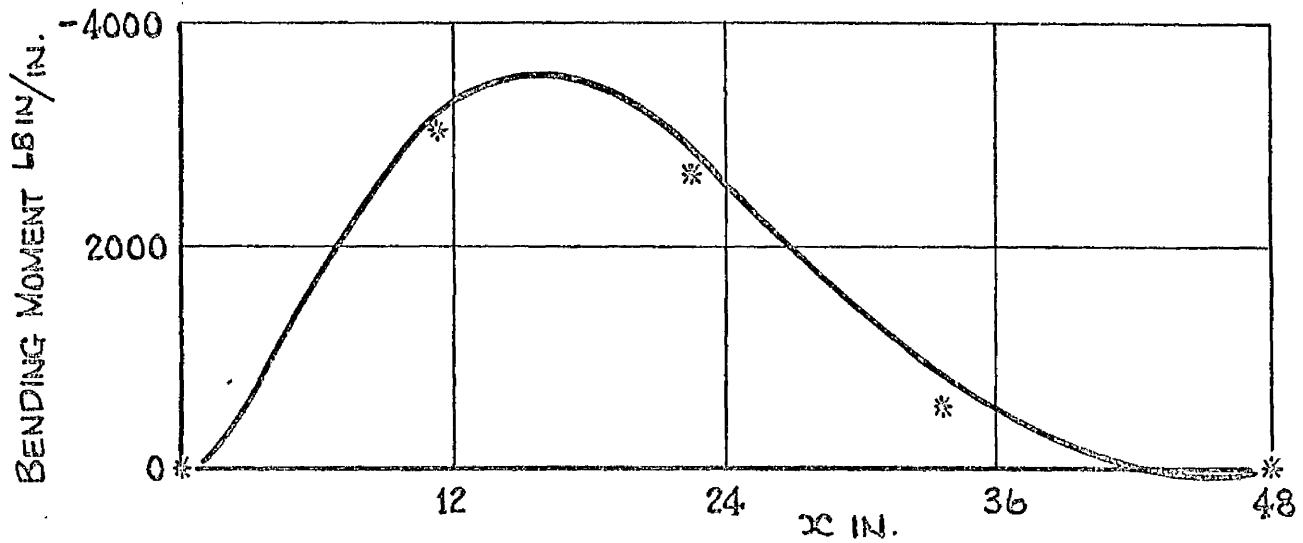


FIGURE (6.8) DISTRIBUTION OF BENDING MOMENT M_y ALONG SHELL

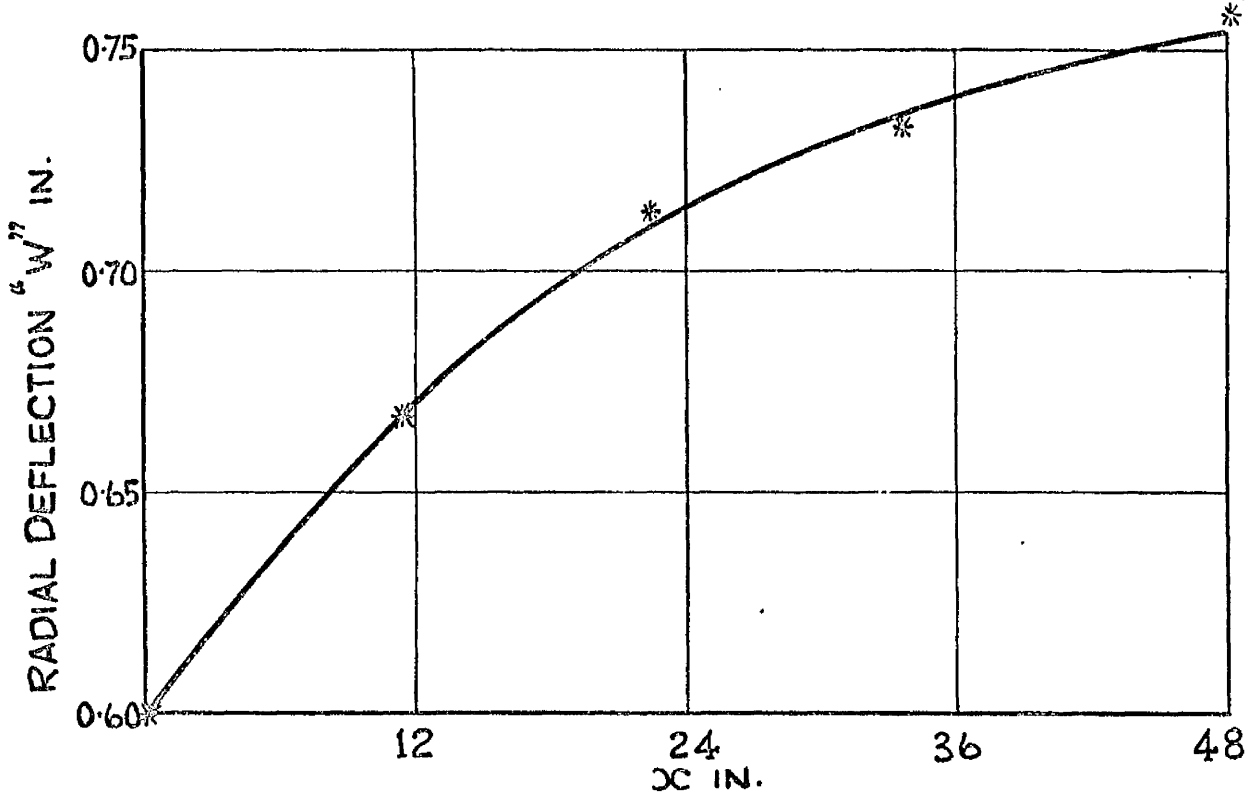


FIGURE (6.9) RADIAL DEFLECTION ALONG SHELL

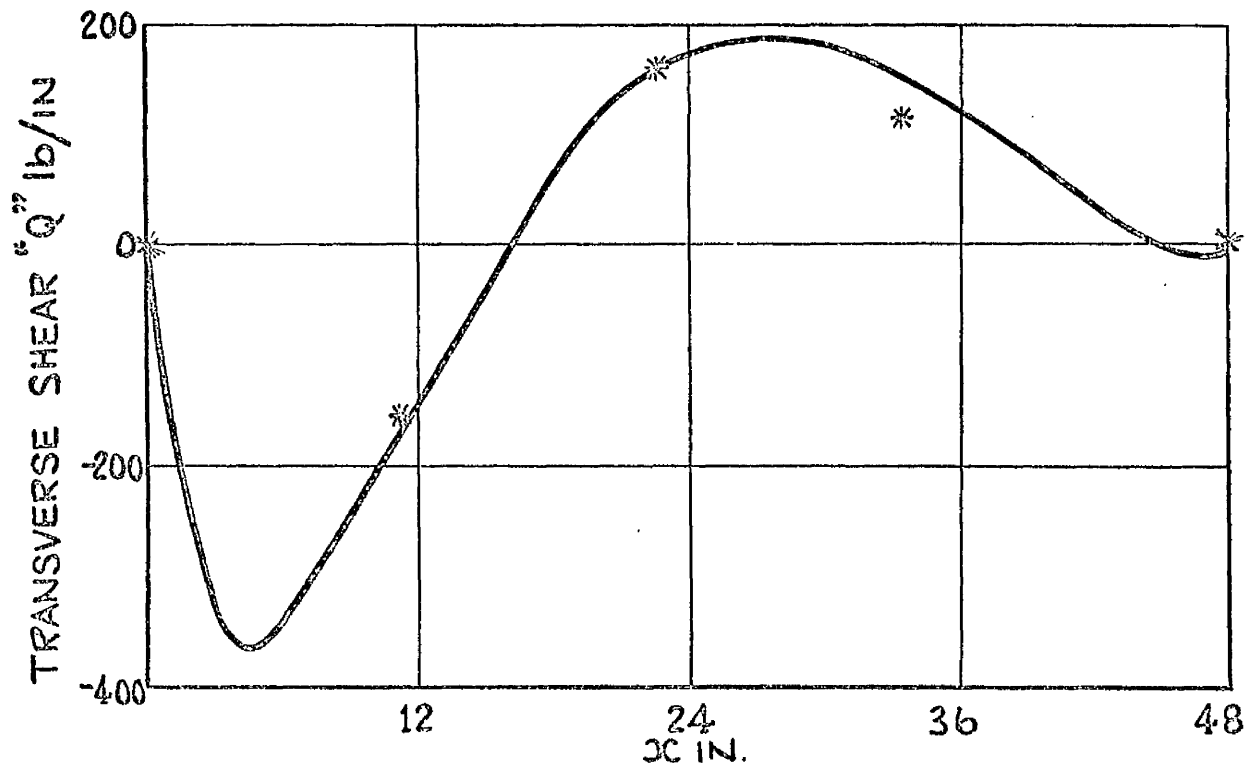


FIGURE (6.10) TRANSVERSE SHEAR DISTRIBUTION ALONG SHELL

EXAMPLE

To evaluate the deflections in a spherical shell using the influence area technique. The shell has similar dimensions and properties to the cylinder of the previous example. The temperature distribution is expressed as

$$t = 100 e^{-0.18x} (1 + \cos 16\theta)$$

where θ is the circumferential angle and x is the distance (in inches) from a great circle around the sphere. This expression for the temperature can be written in terms of the shell parameters as

$$t = 100 e^{-1.786 \sqrt{2} x \frac{x}{a}} (1 + \cos 0.8537 \sqrt{2} x \theta)$$

and it is shown graphically, in this form, in Figure (6.11), for one quarter of the temperature field. This temperature distribution cannot be considered as slowly varying since, in the circumferential direction,

$$n = 16$$

and

$$\sqrt{2} x = 18.741$$

which neither meets the requirement suggested by STEELE that

$$n \ll \sqrt{2} x$$

nor the requirement of the method of solution developed earlier in this Chapter that

$$\frac{n^2}{4x} \ll 1$$

An analytic solution has been obtained however using the simplified results as presented in equations (6.25-26) and the particular values are presented for comparison with the influence area results under the title of simplified theoretical values.

		CIRCUMFERENTIAL DISTANCE $\sqrt{2}x/a$									
		0	0.4	0.8	1.2	1.6	2.0	2.4	2.8	3.2	3.6
LONGITUDINAL DISTANCE $\sqrt{2}x/a$	0	200	194	178	152	120	86	54	27	8	0
	0.4	140	136	124	106	84	60	38	19	6	
	0.8	98	95	87	74	59	42	26	13	4	
	1.2	68	66	61	52	41	30	18	9	3	
	1.6	48	47	43	36	29	21	13	6	2	
	2.0	34	33	30	25	20	14	9	5	1	
	2.4	23	23	21	18	14	10	6	3	1	
	2.8	16	16	15	12	10	7	4	2	1	
	3.2	11	11	10	9	7	5	3	2	0	
	3.6	8	8	7	6	5	4	2	1		
	4.0	6	5	5	4	3	2	2	1		
	4.4	4	4	3	3	3	2	1	1		
	4.8	3	3	2	2	2	1	1	0		
	5.2	2	2	2	1	1	1	0			
	5.6	1	1	1	1	1	1				
	6.0	1	1	1	1	1	0				
6.4	1	1	1	1	0						

FIGURE (6.11) THE TEMPERATURE DISTRIBUTION, °C, OVER ONE QUARTER OF THE SURFACE. (THE TEMPERATURES REFER TO UPPER LEFT-HAND CORNER OF THE BLOCK IN WHICH THEY ARE SITUATED.)

As in the previous example a "unit hot spot" is considered to be acting around the point at which the deflection is required. The remaining surface area of the shell is suitably portioned and the "effect" of the unit hot spot at each of the "centroids" of area is obtained either directly from equation (6.29) by substituting in the appropriate distance or from its graphical form as presented in Figure (6.6). Thus to find the normal deflection at A, in Figure (6.14) first surround the point with a unit hot spot. This unit hot spot will produce a deflection at point B, distance

$$r = \frac{1.0 a}{\sqrt{2} x}$$

from A, a deflection of

$$w_{ba} = -0.5 \frac{x^2}{\pi a}$$

The area surrounding B is

$$A = 0.4 \times 0.4 \cdot \frac{a^2}{2x^2}$$

and the temperature associated with B is, from Figure (6.11), 46°C . Since the definition of a hot spot of intensity μ is

$$\mu = \alpha AT$$

then the deflection at A due to the heated area around B is

$$w_{ab} = -0.5 \frac{x^2}{\pi a} \cdot \alpha \cdot 0.16 \frac{a^2}{2x^2} \cdot 46 = -0.586 \alpha a$$

In/

In a similar manner the deflection at A due to all of the other areas which make up the surface may be added to give

$$W_a = -57.11 \alpha \alpha \quad (C^\circ)$$

The deflections at a number of points on the surface were evaluated using this technique and the results are presented in Figure (6.12). For comparison the results using the simplified approach, which is applicable for slowly varying distributions in the circumferential direction, are included. It is noticeable that the "influence area method" indicates a smaller value of the maximum deflections but a greater "spread" of deflection "into" the shell surface. This effect agrees, of course, with the dropping of the second term in the simplified solution. Figure (6.13) shows the deflection distribution along a longitudinal line at various circumferential values. The similarity of form between the two solutions is noticeable.

The estimation of the membrane and bending stresses by this technique is more laborious. Stress variations from a unit hot spot are much more "severe" than the normal deflection distribution. Furthermore the stress is expressed analytically in polar co-ordinates relative to the hot-spot whereas the stresses which are required do not fit this co-ordinate system.

Thus a stress transformation is required at each point B under consideration.

Referring, once again, to Figure (6.14) the membrane stress resultants N_r and N_ϕ , at the point B relative to the unit hot spot at A are from equations (6.35-36)

$$N_{r_{ba}} = -0.6946 \cdot \frac{2x^2}{2\pi a^2} \cdot Eh$$

$$N_{\phi_{ba}} = +1.1896 \frac{2x^2}{2\pi a^2} Eh$$

However/

		CIRCUMFERENTIAL DISTANCE $\sqrt{R}x$ @			
		0	1.2	2.4	3.6
LONGITUDINAL DISTANCE $\sqrt{R}z$	0	57.11 (67.38)	47.03 (51.21)	25.72 (18.19)	8.44 (0)
	0.5	52.45 (62.94)	43.86 (47.84)	23.75 (16.99)	8.04 (0)
	1.0	43.29 (51.88)	36.61 (39.43)	20.02 (14.00)	
	1.5	32.01 (38.20)	27.42 (29.03)	15.21 (10.31)	2.99 (0)
	2.0	21.65 (25.11)	18.23 (19.09)	9.94 (6.78)	
	3.0	7.13 (6.65)	5.98 (5.06)	3.98 (1.80)	

FIGURE (6.12) THE NORMAL DEFLECTION ($-w/a$ PER $^{\circ}C$) AT SELECTED POINTS ON THE SHELL SURFACE FOUND BY THE "INFLUENCE" TECHNIQUE. SIMPLIFIED THEORETICAL VALUES ARE SHOWN IN BRACKETS.

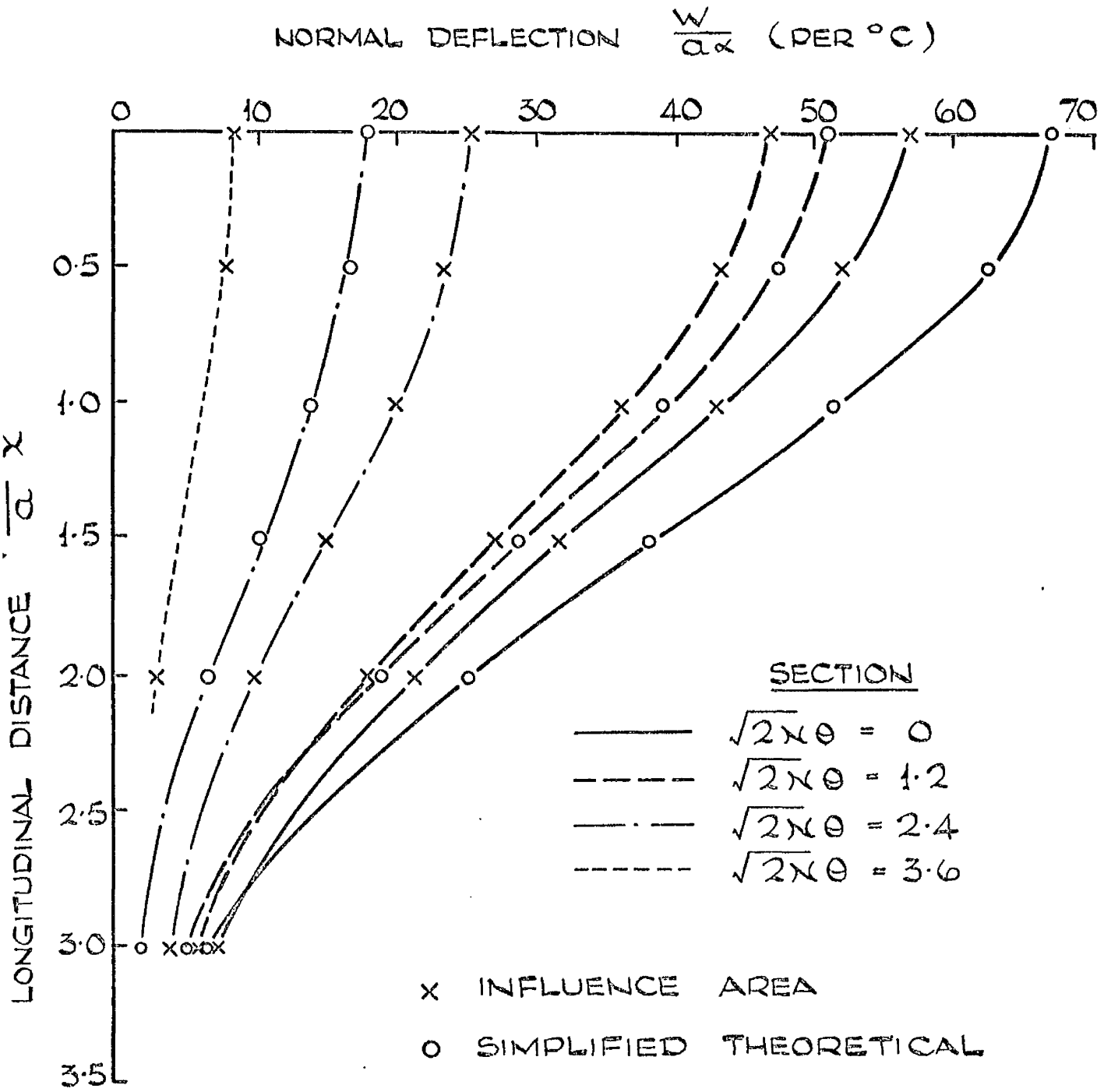


FIGURE (6.13) THE DISTRIBUTION OF THE NORMAL DEFLECTION AT VARIOUS SECTIONS ON THE SURFACE

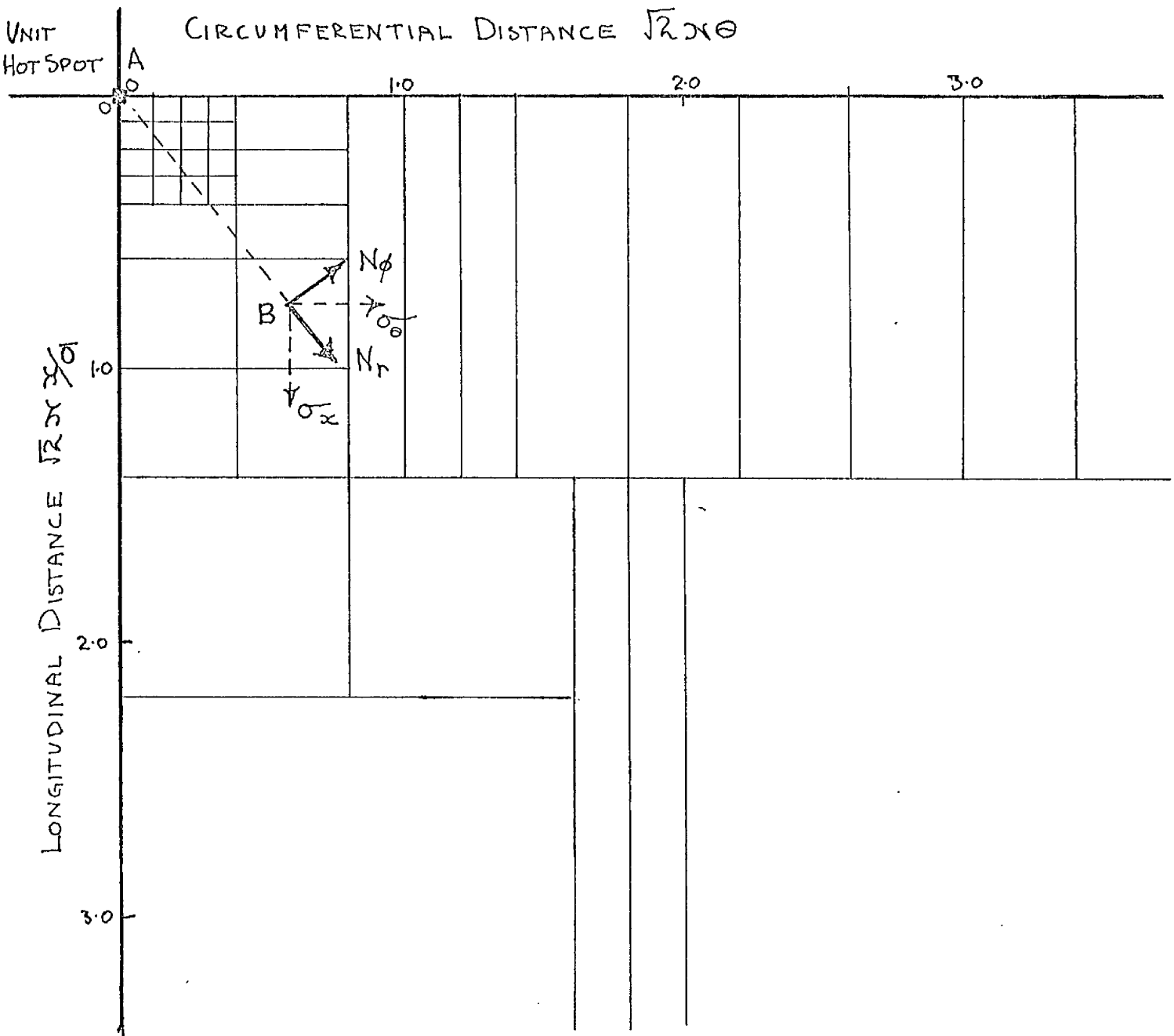


FIGURE (6.14)

THE FIGURE SHOWS HOW THE SURFACE WAS PORTIONED IN ORDER TO FIND THE "EFFECT" AT POINT A. IN PARTICULAR THE "EFFECT" OF THE AREA AND THE TEMPERATURE ASSOCIATED WITH POINT B IS INDICATED.

However these stress resultants must be reorientated into the (x, θ) co-ordinates. Knowing the relevant angle associated with the line joining the two points, AB, and the x ordinate is 51° it is now possible to transform the stresses, by a Mohr circle type transformation, to the cartesian co-ordinate system to give

$$N_{x\ ba} = 0.444 \frac{2x^2}{2\pi a^2} Eh$$

$$N_{\theta\ ba} = 0.0516 \frac{2x^2}{2\pi a^2} Eh.$$

$$\tau_{x\theta\ ba} = -0.922 \frac{2x^2}{2\pi a^2} Eh$$

considering, as before, the area surrounding the point B as

$$A = 0.16 \frac{a^2}{2x^2}$$

and the associated temperature of this area as 46°C then the stress resultants, at A, due to this heated area are

$$N_{x\ ab} = 0.444 \cdot \frac{2x^2}{2\pi a^2} \cdot Eh \times \alpha \times 46 \times \frac{0.16 a^2}{2x^2} = 0.520 Eh\alpha$$

$$N_{\theta\ ab} = 0.0516 \frac{2x^2}{2\pi a^2} Eh \times \alpha \times 46 \times \frac{0.16 a^2}{2x^2} = 0.060 Eh\alpha$$

$$\tau_{x\theta\ ab} = -1.079 Eh\alpha.$$

The resultant stresses at point A can, therefore, be found by summing the component stresses at all of the small areas which make up the heated surface

Stresses at the point A have been estimated using this influence area technique. They are

$$N_{\theta} = -163.71 Eh\alpha$$

$$N_x = -139.66 Eh\alpha$$

$$M_{\theta} = -35.89 Eh\alpha$$

$$M_x = -30.44 Eh\alpha$$

Using/

Using the "simplified theory" the equivalent values for the stresses are

$$N_{\theta} = -132.62 E h \alpha$$

$$N_x = 0$$

$$M_{\theta} = -5.977 E h \alpha$$

$$M_x = -19.920 E h \alpha .$$

As expected the magnitude of the stresses as indicated by the influence area technique is the greater. It could be concluded that the simplified solution does not give a reasonable indication of the magnitude of the stresses for the temperature distribution.

The example considered was laborious to evaluate by the graphical technique employed. Nevertheless a solution was obtainable. This same technique is suitable for computer application provided the KELVIN functions can be expressed suitably in a series form. One major disadvantage of the technique is its inability to handle changes in the material properties with temperature.

CHAPTER 7

EXPERIMENTAL

The experimental work contained in this thesis is partitioned into two main sections .

The first section contains details of the experimental investigation of the temperature distribution on a mild steel shallow spherical shell due to a uniformly heated circular opening . The experimental results which were obtained are compared with the theoretical predictions .

The second subdivision is the measurement of the strains which are incidental to the temperature distributions already considered .

The experimental strain readings are compared with the theoretical predictions .

EXPERIMENTAL

- 7.1 Object of the Experimental Work
- 7.2 Temperature Distribution on a Shallow Spherical Shell due to a Uniformly Heated Circular Opening
- 7.3 Strain Distribution on a Shallow Spherical Shell due to the Uniform Heating of a Circular Opening
- 7.4 Conclusions and Discussion

7.1 The Object of the Experimental Work

One of the philosophical difficulties in a thesis of this nature is to define what should be the object of any experiment performed and what should be its relationship to the overall theoretical development.

The object of the experimental work now being presented is to consider a particular case of temperature distribution and to compare the measured values of the thermal strain with the appropriate theoretical predictions. In particular, the case of a uniformly heated circular opening in a shallow spherical shell, such as would give rise to an axisymmetric temperature distribution, is considered. The opening in the shell and the shell's outer boundary are made free of any external mechanical restraints and the temperature of the shell is allowed to stabilise under the conductive, convective and radiant modes of heat transfer; the latter two modes being relative to a normal laboratory at room temperature.

This experimental work cannot be considered as a confirmation of the theoretical predictions made in the preceding chapters since it is merely an examination of one particular case of thermal stress for one particular set of shell parameters. Despite this, it is valuable to have even one experimental set of results to compare with the theoretical predictions.

Since the theoretical results suggest that the thermal strains/

strains are likely to be small in magnitude , it was considered prudent to be guided further by these predictions and to investigate as small a shell opening as practical since apparently the smaller the opening the greater the magnitude of the maximum stress .

The experimental work has been partitioned under two distinct headings . The first is the temperature distribution and the second is the measurement of the accompanying thermal strains.

From the outset of the experimental work it became obvious that the question of whether thermal strains could be satisfactorily measured or not by the strain gauges currently available had to be considered . It is now obvious that for the earlier work the answer must have been no since the order of the magnitude of errors in the strain gauging was considerably higher than that of the actual strains being measured . Fortunately much improved gauges have recently become available but even with these more sophisticated gauges the same question must still be faced .

7.2 The Temperature Distribution on a Shallow Spherical Shell due to a Uniformly Heated Circular Opening

Three shallow spherical mild steel shells each of the same mean radius but of different thickness of material were made available by the Motherwell Bridge and Engineering Company. These domes had been pressed on the same formers and from the same material which was used in the manufacture of the 1/10th scale model of the Dounreay Sphere upon which much earlier experimental work had been performed, particularly by Tooth.

The dimensions of the domes are detailed in Figure (7.1). From specimen samples of the mild steel, average values of its physical properties were found to be:-

$$\begin{aligned} \text{Young's modulus,} & & & = 13,700 \text{ ton/in}^2 \\ \text{Poisson's ratio} & & & = 0.255 \\ \text{Coefficient of linear thermal expansion,} & & & \\ & & & = 11.3 \times 10^{-6} / ^\circ \text{C}. \end{aligned}$$

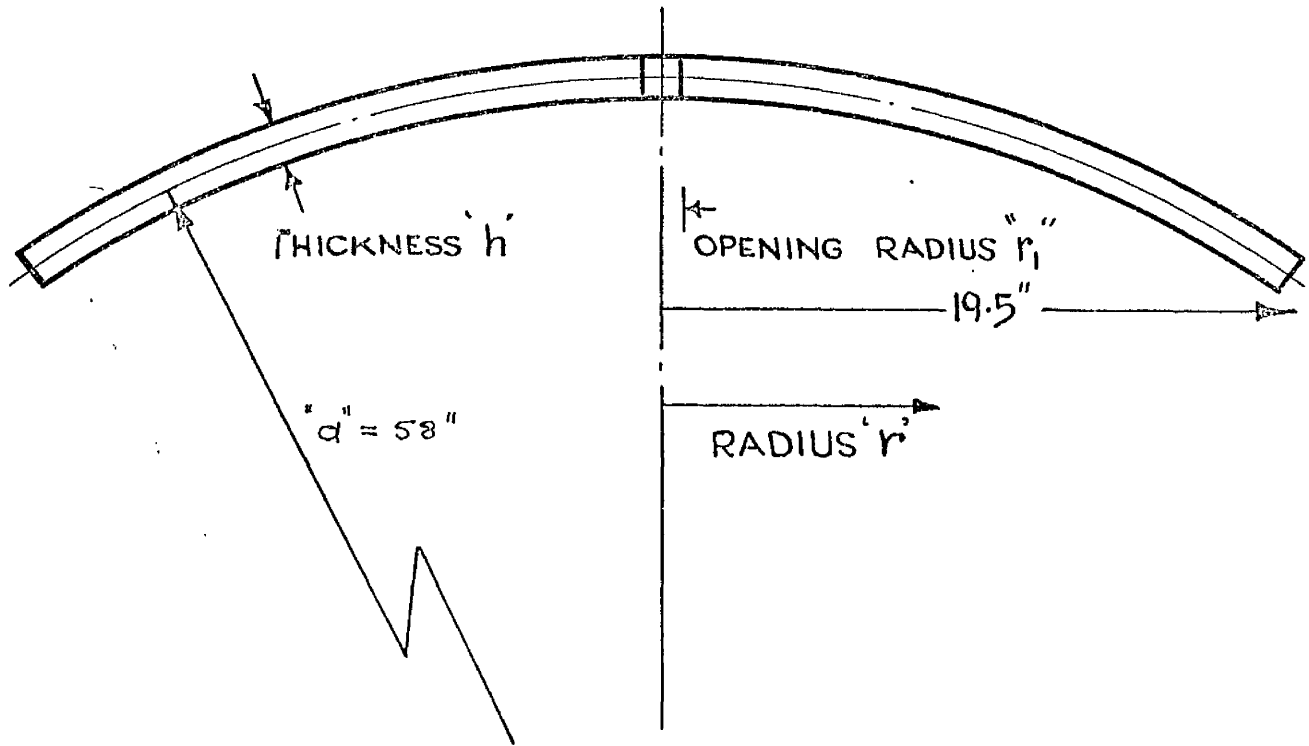
The values of Young's modulus and Poisson's ratio were determined at room temperature whereas the Coefficient of linear expansion is an average value measured over the range $0 \rightarrow 100^\circ \text{C}$.

To determine a suitable size for the circular opening in each of the shells, cognisance was paid to the difficulties which would arise in the ensuing numerical analysis. A common value for the shell parameter z of 0.1 was chosen for all three openings.

Thus

$$z = \sqrt{2} \alpha \phi = 0.1$$

where/



SHELL A

$$r_1 = 0.297''$$

$$h = \frac{1}{2}''$$

SHELL B

$$r_1 = 0.257''$$

$$h = \frac{3}{8}''$$

SHELL C

$$r_1 = 0.21''$$

$$h = \frac{1}{4}''$$

MATERIAL PROPERTIES:-

$$E = 13,700 \text{ ton/in}^2$$

$$\nu = 0.255$$

$$\alpha = 11.3 \times 10^{-6} / \text{C}^\circ$$

FIGURE (7.1) DETAILS OF THE EXPERIMENTAL MILD STEEL SHELLS.

where it is recalled from the theoretical work of the earlier Chapters

$$4\alpha^4 = 12(1-\nu^2) \frac{\sigma_1^2}{h^2}$$

and ϕ is of course the angle of the opening.

The reason for this choice of value is that tabulated values of the Kelvin functions for this argument are available and also this particular value implies a suitably small opening in each of the shells.

The radius of the openings, r_1 , was calculated to be:-

shell A ($\frac{1}{2}$ " thick) $r_1 = 0.2965$ "

shell B ($\frac{3}{8}$ " thick) $r_1 = 0.2573$ "

shell C ($\frac{1}{4}$ " thick) $r_1 = 0.2098$ "

and a hole was drilled and reamed as close to the appropriate dimension as practical in each of shells.

The uniform heating of the circular hole both around its circumference and through the shell thickness proved difficult. To the two major requirements of uniformity and zero force action on the wall of the shell must also be added, what subsequently proved a major obstacle, the stipulation that no radiant heat be transferred from the heating device to the surface of the shell.

After attempts to construct a small electrical element, which would fit into the opening in the manner of a loose plug, had failed, due to the excessive quantity of heat being generated in a small volume, attention was concentrated on the problem of having the source of heat external to the opening and heating the hole by conduction or convection from the heat supply. An electric furnace was constructed round a thin copper tube whose external diameter was the same as the bore of the shell opening.

The/

The heating rig is shown in Figure (7.2a). Both ends of the copper tube were allowed to protrude from this enveloping furnace and, while one end was fitted into the shell, to the other end was attached an air supply which allowed air to be pumped up through the copper tube. This pumping of air proved inconsequential. It was found that excessive temperatures were required to be developed in the furnace to raise the temperature at the opening of the shell to even 100°C . This of course is due to the quantity of heat requiring to be conducted along the copper bit and thus on to the shell. Further, since the furnace was at such elevated temperatures, a great quantity of heat was emitted from the lagging and this heat had to be dispersed without affecting the surfaces of the shell. There was also the problem of a temperature differential through the shell with the surface near the furnace in excess, due to the conduction effect along the tube. This method of heating was also considered unsatisfactory.

The method of heating finally adopted consists, again, of a thin copper tube which mated with the opening in the shell. Through this tube passed the flue gases from the combustion of a calor gas burner situated under the tube. A funnel is brazed to the lower end of the tube to ensure that all the hot gas passes up the tube as shown in Figure (7.2) and schematically in Figure (7.3). This funnel and the lower portion of the tube are lagged to minimise heat loss to the underside of the shell. A cold air supply is also provided around the tube underneath the shell. This colder air can be used to prevent the entrapment of hot air due to the shape of the shell. It is found essential to insert a small piece of wire gauze in the tube above the opening. The heat given off to the gauze/

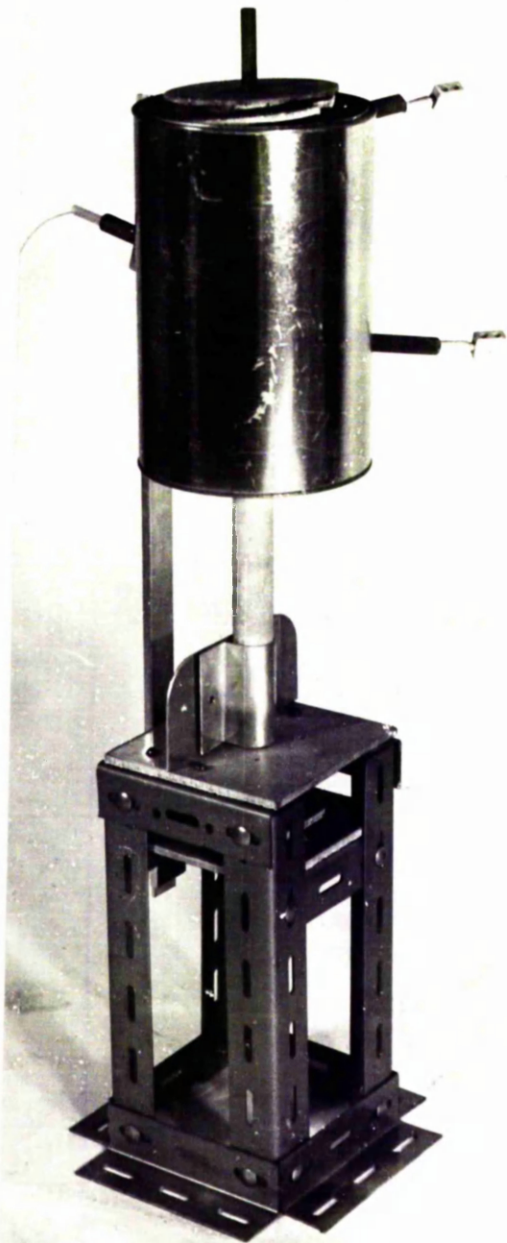


FIGURE (7.2a) ELECTRIC HEATING FURNACE.

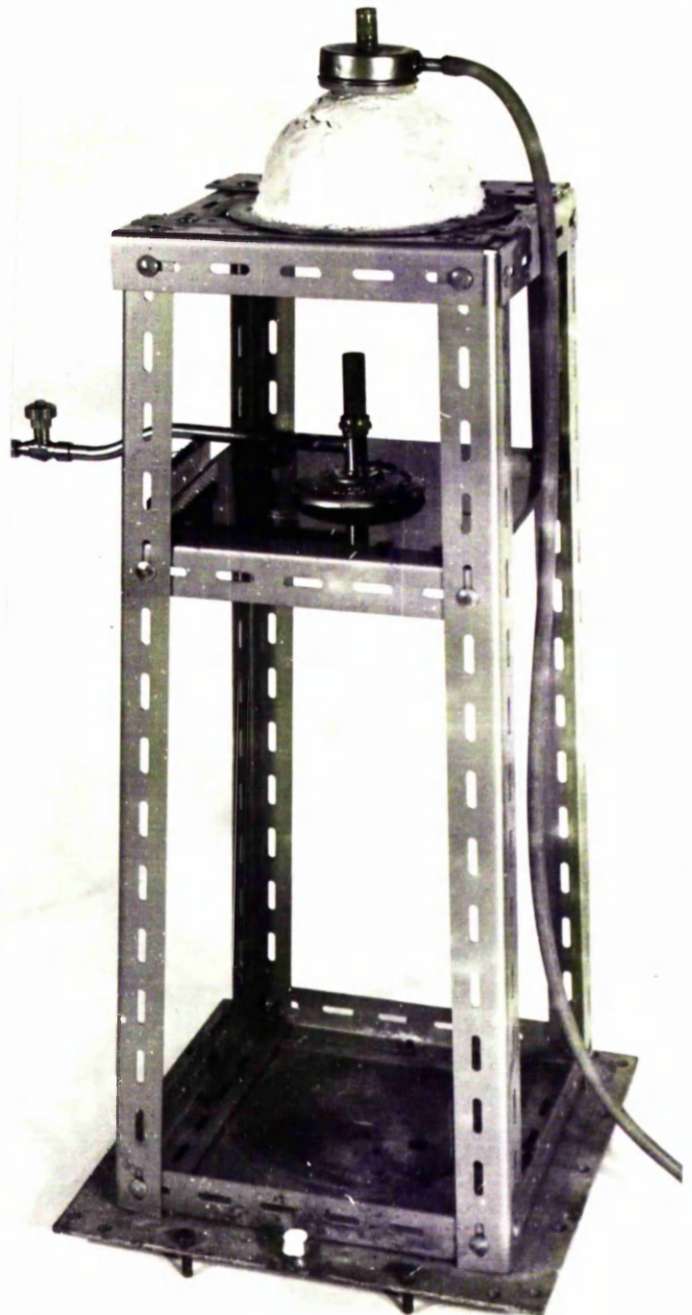


FIGURE (7.2b) ARRANGEMENT OF GAS BURNER AND COPPER TUBE.

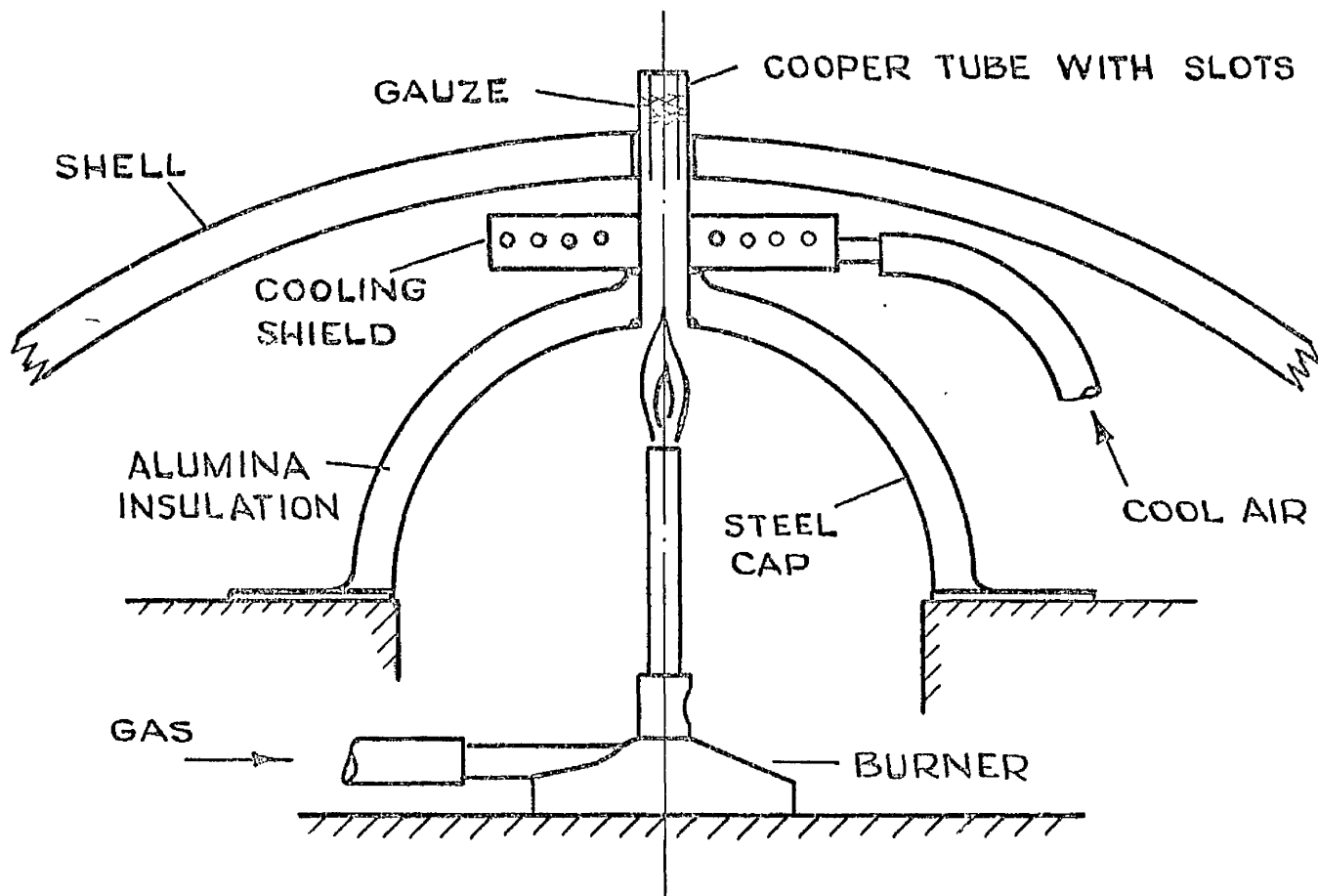


FIGURE (7.3) LAYOUT OF THE HEATING ASSEMBLY

SHELL A ($\frac{1}{2}$)	SHELL B ($\frac{3}{8}$)	SHELL C ($\frac{1}{4}$)
5	5.7730	7.0705
7	8.0797	9.8959
9	10.3922	12.7279

TABLE (7.1) EQUIVALENT VALUES OF THE PARAMETER 'S' FOR THE THREE EXPERIMENTAL SHELLS.

gauze tends to balance that tendency for the lower surface of the shell to be warmer, near the opening, than the upper surface. The calor gas burner is easily controllable and steady temperature conditions can be maintained.

It is found that the degree of pressure between the tube and the opening wall is of the utmost importance. Any lack of uniformity of pressure results in large discrepancies from the axisymmetric temperature distribution which is required. To ensure that the temperature distribution is axisymmetric, thermocouples have been attached, to the surface of the sphere near to the opening, on the same hoop circles but at different meridional angles. These thermocouples along with the thermocouples along the radial line, which indicate the axisymmetric temperature distribution, can be seen on the photograph of the top surface of the $\frac{1}{2}$ " thick shell, Figure (7.4). Any difference in readings between the circumferentially displaced thermocouples would indicate a lack of symmetry in the heating of the shell and this would require to be corrected by the appropriate orientation of the pressure of the heating tube.

The axisymmetric temperature distribution is measured by the same radial line of thermocouples on both surfaces of the sphere, Since the temperatures are required to be measured relative to room temperature there is no need for any cold junction other than the potentiometer box itself upon which a reading in millivolts, corresponding to the temperature, can be measured. The general layout including the temperature measuring equipment is shown in the photograph, Figure (7.4b).

After/

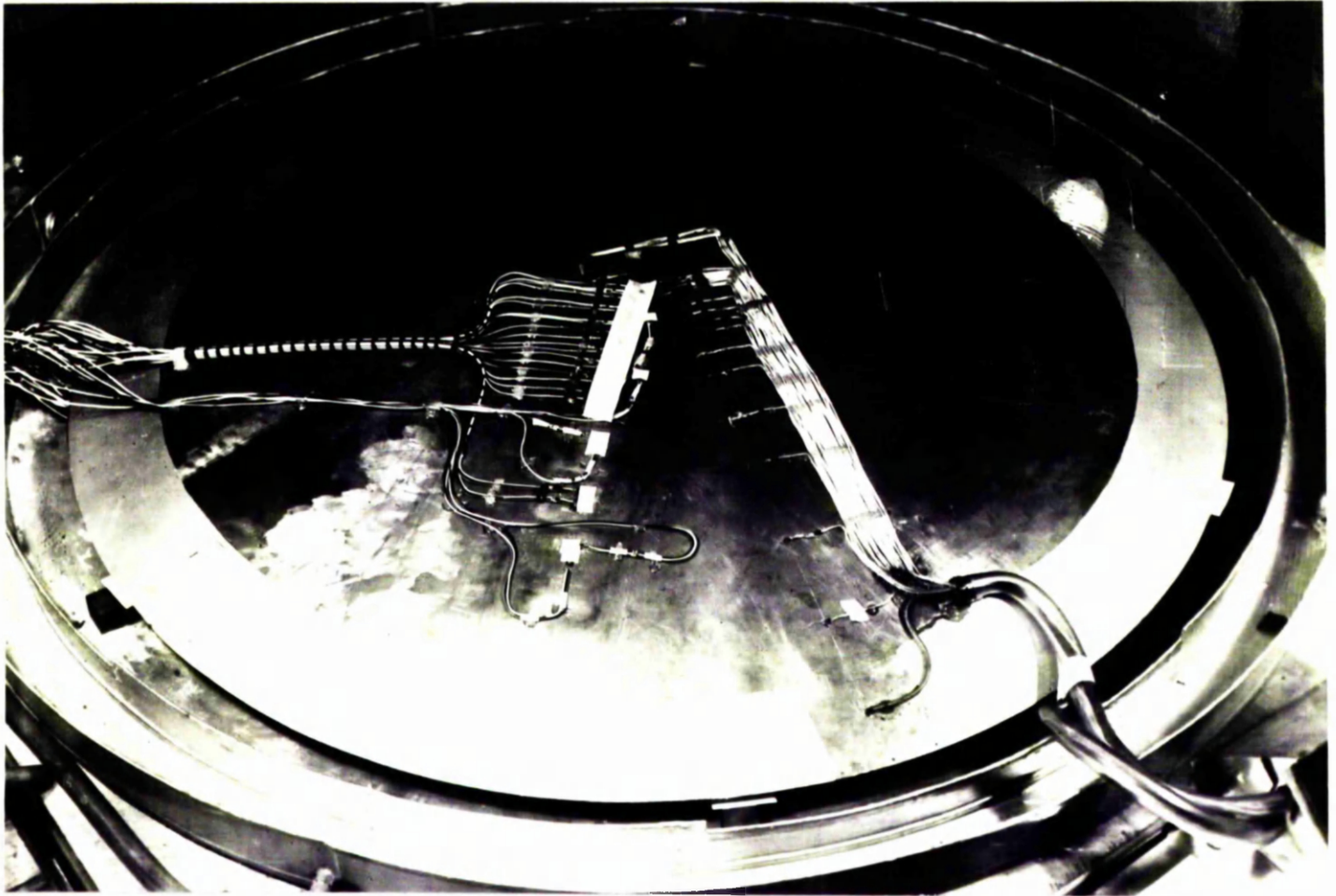


FIGURE (7.4) PHOTOGRAPH SHOWING THE TOP SURFACE OF SHELL A WITH THE STRAIN GAUGES ON THE LEFT AND THE THERMOCOUPLES ON THE RIGHT.

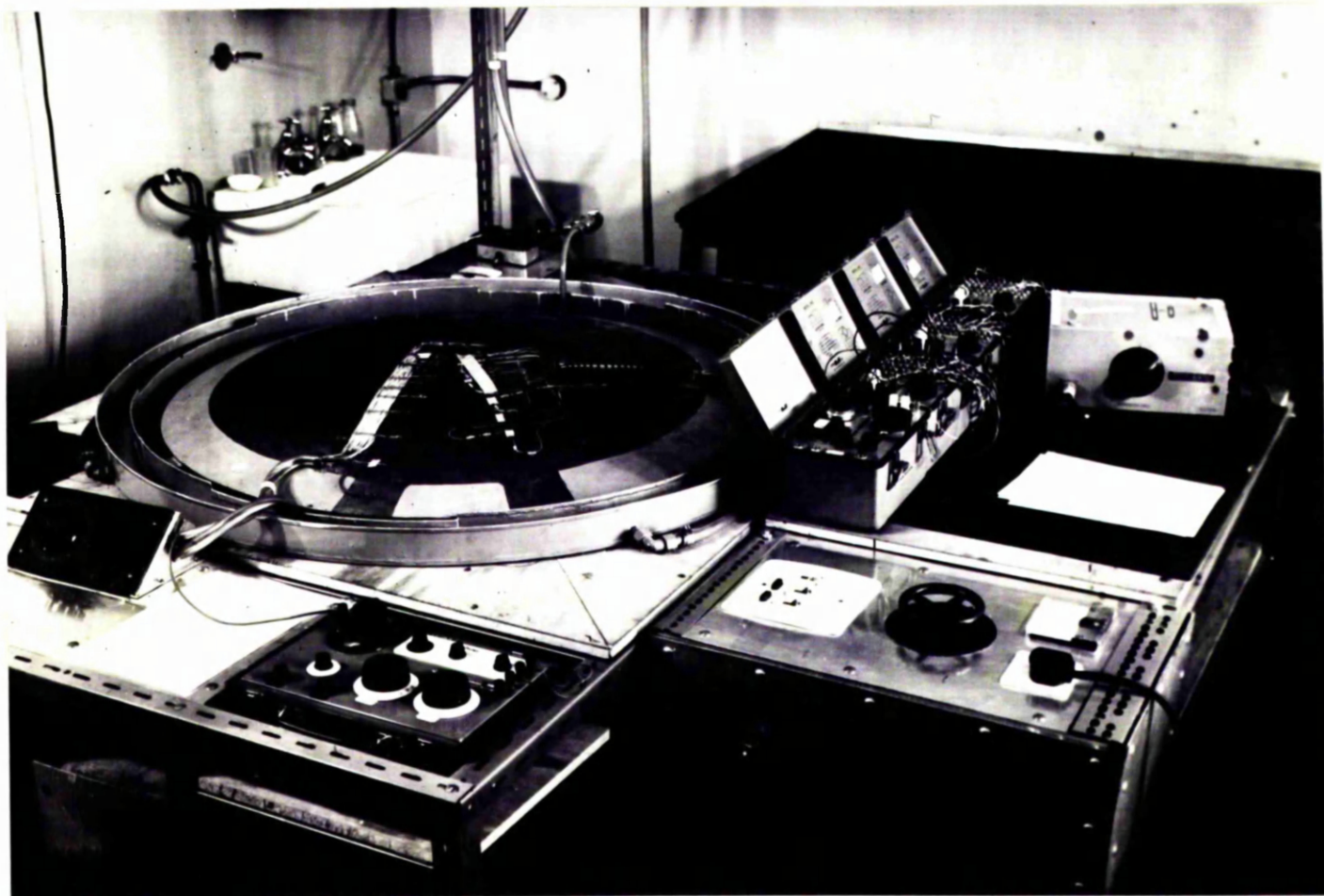


FIGURE (7.4b) THE GENERAL LAYOUT OF THE EXPERIMENTAL RIG.

After several tests the most satisfactory method of affixing the hot thermocouple junctions to the material was found to be by spot welding. To strengthen the weld and also to provide a protective coating, a blob of Araldite was put over the junction. The lead wires to the junction were run for a short way along a path of uniform temperature with that junction.

No difference in temperature through the thickness of the plate was found beyond the first 4" radius from the axis. Within the first 4" gradients through the plate could be corrected by the pressure of the tube, position of the gauze in the tube and cool air being pumped round the heater.

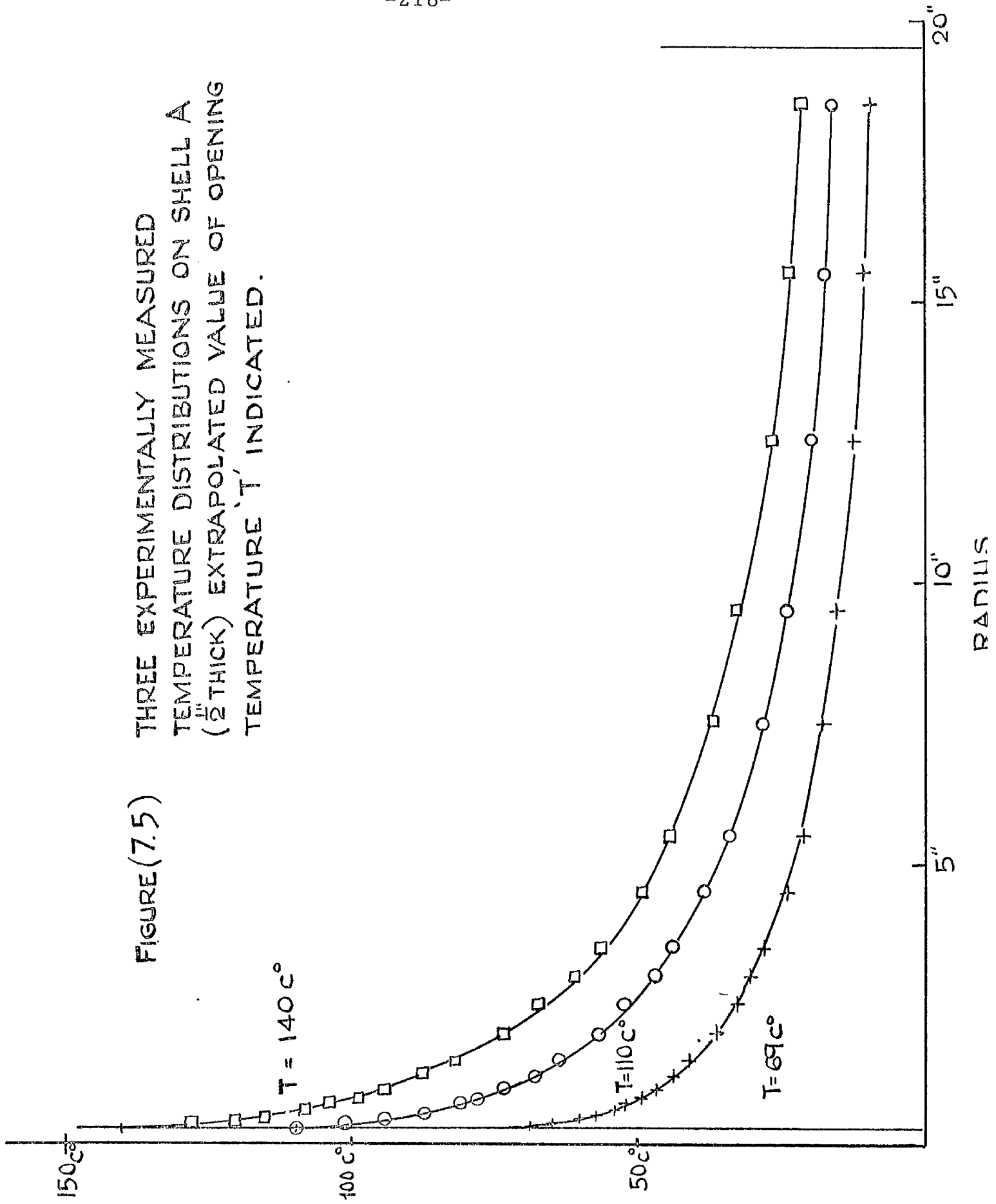
Results for three distinct temperature distributions are presented in graphical form in Figures (7.5 - 7) for each of the shells.

Each of the traces on the temperature graphs was extrapolated to give a temperature value at its particular opening; this is the opening value of the temperature, T , which figured so prominently in the theoretical development. As is common with all extrapolation there is a degree of human judgement required and hence a degree of error can be introduced.

After determining the opening values of the temperature each of the distributions was normalised to its own particular value and Figures (7.8 - 10) present the temperature distribution as a function of the opening value. The results are promising in that they show that it is not unreasonable to express the temperature distribution as a function of the opening temperature, T .

We can now investigate the suitability of the theoretical/

FIGURE (7.5)
THREE EXPERIMENTALLY MEASURED
TEMPERATURE DISTRIBUTIONS ON SHELL A
($\frac{1}{2}$ " THICK) EXTRAPOLATED VALUE OF OPENING
TEMPERATURE 'T' INDICATED.



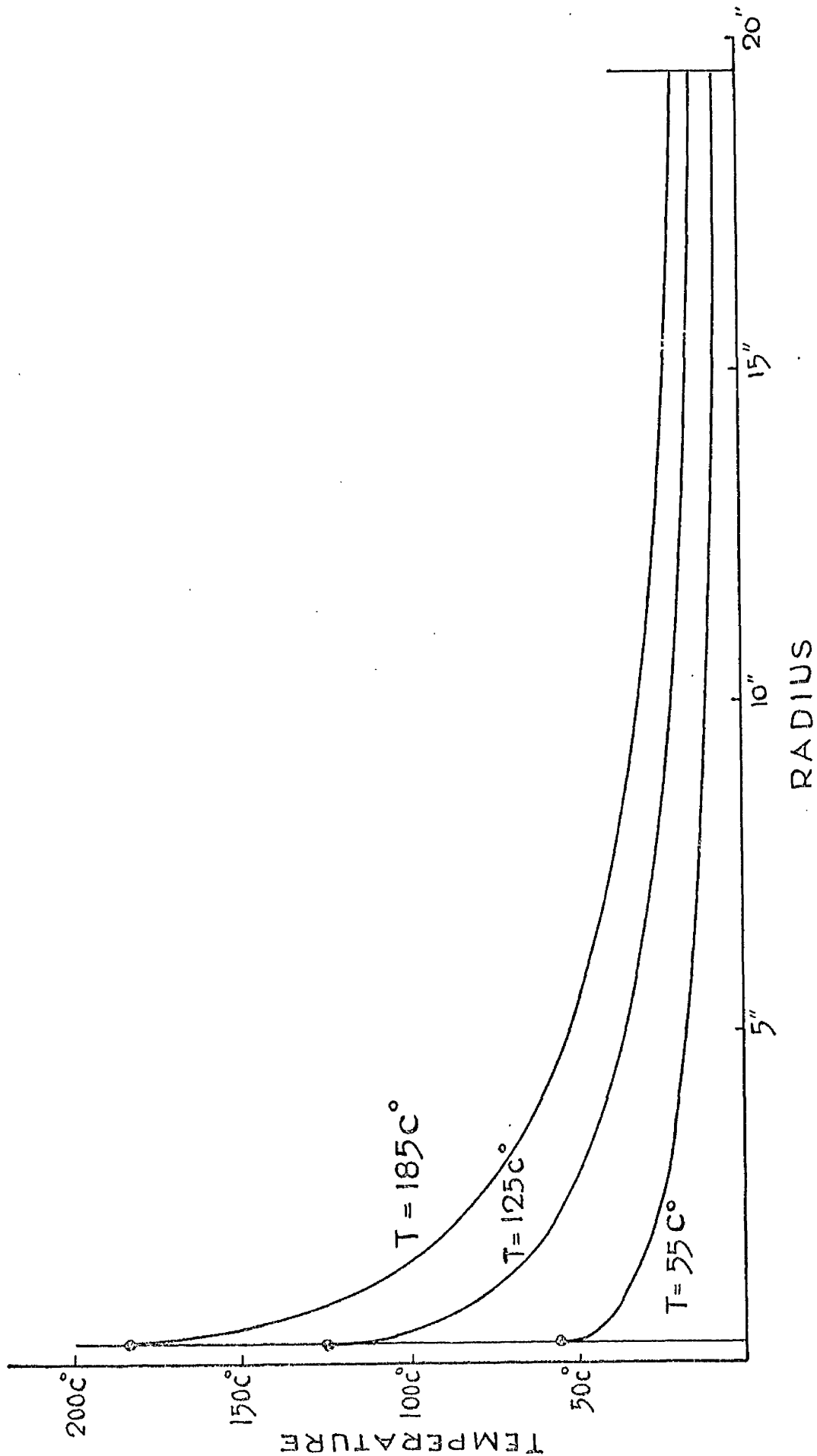


FIGURE (7.6) THREE EXPERIMENTALLY MEASURED TEMPERATURE DISTRIBUTIONS ON SHELL B ($\frac{3}{8}$ THICK)

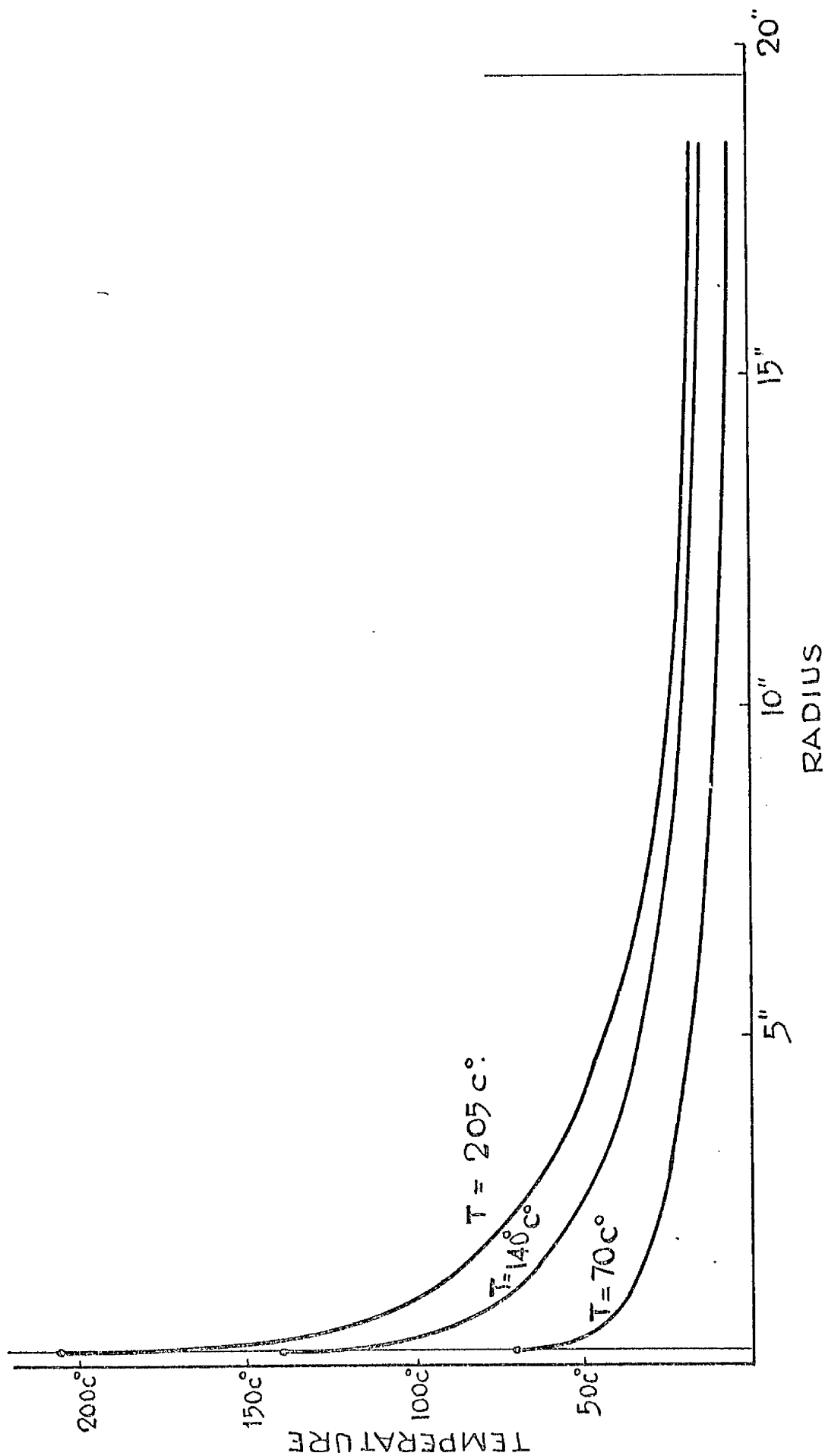


FIGURE (7.7) THREE EXPERIMENTALLY MEASURED TEMPERATURE DISTRIBUTIONS ON SHELL C ($\frac{1}{4}$ THICK)

FIGURE (7.8) NORMALISED VALUES OF THE EXPERIMENTAL POINTS, SHOWN IN FIGURE (7.5) FOR SHELL 'A'. THEORETICAL TEMPERATURE DISTRIBUTIONS FOR DIFFERENT 'S' VALUES ARE INCLUDED.

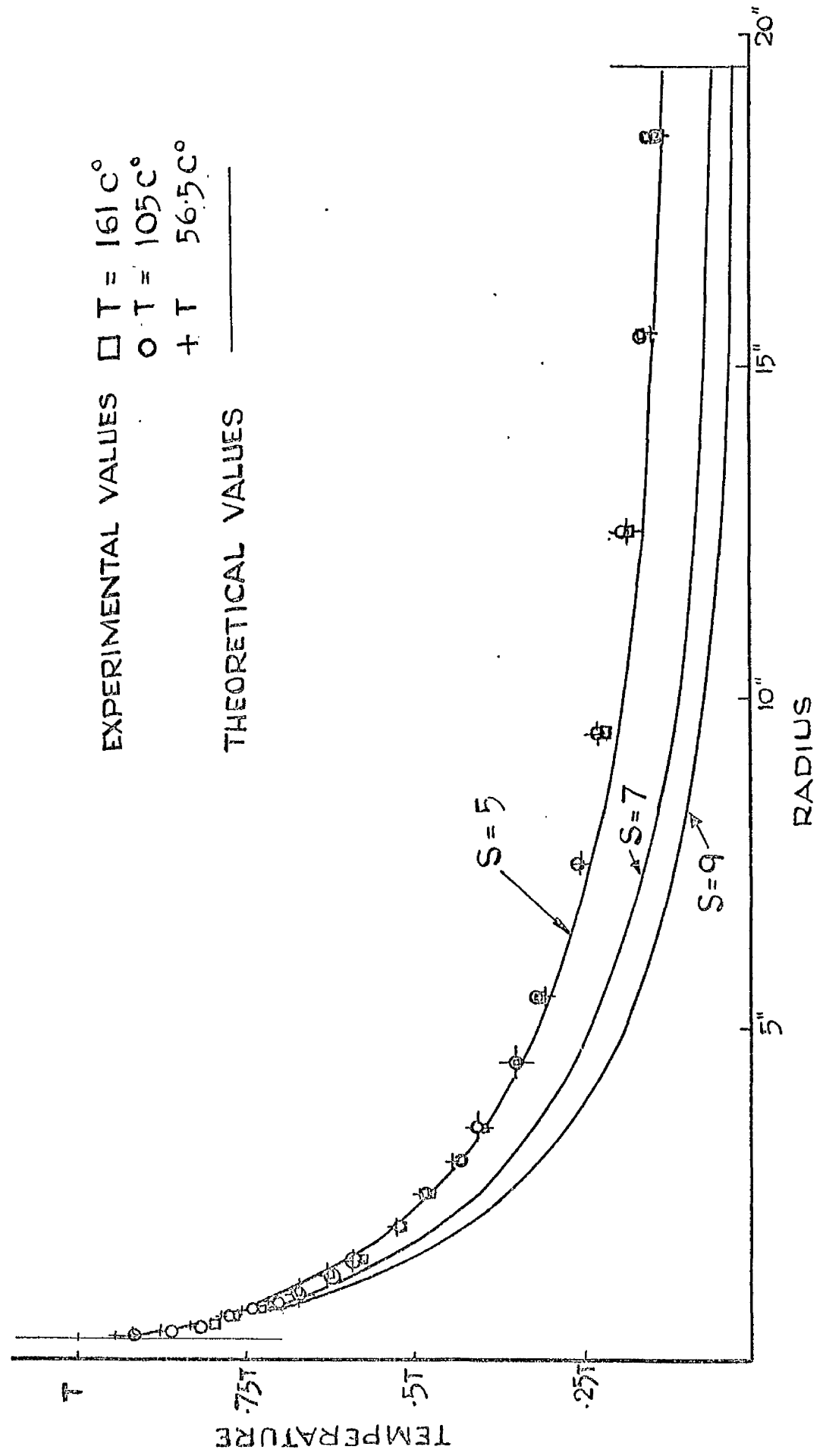


FIGURE (7.8b) THE NORMALISED VALUES OF FIGURE (7.8) SHOWN IN GREATER DETAIL FOR SMALL VALUES OF THE RADIUS.

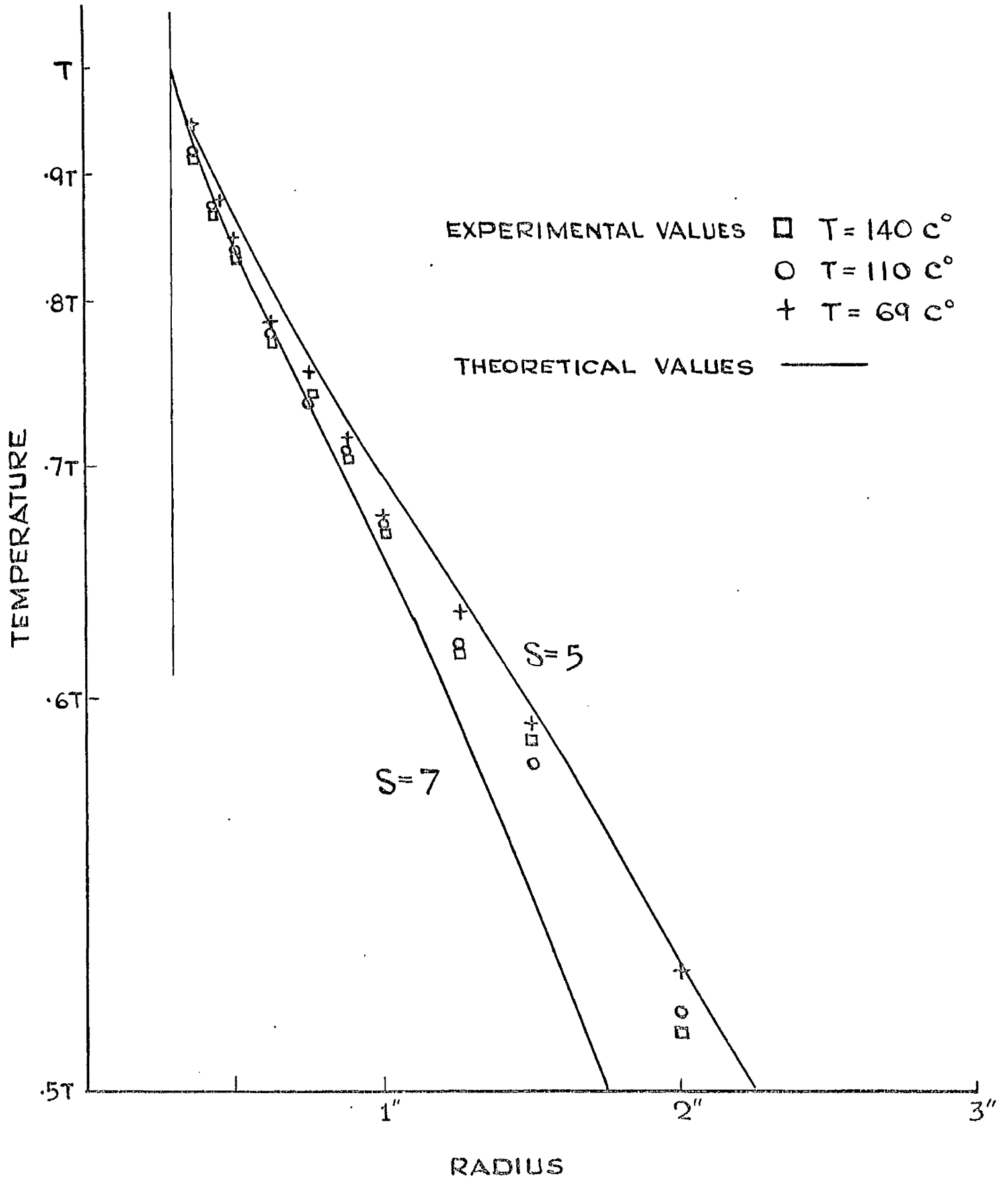


FIGURE (7.9) NORMALISED VALUES OF THE EXPERIMENTAL POINTS, SHOWN IN FIGURE (7.6), FOR SHELL 'B', THEORETICAL TEMPERATURE DISTRIBUTIONS FOR DIFFERENT S VALUES ARE INCLUDED

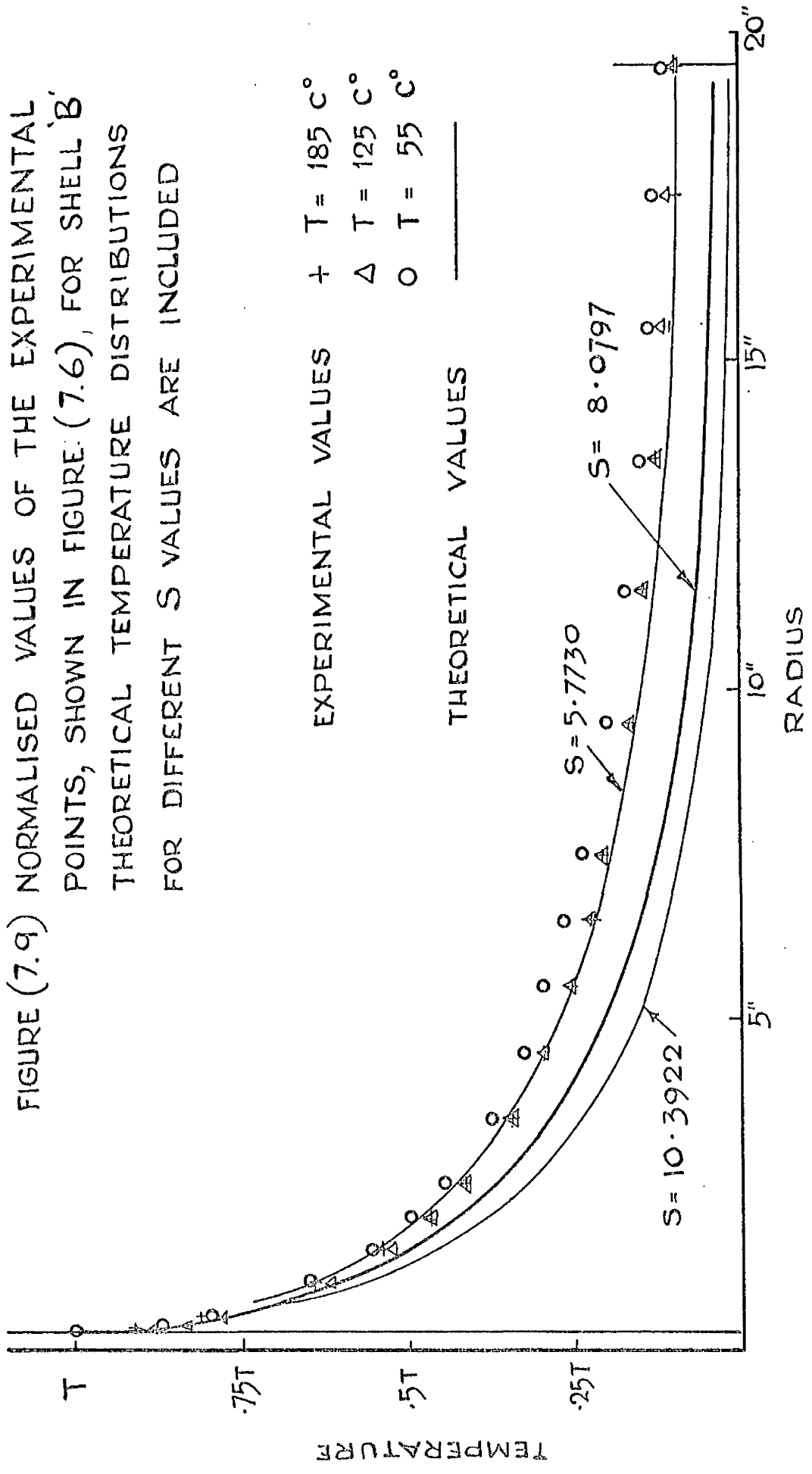
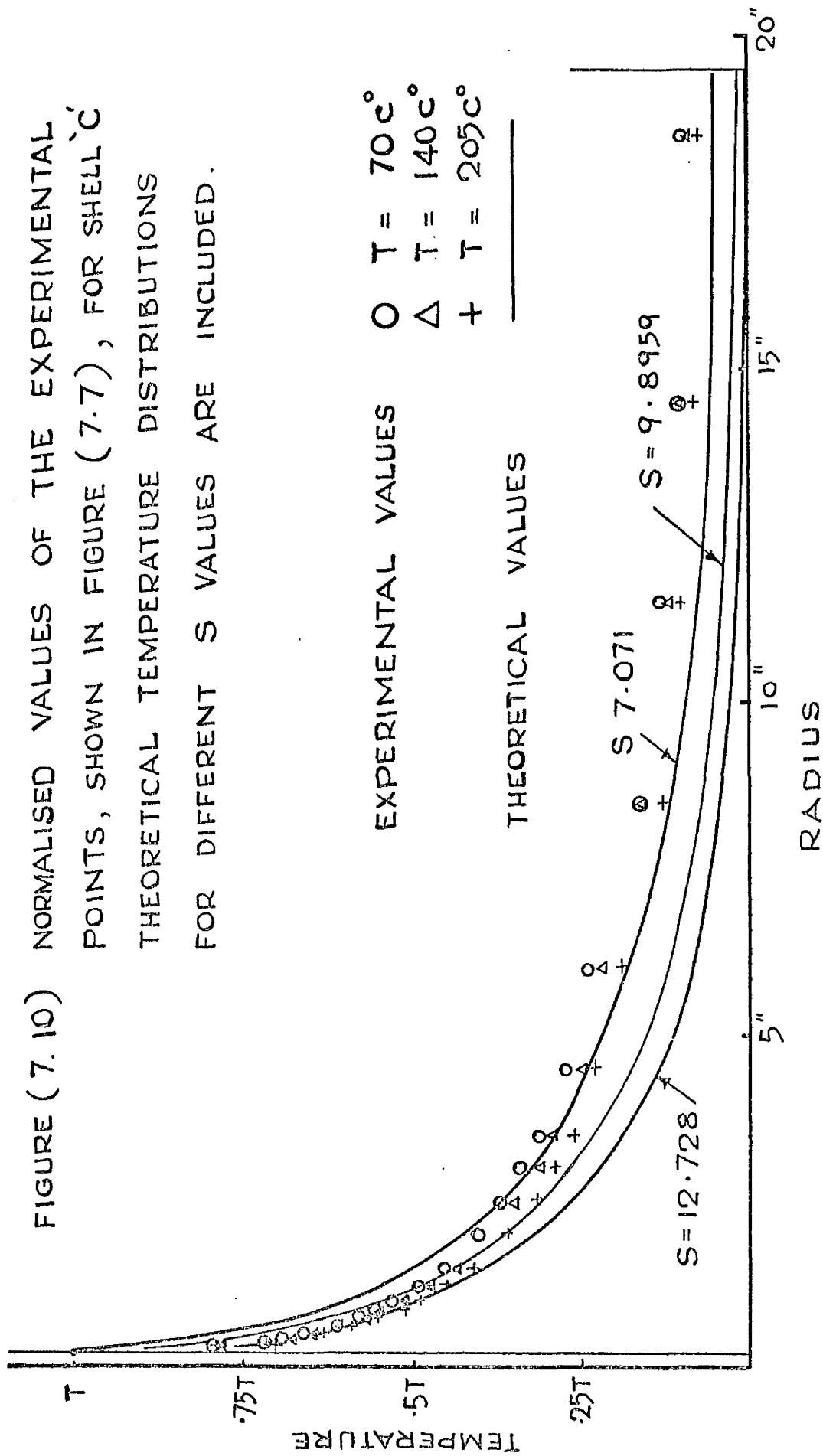


FIGURE (7.10) NORMALISED VALUES OF THE EXPERIMENTAL POINTS, SHOWN IN FIGURE (7.7), FOR SHELL C THEORETICAL TEMPERATURE DISTRIBUTIONS FOR DIFFERENT S VALUES ARE INCLUDED.



theoretical predictions for the temperature made in Chapter 1.

Equation (1.17) gives for a shallow spherical shell

$$t = AI_0(s\phi) + BK_0(s\phi)$$

where, from equation (1.4),

$$S^2 = \frac{2m}{kh} \cdot a^2$$

Let us consider an estimate of the value of this thermal parameter S for shell A. Whereas there is no difficulty with the thickness of the shell, h , and the mean radius of the shell, a , much judgement is required in the selection of the values of the thermal conductivity of the material, k , and the combined convective and radiation coefficient, m .

Table (A3.2) would suggest that a value of 30 Btu/ft hr^{°F} for the thermal conductivity, k , would not be unreasonable.

Recalling from equation (1.2) that the coefficient m is the sum of the two coefficients m_c and m_r we find in Appendix 3 that McADAMS⁽⁵⁶⁾ gives two empirical results, one for a horizontal plate facing upward, equation (A3.1) and the other for the same plate facing downward, equation (A3.2). Since we have the situation of one surface facing upwards and the other downwards, let us take a value between the two given by McADAMS and consider

$$m_c = 0.3 (t_s - t_f)^{\frac{1}{4}}$$

A greater problem is the determination of a suitable value for the "constant" t_s , the surface temperature of the plate. Though the temperature at the opening is relatively high the main surface is relatively cool. However, to arrive at some value let us consider/

consider values of 212°F for t_s and 75°F for the room temperature t_f , thus

$$\begin{aligned} m_c &= 0.3 (212 - 75)^{\frac{1}{4}} \\ &= 1.02 \text{ Btu/ft}^2 \text{ hr}^{\circ}\text{F} \end{aligned}$$

The radiation coefficient m_r is given by equation (A3.7) as

$$m_r = \epsilon (t_s + t_f)(t_s^2 + t_f^2).$$

where the temperatures are in absolute scale. Table (A3.3) confirms that a value of 0.3 is not unreasonable for the emissivity, ϵ , of the material. Thus, assuming the same values for the temperature as used earlier for the convective coefficient, we have

$$\begin{aligned} m_r &= 0.1717 \times 0.3 (530 + 672) (530^2 + 672^2) \times 10^{-8} \\ &= 0.454 \text{ Btu/ft}^2 \text{ hr}^{\circ}\text{F} \end{aligned}$$

and the value for the composite coefficient is

$$\begin{aligned} m &= m_r + m_c \\ &= 0.454 + 1.02 = 1.474 \text{ Btu/ft}^2 \text{ hr}^{\circ}\text{F} \end{aligned}$$

It is of interest to note that CHAPMAN⁽⁵⁷⁾ uses, in his examples involving mild steel plates, for the conductivity constant $33 \text{ Btu/ft hr}^{\circ}\text{F}$ and for the coefficient m , $1.4 \text{ Btu/ft}^2 \text{ hr}^{\circ}\text{F}$.

Using the values developed the thermal parameter S becomes

$$\begin{aligned} S &= \left(\frac{2 \times 1.474 \times 12}{30 \times \frac{1}{2}} \right)^{\frac{1}{2}} \times 5 \\ &= 7.66 \end{aligned}$$

Since/

Since there are so many approximations and assumptions made it would suffice to consider the value of

$$S = 7$$

and for comparison with the experimental results to consider as outside bounds the values of $S = 5$ and $S = 9$.

The equivalent S values, using the same conductivity and overall heat transfer coefficient, for the other two shells are shown in Table (7.1).

Recalling once again that the theoretical expression for the temperature distribution is, from equation (1.21),

$$t = AI_0(S\phi) + BK_0(S\phi)$$

we can differentiate to find the thermal gradient as

$$t' = SA I_1(S\phi) - SB K_1(S\phi).$$

With the appropriate boundary conditions appertaining to the experimental shells namely

$$\begin{aligned} t &= T \quad \text{at} \quad \phi = \phi_1 \\ t' &= 0 \quad \text{at} \quad \phi = \phi_2 \end{aligned}$$

where ϕ_1 and ϕ_2 are the inner and outer shell boundary values, the integration constants then become

$$A = \frac{K_1(S\phi_2)}{I_0(S\phi_1)K_1(S\phi_2) + K_0(S\phi_1)I_1(S\phi_2)}$$

$$B = \frac{I_1(S\phi_2)}{I_0(S\phi_1)K_1(S\phi_2) + K_0(S\phi_1)I_1(S\phi_2)}$$

With the tabulated values of S and the appropriate values/

values of ϕ_1 and ϕ_2 it is now possible to complete the corresponding theoretical temperature distributions.

These distributions have been included in Figures (7.8-10).

It is observed that the theoretical temperature distributions adequately represent the form or shape of the curve given by the experimental values.

Consider in detail the shell A, Figure (7.8). At first glance the theoretical trace given by $S = 5$ seems to most closely represent the experimental points. However, it can be seen that this theoretical trace overestimates the temperatures close to the opening and in consequence underestimates the thermal gradient at the opening. This can be seen more clearly in Figure (7.8b), which shows the values near the opening in greater detail. It is this thermal gradient which seems so important in the determination of the theoretical values of the stress distribution in the shell. The experimental trace of $S = 7$ would appear to be more suitable in describing the conditions near the opening and hence 7 would be a more suitable value to use in the theoretical calculations appropriate to the $\frac{1}{2}$ inch shell A.

In all cases the theoretical temperatures diverge from and become less than the actual temperatures towards the outside boundary. This can mean, physically, that not as much heat has been lost from the shell surface as has been predicted theoretically. A closer examination of the surface of the shell, the upper surface of which is shown in Figure (7.4), can provide one reason for this discrepancy. It is observed from the photograph that a small part of the surface of the sphere has a partial insulation in the form of thermocouple wires, strain gauges and their leads, and of course Araldite. This insulation will be particularly effective near the opening where the temperatures/

temperatures are relatively high. Because of this insulation the heat which could have been lost will be conducted down the sphere to the outer boundary and will of course cause higher temperatures on the shell. This effect was not taken into account in the theoretical considerations.

This experimental error aside it is surprising considering the coarseness of the approximations made in forming our heat transfer coefficient S that one theoretical curve so closely fits the experimental values, particularly since so much of the heat loss from the surface is not a linear function of the temperature.

It is appreciated that if the shell were broken up into a number of bands, each with their own S value, then a much better correspondence could be achieved. Since, however, we are requiring a value of S for our subsequent theoretical stress calculations, there appears no need to do this as we have adequately shown the reasonableness of the theoretical predictions close to the important heated boundary.

Examining now the results for the other two shells, Figures (7.9 - 10), we see that they confirm what has already been said for the $\frac{1}{2}$ " shell but also since they represent another two different thicknesses further confirm the validity of the theoretical expression for the temperature distribution

$$\tau = A I_0(S\phi) + B K_0(S\phi)$$

where the thickness of the shell, h , is contained in the constant S which is given by

$$S^2 = \frac{2m}{kh} a^2$$

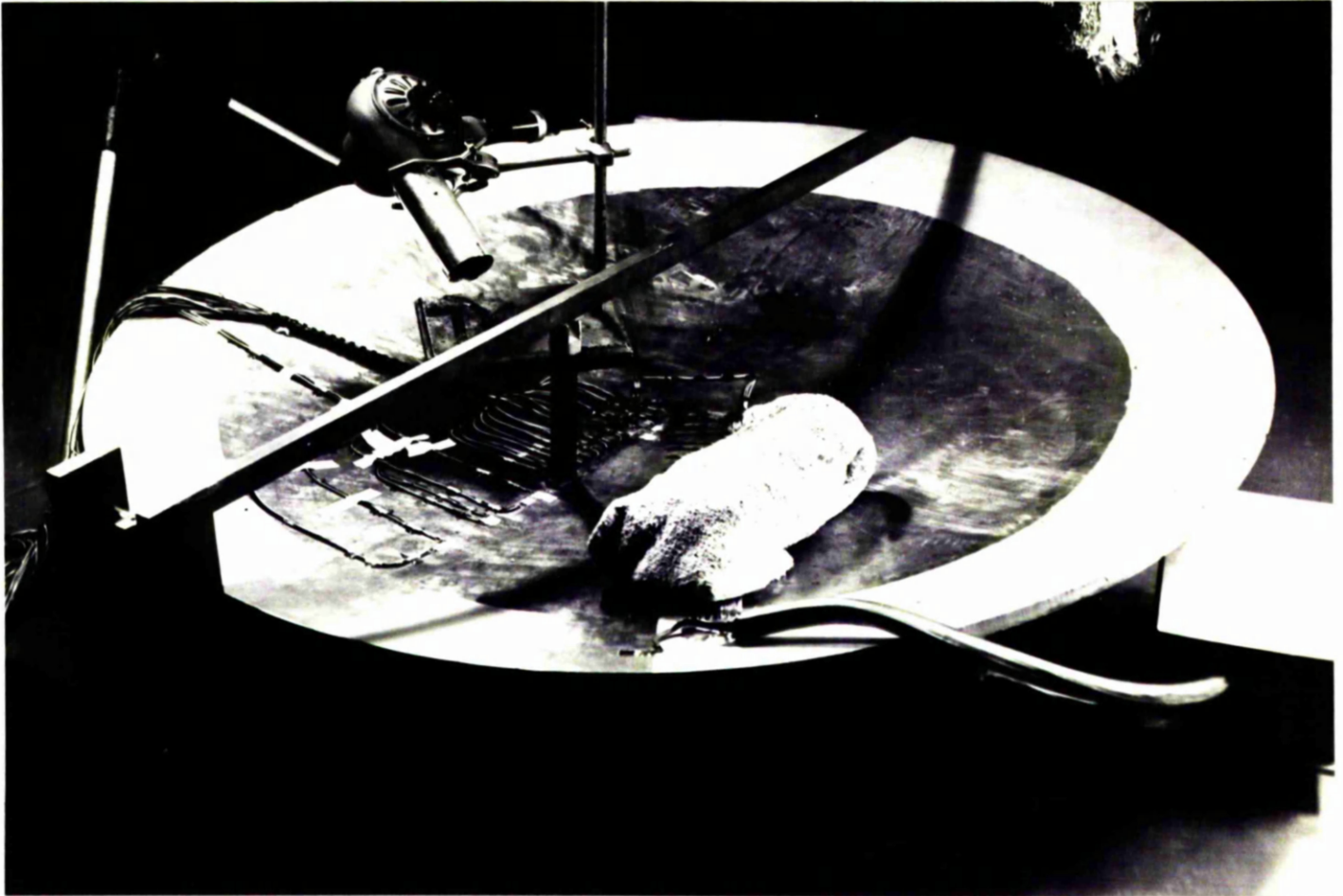


FIGURE (7.11) A STRAIN GAUGE DURING THE CURING CYCLE.

7.3 Strain Distribution on a Shallow Spherical Shell due to the Uniform Heating of a Circular Opening

With all the preliminary tests carried out, the selection of the type of gauge, its cement and the method of wiring made, it is then possible to proceed with the gauging of one of the shallow shells.

The shell selected for gauging was shell A, which is the thickest of the three shells considered earlier, namely, $\frac{1}{2}$ inch. With all the shells having a common spherical radius, a , the a/h ratio of shell A is therefore the least. The theoretical work of the earlier chapters has indicated that the lower the a/h ratio the higher is likely to be the magnitude of the maximum stresses (provided S remains constant).

Despite the great care taken in the surface preparation, the application of the adhesive and in the curing of the cement, it was found that the first two gauges had not properly bonded to the shell surface, there being slight gaps between the gauge backings and the shell. It was felt that this fault was due to insufficient or unevenly divided pressure on the gauge during curing. As has been indicated earlier, a pressure jig was constructed round the shell and the bonding of the subsequent gauges proved satisfactory.

Forty gauges were attached to the shell, equally divided between the two surfaces and oriented in circumferential and radial directions, all along the same radial line as can be seen in Figures (7.4) and (7.11). Most of the gauges were positioned as close to the opening as possible as it was felt that the more interesting strain distribution/

distribution would be in this region.

After the shell had been positioned in the heating rig and the first full temperature tests carried out, it was found that five of the gauges were unsatisfactory in so far as they gave an erratic response or no response at all. The shell was removed from the rig and these gauges repaired. Three of these gauges were found to be damaged and were replaced while the soldering at the other two was found to be "dry". The opportunity was then taken to attach a further ten gauges to give a more complete description of the strain distribution further away from the opening. The shell was then replaced on the rig and once again the experiment continued.

The shell was heated, through its opening, a number of times up to a maximum opening temperature of about 200°C to allow the gauges, etc. to settle and to subject them to a few loading cycles.

Full scale tests were then carried out heating the opening to various temperatures and when steady temperature conditions prevailed upon the sphere strain readings were taken. These readings were corrected, once a curve for the temperature distribution had been plotted, for the apparent strain and curves for the hoop and radial strains on both surfaces plotted.

It was observed that a further four gauges gave readings which were rather peculiar and did not fit into any recognisable pattern. By means of an Avometer it was quickly confirmed that there was some leakage from these gauges to the shell, although earlier resistance checks had proved satisfactory. Unfortunately all these gauges were situated on the lower surface and so once again the shell had to be removed from the rig. Three of these gauges were removed/

removed and replaced. It was found on all of them that the "earthing" took place at the soldered point of attachment of the leads. In the case of the fourth gauge there was a minor fault at its tabs.

During all this preliminary testing, one peculiarity arose which had not previously been considered and which is not mentioned in the literature. Whilst taking readings from a strain gauge, it was found that there was an erratic movement of the galvanometer needle. This movement became associated with the opening and shutting of doors in the room, draughts and movement close to the gauge. The slightest draught over a gauge was found to cause a very large movement of the galvanometer and hence a large reading of strain. The draught did not affect the lead wires. At first this may appear to be somewhat of a contradiction since self-temperature compensated gauges should be insensitive to small changes in temperature such as are caused by draughts in a room. However, it was realised that the boundary air in close proximity to the gauges must be at a temperature comparable with that of the gauge itself. Even the smallest draught would disturb this warm boundary layer and thus cause a change in the thermal gradient through the gauge. It is recalled that the earlier tests for apparent strain were like those of the strain gauge manufacturer, performed within an oven where the air temperature matched that of the specimen. This of course raises the question of whether an apparent strain recorded within an oven is the same as the apparent strain on a specimen where the gauge is itself transferring heat to a much colder atmosphere. To overcome the difficulty of the fluctuations of the galvanometer, it was found essential to cover the matrix of the gauge with a piece of/

of tape capable of providing thermal insulation. This eliminated the fluctuations but obviously further interfered with the heat transfer from the shell.

The readings are presented graphically in Figures (7.14 - 17) as (O,+). The results are for only two distinct temperature distributions but are quite representative of the many similar tests carried out at different temperature levels. The Figures (7.12 - 13) also show the relevant theoretical predictions which are now derived.

The dimensions of the Shell A, Figure (7.1), upon which the experimental thermal strain measurement was performed are such that it falls well within the category of a shallow spherical shell. The simplifications to the general case of a spherical shell, given in Chapter 4 under the heading of Shallow Spherical Shells, are thus permissible. Further, since the temperature effects are almost zero at the outer boundary it is possible to consider only the integration constants associated with the heated opening. The conditions at this heated opening are

$$t = T, N_r = 0, M_r = 0 \quad \text{where} \quad r = r_1.$$

The analysis of this particular case is treated in some detail in Section (4.2) where the above boundary conditions lead to

$$\begin{bmatrix} N_{r_1} \\ M_{r_1} \end{bmatrix} = \begin{bmatrix} 0 \\ 0 \end{bmatrix} = \begin{bmatrix} \frac{2\alpha^2}{a^2} \frac{\ker' z_1}{z_1} & \frac{2\alpha^2}{a^2} \ker' z_1 \\ -\frac{1}{a} \left(\ker z_1 - \frac{1-\nu}{z_1} \ker' z_1 \right) & -\frac{1}{a} \left(\ker z_1 + \frac{1-\nu}{z_1} \ker' z_1 \right) \end{bmatrix} \begin{bmatrix} A_3 \\ A_4 \end{bmatrix} + \frac{Eh\alpha}{s^4 + 4\alpha^4} \begin{bmatrix} -\sqrt{2}\alpha s^2 t_1 \\ a[s^2 - \frac{(1-\nu)\ker' z_1}{z_1}] \end{bmatrix}$$

and the integration constants are given by

$$\begin{bmatrix} A_3 \\ A_4 \end{bmatrix} = \frac{Eh\alpha}{s^4 + 4\alpha^4} \begin{bmatrix} \frac{2\alpha^2}{a^2} \frac{\ker' z_1}{z_1} & \frac{2\alpha^2}{a^2} \ker' z_1 \\ -\ker z_1 + \frac{1-\nu}{z_1} \ker' z_1 & -\ker z_1 - \frac{1-\nu}{z_1} \ker' z_1 \end{bmatrix} \begin{bmatrix} \sqrt{2}\alpha s^2 t_1 \\ -s^2 t_1 + \frac{(1-\nu)\ker' z_1}{z_1} \end{bmatrix}$$

where

$$z = \sqrt{2} \alpha \phi \approx \sqrt{2} \alpha \frac{r}{a}$$

Equation (4.21) gives for the temperature gradient at the opening

$$t_1 = -\frac{T S}{a} \frac{K_1\left(\frac{S}{a} r_1\right)}{K_0\left(\frac{S}{a} r_1\right)}$$

We can now evaluate the constants A_3 and A_4 for particular values of the parameters T and S and hence, by substituting back into equations (4.12 - 18) find the stress distribution into the shell from the opening. For comparison with the experimental results, the strain distributions on the upper and lower surfaces of the shell have been computed for shell A for three distinct values of S ($S = 5, 7$ and 9) and the results are presented in Tables (7.2 - 5) as functions of αT . Since the strains for the different values are so close to one another, only the strain distributions for the case $S = 7$ are presented graphically in Figures (7.12-13).

It is observed from the tables that the greater value of S the greater the intensity of the strain and the quicker the "die out" with distance from the opening. The feature of the graphs is the remarkable pattern of the strain distribution near the opening where for three of the strains there is a rapid changing of sign leading to a turning value and almost all of this taking place within the first inch from the opening.

With the experimentally derived value for the coefficient of linear expansion, $\alpha = 11.3 \times 10^{-6}/C^{\circ}$, and the extrapolated values for the opening temperatures, $T = 72C^{\circ}$ and $T = 140C^{\circ}$, the parameters of Figures (7.12-13) can be specialised to those of the actual tests whose experimental results are reported in Figures (7.14-17).

The/

The theoretical predictions of the strain distributions for the actual opening temperature can then be evaluated. They are indicated by continuous lines in Figures (7.14 - 17) whereas the strain gauge readings are shown as discrete values.

It is encouraging to see the large measure of agreement between the experimental values and theoretical predictions shown on these graphs.

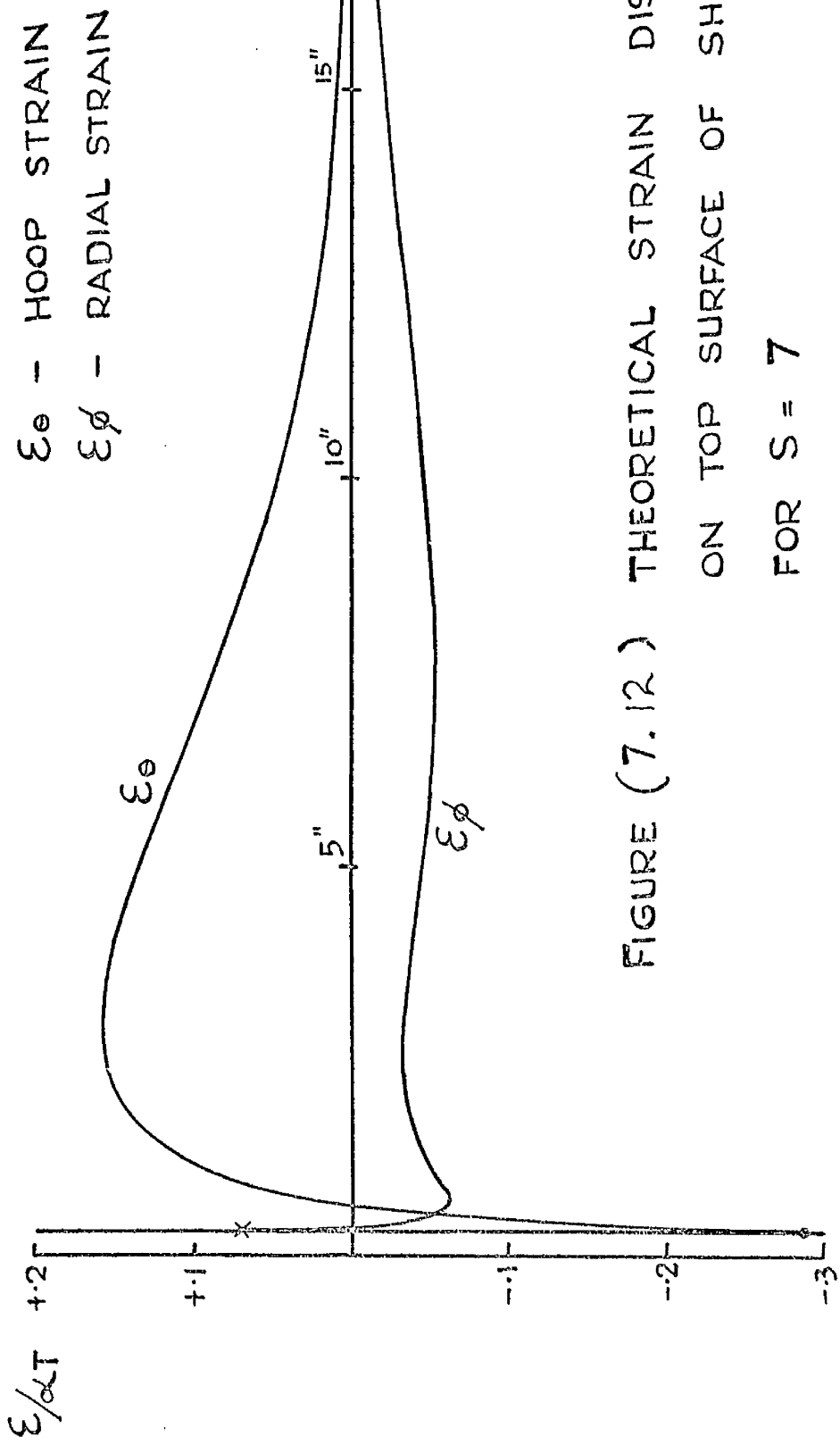


FIGURE (7.12) THEORETICAL STRAIN DISTRIBUTION
ON TOP SURFACE OF SHELL 'A'
FOR S = 7

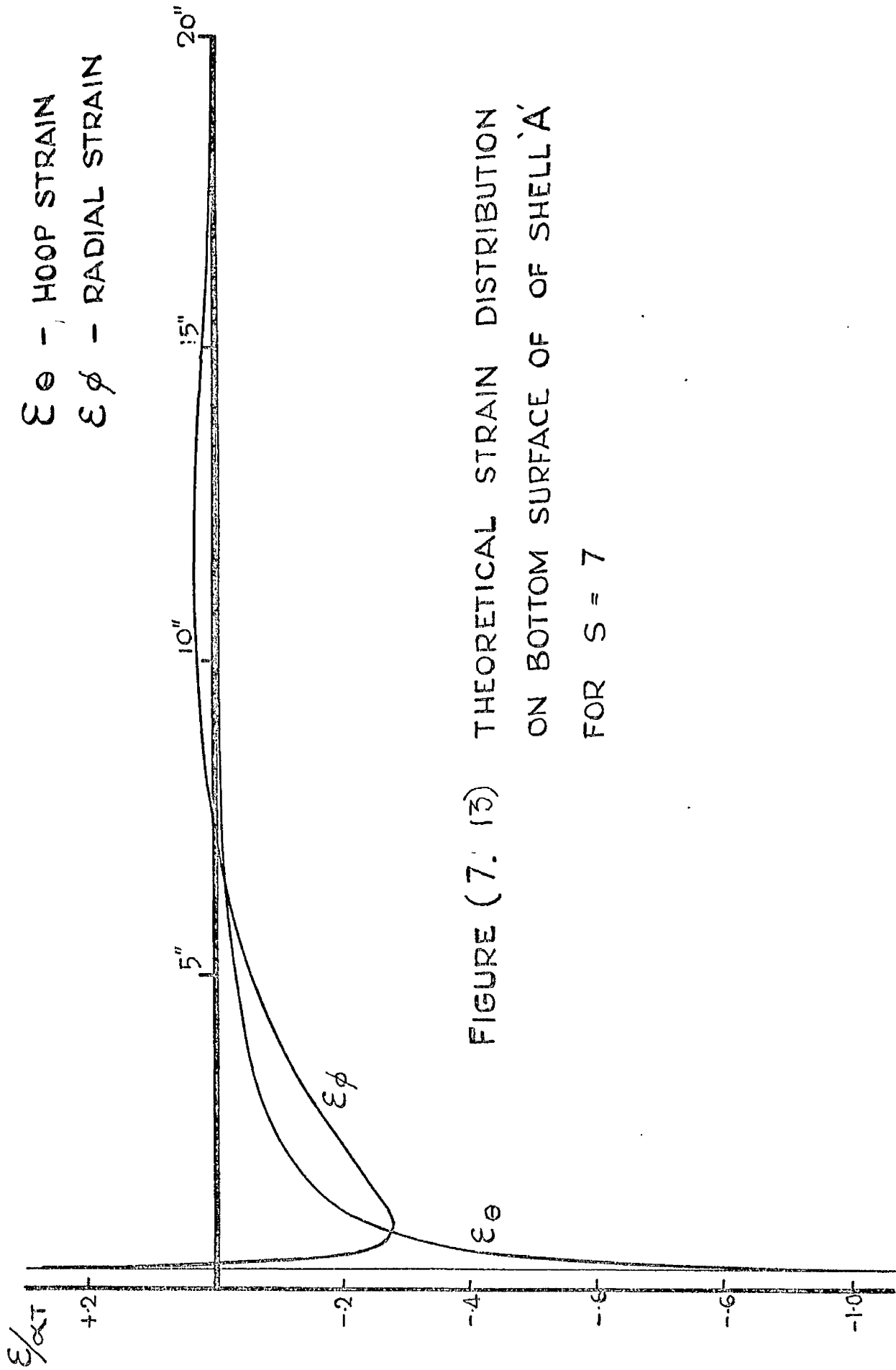


FIGURE (7.13) THEORETICAL STRAIN DISTRIBUTION
 ON BOTTOM SURFACE OF SHELL 'A'
 FOR $S = 7$

Hoop Strain $\times (\alpha T)^{-1}$			
Bottom Surface			
Radius r ins.	S = 5	S = 7	S = 9
.297	-1.008364	-1.06467	-1.10187
.445	- .572175	- .60073	- .61785
.594	- .405389	- .42293	- .43194
.742	- .319388	- .33108	- .33568
.890	- .266653	- .27465	- .27649
1.039	- .230477	- .23589	- .23580
1.187	- .203682	- .20720	- .20565
1.335	- .182720	- .18472	- .18209
1.484	- .165654	- .16645	- .16293
1.632	- .151340	- .15116	- .14692
1.781	- .139059	- .13804	- .13323
2.077	- .118863	- .11653	- .11087
2.226	- .110386	- .10755	- .10156
2.374	- .102744	- .09945	- .09322
2.671	- .089478	- .08547	- .08089
2.968	- .078339	- .07380	- .06695
4.155	- .047644	- .04212	- .03531
4.748	- .037802	- .03222	- .02573
5.342	- .030391	- .02491	- .01886
5.935	- .024833	- .01956	- .01399
7.122	- .017647	- .01298	- .00838
8.309	- .013810	- .00982	- .00612
9.496	- .011812	- .00811	- .00550
10.683	- .010722	- .00791	- .00556
11.870	- .009996	- .00763	- .00575
13.350	- .009173	- .00723	- .00578
14.838	- .008252	- .00663	- .00545
16.322	- .007212	- .00582	- .00484
17.805	- .006029	- .00470	- .00369
19.289	- .005597	- .00377	- .00307

Table 7.2

Radial Strain $\times (\Delta T)^{-1}$ Bottom Surface			
Radius r ins.	S = 5	S = 7	S = 9
.297	+.257133	+.27149	+.28098
.445	-.099472	-.10524	-.10916
.594	-.208275	-.21958	-.22688
.742	-.248001	-.26087	-.26892
.890	-.261809	-.27484	-.28267
1.039	-.264105	-.27671	-.28398
1.187	-.260719	-.27262	-.27919
1.335	-.254338	-.26543	-.27124
1.484	-.246321	-.25655	-.26162
1.632	-.237411	-.24676	-.25109
1.781	-.228030	-.23653	-.24014
2.077	-.208775	-.21562	-.21792
2.226	-.199164	-.20523	-.20693
2.374	-.189660	-.19498	-.19613
2.671	-.171145	-.17509	-.16720
2.968	-.153442	-.15612	-.15537
4.155	-.092049	-.09099	-.08787
4.748	-.067091	-.06480	-.06108
5.342	-.045760	-.04258	-.03858
5.935	-.027806	-.02407	-.02000
7.122	-.000881	+.00328	+.00693
8.309	+.016111	+.02002	+.02286
9.496	+.025556	+.02873	+.03068
10.683	+.029592	+.03203	+.03293
11.870	+.030003	+.03159	+.03162
13.350	+.027510	+.02811	+.02731
14.838	+.023464	+.02325	+.02189
16.322	+.019082	+.01829	+.01662
17.805	+.012181	+.01074	+.00873
19.289	+.011632	+.01003	+.00827

Table 7.3

Hoop Strain $\times (\alpha T)^{-1}$			
Top Surface			
Radius r ins.	S = 5	S = 7	S = 9
.297	-.241738	-.28656	-.32923
.445	-.073037	-.09412	-.11482
.594	-.000718	-.01230	-.02425
.742	+.040403	+.03394	+.02713
.890	+.067501	+.06419	+.05965
1.039	+.086931	+.08579	+.08314
1.187	+.101590	+.10201	+.10070
1.335	+.113006	+.11461	+.11426
1.484	+.122065	+.12453	+.12492
1.632	+.129327	+.13249	+.13340
1.781	+.35166	+.13884	+.14017
2.077	+.143573	+.14793	+.14976
2.226	+.146485	+.15106	+.15302
2.374	+.148700	+.15342	+.15546
2.671	+.151399	+.15625	+.15829
2.968	+.152237	+.15707	+.15895
4.155	+.143729	+.14741	+.14814
4.748	+.135268	+.13813	+.13812
5.342	+.125413	+.12741	+.11597
5.935	+.114837	+.11599	+.11458
7.122	+.093346	+.09299	+.09050
8.309	+.073284	+.07176	+.06858
9.496	+.055847	+.05351	+.04999
10.683	+.041443	+.03863	+.03506
11.870	+.030026	+.02701	+.02360
13.350	+.019480	+.01648	+.01345
14.838	+.012301	+.00953	+.00695
16.322	+.007639	+.00518	+.00308
17.805	+.004832	+.00285	+.00135
19.289	+.003254	+.00153	+.00028

Table 7.4

Radius r ins	Radial Strain $\times (\alpha T)^{-1}$ Top Surface		
	S = 5	S = 7	S = 9
.297	+.061643	+.07307	+.08395
.445	-.029617	-.03447	-.03903
.594	-.049235	-.05855	-.06743
.742	-.051508	-.06222	-.07470
.890	-.048711	-.05972	-.07034
1.039	-.04449	-.05549	-.06604
1.187	-.040313	-.05100	-.06136
1.335	-.036474	-.04689	-.05696
1.484	-.033187	-.04330	-.05308
1.632	-.030476	-.04031	-.04980
1.781	-.028314	-.03788	-.04710
2.077	-.025439	-.03453	-.04327
2.226	-.024618	-.03353	-.04203
2.374	-.024139	-.03287	-.04117
2.671	-.024026	-.03246	-.04036
2.968	-.024782	-.03297	-.04050
4.155	-.032121	-.03950	-.04576
4.748	-.036446	-.04343	-.04907
5.342	-.040370	-.04692	-.05192
5.935	-.043588	-.04968	-.05400
7.122	-.047448	-.05246	-.05547
8.309	-.047940	-.05180	-.05355
9.496	-.045731	-.04845	-.04906
10.683	-.041699	-.04334	-.04301
11.870	-.036674	-.03738	-.03633
13.350	-.030003	-.02978	-.02809
14.838	-.022009	-.02281	-.02079
16.322	-.018286	-.01694	-.01480
17.805	-.011074	-.00928	-.00706
19.289	-.010716	-.00907	-.00714

Table 7.5

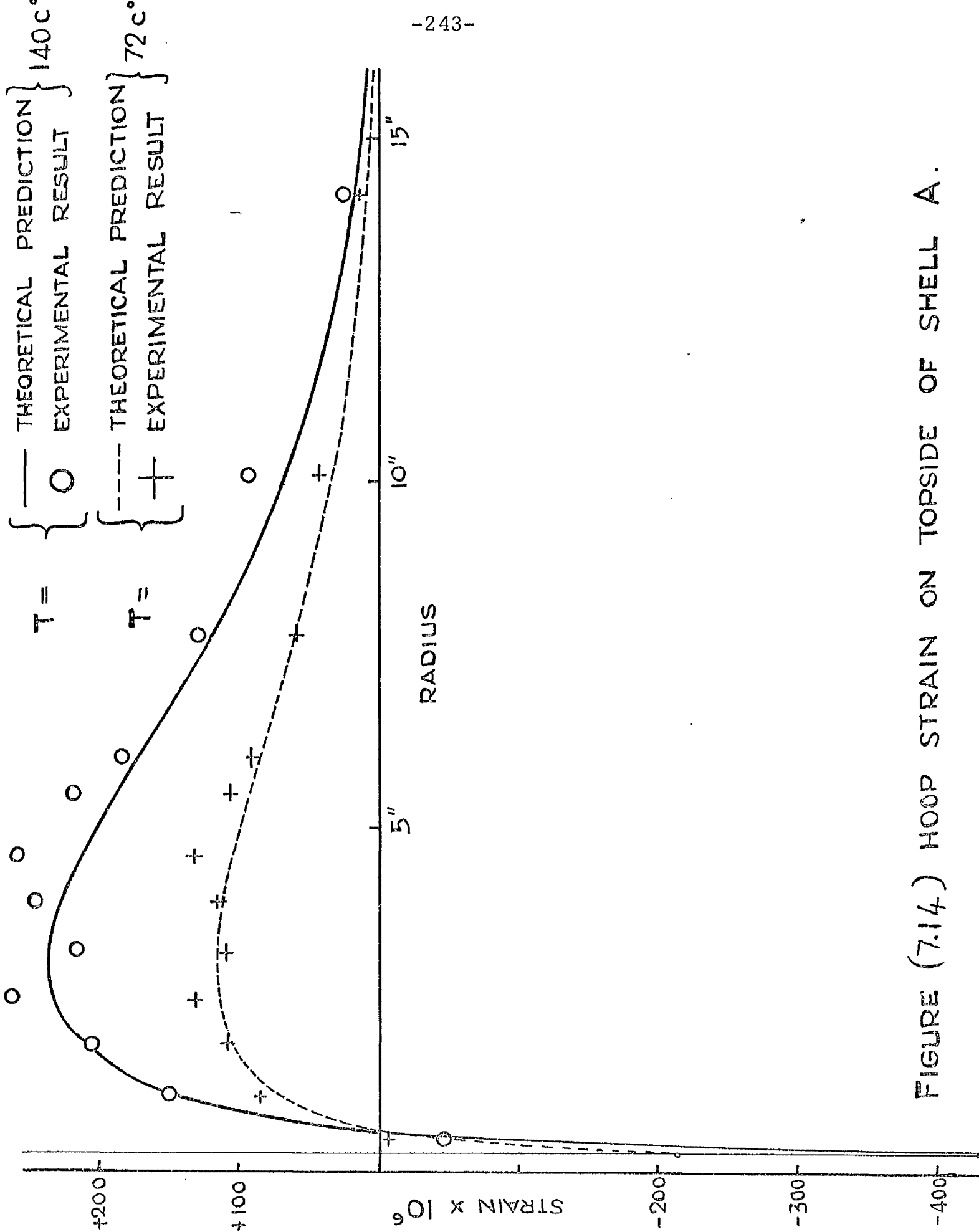


FIGURE (7.14) HOOP STRAIN ON TOPSIDE OF SHELL A.

$T =$ { — THEORETICAL PREDICTION } 140c°
 { ○ EXPERIMENTAL RESULT }
 $T =$ { - - - THEORETICAL PREDICTION } 72c°
 { + EXPERIMENTAL RESULT }

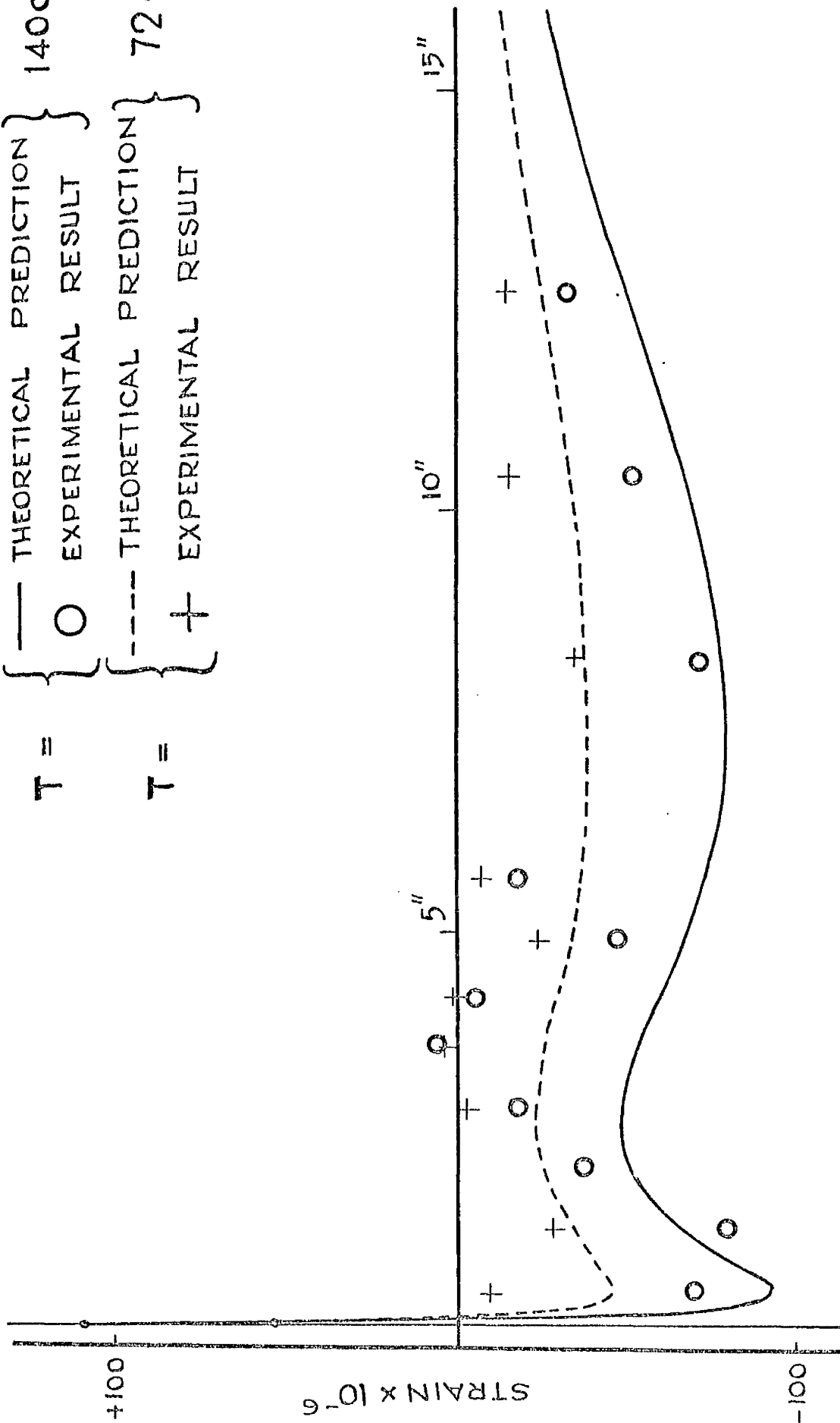


FIGURE (7.15.) RADIAL STRAIN ON TOPSIDE OF SHELL A

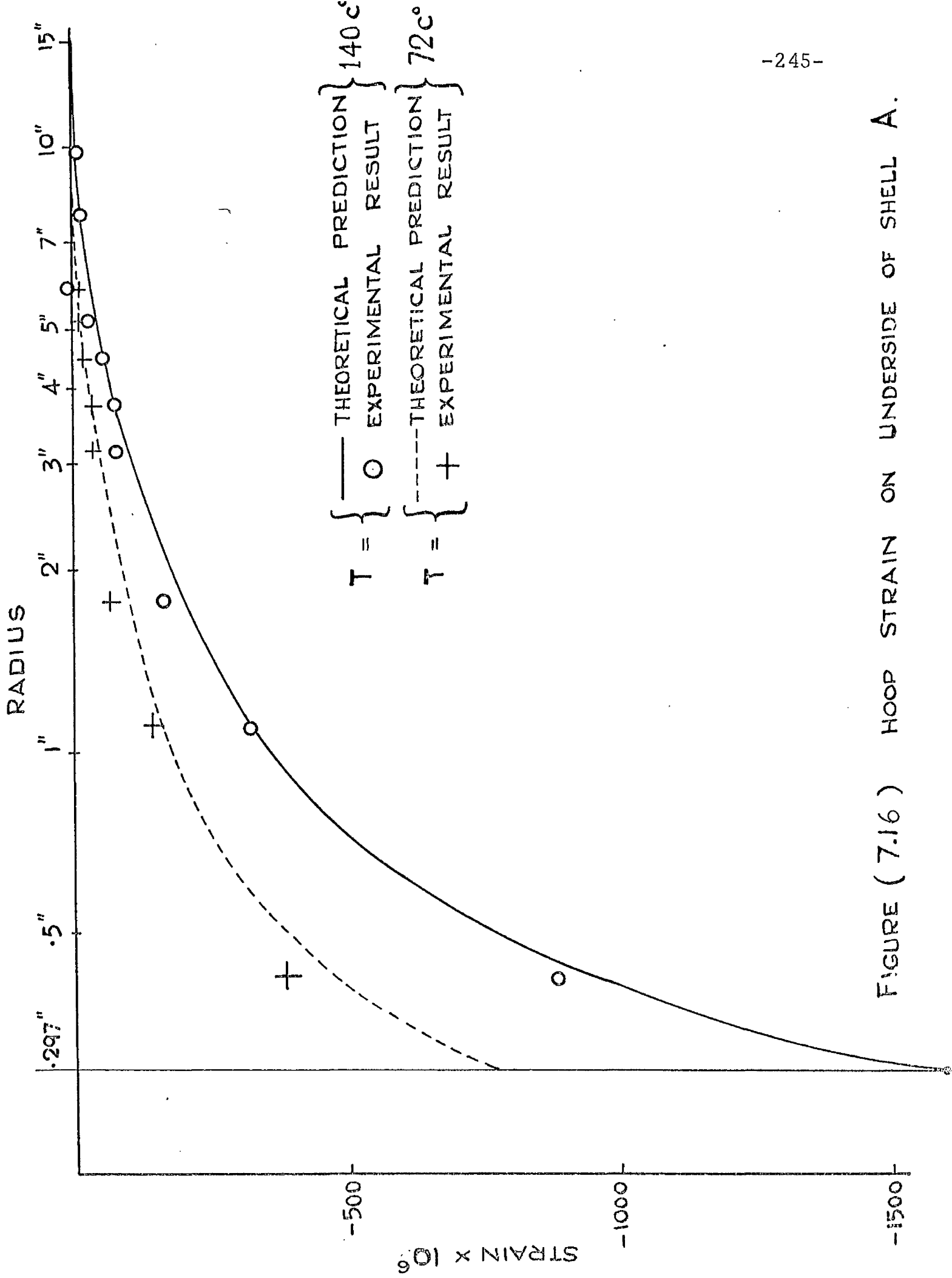
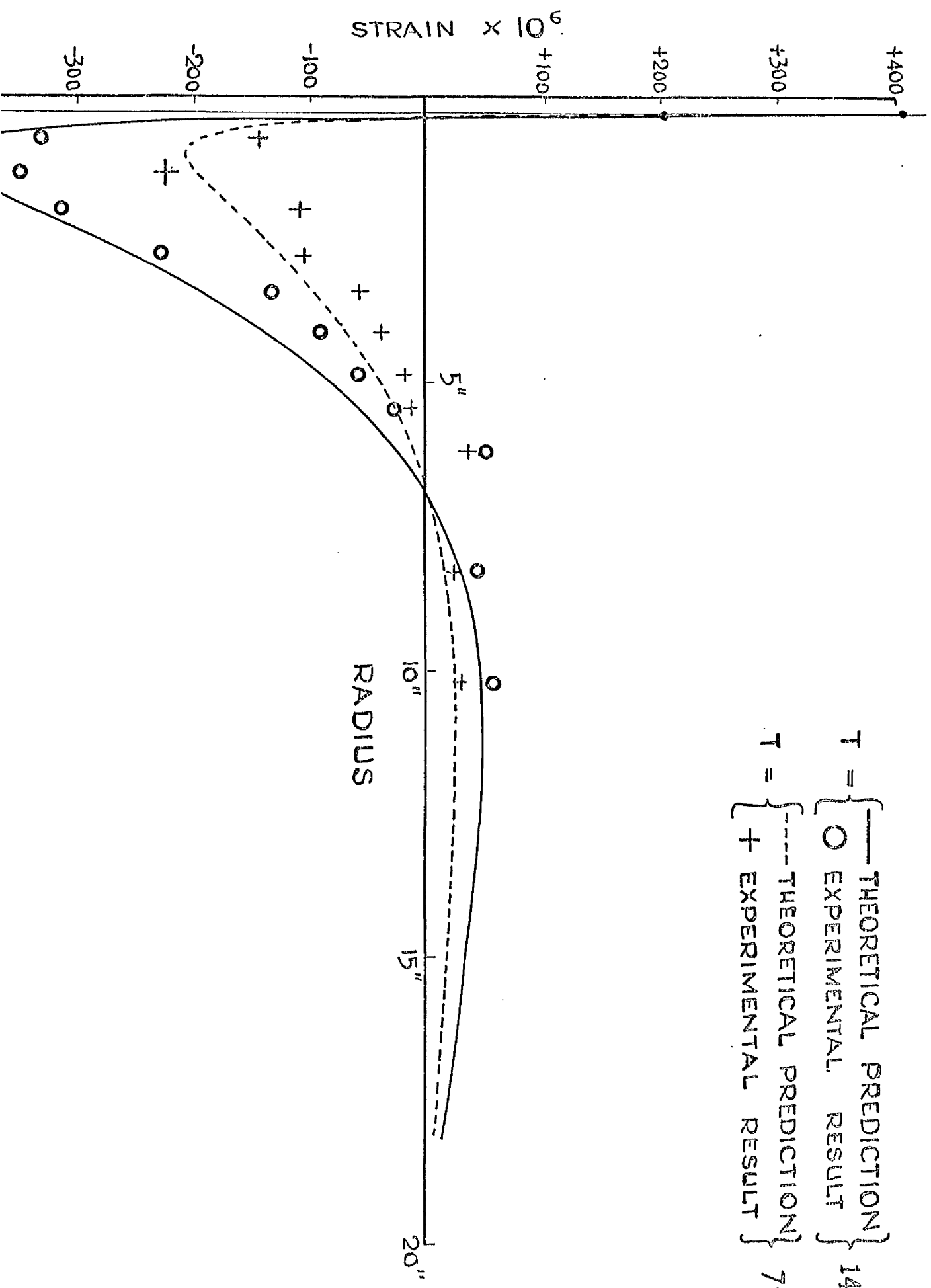


FIGURE (7.16) HOOP STRAIN ON UNDERSIDE OF SHELL A.



T = { — THEORETICAL PREDICTION } 140 c°
O EXPERIMENTAL RESULT
T = { - - - - - THEORETICAL PREDICTION } 72 c°
+ EXPERIMENTAL RESULT

7.4 Conclusions and Discussion

The temperature distributions into a shallow spherical shell from a uniformly heated axisymmetric circular opening were measured for various values of the opening temperature and for different shell thicknesses. Free convection and radiation of heat was allowed from both the upper and lower surfaces of the shells. Some of the experimental results are presented in Figures (7.5 - 7). These results have been normalised in terms of the opening temperature, T , and the resulting non-dimensional temperature distributions are shown in Figures (7.8 - 10). Although there is some slight scatter of the results it appears reasonable, from these results, to express the temperature distribution into the shell as

$$t = T \times f_n(\phi, h) .$$

The theoretical relationship developed in Chapter 1 for such a temperature distribution is

$$t = A I_0(S\phi) + B K_0(S\phi)$$

where the heat transfer parameter S is given as

$$S = \left(\frac{2m}{kh} \right)^{\frac{1}{2}} \alpha$$

The heat conduction coefficient k is empiric and it can be seen, from Table (A.3.2), that it is, to an extent, temperature dependent. The assumption that the heat exchanged by the radiation mode of heat transfer can be expressed in terms of the temperature difference is less satisfactory, although it is not too unreasonable for/

for a small temperature range. The degree of agreement between the normalised experimental results, for each shell thickness, taken over the surface of the shell and hence over the various temperature fields, indicates that the value for the radiation coefficient is not critical for the range of temperature, $0 - 200^{\circ}\text{C}$ investigated. The theoretical temperature distribution graphs, for different values of parameter S , faithfully reflect the form of the experimental results. Some difficulties exist, however, in determining which particular value of S most closely represents a particular experimental result. A theoretical curve, for a lower value of S , which gives a better overall picture of the temperature distributions may not however give the best representation of the conditions near the opening. For a better representation of the situation close to the opening, where there are rapid changes in temperature, a higher value of the coefficient, S , is required. For a more accurate theoretical description of the temperature distribution over the shell, the surface would require to be "broken into" a number of temperature zones each with its own value of the parameter, S . The temperatures at each of the zone boundaries could then be equated to give an overall description. Such a procedure could also account for variations in the other shell parameters with temperature and would be ideally suited to the finite element technique discussed in Appendix 4. For the theoretical determination of the thermal stresses within a shell from a heated opening, it is the temperature distribution close to the opening which appears the more pertinent to the calculations. The value of the coefficient S , selected for any stress calculation should be the value estimated for the opening conditions.

Tables/

Tables (7.2 - 5) which give the strain distribution in the $\frac{1}{2}$ " shell for these values of the parameter S , show that neither the magnitude of the strain nor its distribution is over-sensitive to the large variations of S represented. For example, the largest values of the strains are those given in Table (7.2) for the circumferential strain at opening; they are

$$\text{Circumferential strain (S = 5)} = -1.008364 \times \alpha T$$

$$\text{Circumferential strain (S = 9)} = -1.10187 \times \alpha T$$

The paucity of published experimental strain gauge results in the thermal strain field led the author to examine critically the techniques available. To this end, one shell was strain gauged in order to investigate the strain pattern due to a particular temperature distribution. Two complete sets of experimental results are presented in this Chapter. These are typical of the results from the many similar tests which were performed. Repeatability was found for the strain gauge readings and, indeed, any lack of repeatability was taken as indicative of an unsatisfactory strain gauge.

The experimental results are compared with those derived earlier by the analysis. On the whole it is felt that the experimental results obtained confirm the general analytical approach used in the thesis and emphasise the importance of testing the shell in the correct environment. Regarding this latter point, it is clear that thermal strain measurement can only satisfactorily take place in ideal laboratory conditions.

BIBLIOGRAPHY

1. DUHAMEL, J. M.C. 'Memoire sur le calcul des actions moleculaires developpees par les changements de temperature dans les corps solides'. Mem. inst. France, vol. 5, pp. 440-498, 1838.

'Second memoire sur les phenomenes thermomechaniques'. J. ecole polytech. (Paris), vol. 15, pp. 1-57, 1837.

'Memoire sur le mouvement des differents points d'une barre cylindrique dont la temperature varie'. J. ecole polytech. (Paris), vol. 21, pp. 1-33, 1856.
2. POISSON, S. D. 'Memoire sur l'equilibre et le mouvement des corps elastiques'. Mem. Paris Acad., 8:357-570, 1829.
3. BOLEY, B. A. & WEINER, J. H. 'Theory of Thermal Stresses'. John Wiley & Sons, Inc., New York, 1960.
4. JOHNS, D. J. 'Thermal Stress Analyses'. Pergamon Press Ltd., 1965.
5. NEUMANN, F. E. 'Die Gesetze der Doppelbrechung des Lichts in Comprimirten oder ungleichformig erwarmten unkrystal-linischen Dorpern'. Abhandl, koniglichen Akad. Wiss. Berlin, Zweiter Teil, pp. 1-254, 1841.
6. HOPKINSON, J. 'On the Stresses Caused in an Elastic Solid by Inequalities of Temperature'. Messenger Math., 8:168-174, 1879.
7. TIMOSHENKO, S. & GOODIER, J. N. 'Theory of Elasticity'. McGraw-Hill, New York. 2nd Edition, 1951.
8. BIOT, M. A. 'Thermoelasticity and Irreversible Thermodynamics'. Journal of Applied Physics, vol. 22, pp. 240-253, March, 1956.
9. PRZEMIENICKI, J. S. 'The General Theory of Axisymmetrical Shells under Temperature Loading'. Bristol Aircraft Ltd. Technical Office Report, No.88 (1956).

10. HIESLER, M. P. 'Transient thermal stresses in slabs and circular pressure vessels'. J. Appl. Mech., 20, 261, 1953.
11. HLINKS, J. W. 'Charts on Elastic Thermal Stresses in Heating and Cooling of Slabs and Cylinders'. A.S.M.E. paper 57-A-238, 1957.
12. MEISSNER, E. 'Über Elastizität und Festigkeit dünner Schalen'. Vierteljahrsschrift der Naturforschenden Gesellschaft in Zurich. Vol. 60, 1915, pp. 111-113.
13. EICHELBERG, G. 'Temperatureverlauf und Warmespannungen in Verbrennungsmotoren'. Forschungsarbeiten Ing. Wesen, Berlin, No. 263, 1923.
14. PARKUS, H. 'Warmespannungen in Rotationschalen mit dreh-symmetrischer Temperaturverteil'. Österreichische Akademie der Wissenschaften (math.-natur. Klasse) 2a, volume 160, pp. 1-13, 1951.
15. FLUGGE, W. 'Stresses in Shells'. Springer-Verlag. Berlin, 1960.
16. REISSNER, H. 'Spannungen in Kugelschalen'. (Kuppeln). Festschrift Mueller-Breslaw, 1912, pp. 181-193.
17. NOWACKI, W. 'Thermoelasticity'. Pergamon Press Ltd., 1962.
18. WATSON, G. N. 'Theory of Bessel Functions'. Cambridge University Press, 1958.
19. EKSTROM, J. E. 'Studien über dünne Schalen von rotations-symmetrischer Form und Belastung mit konstanter oder veränderlicher Wandstärke'. Ing. Vetenskaps. Akad., Pamphlet No. 121, 1933.
20. NOVOZHILOV, V. V. 'The Theory of Thin Shells'. P. Noordhoff Ltd., Groningen, 1959.
21. JEFFREYS, H. & JEFFREYS, H. B. 'Methods of Mathematical Physics'. Cambridge University Press, p. 491, 1946.

22. PRZEMIENICKI, J. S. 'Thermal Stresses'. Course of lectures given at the University of Southampton (1959).
23. BLUMENTHAL, O. 'Uber Asymptotische Integration von Differential-Gleichungen mit Anwendung auf die Berechnung von Spannungen in Kugelschalen'. 5th Inter. Congress Math. 1912. Prov. vol. 2, pp. 319-327.
24. HETENYI, M. 'Beams on Elastic Foundations'. University of Michigan Studies. Vol. 16.
25. GECKELER, J. W. 'Uber die Festigkeit Achsensymmetrischer Schalen'. Forschungsarbeiten. Ing. Wes. Vol. 276, 1926. pp. 1-52.
26. LECKIE, F. A. 'Asymptotic Solutions for the Spherical Shell subjected to axially symmetrical Loading'. Nucl. Reactor Cont. Bldg. & Press. Vessels Symp., 1960, Butterworths, London. pp. 286-297.
27. LANGER, R. E. 'On the Asymptotic Solutions of Ordinary Differential Equations with reference to the Stokes' Phenomenon about a Singular Point'. Trans. Amer. Math. Soc., vol. 37, 1935. pp. 397-416.
28. TOOTH, A. S. 'Ph.D. Thesis'. University of Glasgow, 196
29. AMBARTSUMYAN, S. A. 'On the Calculation of Shallow Shells'. Prikladnaia Matematika i Mekhanika, vol. 11, pp. 527-532. 1947. Translated as NACA TM, 1425, December, 1956.
30. GRADOWCZYK, M. H. 'On Thermal Stresses in Thin Shallow Shells'. I.A.S.S. Symposium, 1963.
31. CONRAD, D. A. & FLUGGE, W. 'Ph.D. Thesis of Conrad'. Stanford University, September, 1956.
32. HAVERS, A. 'Asymptotische Biegetheorie der unbelasteten Kugelschale'. Ingenieur - Archiv. vol. 6, 1935. pp. 282-312.

33. STEELE, C. R. 'A Systematic Analysis for Shells of Revolution with Nonsymmetric Loads'. Proc. 4th U.S. Nat. Cong. Appl. Mech., 2. pp. 783-792 (1962).
34. BOUMA, A. L. 'Some Applications of the Bending Theory Regarding Doubly Curved Shells'. I.U.T.A.M. Symposium, Delft, 1959. North Holland Publishing Co. pp. 202-234.
35. PENNY, R. K. 'Stress Concentrations at the Junction of a Spherical Pressure Vessel and Cylindrical Duct caused by certain Axisymmetric Loadings'. Nucl. Reactor Cont. Bldg. & Press. Vessels Symp., 1960. Butterworths, London. pp. 347-368.
36. LECKIE, F. & LIVESLEY, R. K. 'Stress Analysis of a Containment Vessel Subjected to Lateral Loads'. Nucl. Reactor Cont. Bldg. and Press. Vessel Symp., 1960. Butterworths, London. pp. 150-163.
37. BAILEY, R. W. & HICKS, R. 'Stress Analysis Problems Associated with the Design of Reactor Pressure Vessels'. Symp. on Nucl. React. Cont. Bldgs. and Press. Vessels. Butterworths, London, 1960. pp. 134-149.
38. BIJLAARD, P. P. 'On the Stresses from Local Loads in Spherical Pressure Vessels or Pressure Vessel Heads'. Bulletin No.34, Welding Research Council, 1956.
39. WOLOSEWICK, F. E. 'Supports for Vertical Pressure Vessels'. Petroleum Refiner, August, 1951.
40. BERGMAN, D. J. 'Temperature Gradients in Skirt Supports of Hot Vessels'. Journal of Engineering for Industry, May, 1963.
41. BALDWIN-LIMA-HAMILTON. 'Measurement Topics'. Published quarterly by BLH Electronics Inc., Waltham, Mass., U.S.A.
42. BERTODO, R. 'Development of High-Temperature Strain Gauges'. Inst. Mech. Eng. Ads. Pap. 35/38, 1959.

43. BROAD, M. S. 'Measurement of Static Strain under Rapid Heating'. pp. 22-30, Strain, vol.4, No.4, 1968.
44. HILDEBRAND, F. B. 'An Asymptotic Integration in Shell Theory'. Proc. of Symp. in App. Maths. vol.3, 1950. pp. 53-66.
45. JAKOB, M. 'Heat Transfer'. Vols. I, II, John Wiley & Sons, Inc., New York, 1949.
46. GALLETLY, G. D. 'Ring Loads on Spherical Shells'. 1 Theoretical Analysis. Batafse Internationale Petroleum Maatschappu N.V., The Hague.
47. HICKS, R. 'Theoretical Analysis of the Stress induced in a Spherical Vessel due to the Constraining Effect of a Cylindrical Skirt'. Proc. Inst. Mech. Engrs. Vol. 172, No. 21, 1958.
48. REISSNER, E. 'Stresses and Small Displacements of Shallow Spherical Shells'. Amer. Jn. Math. Phys. Vol. 25, 1946, pp. 80-85 and 279-300.
49. TIMOSHENKO, S. P. & S. WOINOWSKY-KRIEGER. 'Theory of Plates and Shells'. McGraw-Hill, 1959.
50. DEN HARTOG, J. P. 'Temperature Stresses in Flat Rectangular Plates and in Thin Cylindrical Tubes'. J. Franklin Inst., 222, 149. (1936).
51. WEIL, N. A. & MURPHY, J. J. 'Design and Analysis of Welded Pressure-Vessel Skirt Supports'. Journal of Engineering for Industry, Feb., 1960.
52. BIEZENO & GRAMMEL. 'Engineering Dynamics'. Vol. 1, Blackie, 1955.
53. GIBBS, J. P. 'Two Types of High-Temperature Weldable Strain Gauges'. Experimental Mechanics 7, 8, 19A-26A. (Aug., 1967).

54. JUVINALL, R. C. 'Engineering Considerations of Stress, Strain and Strength'. McGraw-Hill, 1967.
55. KESTENS, J. 'Applied Mechanics Review'. No.1816, 1967.
56. McADAMS, W. H. 'Heat Transmission'. McGraw-Hill, 1967.
57. CHAPMAN, A. J. 'Heat Transfer'. MacMillan, 1960.
58. TATNALL, F. G. 'Summary Report on High Temperature Strain Gauge Research'. BLH Naval Contract No.NR845(00), 1955.
59. CROWDER, H. K. & McCUSKEY, S. W. 'Topics in Higher Analysis'. MacMillan, 1964.
60. HICKS, R. 'Asymmetrically ring reinforced circular hole in a uniformly end-loaded flat plate with reference to pressure-vessel design'. Inst. Mech.Eng. adv. pap. 15/58. 1958.
61. WATERS, E. O. 'Theoretical Stresses near a circular opening in a flat plate, reinforced with a cylindrical outlet'. Weld. Res. Coun. Bull. No. 51, June, 1959.
62. TOOTH, A. S. & KENEDI, R. M. 'The Influence Line Technique of Shell Analysis'. Colloquium or Simplified Calculation Methods, Brussels, 1961. North-Holland Publishing Coy.
63. McLACHLAN, N. W. 'Bessel Functions for Engineers'. Oxford, 1955.
64. NOSOVA, L. N. 'Tables of Thomson Functions and Their Derivatives'. Pergamon Press Limited, 1961.
65. ABRAMOWITZ, M. & STEGUN, I. A. 'Handbook of Mathematical Functions'. Dover, 1965.
66. HSU, S. T. 'Engineering Heat Transfer'. D. Van Nostrand. (1963).

APPENDIX 1

COMPUTATION

INTRODUCTION

The computation required for the production of the graphs and the tables presented in this thesis was performed on a Sirius Digital Computer. This model of computer, which was designed primarily for teaching purposes, is limited in its storage capacity to 4,000 words each of 10 digits and in its speed of operation to 4 milli-seconds access time. These limitations are rather severe and of course affect the numerical methods used in the solving of the various equations. With the larger computers now available, greater possibilities arise. For example, a more satisfactory program for the Kelvin functions could be written and the thermal stress problem could be solved using the appropriate Greens function.

The Modified Bessel Functions

The Modified Bessel functions $I_0(z)$, $I_1(z)$, $K_0(z)$ and $K_1(z)$ are required for the computation of the temperature and the temperature gradient throughout the shell. A standard autocode program is available for these functions for values of argument less than 10. This program uses the Chebyshev series with the appropriate Chebyshev polynomials. It was found, however, that the accuracy of the functions obtained by using this program fall away as the argument approached the limiting value of 10. This, of course, affected the results for the stress functions and in the graphs/

graphs produced a "kink" in the region where the argument was just less than 10. It also made the matching of the effects due to an opening on one side of $Z = 10$ with the effects on the other side of this value meaningless. The N.P.L. Tables for the Chebyshev Polynomials (volume 5) give for the range of acceptable validity of their polynomials for the Modified Bessel functions

$$- 8 \leq Z \leq + 8 .$$

For values of argument greater than 10 the series form for the Bessel functions as given by McLAUCHLIN⁽⁶³⁾ was used. He gives the series for $K_0(Z)$ and $K_1(Z)$ as

$$K_0(Z) \approx \frac{1.2533}{Z^{\frac{1}{2}}} e^{-Z} \left\{ 1 - \frac{1}{8Z} + \frac{9}{128Z^2} - \frac{75}{1024Z^3} + \dots \right\}$$

$$K_1(Z) \approx \frac{1.2533}{Z^{\frac{1}{2}}} e^{-Z} \left\{ 1 + \frac{3}{8Z} - \frac{15}{128Z^2} + \frac{105}{1024Z^3} - \dots \right\}$$

A.1.1-2

The values obtained using these series compare favourably with the corresponding values in the standard tables.

The two distinct series forms which were used give a satisfactory solution for the Modified Bessel functions over the whole range of argument except in the region $8 \leq Z \leq 10$. For accurate values in this region a further set of Chebyshev polynomials would be required to cover the range $8 \leq Z \leq 10$ and thus provide better continuity over the whole shell. It is probable however that these are now available as one of the standard subroutines of the larger computers.

The Kelvin Functions

The series representation of the Kelvin functions in powers of Z is

$$\text{ber } Z = \sum_{k=0}^{\infty} \frac{(-1)^k Z^{4k}}{2^{4k} [(2k)!]^2},$$

$$\text{bei } Z = \sum_{k=0}^{\infty} \frac{(-1)^k Z^{4k+2}}{2^{4k+2} [(2k+1)!]^2},$$

$$\text{ker } Z = \left(\ln \frac{Z}{Z} - c \right) \text{ber } Z + \frac{\pi}{4} \text{bei } Z + \sum_{k=0}^{\infty} \frac{(-1)^k Z^{4k}}{2^{4k} [(2k)!]^2} \sum_{m=0}^{2k} \frac{1}{m},$$

$$\text{kei } Z = \left(\ln \frac{Z}{Z} - c \right) \text{bei } Z - \frac{\pi}{4} \text{ber } Z + \sum_{k=0}^{\infty} \frac{(-1)^k Z^{4k+2}}{2^{4k+2} [(2k+1)!]^2} \sum_{m=1}^{2k+1} \frac{1}{m}$$

where C is Euler's constant.

A.1.3-6

The slow convergence of these series makes them impractical for use in our involved program where a great number of Kelvin functions may be required. Indeed, NOSOVA⁽⁶⁴⁾, who is responsible for the most recent tables of these functions, used an asymptotic representation for obtaining his tabulated values at the larger values of argument. This asymptotic series for ker Z and kei Z is

$$\text{ker } Z \approx \left(\frac{\pi}{2Z} \right)^{\frac{1}{2}} e^{-\left(\frac{Z}{\sqrt{2}} \right)} \left[L_0(-Z) \cos \left(\frac{Z}{\sqrt{2}} + \frac{\pi}{8} \right) + M_0(-Z) \sin \left(\frac{Z}{\sqrt{2}} + \frac{\pi}{8} \right) \right]$$

$$\text{kei } Z \approx \left(\frac{\pi}{2Z} \right)^{\frac{1}{2}} e^{-\left(\frac{Z}{\sqrt{2}} \right)} \left[M_0(-Z) \cos \left(\frac{Z}{\sqrt{2}} + \frac{\pi}{8} \right) - L_0(-Z) \sin \left(\frac{Z}{\sqrt{2}} + \frac{\pi}{8} \right) \right]$$

where/

A.1.7-8

where

$$L_0(z) = 1 + \frac{1^2}{1! 8z} \cos \frac{\pi}{4} + \frac{1^2 \cdot 3^2}{2! (8z)^2} \cos \frac{2\pi}{4} + \frac{1^2 \cdot 3^2 \cdot 5^2}{3! (8z)^3} \cos \frac{3\pi}{4} +$$

$$M_0(z) = -\frac{1}{1! 8z} \sin \frac{\pi}{4} - \frac{1^2 \cdot 3^2}{2! (8z)^2} \sin \frac{2\pi}{4} - \frac{1^2 \cdot 3^2 \cdot 5^2}{3! (8z)^3} \sin \frac{3\pi}{4} -$$

A.1.9-10

and the argument z is large.

For even larger values of argument the functions $M_0(z)$ and $L_0(z)$ can be approximated by

$$L_0(z) = 1$$

$$M_0(z) = 0$$

and here the functions $\ker(z)$ and $\kei(z)$ should become

$$\ker(z) \approx \left(\frac{\pi}{2z}\right)^{\frac{1}{2}} e^{-\frac{z}{\sqrt{2}}} \cos\left(\frac{z}{\sqrt{2}} + \frac{\pi}{8}\right)$$

$$\kei(z) \approx -\left(\frac{\pi}{2z}\right)^{\frac{1}{2}} e^{-\frac{z}{\sqrt{2}}} \sin\left(\frac{z}{\sqrt{2}} + \frac{\pi}{8}\right)$$

A.1.11-12

These are the representations commonly used in shell theory and which were discussed earlier in Chapter 3. There it was stated that these approximations were reasonably valid for $z > 10$ and that the range of validity $z > 6$, as given by REISSNER, is rather optimistic.

Since a series of representation of the Kelvin functions for the larger values of the argument was readily available and was suitable for inclusion in a computer program, an attempt was made to find the appropriate Chebyshev polynomials for the lower arguments. The values obtained were rather limited in their accuracy. After correspondence with C. W. Clenshaw of N.P.L. more/

more accurate values and these polynomials to a greater number of digets than would be possible to obtain on the Sirius computer, were provided by him. Since these values have not yet been published, they are included now for the sake of completeness.

For the computation of the functions $\ker z$ and $keiz$ for arguments less than 8 write

$$\ker z + i keiz = - \left\{ \ln\left(\frac{x}{2}\right) + \left(\frac{i\pi}{4}\right) \right\} \sum A_r T_r(x) + \sum B_r T_r(x) \tag{A.1.13}$$

where

$$x = \left(\frac{z}{8}\right)^2$$

Here the sum $\sum A_r T_r(x)$ is the function $\ker z + i keiz$.

The coefficients A_r and B_r are now presented to 10 decimal places-

<u>r</u>	<u>A_r</u>	<u>B_r</u>
0	+ 4.51042 30966	+ 33.42583 45543
1	-29.34949 10970 i	- 33.85929 29333 i
2	+10.84058 01738	+ 30.13631 27446
3	- 8.98868 87413 i	- 3.51819 48725 i
4	+ 8.71271 74102	+ 11.24784 41174
5	+ 3.46690 09758 i	+ 5.59593 16514 i
6	- 0.85344 63697	- 1.55752 23300
7	- 0.14735 80153 i	- 0.29293 75949 i
8	+ 0.01904 82639	+ 0.04044 62330
9	+ 0.00192 21032 i	+ 0.00430 62257 i
10	- 0.00015 59976	- 0.00036 56490
11	- 0.00001 04179 i	- 0.00002 53896 i
12	+ 5830	+ 14702
13	+ 277 i	+ 721 i
14	- 11	- 30
15	- 0 i	- 1 i

The coefficients of the derivatives of the Kelvin functions can be obtained easily by the standard procedure for the differentiation of a Chebyshev series. Unfortunately, one loses one or two decimal places on each differentiation and since, in calculating certain of the stress resultants more than one differentiation is involved, we have what could be a serious loss of accuracy.

In testing this Chebyshev series on the Sirius computer, the limitation on the size of a word to 10 digits becomes rather severe since one cannot make full use of the tabulated coefficients. Indeed, only the first 11 coefficients can be used, and these to a lesser accuracy. Tests showed good correspondence between the tabulated values of ber , bei , ker and kei and those obtained using the modified polynomials except approaching the limit of $z = 8$ where there were growing discrepancies especially in the case of the ker and kei functions. The first derivatives of the Kelvin functions were also satisfactory over most of the range until the upper limit was approached when the discrepancies were even greater (to the order of 10% error) than for the function itself.

Since this source of error would require to be modified and also since the range of argument $8 \leq z \leq 10$ would require investigation, it was felt that it would be unwise to proceed with the attempt to program the Kelvin functions for the full range of argument. It was decided to write into each program the values of the required Kelvin functions at a number of discrete points over the required range.

With the great improvement of computer facilities now available, there is now a distinct possibility of preparing a program for the Kelvin functions which will cover all arguments. It this is done/

done one could consider a numerical solution to many of the shell problems where the Greens function involves these Kelvin functions.

The Computer Programs

The computer programs for the evaluation of the stress resultants for the various shell parameters and conditions of loading were prepared using the series representation of the Modified Bessel functions and a set of values for the Kelvin functions at a finite number of points.

Difficulty was experienced over that part of the range involving $8 \leq 5\phi \leq 10$ for the reason mentioned earlier but over the rest of the range the various graphs appear smooth and continuous.

In the case of the interaction of the cylinder with the sphere it was found that the full problem of finding the stresses into the sphere from a particular opening value required a greater machine capacity than was available in Sirius. It was just possible to obtain the appropriate integration constants and also the opening values for the stress resultants. A further program is therefore required to obtain the stresses into the sphere. This difficulty no longer obtains with the larger computers available.

No attempt is made here to present any of the programs, which are written in Sirius Autocode, since they contain no matter which would contribute to computational technique.

APPENDIX 2

THE CIRCULAR DISC

The radial displacement $u(r)$ of a circular disc which has an axisymmetric temperature distribution is, by TIMOSHENKO and GOODIER ⁽⁴⁹⁾, expressed in the form

$$\frac{d}{dr} \left[\frac{1}{r} \frac{d(ru)}{dr} \right] = \alpha (1 + \nu) \frac{dt}{dr}$$

The general solution of this equation is substituted, by them, into the stress-strain and the strain-displacement relationships to give the following expressions for the displacement and the stresses

$$u(r) = (1 + \nu) \frac{\alpha}{r} \int_a^r tr \, dr + C_1 r + \frac{C_2}{r}$$

$$\sigma_r = -\frac{\alpha E}{r^2} \int_a^r tr \, dr + \frac{E C_1}{1 - \nu} - \frac{E C_2}{(1 + \nu) r^2}$$

$$\sigma_\theta = \frac{\alpha E}{r^2} \int_a^r tr \, dr - E \alpha t + \frac{E C_1}{1 - \nu} + \frac{E C_2}{(1 + \nu) r^2} \quad \text{A.2.1-3}$$

where, $r = a$ is the inner boundary, C_1 and C_2 are the constants of integration.

Impose the boundary condition that $\sigma_r = 0$ at $r = a$ and $r = b$ and determine these integration constants.

The expressions for the stresses and displacement then become

$$\sigma_r = \frac{\alpha E}{r^2} \left[\frac{r^2 - a^2}{b^2 - a^2} \int_a^b tr \, dr - \int_a^r tr \, dr \right]$$

$$\sigma_\theta = \frac{\alpha E}{r^2} \left[\frac{r^2 - a^2}{b^2 - a^2} \int_a^b tr \, dr + \int_a^r tr \, dr - tr^2 \right]$$

$$u(r) = \frac{\alpha}{r} \left[(1 + \nu) \int_a^r tr \, dr + \frac{(1 - \nu)r^2 + (1 + \nu)a^2}{b^2 - a^2} \int_a^b tr \, dr \right] \quad \text{A.2.4-6}$$

It was shown in Chapter I, equation (1.17) that the axisymmetric temperature distribution in a flat plate is given by

$$t = A I_0(cr) + B K_0(cr)$$

where A and B are constants and

$$c = \left(\frac{2m}{kh}\right)^{\frac{1}{2}} .$$

If then the temperature at the inner boundary $r = a$ is T and provided the temperature gradient becomes zero before the outer boundary $r = b$ is reached, equation (1.6) will give

$$t = T \frac{K_0(cr)}{K_0(ca)} \tag{A.2.7}$$

and, upon differentiating, the thermal gradient will be

$$t' = \frac{dt}{dr} = -cT \frac{K_1(cr)}{K_0(ca)} . \tag{A.2.8}$$

Examine the opening values of the stresses and the displacement for the temperature distribution. The radial stress at the opening is, of course, zero. Substituting in equations (A.2.5-6) the expression for the temperature as given in equation (A.2.7) will give

$$[u(r)]_{r=a} = \frac{2a\alpha}{b^2 - a^2} \frac{T}{K_0(ca)} \int_a^b K_0(cr) r dr$$

$$[\sigma_r]_{r=a} = \frac{2\alpha E}{b^2 - a^2} \frac{T}{K_0(ca)} \int_a^b K_0(cr) r dr - E\alpha T$$

Making use of the recurrence relationship for Bessel functions

$$\int K_0(z) z dz = [-z K_1(z)]$$

which is as given by ABRAMOWITZ and STEGUN ⁽⁶⁵⁾, these equations may be integrated to/

may be integrated to

$$\left[u(r) \right]_{r=a} = \frac{2a^2 \alpha}{(b^2 - a^2)c} T \frac{[K_1(ca) - K_1(cb)]}{K_0(ca)}$$

$$\left[\sigma_{\theta} \right]_{r=a} = \frac{2a \alpha}{(b^2 - a^2)c} T \frac{[K_1(ca) - K_1(cb)]}{K_0(ca)} - E \alpha T$$

A.2.9-10

Recalling, from equation (A.2.8) that

$$t' = -cT \frac{K_1(cr)}{K_0(cr)}$$

and further, from our boundary condition that $t' = 0$ at $r = b$

we can write equations (A.2.9-10) as

$$\left[u(r) \right]_{r=a} = -\frac{2a^2}{b^2 - a^2} \frac{\alpha}{c^2} t'_a$$

$$\left[\sigma_{\theta} \right]_{r=a} = -\frac{2a}{b^2 - a^2} \frac{\alpha E}{c^2} t'_a - E \alpha T$$

A.2.11-12

For small values of opening in the circular plate we can once again make use of the limiting forms of the Bessel functions for small arguments. They were

$$K_0(z) \approx -\ln(z)$$

$$K_1(z) \approx z^{-1}$$

Substituting these values therefore in equations

(A.2.11-12) and with $z \rightarrow 0$ we have

$$\left[u(r) \right]_{r=a} \approx 0$$

$$\left[\sigma_{\theta} \right]_{r=a} \approx E \alpha T$$

A.2.13-14

The general expressions for the stress distribution into the/

the plate from the opening can be written as

$$u(r) = \frac{\alpha}{c^2 r} \left[(1-\nu)(rt_r^{\cdot} - at_a^{\cdot}) + \frac{(1+\nu)r^2 + (1-\nu)a^2}{b^2 - a^2} \cdot (-at_a^{\cdot}) \right]$$

$$\sigma_r = \frac{\alpha E}{c^2 r^2} \left[-\frac{r^2 - a^2}{b^2 - a^2} at_a^{\cdot} - (rt_r^{\cdot} - at_a^{\cdot}) \right]$$

$$\sigma_{\theta} = \frac{\alpha E}{c^2 r^2} \left[-\frac{r^2 + a^2}{b^2 - a^2} at_a^{\cdot} + (rt_r^{\cdot} - at_a^{\cdot}) \right] - E \alpha t$$

A.2.15-17

where the thermal gradient is

$$t^{\cdot} = -cT \frac{K_1(cr)}{K_0(cr)} .$$

APPENDIX 3

CONVECTIVE AND RADIANT HEAT TRANSFER

Convection is the term applied to the heat transfer mechanism which takes place in a fluid because of a combination of conduction within the fluid and energy transport which is due to the fluid motion itself. The distinguishing feature therefore of heat convection is this fluid motion.

When a fluid moves past a solid surface it is observed that the fluid velocity varies from zero at that surface to some finite value at some distance away. The velocity gradient is affected by the condition of the boundary layer in this region and by the actual geometric position of the surface whether it be lying vertically or horizontally and whether it faces up or down.

It must be appreciated that the convective heat transfer coefficient which was introduced in equation (1.2) as m_c is only an attempt to rationalise a rather complex and variable quantity for computational purposes.

Experimental work has been performed in estimating the rate of heat loss from flat plates to the still air which surrounds them. It was found that the rate of heat loss depended upon the size of the plate and for plates 3 to 4 feet square the following simplified formulae are recommended by McADAMS⁽⁵⁶⁾ for the heat transfer coefficient due to convection only -

$$m_c = 0.38 (t_s - t_f)^{\frac{1}{4}}$$

A.3.1

for a horizontal surface facing upward.

$$m_c = 0.20 (t_s - t_f)^{\frac{1}{4}} \quad \text{A.3.2}$$

for a horizontal surface facing downwards, and for a vertical surface

$$m_c = 0.27 (t_s - t_f)^{\frac{1}{4}} \quad \text{A.3.3}$$

where all three equations are for turbulent flow only.

It is apparent that the value of m_c for an upward facing surface is almost double that for a downward facing one whereas the value for a vertical surface is almost equal to their arithmetic mean.

THERMAL RADIATION

The rate at which heat is radiated from an emitting surface A is given by the Stefan-Boltzmann law as

$$q = \epsilon \sigma A T^4 \quad \text{A.3.4}$$

where T is the absolute temperature of the surface, σ is a universal constant and ϵ is a property of the particular emitting surface known as its emissivity. For an ideal radiator, a "black body" the value of the emissivity is unity.

The heat loss, by radiation, from a body of surface temperature T_s (absolute) to ambient surroundings at temperature T_f (absolute) is therefore given by the relationship

$$q_r = \sigma A \epsilon (T_s^4 - T_f^4) \quad \text{A.3.5}$$

provided the area of the surface of the surroundings is very large in comparison with the emitting area.

It/

It is found expedient to define a radiant heat transfer coefficient m_r using the same linear temperature relationships which are involved with the convective heat transfer coefficient. Postulate the following relationship

$$\bar{q}_r = m_r A (t_s - t_f) \tag{A.3.6}$$

and although it is realised that this empirical formula is convenient for design and some computational purposes, it obscures the real nature of the radiant exchange mechanism since m_r must be some function of σ , ϵ and the absolute temperatures T_s and T_f . Indeed combining these two equations (A.3.5) and (A.3.6) gives

$$\begin{aligned} m_r &= \frac{T_s^4 - T_f^4}{t_s - t_f} \cdot \sigma \epsilon \\ &= \sigma \epsilon (T_s + T_f)(T_s^2 + T_f^2) \end{aligned} \tag{A.3.7}$$

Values for the emissivity of some common metallic surfaces are given in Table (A.3.1). These values are after HSU⁽⁶⁶⁾.

Material Condition	Emissivity	
	100°F	500°F
Iron		
Pure polished	0.06	0.08
Electrolytically deposited	0.05	0.07
Freshly rubbed with emery	0.24	-
Wrought polished	0.28	0.27
Wrought smooth	0.35	-
Wrought smooth but rifled	0.75	-
Cast freshly turned	0.44	-
Cast	0.21	-
Cast oxidized	0.63	0.66
Red rushed	0.62	-
Rolled oxidized	0.66	-
Very rusted	0.69	-
Electrolytically oxidized	0.79	0.80
Rough oxide layer	0.81	-
Matt oxidized wrought	0.95	0.95
Rough oxidized cast	0.98	-
Red iron oxide	0.96	-
Steel		
Polished	0.07	0.10
Carbonized	0.52	0.53
Oxidized	0.79	0.79
Plate rough	0.94	-

Table A.3.1

The emissivity of iron and steel for various surface conditions - HSU.

Alloy	Temperature Range °F	Thermal Conductivity (k) Btu/ft hr °F
Steels		
0.5% C Carbon steel	-212	31.6
	68	30.2
	212	28.2
	392	25.5
	572	24.2
	752	20.2
	1112	18.1
1.0% C Carbon steel	-212	
	68	24.8
	212	24.8
	392	24.2
	572	22.8
	752	21.5
	1112	18.8
1.5% C Carbon steel	-212	
	68	20.8
	212	20.8
	392	20.8
	572	20.2
	752	19.5
	1112	18.2

Table A.3.2

The thermal conductivity of some alloy steels for various temperature values.

APPENDIX 4

FINITE ELEMENT SOLUTIONS

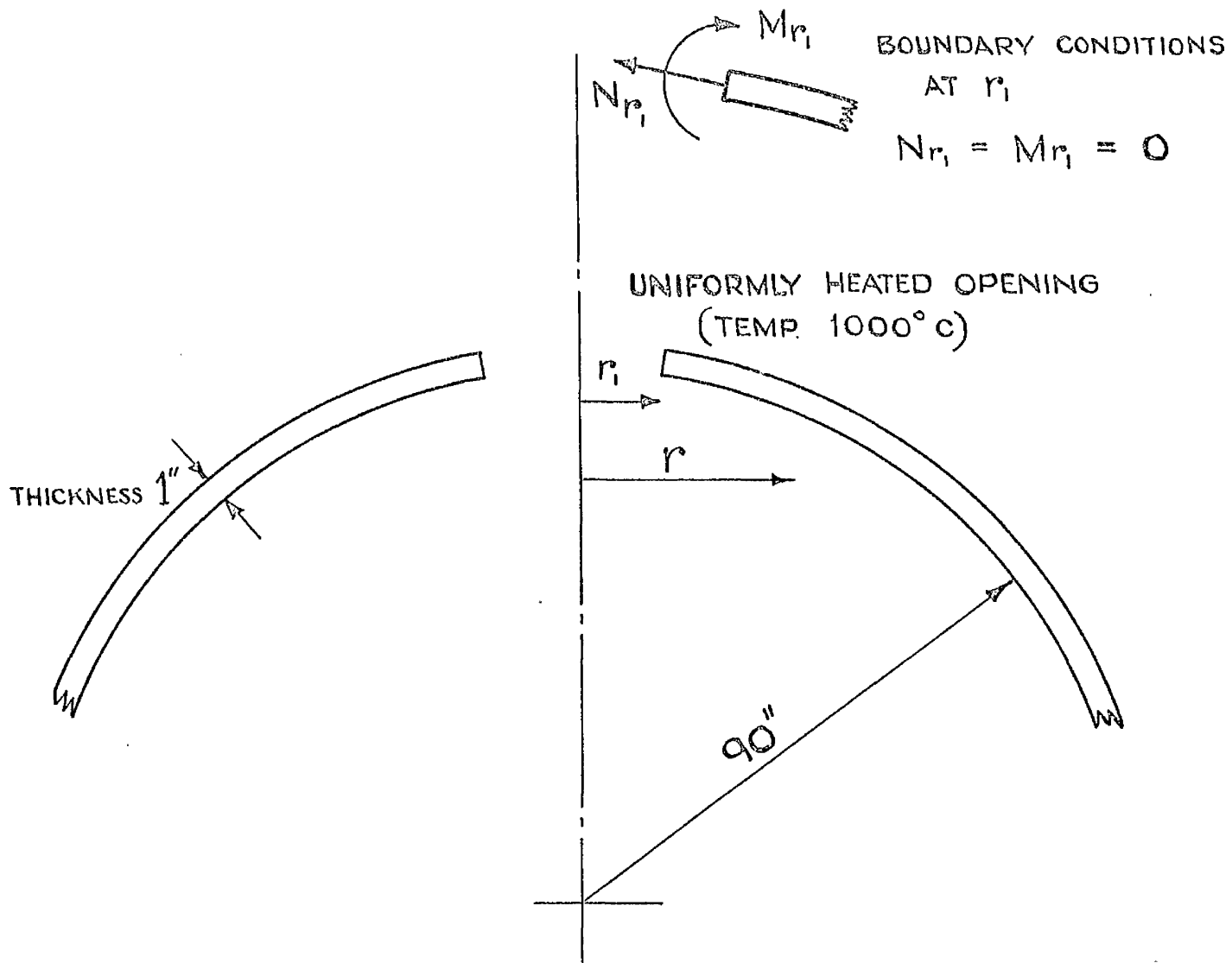
With the advent of the modern high speed digital computer has grown an interest in the numerical methods suitable for solving the problems associated with shells structures. One such numerical procedure is known as the finite element technique. This technique consists of "breaking" the shell up into a number of elements. These elements must subsequently be "matched" at their boundaries to give either continuity of stress or of displacement. The solution of a shell problem by this method requires the use of a computer with a storage capacity capable of handling the inversion of the large matrix which is involved.

One commercial organisation which has a finite element program for spherical shells is Babcock and Wilcox. Their program is capable of evaluating the thermal stresses on a spherical shell due to an axisymmetrical temperature distribution. S. H. Dance of this company, when approached by the author, agreed to evaluate, using this finite element program, two cases of a heated opening in a spherical shell with a specified temperature distribution.

The values of the shell parameters subsequently supplied to him were as shown in Figure (A.4.1). The two opening values for which the thermal stress distribution was requested were

$$r_1 = 0.518" \quad ; \quad r_2 = 25.557 \quad .$$

The temperature distribution arising from such heated openings can be/



YOUNG'S MODULUS, E , = $30 \times 10^6 \text{ lb/in}^2$
 COEFFICIENT OF LINEAR THERMAL EXPANSION, α , = $11 \times 10^{-6} \text{ in/in } ^\circ\text{C}$
 POISSON'S RATIO, ν , = 0.255

ASSUMED CONSTANT OVER WHOLE SHELL

OPENING TEMPERATURE, T , = 1000°C

TEMPERATURE DISTRIBUTION, t , = $T \frac{K_o(S \frac{r}{a})}{K_o(S \frac{r_i}{a})}$

TEMPERATURE PARAMETER, S , = 12

FIGURE (A4.1) DETAILS OF THE SHELL FOR WHICH THE THERMAL STRESSES ARE EVALUATED.

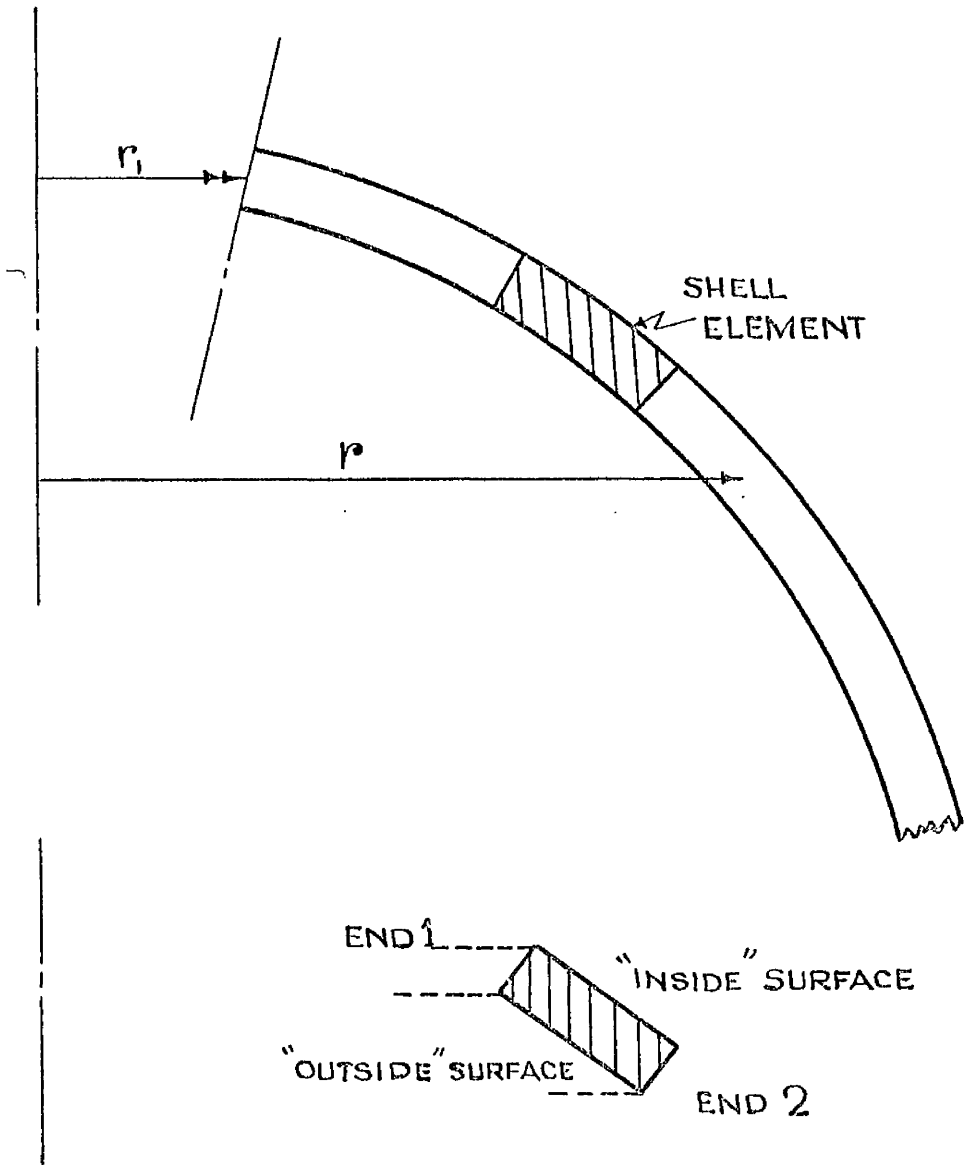


FIGURE (A4.2)

TYPICAL SHELL ELEMENT FOR THE FINITE ELEMENT TECHNIQUE.

N.B. SINCE THE PROBLEM HAS BEEN SOLVED "UPSIDE DOWN" THE LOWER DIAGRAM IS REQUIRED TO INTERPRET THE RESULTS.

be evaluated, using the relationship

$$t = \frac{T K_o(s \frac{r}{a})}{K_o(s \frac{r_1}{a})}$$

since all of the parameters have been prescribed. These temperature distributions are shown in Table (A.4.5).

For the finite element method Dance divided the surface of the shell, over which there was a non-zero temperature distribution, into 40 equal tapered conical elements, where the taper is, of course, zero in this problem. The surfaces of the sphere thus considered were

$$\begin{array}{l} \text{for } r_1 = 0.518" \quad , \quad 0.518" \leq r \leq 43.953" \\ \text{for } r_1 = 25.557" \quad 25.557" \leq r \leq 62.997" \end{array}$$

The problem was then solved using a stiffness method. This method should ensure reasonable accuracy of displacement but the stresses could be subject to some error due to the approximations inherent in the method. This type of problem is solved "upside down". Computation begins on the outer element, where the temperature is zero, and proceeds to the opening. The assumption is made that there is zero displacement and rotation of the outer element. It is of interest to note that the meanings of "inside" and "outside" surfaces, see Figure (A.4.2), as used in the program, do not correspond with the usual connotation.

The results obtained by Dance, for certain of the elements, are presented in Tables (A.4.1 and 3). It is observed that results are presented for both "ends" of each element so that the values for "end two" of an element should agree with the values of "end one" of the consecutive element. The tables show perfect agreement/

agreement between the end values of both the horizontal displacement and of the rotation. There is good correspondence between the hoop stress values. The axial stress values show wide disparity particularly near the heated opening. The large value given for the axial stress at this boundary is disconcerting.

An analytic solution for this same problem is presented in Section 2 of Chapter 2. Substituting into this solution the appropriate values of the parameters and of the boundary conditions "analytic" solutions for the stress distributions are obtained. The analytic results are presented in Tables (A.4, 2 and 4). It is unfortunate that, because of the computational difficulties outlined in Appendix 1, the stress values cannot be calculated for the exact values of the radii given in the finite element results.

It is observed that there is reasonable agreement between all the computed and the analytic results except for the axial stress values near the opening. The mean of the two adjacent computed axial stress values does however give better agreement with the analytic results. Rather surprisingly there is better agreement between the stress values for the smaller value of opening, $r_1 = 0.518"$, than between the stress values for the larger opening where $r_1 = 25.557"$. The same is not true for the horizontal displacement. In the case of $r_1 = 0.518"$

$$\begin{aligned} u \text{ (computed)} &= 0.1233 \times 10^{-2} \text{ in} \\ u \text{ (analytic)} &= 0.2116 \times 10^{-2} \text{ in} . \end{aligned}$$

Once again, however, the correspondence between the two sets of values improves with distance from the opening.

As with many other numerical procedures it would be valuable to perform the finite element technique on the same problems using/

using different numbers of elements each time. The convergence of the various results obtained for the stresses could then be compared.

The earlier graphical results presented in this thesis indicate rapid changes in the stresses within a region close to the opening. An element size of approximately 1" in this region is rather large. It would be more satisfactory to have an element whose size varies with the radius. Thus would be provided small elements in the region of the opening where the rapid changes take place and large elements far removed from the opening where the effects have reduced almost to zero.

Element	End	Radius (ins)	Stresses (lb/in ²)				Horizontal Displacement (ins)	Rotation
			Inside		Outside			
			Axial	Hoop	Axial	Hoop		
1	1	25.557	.6579	.1110	.5555	.48784	.2144	.5511
	2		.4537	.7237	.1969	.1427	.2080	.5450
2	1	26.633	.5133	.7472	.7846	.1689	.2080	.5450
	2		.7221	.4550	.6836	.6305	.1989	.5367
3	1	27.706	.9984	.4698	.1328	.4552	.1989	.5367
	2		.1307	.2530	.1610	.1913	.1879	.5239
4	1	28.774	.9377	.2613	.2003	.1802	.1879	.5239
	2		.2016	.1049	.2475	.2617	.1753	.5061
5	1	30.896	.2671	.5994	.3321	.2863	.1619	.4833
	2		.3381	.7048	.3848	.2875	.1477	.4561
9	1	34.043	.4367	.1411	.4490	.2344	.1194	.3923
	2		.4512	.1468	.4725	.1937	.1058	.3577
14	1	39.179	.4305	.1078	.4072	.4732	.5930	.2228
	2		.3949	.8801	.3839	.1879	.5015	.1931
21	1	46.109	.1989	.8623	.1821	.5115	.1514	.6718
	2		.1695	.1176	.1548	.5181	.1201	.5450
25	1	49.919	.9761	.1164	.8819	.4534	.5722	.2746
	2		.8028	.1335	.7024	.4125	.4410	.2144
28	1	52.686	.5010	.1505	.4451	.3330	.2593	.1278
	2		.4000	.1470	.3321	.2895	.1987	.9791
35	1	58.860	.6791	.9753	.5230	.1192	.3895	.2340
	2		.5951	.8584	.3679	.1030	.2750	.1953
40	1	62.997	.6952	.4209	.6358	.7425	.2368	.5268
	2	63.795	.8875	.2779	.7818	.7036	0	0

TABLE (A4.1) Computed results for the stress distribution into a spherical shell from a heated opening at = 25.557 in. using the finite element technique

Radius (ins)	Stresses (lb/in ²)						Horizontal Displacement (ins)	Rotation
	Inside			Outside				
	Axial	Hoop		Axial	Hoop			
25.558	0	- .1103 6		0	- .4859 5	.2135	.5483 -1	
26.058	- .3653 3	- .9279 5		- .4539 3	- .3274 5	.2109	.5456 -1	
26.553	- .2966 3	- .7722 5		- .1133 4	- .1935 5	.2076	.5426 -1	
27.048	+ .4501 3	- .6343 5		- .6606 4	- .8186 4	.2039	.5392 -1	
29.508	+ .1627 5	- .1603 5		- .2410 5	+ .2252 5	.1787	.5086 -1	
31.459	+ .3017 5	- .1233 5		- .3619 5	+ .2774 5	.1538	.4654 -1	
34.354	+ .4314 5	+ .1357 5		- .4564 5	+ .2147 5	.1152	.3785 -1	
40.016	+ .3958 5	+ .8991 4		- .3836 5	+ .2319 4	.5220 -1	.1966 -1	
46.823	+ .1757 5	+ .4270 3		- .1640 5	- .5118 4	.1372 -1	.5698 -2	
50.314	+ .9028 4	- .1054 4		- .8323 4	- .4270 4	.5905 -2	.2445 -2	
53.280	+ .4593 4	- .1232 4		- .4218 4	- .3048 4	.3304 -2	.9501 -3	
59.340	+ .5254 3	- .5854 3		- .4613 3	- .7795 3	.1081 -2	.1517 -3	
64.958	+ .2115 2	- .9032 2		- .2049 2	- .7685 2	.7279 -3	.7520 -4	

TABLE (A4.2) Analytic Results for the stress distribution into a spherical shell from a heated opening at = 25.558 in.

Element	End	Radius (ins)	Stresses (lb/in ²)						Horizontal Displacement (ins)	Rotation
			Inside		Outside					
			Axial	Hoop	Axial	Hoop				
1	1	0.518	- .1512 6	- .3708 6	- .8057 5	- .1031 6	.2116 -2	- .4312 -2		
	2		- .1245 6	- .1020 6	- .3158 4	.3677 5	.1012 -1	- .6026 -2		
2	1	1.682	- .1270 6	- .1027 6	- .2056 5	.3192 5	.1012 -1	- .6026 -2		
	2		- .1138 6	- .6802 5	- .2109 5	.4683 5	.1393 -1	- .8656 -2		
3	1	2.846	- .9840 5	- .6408 5	- .6501 4	.5053 5	.1393 -1	- .8656 -2		
	2		- .8631 5	- .4610 5	- .1332 5	.5324 5	.1631 -1	- .1080 -1		
4	1	4.009	- .7435 5	- .4303 5	- .1653 4	.5619 5	.1631 -1	- .1080 -1		
	2		- .6356 5	- .3127 5	- .1004 5	.5383 5	.1773 -1	- .1233 -1		
7	1	7.494	- .2466 5	- .1159 5	- .4841 4	.4807 5	.1551 -1	- .1370 -1		
	2		- .1849 5	- .7575 4	- .1170 5	.4137 5	.1814 -1	- .1367 -1		
10	1	10.968	+ .4697 3	- .2529 3	- .1092 5	.3119 5	.1643 -1	- .1266 -1		
	2		+ .2742 4	+ .7006 3	- .1444 5	.2535 5	.1522 -1	- .1183 -1		
15	1	16.718	+ .1191 5	+ .2701 4	- .1241 5	.1018 5	.9739 -2	- .7769 -2		
	2		+ .1112 5	+ .2240 4	- .1246 5	.7398 4	.8422 -2	- .6777 -2		
23	1	25.764	+ .5827 4	+ .1752 3	- .5149 4	- .4954 3	.2101 -2	- .1911 -2		
	2		+ .4920 4	- .1659 2	- .4356 6	- .7536 3	.1625 -2	- .1525 -2		
27	1	30.189	+ .2757 4	- .3325 3	- .2402 4	- .9767 3	.6727 -3	- .7195 -3		
	2		+ .2239 4	- .3698 3	- .1882 4	- .9289 3	.4315 -3	- .5455 -3		
36	1	39.832	+ .1760 3	- .2702 3	- .1655 3	- .3283 3	.1009 -4	- .4298 -4		
	2		+ .1389 3	- .2347 3	- .1060 3	- .2760 3	.3376 -5	- .3209 -4		
40	1	43.953	+ .9745 2	- .1408 3	- .1239 3	- .1918 3	- .3276 -5	- .9125 -5		
	2	44.965	+ .1341 3	- .1024 3	- .1462 3	- .1739 3	0	0		

TABLE (A4.3) Computed results for the stress distribution into a spherical shell from a heated opening at $r = 0.518$ in. using the finite element technique

Radius (ins)	Stresses (lb/in ²)				Horizontal Displacement (ins)	Rotation
	Inside		Outside			
	Axial	Hoop	Axial	Hoop		
0.518	0	- .3788 6	0	- .1385 6	.1233 -2	.4153 -2
1.555	- .1264 6	- .1205 6	- .2833 5	+ .8765 4	.8651 -2	.5407 -2
2.850	- .1000 6	- .6807 5	- .1259 5	+ .4043 5	.1307 -1	.8192 -2
3.886	- .7864 5	- .4709 5	- .7045 4	+ .4869 5	.1522 -1	.1005 -1
7.249	- .3113 5	- .1358 5	- .8908 4	+ .4575 5	.1758 -1	.1298 -1
10.344	- .4224 4	- .1931 5	- .1109 5	+ .3223 5	.1606 -1	.1241 -1
16.494	+ .1093 5	+ .2442 4	- .1244 5	+ .1015 5	.9287 -2	.7558 -2
25.561	+ .5693 4	+ .1452 3	- .5059 4	- .4452 3	.1867 -2	.1833 -2
30.485	+ .1360 4	- .3399 3	- .9966 3	- .3795 3	.7269 -3	.5843 -3
40.017	+ .1386 3	+ .2508 3	- .9901 2	+ .1914 3	.2143 -4	.3518 -5
44.591	- .231 2	- .759 2	+ .297 2	- .627 2	-	-

TABLE (A4.4) Analytic results for the stress distribution into a spherical shell from a heated opening at $r = 0.518$ in.

$r_1 = 0.518''$		$r_1 = 25.557''$	
r_{in}	$t^{\circ}C$	r_{in}	$t^{\circ}C$
0.518	1000.000	25.557	1000.000
1.682	597.279	26.633	843.628
2.846	425.105	27.706	712.263
4.009	320.497	28.774	601.787
5.172	248.959	29.837	508.786
6.334	197.008	30.896	430.424
7.494	157.891	31.950	364.342
8.654	127.722	32.999	308.573
9.812	104.053	34.043	261.473
10.986	85.247	35.081	221.668
12.123	70.159	36.115	188.006
13.275	57.960	37.142	159.524
14.425	48.034	38.164	135.410
15.573	39.917	39.179	114.985
16.718	33.249	40.189	97.676
17.861	27.751	41.192	83.000
19.000	23.205	42.189	70.552
21.270	16.300	44.163	51.023
23.524	11.509	46.109	36.940
25.764	8.161	48.026	26.772
27.986	5.807	49.914	19.420
30.189	4.145	51.770	14.099
32.372	2.966	53.594	10.245
34.533	2.127	55.384	7.449
36.671	1.529	57.140	5.420
38.785	1.101	58.860	3.946
40.873	0.794	60.543	2.875
42.933	0.573	62.189	2.095
43.953	0.487	62.997	1.789

TABLE (A4.5) Temperature distributions into the spherical shell from two distinct opening values.

ACKNOWLEDGEMENTS

The author wishes to thank Professor J.M. Harvey, Head of the Department of Mechanics of Materials at the University of Strathclyde, for the use of the facilities of the Department.

The author also wishes to thank his many colleagues at the University of Strathclyde for their encouragement in the research programme. In particular, he would like to thank Dr. A.S. Tooth for his continuing advice during the whole period of the investigation.